The influences of medial-diencephalic lesions on hippocampal and cortical function and plasticity.

Aura Frizzati

A dissertation submitted for the higher degree of PhD

School of Psychology

2015

CONTENTS

DECLARATION

This work has not been submitted in substance for any other degree or award at this or any other university or place of learning, nor is being submitted concurrently in candidature for any degree or other award.

Signed …… (candidate)
Date ……

STATEMENT 1

This thesis is being submitted in partial fulfillment of the requirements for the degree of ……(insert MCh, MD, MPhil, PhD etc, as appropriate)

Signed …… (candidate)
Date ……

STATEMENT 2

This thesis is the result of my own independent work/investigation, except where otherwise stated.
Other sources are acknowledged by explicit references. The views expressed are my own.

Signed …… (candidate)
Date……

STATEMENT 3

I hereby give consent for my thesis, if accepted, to be available online in the University's Open Access repository and for inter-library loan, and for the title and summary to be made available to outside organisations.

Signed …… (candidate)
Date ……

STATEMENT 4: PREVIOUSLY APPROVED BAR ON ACCESS

I hereby give consent for my thesis, if accepted, to be available online in the University's Open Access repository and for inter-library loans **after expiry of a bar on access previously approved by the Academic Standards & Quality Committee.**

Signed …… (candidate)
Date ……

SUMMARY

The medial diencephalon, comprising the mammillary bodies and anterior thalamic nuclei, is important for memory in both humans and animals. However, there is still uncertainty regarding how this region supports memory processes. The mammillary bodies and anterior thalamic nuclei form part of the Papez circuit, a network of brain regions important for episodic memory. Lesions within the medial diencephalon cause distal hypofunctionality in the rest of the Papez circuit, and most consistently in the retrosplenial/posterior cingulate cortex. Patients with diencephalic amnesia often exhibit glucose hypometabolism in the posterior cingulate cortex and animals with medial diencephalic lesions dramatically reduce immediate early gene expression in the retrosplenial cortex. It is still unknown whether these distal effects contribute to the memory impairments.

This body of work investigated the distal hypofunctionality following lesions of the mammillothalamic tract in rats, a white matter bundle that connects the mammillary bodies to the anterior thalamic nuclei within the medial diencephalon. Mammillothalamic tract lesions were found to reduce expression levels of the immediate early gene *zif268* in the retrosplenial cortex. However, no significant changes were found in the fine dendritic microstructure of the small pyramidal neurones located in the superficial layers of the rostral granular retrosplenial cortex, which receive the anterior thalamic nuclei input.

To determine whether the reduced immediate early gene expression contributes to the spatial memory impairments associated with mammillothalamic tract lesions, antisense oligodeoxynucleotides were infused into either the retrosplenial cortex or the dorsal hippocampus. These infusions had no effect on spatial memory performance; however, it was not possible to verify that they were effective in knocking-down *zif268* or *c-fos* at the molecular level. This work expands our understanding of the distal effects of mammillothalamic tract lesions but further studies are needed to determine whether they contribute to the memory impairments observed.

ACKNOWLEDGEMENTS

I would like to thank my main supervisor Seralynne Vann who has really helped me a lot in these three years and who gave me all the support necessary to complete all of the work on time. I would also like to thank Kerrie Thomas for her precious co-supervision, helping me with the molecular part of the experiments; John Aggleton, who has helped me to plan the experiments and monitored on my progresses; Andrew Nelson, who has supported me so much in these three years in all the experiments, helping me with behavioural testing, surgeries, infusions, statistics and experimental planning; Christopher Dillingham, Simon Trent, Anna Powell and Nichola Brydges for helping me a lot with staining, western blot, statistics, surgeries, infusions and microdissections.

A huge thanks also to all the lab staff, particularly Moira Davies, Clive Mann, Heather Phillips and Eman Amin, I have learned so much from all of them and they have been just amazing in cheering me up and made me smile also in the most difficult moments.

I also thank Kat, who joined me in the office in the last year of this experience and with whom it was really a pleasure sharing some of my time at work.

Finally I want to dedicate this thesis to my wonderful parents, who, with their love, have always listened to me, helped me and have been obliged to become sort of neuroscience experts. Vi voglio bene.

This work in this thesis was supported by a Wellcome Trust Studentship.

Chapter 1 : Introduction

Memory is hugely important for our everyday lives and memory impairments can have devastating consequences. Therefore, understanding how brains support memory continues to be one of the key goals of neuroscience. There is a network of brain regions, known as the Papez circuit, which appears to support memory. This circuit comprises structures within the medial temporal lobe, the medial diencephalon and the cingulate cortex. Within this circuit, the main focus has typically been the medial temporal lobe (i.e. hippocampus) with the medial diencephalon receiving far less attention. However, findings from both patients and animals have repeatedly shown the importance of the medial diencephalon for memory. Despite this, there is still very little known about why this region is important for memory.

To try and understand why damage to the medial diencephalon disrupts memory, it may be important to look beyond the medial diencephalon and consider how damage to this region impacts on other structures that have been implicated in memory. For example, there is evidence that damage to one component of the Papez circuit can cause hypofunctionality in the other components. The aim of this body of work, therefore, was to investigate the distal effects of damage to the medial diencephalon and whether these changes may contribute to the observed memory impairments. Microstructural and functional changes following mammillothalamic tract lesions were assessed using dendritic analysis and immediate early gene imaging. The functional effects were then investigated artificially knocking-down levels of immediate early gene expression in structures within the Papez circuit to determine whether this was sufficient to impair memory.

1.1. The Papez circuit

In order to understand the effects of lesioning the medial diencephalon on memory, it is important to consider its anatomical connections. For this thesis, I will describe the anatomy of the Papez circuit, a brain circuit that comprises the medial diencephalon and that has been repeatedly implicated in supporting spatial memory processes.

Papez (1937) described a functional circuit within the limbic system that originates in the hippocampal formation and includes the mammillary bodies, anterior thalamic nuclei and cingulate gyrus (Figure 1-1). Papez proposed that this circuit supported the expression and subjective experience of emotions, however, it subsequently became recognised as a "memory" circuit (Aggleton & Brown, 1999; Barbizet & Jardine, 1971; Delay & Brion, 1969). Consistent with this, lesions of the principal components of the circuit have been associated with anterograde amnesia in humans (e.g. Scoville & Milner, 1957; Valenstein et al., 1987; Van der Werf, Witter, Uylings, & Jolles, 2000) and spatial memory impairments in animals (e.g. Aggleton, Hunt, Nagle, & Neave, 1996; Aggleton, Hunt, & Rawlins, 1986; Vann & Aggleton, 2002, 2003)

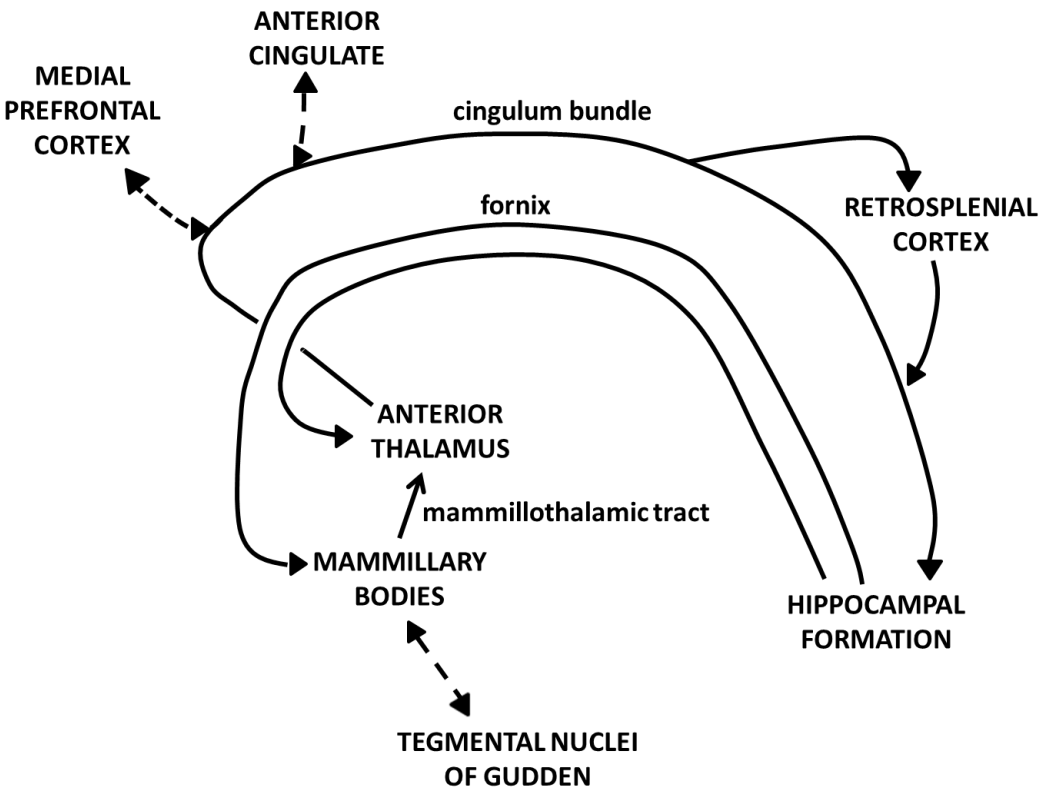

Figure 1-1. Schematic representation of the connections within the modified Papez circuit. In addition to the connections described in the main text, the circuit is reciprocally connected with the medial prefrontal and anterior cingulate cortices (mainly via the cingulum bundle) and with the tegmental nuclei of Gudden, located in the mesencephalon (dashed arrows).

The following sections will give an anatomical description of the main structures within the Papez circuit and their interconnections. While the focus will be on the rodent brain, the main connections appear very similar across species.

1.1.1 The hippocampal formation

The hippocampal formation comprises a series of interconnected regions which form a circuit (Amaral, 1993): the dentate gyrus, the hippocampus proper (subfields CA1 and CA3), the subicular complex (subiculum, presubiculum, parasubiculum and postsubiculum) and the entorhinal cortex (Figure 1-2).

1.1.1.1 Connectivity of the hippocampal formation

The entorhinal cortex sends projections to the circuit via the perforant path; neurones located in layer II of the entorhinal cortex project to the dentate gyrus and CA3, while neurones in layer III of the entorhinal cortex project to CA1 and subiculum (Amaral,

1993). The granule cells of the dentate gyrus send their synapses to the pyramidal neurones of CA3 hippocampal subfield via the mossy fibres. In turn, CA3 pyramidal neurones send their efferents to CA1 subfield via the Schaffer collaterals; the same axons also give rise to associational connections, collateralising and projecting to CA3 itself (Ishizuka, Weber, & Amaral, 1990). CA1 pyramidal cells send their outputs to the subiculum, which mainly projects to the anterior thalamic nuclei (the anteroventral and the anteromedial thalamic nuclei), mammillary bodies (medial mammillary nuclei), nucleus accumbens, postsubiculum and retrosplenial cortex (Amaral, 1993; Dillingham, Erichsen, O'Mara, Aggleton, & Vann, 2015; Van Groen & Wyss, 1990c; Wright, Vann, Erichsen, O'Mara, & Aggleton, 2013; Wyss & Van Groen, 1992). The information from CA1 and the subicular complex also flows back to the deep layers of the entorhinal cortex, closing the circuit (Van Groen & Wyss, 1990b, 1990c).

The components of the subicular complex can be dissociated in terms of their cytoarchitecture and connectivity. However, there is disagreement as to existence of the postsubiculum in the rat, as there is no corresponding postsubiculum in the primate. Some consider the rat postsubiculum to be dorsal presubiculum (Blackstad, 1956; Honda & Ishizuka, 2004; Honda, Umitsu, & Ishizuka, 2008), however, for this body of work, the term postsubiculum (Rose & Woolsey, 1948; Van Groen & Wyss, 1990c) will be used, acknowledging the anatomical and electrophysiological differences between pre- and postsubiculum. The postsubiculum is reciprocally connected with the anterodorsal nucleus of the thalamus and receives light projections from the anteroventral nucleus. It also has reciprocal connections with the retrosplenial cortex, sending most of its projections to the Rgb subregion (Van Groen & Wyss, 1990c). Furthermore, the postsubiculum is one of the major sources of visual information for the hippocampal formation, given its reciprocal connections with visual cortical area 18b and with the laterodorsal thalamic nucleus, a structure connected with the visual system (Van Groen & Wyss, 1990c, 1992). The presubiculum is reciprocally connected with the anteroventral and dorsolateral thalamic nuclei, and receives input from the claustrum. The parasubiculum, instead, is reciprocally connected with the anterodorsal thalamic nucleus and receives afferents from the anteroventral and the laterodorsal thalamic nuclei, CA1 and amygdala. Both the presubiculum and parasubiculum send commissural projections to each other and to their corresponding controlateral areas; furthermore, they both have reciprocal connections with the retrosplenial cortex and receive fibres from the diagonal band of Broca, the nucleus reuniens, the supramammillary nucleus, the ventral tegmental area, the raphe nuclei and the locus coeruleus (Van Groen & Wyss, 1990b).

The fimbria/fornix is the main white matter tract associated with the hippocampal formation, connecting it to cortical and subcortical structures. At the level of the anterior commissure, the fornical fibres divide into two bundles, either continuing rostrally and forming the precommissural fornix (whose two main target structures are the basal forebrain and the prefrontal cortex), or turning caudally to become the postcommissural fornix (which innervates the anterior thalamic nuclei and the hypothalamus, including the mammillary bodies) (Vann, Erichsen, O'Mara, & Aggleton, 2011). The fornical projection to the anterior thalamic nuclei principally involves the anteromedial and anteroventral thalamic nuclei which are innervated by the entorhinal cortex, subiculum, presubiculum and parasubiculum (Dillingham, Erichsen, et al., 2015; Meibach & Siegel, 1977; Swanson & Cowan, 1975; Wright, Erichsen, Vann, O'Mara, & Aggleton, 2010). In contrast, projections from the postsubiculum to the anterodorsal thalamic nucleui travel through a non-fornical route, the internal capsule (Dillingham, Erichsen, et al., 2015).

The descending columns of the postcommissural fornix, which are distinct from the portion of the tract targeting the anterior thalamic nuclei, carry projections from the subiculum, postsubiculum and parasubiculum, and project to the mammillary bodies and surrounding hypothalamic regions (Allen & Hopkins, 1989; Swanson & Cowan, 1975; Van Groen & Wyss, 1990b). The projections to the anterior thalamic nuclei and mammillary bodies arise from separate populations within the subiculum (Wright et al., 2010).

The fornix also carries return projections back to the hippocampus, most notably the dense cholinergic projections from the septal nuclei, via the precommissural fornix, as well as projections from the hypothalamus and midbrain via the postcommissural fornix (Poletti & Creswell, 1977; Saunders & Aggleton, 2007; Swanson, Kohler, & Bjorklund, 1987).

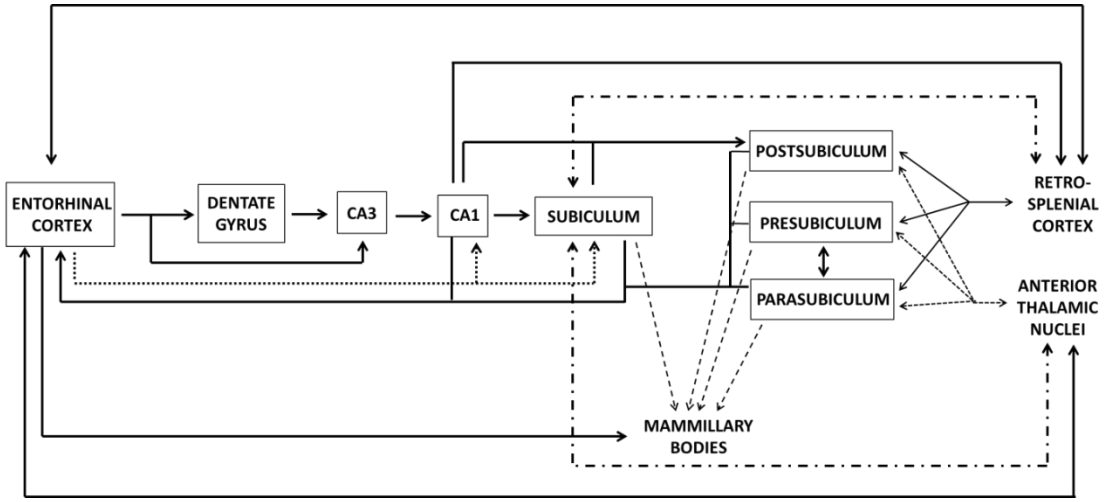

Figure 1-2. Schematic representation of the connections within the hippocampal formation and with the other brain structures relevant for this thesis (mammillary bodies, anterior thalamic nuclei and retrosplenial cortex). Connections among these other structures are not represented. The arrows indicate if the connections are afferent, efferent or reciprocal.

1.1.2 The anterior thalamic nuclei

The anterior thalamic nuclei are located in the rostral part of the dorsomedial thalamus (a component of the medial diencephalon). They are separated from the rest of the thalamus by the internal medullary lamina (Child & Benarroch, 2013). The anterior thalamic nuclei consist of three bilateral pairs of nuclei: the anterodorsal, anteromedial and anteroventral thalamic nuclei. The anterodorsal nuclei are the smallest in size, while the anteroventral nuclei are the largest. There are also differences in neuronal size and packing density across the anterior thalamic nuclei (Morel, Magnin, & Jeanmonod, 1997).

1.1.2.1 Connectivity of the anterior thalamic nuclei

The individual anterior thalamic nuclei can also be dissociated in terms of their connectivity; while they are connected with the same overall structures, i.e. the hippocampal formation, cingulate cortex (anterior and retrosplenial) and the mammillary bodies, they are connected to different subregions within these structures (Aggleton et al., 2010) (Figure 1-3, Figure 1-4 and Figure 1-5).

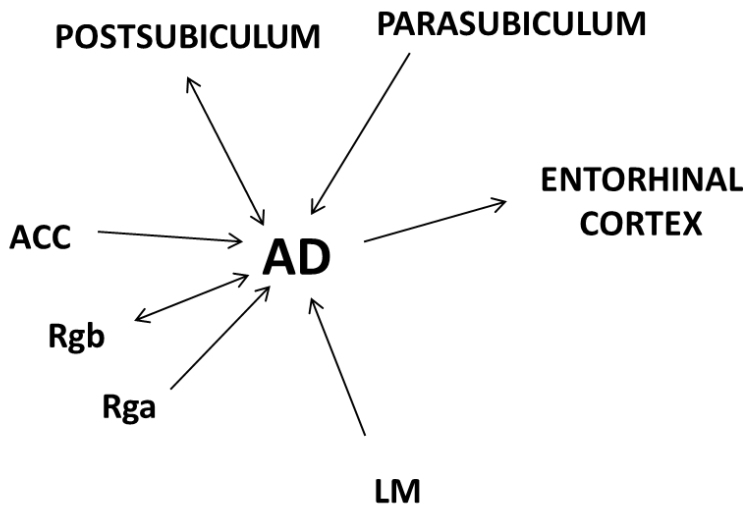

Figure 1-3. Diagram of some input/output connections of the anterodorsal thalamic nuclei (AD).Only a selection of areas relevant for the current piece of work is reported. The arrows indicate if the connections are afferent, efferent or reciprocal. ACC = anterior cingulate cortex; LM = lateral mammillary nuclei; Rga = granular retrosplenial subregion a; Rgb = granular retrosplenial subregion b.

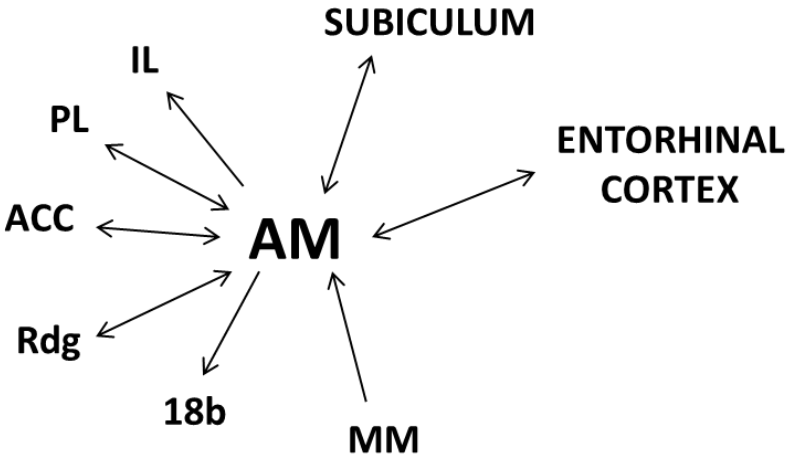

Figure 1-4. Diagram of some input/output connections of the anteromedial thalamic nuclei (AM).Only a selection of areas relevant for the current piece of work is reported. The arrows indicate if the connections are afferent, efferent or reciprocal. ACC = anterior cingulate cortex; IL = infralimbic cortex; MM = medial mammillary nuclei; PL = prelimbic cortex; Rdg = dysgranular retrosplenial subregion.

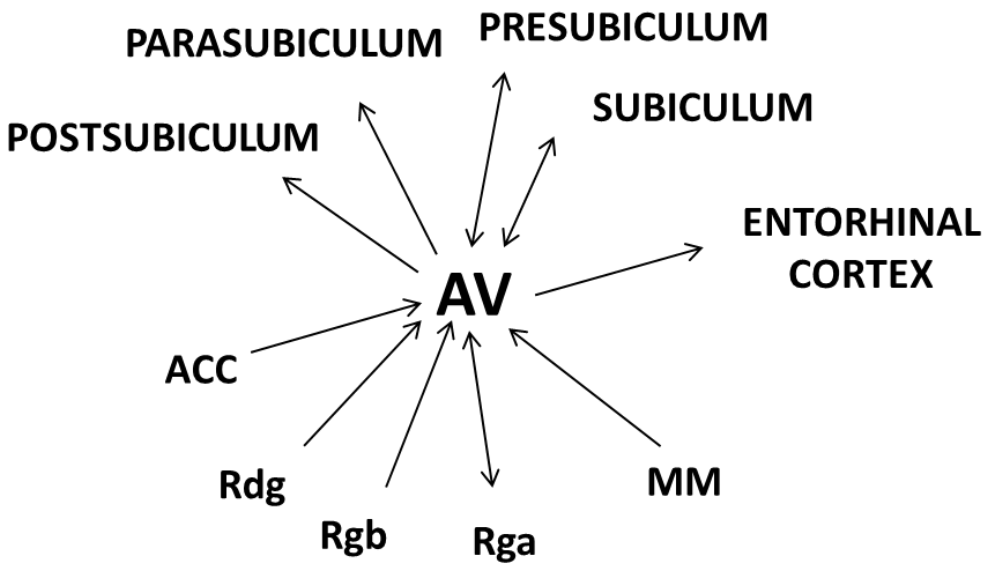

Figure 1-5. Diagram of some input/output connections of the anteroventral thalamic nuclei (AV).Only a selection of areas relevant for the current piece of work is reported. The arrows indicate if the connections are afferent, efferent or reciprocal. ACC = anterior cingulate cortex; MM = medial mammillary nuclei; Rdg = dysgranular retrosplenial subregion; Rga = granular retrosplenial subregion a; Rgb = granular retrosplenial subregion b.

Connections with the hippocampal formation

As previously described (Section 1.1.1), the anterior thalamic nuclei receive dense inputs from the hippocampal formation through the fornix. Both the anteroventral and anteromedial thalamic nuclei are innervated by the subiculum, but their inputs originate from distinct subicular populations (Dillingham, Erichsen, et al., 2015; Wright et al., 2013). The presubiculum projects to the anteroventral thalamic nuclei (Van Groen & Wyss, 1990b) while the parasubiculum targets the anterodorsal thalamic nuclei (Van Groen & Wyss, 1990b). The postsubiculum projections to the anterodorsal thalamic nuclei are carried via the internal capsule (Dillingham, Erichsen, et al., 2015). Finally, the entorhinal cortex sends sparse fibres mainly to the anteromedial thalamic nuclei (Wright et al., 2010).

The anterior thalamic nuclei send return projections back to the hippocampal formation through the cingulum bundle (Shibata, 1993a). All three anterior thalamic nuclei send outputs to the entorhinal cortex. Both the anteromedial and anteroventral thalamic nuclei project to the subiculum, while both the anterodorsal and anteroventral thalamic nuclei send fibres to the presubiculum and parasubiculum (Shibata, 1993a; Van Groen & Wyss, 1990b). The postsubiculum is the target of dense connections

from the anterodorsal thalamic nuclei and lighter connections from the anteroventral thalamic nuclei (Van Groen & Wyss, 1990c).

Connections with the mammillary bodies

The anterior thalamic nuclei receive dense inputs from the mammillary bodies via the mammillothalamic tract. Specifically, the anterodorsal thalamic nuclei are the target of bilateral projections from the lateral mammillary nuclei, while the anteromedial and anteroventral thalamic nuclei are reached by fibres from the ipsilateral medial mammillary nuclei (Cruce, 1975). The connections from the mammillary bodies to the anterior thalamic nuclei are topographically organised, and distinct portions of the medial mammillary nuclei target either the anteromedial or the anteroventral thalamic nuclei (Shibata, 1992) (further detail given in Section 1.1.3.1).

Connections with the other subcortical structures

The laterodorsal tegmental nucleus projects to both the anteroventral and anteromedial thalamic nuclei, providing a strong cholinergic input (Shibata, 1992; Wright et al., 2013). The caudo-dorsal portion of the thalamic reticular nucleus projects to both the anteroventral and anterodorsal thalamic nuclei, while its rostro-dorsal portion targets the anteromedial thalamic nuclei (Shibata, 1992).

Connections with the retrosplenial cortex

The anterior thalamic nuclei are densely connected with the retrosplenial cortex through the cingulum bundle. These connections are topographically organised, linking specific thalamic nuclei to specific subregions of the retrosplenial cortex (further detail given in Section 1.1.4.1).

Connections with other cortical areas

All three anterior thalamic nuclei receive projections from the anterior cingulate cortex, and for the anteromedial and anteroventral thalamic nuclei these projections are reciprocal (Shibata & Kato, 1993; Shibata & Naito, 2005; Shibata, 1993b). Both the anteromedial and the anteroventral thalamic nuclei are reciprocally connected with the agranular medial cortex (Shibata & Naito, 2005). In addition, the anteromedial thalamic nuclei are reciprocally connected with the prelimbic cortex, and send fibres to the infralimbic and perirhinal cortices and to visual area 18b (Shibata, 1993a; Van Groen, Kadish, & Wyss, 1999).

1.1.3 The mammillary bodies

The mammillary bodies are part of the medial diencephalon and are located in the caudal portion of the hypothalamus. They are delimited rostrally by the premammillary nuclei, dorsally by the supramammillary nucleus, and laterally and ventrally by the tuberomammillary nucleus (Allen & Hopkins, 1988). The mammillary bodies are subdivided into two pairs of bilateral and symmetrical nuclei (Figure 1-6): two larger medial mammillary nuclei and two smaller lateral mammillary nuclei located in the anterior two thirds of the structure and flanking the medial nuclei.

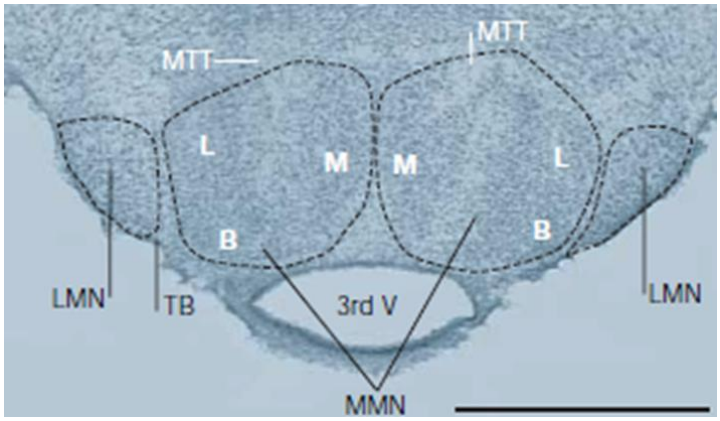

Figure 1-6. Nissl-stained coronal section of the rat mammillary bodies. The cytoarchitectonic divisions are indicated. 3rd V = third ventricle; B = pars basalis; L = pars lateralis; M = Pars medialis; LMN = lateral mammillary nuclei; MMN = medial mammillary nuclei; MTT = mammillothalamic tract; TB = tuberomammillary nucleus. Scale bar 1 mm. Figure adapted from Vann & Aggleton (2004).

The neurones in the mammillary bodies are small to medium in size, and those located in the lateral mammillary nuclei are larger than those found in the medial mammillary nuclei. In the rodent, no interneurones have been found within the mammillary bodies, and all neurones are projection neurones (Allen & Hopkins, 1988). However, interneurones have been reported in the human mammillary bodies (Dixon et al., 2004). On the basis of cytoarchitectural properties and organisation of connections with other brain areas, the medial mammillary nuclei have been further divided into smaller subnuclei, from three to six (Allen & Hopkins, 1988; Gurdjian, 1927; Krieg, 1932; Seki & Zyo, 1984), with pars medialis, pars lateralis and pars basalis being the most common subdivisions (Vann, 2010).

1.1.3.1 Connectivity of the mammillary bodies

The mammillary bodies have limited connections with other brain structures; the main connections are the inputs from the hippocampal formation, the outputs to the anterior thalamic nuclei and the reciprocal connections with the tegmental nuclei of Gudden (Figure 1-7).

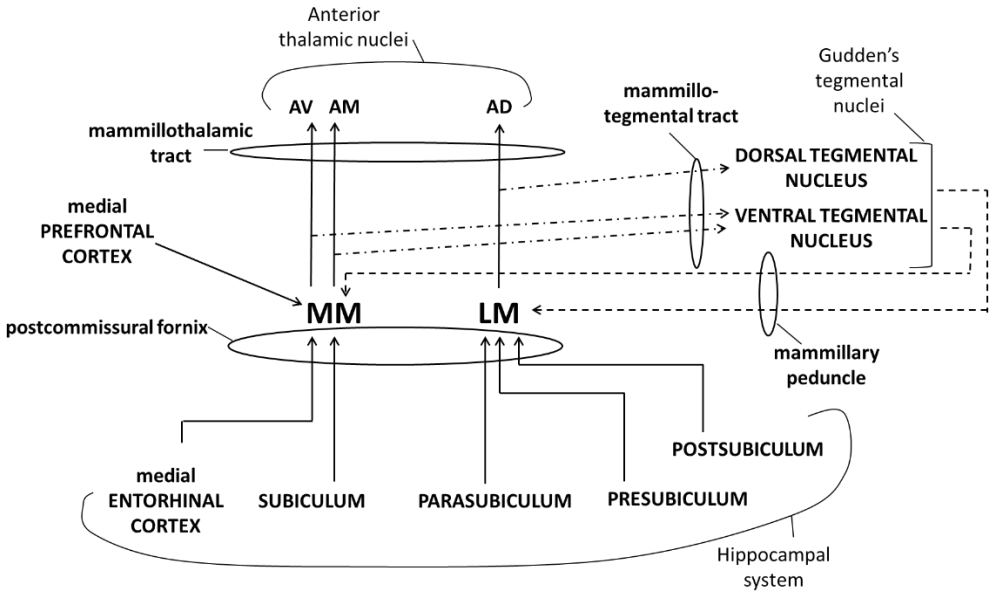

Figure 1-7. Diagram of the main input/output connections of the mammillary bodies. The arrows indicate if the connections are afferent or efferent. AD = anterodorsal thalamic nuclei; AM = anteromedial thalamic nuclei; AV = anteroventral thalamic nuclei; LM = lateral mammillary nuclei; MM = medial mammillary nuclei.

Connections with the hippocampal formation

The hippocampal formation sends its projections to the mammillary bodies via the descending columns of the postcommissural fornix (Vann et al., 2011; Vann, 2013). The medial mammillary nuclei receive dense inputs from both the dorsal and ventral subiculum and from the medial entorhinal cortex, while the lateral mammillary nuclei are targeted by the presubiculum, parasubiculum and postsubiculum (Allen & Hopkins, 1989; Shibata, 1988; Van Groen & Wyss, 1990c; Wright et al., 2010). The connections from the hippocampal formation to the mammillary bodies have shown to be excitatory, releasing glutamate, aspartate and neurotensin (Kiyama et al., 1986; Storm-Mathisen & Woxen Opsahl, 1978).

Connections with the anterior thalamic nuclei

The mammillary bodies send projections to the anterior thalamic nuclei via the mammillothalamic tract, which emerges as the ascending branch of the principal mammillary tract. The same neurones in the mammillary bodies have been shown to send axon collaterals to both the anterior thalamic nuclei via the mammillothalamic tract and to the midbrain via the mammillotegmental tract (see next Section and Takeuchi, Allen, & Hopkins, 1985). As already mentioned, the lateral mammillary nuclei project bilaterally to the anterodorsal thalamic nuclei, while the medial mammillary nuclei send unilateral projections to the anteromedial and anteroventral thalamic nuclei (Cruce, 1975); specifically, the medial portions of the medial mammillary nuclei send ipsilateral projections to the anteromedial thalamic nuclei, while the lateral portions ipsilaterally target the anteroventral thalamic nuclei (Shibata, 1992). All these projections are excitatory, releasing glutamate and aspartate as the main neurotransmitters (Gonzalo-Ruiz, Morte, & Sanz, 1998).

Connections with Gudden's tegmental nuclei

Gudden's tegmental nuclei are located in the midbrain and are divided into a dorsal and a ventral nucleus. The mammillary bodies send projections to these nuclei via the mammillotegmental tract, which emerges as the descending branch of the principal mammillary tract (Allen & Hopkins, 1990). In particular, the medial mammillary nuclei target Gudden's ventral tegmental nucleus, while the lateral mammillary nuclei target Gudden's dorsal tegmental nucleus (Cruce, 1977). The tegmental nuclei of Gudden send return projections to the mammillary bodies via the mammillary peduncle: the ventral tegmental nucleus of Gudden sends afferents to the medial mammillary nuclei, while the dorsal nucleus projects to the lateral mammillary nuclei (Allen & Hopkins, 1989). The tegmental afferents to the mammillary bodies are inhibitory, i.e. they release GABA or leu-enkephalin (Gonzalo-Ruiz, Alonso, Sanz, & Llinas, 1992; Gonzalo-Ruiz, Romero, Sanz, & Morte, 1999); a large proportion of neurones in Gudden's ventral tegmental nucleus that project to the mammillary bodies are parvalbuminergic (Dillingham, Holmes, et al., 2015).

Connections with other subcortical structures

The mammillary bodies receive inputs from the septal nuclei, with the medial septal nucleus and the nucleus of the diagonal band of Broca projecting to the medial mammillary nuclei, while the lateral septal nucleus sends connections to the lateral mammillary nuclei (Swanson & Cowan, 1979). Within the hypothalamic area, both the medial and lateral mammillary nuclei receive afferents from the supramammillary and

tuberomammillary nuclei, and the medial mammillary nuclei project back to the supramammillary nucleus (Gonzalo-Ruiz et al., 1992); the afferents from the supramammillary nucleus to the mammillary bodies are dopaminergic (Gonzalo-Ruiz et al., 1992). Finally, both the lateral and medial mammillary nuclei send, via the mammillotegmental tract, non-overlapping projections to the tegmental reticular nucleus and the median pontine nuclei (Allen & Hopkins, 1990; Cruce, 1977); these latter nuclei are reciprocally connected with the cerebellum (Allen & Hopkins, 1990).

Connections with other cortical areas

The medial mammillary nuclei are innervated by the medial prefrontal cortex; the largest projections comes from the infralimbic cortex, with lighter projections originating from the prelimbic and anterior cingulate areas (Allen & Hopkins, 1989). Finally, the granular retrosplenial cortex subregions a and b (Rga and Rgb) send very light projections to the mammillary bodies (Wright et al., 2010).

1.1.4 The retrosplenial cortex

The retrosplenial cortex is included in the posterior portion of the cingulate cortex, extending around the splenium of the corpus callosum, as the name “retrosplenial” suggests. It comprises Brodmann’s areas (BA) 29 and 30.

In primates, it is located deep in the cerebral cortex, along the midline, and with BA 23 and 31 (which are exposed on the surface of the gyrus) forms the caudal portion of the posterior cingulate cortex (Sugar, Witter, Strien, & Cappaert, 2011; Vann, Aggleton, & Maguire, 2009; Vogt, Vogt, & Farber, 2004).

There is not an exact match between the primate and the rodent posterior cingulate cortex (Vogt et al., 2004). In the rodent brain there is no cingulate sulcus, so the cingulate gyrus is not present; as there are no equivalent areas 23 and 31, the retrosplenial cortex makes up the whole posterior cingulate cortex (Vann et al., 2009; Vogt et al., 2004; Vogt & Peters, 1981). Thus, in rodents, the retrosplenial cortex extends over a considerable portion of the brain, stretching along the rostro-caudal axis from the anterior border of the hippocampus to almost the cerebral posterior extremity (Vann et al., 2009).

In rats, the retrosplenial cortex has been divided into different subregions, on the basis of changes in cytoarchitectonic properties. Different nomenclatures are used in the literature. Wyss & Van Groen (1992) divided it into a dysgranular (Rdg) and two

granular (Rga and Rgb) subregions (Figure 1-8). Other authors, such as Vogt & Peters (1981), adopted a different (but partially overlapping) partition of the retrosplenial cortex, subdividing it into four areas: they defined the dysgranular retrosplenial cortex (Rdg) as area 29d (Vogt & Peters, 1981) or 30 (B. A. Vogt et al., 2004), while the granular retrosplenial cortex was parcellated into areas 29a, 29b and 29c (area 29c equivalent to Rgb, while areas 29a and 29b equivalent to Rga; Van Groen & Wyss, 2003). In the present thesis, the nomenclature adopted by Wyss & Van Groen (1992) will be used, to provide direct comparisons with previous studies using the same nomenclature (e.g. Vann & Albasser, 2009).

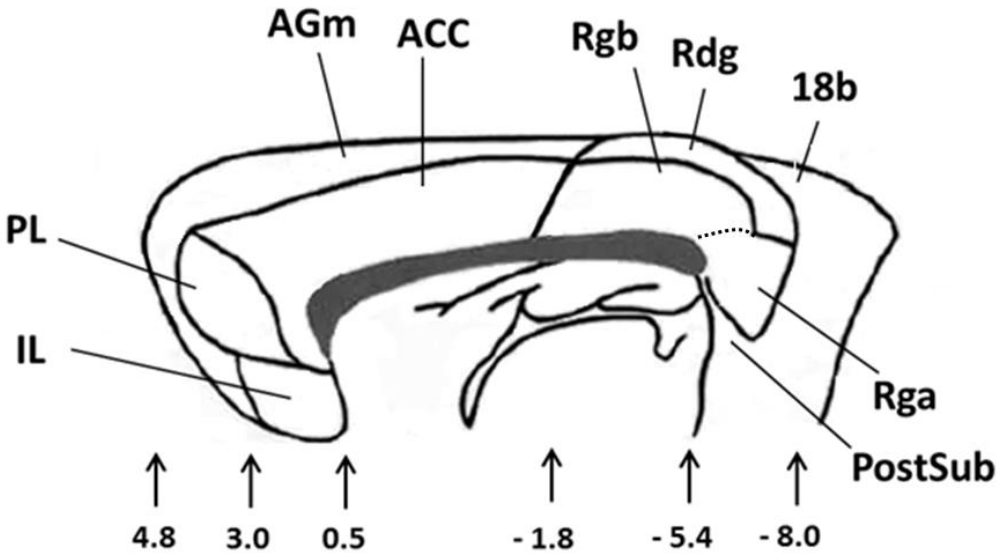

Figure 1-8. Schematic drawing of the sagittal view of the rat brain (rostral extremity on the left), showing some main areas, including the retrosplenial cortex and its main subregions Rdg, Rgb and Rga. 18b = visual area, ACC = anterior cingulate cortex; AGm = agranular medial cortex; IL = infralimbic cortex; PL = prelimbic cortex; PostSub = postsubiculum. The number indicates the approximate antero-posterior level at the arrow point. Figure adapted from Vogt et al. (2004).

Rdg shares its borders with the agranular motor cortex, visual area 18b, Rgb and Rga. Rgb is bordered by Rdg, Rga, the corpus callosum, the anterior cingulate cortex and the agranular motor cortex (Wyss & Van Groen, 1992). Rga shares its boundaries with Rgb, Rdg, the postsubiculum and the corpus callosum (Wyss & Van Groen, 1992). A characteristic cytoarchitectural feature of Rdg is the lack of a properly formed internal granular layer IV (Van Groen & Wyss, 1992). Layer II in Rga is narrower than

Rgb and its neurones appear larger; furthermore, layer VI, which is present in Rdg and Rgb is almost absent in Rga (Van Groen & Wyss, 2003).

Along the antero-posterior axis, Rgb and Rdg can be separated into a rostral portion (anterior to the splenium of the corpus callosum), and a caudal portion (posterior to the splenium). Rga is only present caudally (Pothuizen, Davies, Albasser, Aggleton, & Vann, 2009).

1.1.4.1 Connectivity of the retrosplenial cortex

The connections of the three subregions of the retrosplenial cortex are reported below (Figure 1-9, Figure 1-10 and Figure 1-11). The connected areas have been divided into three groups on the basis of their anatomical location (cortical or subcortical) or whether they belong to the hippocampal formation. The connectivity reported below is based on the studies by Shibata, Kondo, & Naito (2004), Van Groen & Wyss (1990a, 2003, 1992) and Wyss & Van Groen (1992), unless otherwise stated.

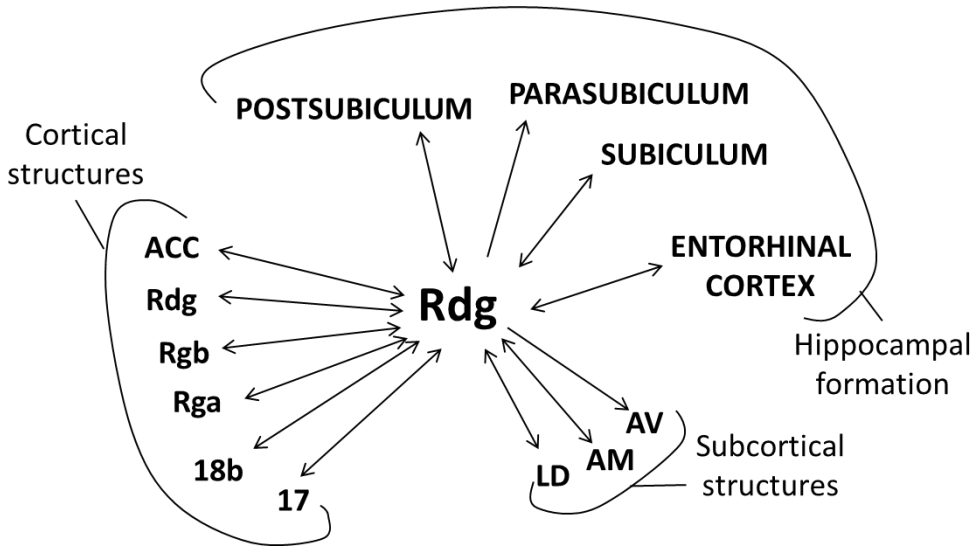

Figure 1-9. Diagram of some input/output connections of the retrosplenial subregion Rdg. Only a selection of areas relevant for the current piece of work is reported. The arrows indicate if the connections are afferent, efferent or reciprocal. 17 = visual area 17; 18b = visual area 18b; ACC = anterior cingulate cortex; AM = anteromedial thalamic nuclei; AV = anteroventral thalamic nuclei; LD = laterodorsal thalamic nuclei.

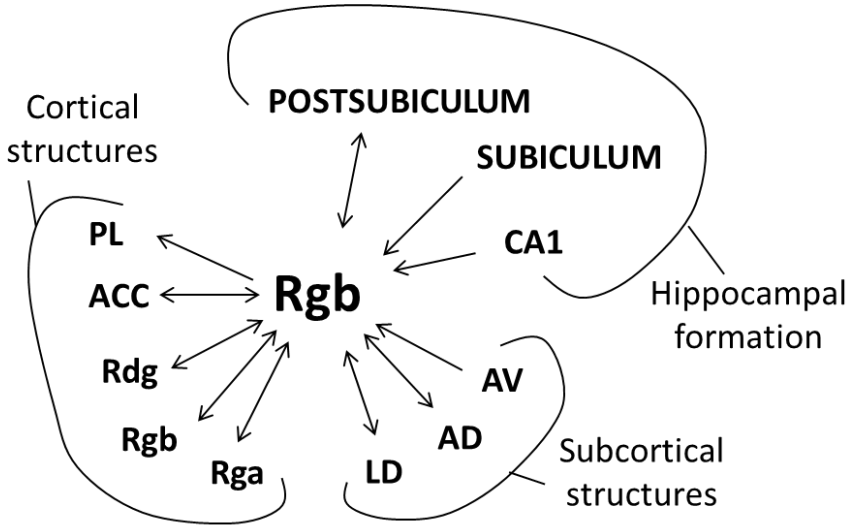

Figure 1-10. Diagram of some input/output connections of the retrosplenial subregion Rgb. Only a selection of areas relevant for the current piece of work is reported. The arrows indicate if the connections are afferent, efferent or reciprocal. ACC = anterior cingulate cortex; PL = prelimbic cortex; AD = anterodorsal thalamic nuclei; AV = anteroventral thalamic nuclei; LD = laterodorsal thalamic nuclei.

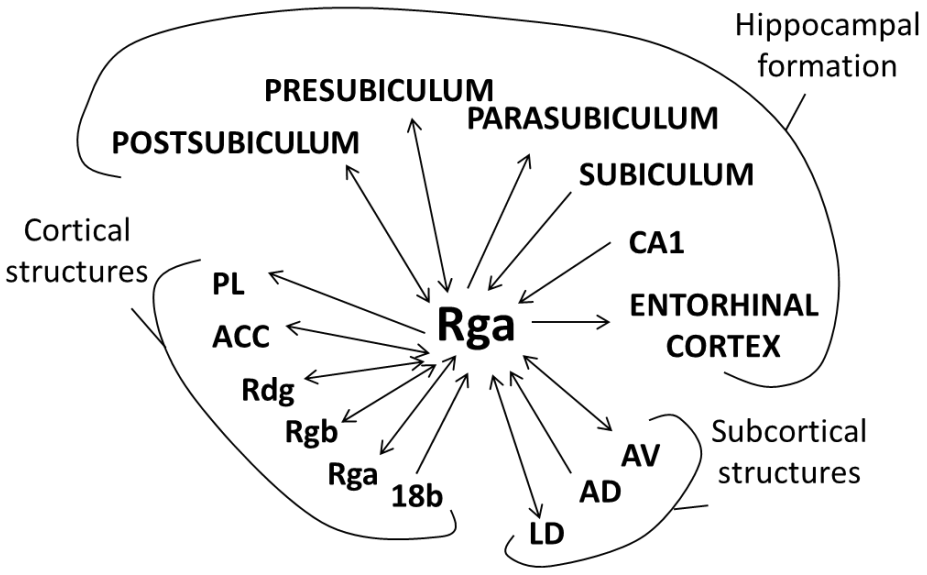

Figure 1-11. Diagram of some input/output connections of the retrosplenial subregion Rga. Only a selection of areas relevant for the current piece of work is reported. The arrows indicate if the connections are afferent, efferent or reciprocal. 18b = visual area 18b; ACC = anterior cingulate cortex; PL = prelimbic cortex; AD = anterodorsal thalamic nuclei; AV = anteroventral thalamic nuclei; LD = laterodorsal thalamic nuclei.

Connections with the hippocampal formation

All three retrosplenial subregions have reciprocal connections with the postsubiculum. In addition, Rdg is reciprocally connected with the entorhinal cortex and subiculum, while Rga is reciprocally connected with the presubiculum and sends efferents to the entorhinal cortex. Both Rdg and Rga send outputs to the parasubiculum. Both Rgb and Rga receive afferents from the hippocampal subfield CA1 and the subiculum.

Connections with the anterior thalamic nuclei

The retrosplenial cortex has dense connections with the anterior thalamic nuclei. Rdg is reciprocally connected with the anteromedial thalamic nuclei, Rgb with the anterodorsal thalamic nuclei, and Rga with the anteroventral thalamic nuclei. Furthermore, Rdg projects to the anteroventral thalamic nuclei while Rgb is innervated by the anteroventral thalamic nuclei (Wright et al., 2013). Rga also receives inputs from the anterodorsal thalamic nuclei.

Connections with other subcortical structures

The laterodorsal thalamic nuclei have reciprocal connections with all the three retrosplenial subregions, but especially dense with Rdg (Van Groen & Wyss, 1992). Both Rdg and Rga are reciprocally connected to the reuniens thalamic nucleus. All three subregions project to the thalamic reticular nucleus, the superior colliculus and the ventral pontine nuclei. Both Rdg and Rgb project to the periaqueductal gray. Rdg projects also to the caudate/putamen and zona incerta. All three subregions are innervated by the claustrum but for Rgb this connection is reciprocal. All three subregions receive inputs from the diagonal band of Broca, midbrain raphe nuclei and locus coeruleus. Rdg and Rgb also receive projections from the medial septal nucleus.

Connections with other cortical areas

All three retrosplenial subregions are reciprocally connected with the anterior cingulate cortex. Rdg is also reciprocally connected with visual cortical areas 17 and 18b and projects to the perirhinal cortex and the orbital and agranular medial cortices. Rgb and Rga send light projections to the prelimbic cortex. Rgb projects to both agranular medial and agranular lateral cortex. Rga receives inputs from area 18b. All three retrosplenial cortex subregions have dense intrinsic connections, including connections with their contralateral counterparts.

1.1.5 The anterior cingulate cortex

The anterior cingulate cortex is part of the dorsal portion (together with the agranular medial cortex; Figure 1-8) of the rat medial prefrontal cortex (Vertes, 2004). The anterior cingulate connections that are relevant for this thesis are reported here. The anterior cingulate cortex receives projections from the anteromedial thalamic nuclei (Shibata, 1993b), and it is reciprocally connected with all subregions within the retrosplenial cortex (Wyss & Van Groen, 1992). No afferents have been reported from the hippocampal formation (Jay, Glowinski, & Thierry, 1989).

1.1.6 The prelimbic and the infralimbic cortex

Both prelimbic and infralimbic cortices constitute the ventral portion of the rat medial prefrontal cortex (Figure 1-8). The connections of these areas with other brain structures relevant for this thesis are reported here. Both the infralimbic and prelimbic cortices send their projections to the anteromedial thalamic nuclei (Vertes, 2004), and the anterior medial nuclei send projections back to the prelimbic cortex (Conde', Audinat, Maire-Lepoivre, & Crepel, 1990). The ventral CA1 subfield and subiculum send projections to both the infralimbic and prelimbic cortices (Chudasama, Doobay, & Liu, 2012; Jay et al., 1989; Jay & Witter, 1991). Finally the prelimbic cortex receives light projections from the retrosplenial subregions Rgb and Rga (Shibata et al., 2004; Van Groen & Wyss, 2003).

1.1.7 Systems within the Papez circuit

As previously described, there are distinct patterns of connectivity within the Papez circuit. Furthermore, some of these connected structures share some electrophysiological properties. These observations have led to the proposal of the presence of three different parallel systems with distinct functionalities embedded within the same general circuit, each one relying on a specific component of the anterior thalamus (Aggleton & Nelson, 2014; Aggleton et al., 2010; Vann & Aggleton, 2004b).

1.1.7.1 The "head-direction" system (anterior dorsal thalamic nuclei)

This system includes areas that contains "head-direction" neurones, i.e. cells that fire only when the animal is facing a specific direction on the horizontal plane regardless of its actual position (Taube, Muller, & Ranck, 1990). These particular neurones have been found in different structures either within the Papez circuit or connected with it: the dorsal Gudden's tegmental nucleus (P. E. Sharp, Tinkelman, & Cho, 2001), the lateral mammillary nuclei (Blair, Cho, & Sharp, 1998), the anterodorsal thalamic nuclei (Taube, 1995), the postsubiculum (Taube et al., 1990), the laterodorsal thalamic nuclei and the retrosplenial cortex (Chen, Green, Barnes, & McNaughton, 1994). The connectivity of these structures is shown in Figure 1-12.

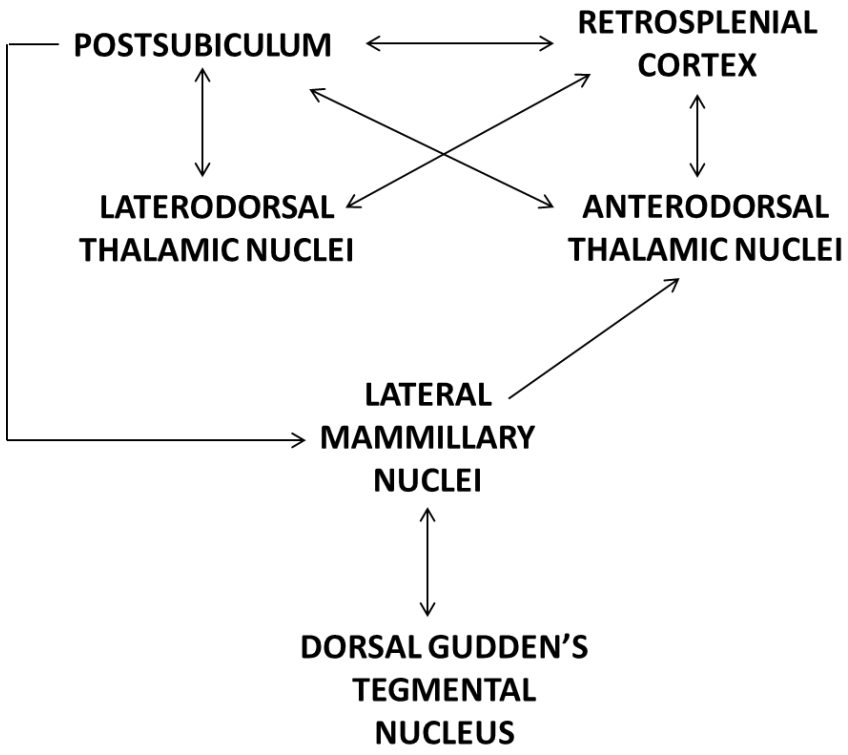

Figure 1-12. Diagram of the "head-direction" system.

If the lateral mammillary nuclei are lesioned, the head-direction neurones in the anterodorsal thalamic nuclei (Blair et al., 1998), postsubiculum and retrosplenial cortex (P. E. Sharp & Koester, 2008) lose their direction-firing properties. The influence the lateral mammillary nuclei have on the rest of the head-direction system has been shown to depend on the integrity of its inputs from Gudden's dorsal tegmental nucleus, which provides vestibular information to the system (Bassett, Tullman, & Taube, 2007).

1.1.7.2 The "return-loop" system (anteroventral thalamic nuclei)

The information that reaches the anterior thalamic nuclei from the hippocampal formation (subiculum and presubiculum), the retrosplenial cortex and the medial mammillary nuclei is conveyed back to the hippocampal formation by the anteroventral thalamic nuclei, which send their projections to the entorhinal cortex and the subicular complex (see Figure 1-5). Studies have found that within the medial mammillary nuclei (Kocsis & Vertes, 1994), the anteroventral thalamic nuclei (Vertes, 2004), the entorhinal cortex (Mitchell & Ranck, 1980), the subiculum (Jackson, Goutagny, & Williams, 2011) and the retrosplenial cortex (Borst, Leung, & MacFabe, 1987; Foster, Kaveh, Dastjerdi, Miller, & Parvizi, 2013) there are cells whose discharge is synchronised with the hippocampal theta rhythm. Theta rhythm is a large oscillatory (4-12 Hz) electrical brain signal and it has been implicated in memory and spatial processing (Burgess & O'Keefe, 2011; Vertes, 2005). Theta rhythm in the medial mammillary nuclei is at least partially driven by the activity in CA1 hippocampal subfield, conveyed mainly through the subiculum (Kocsis & Vertes, 1994). It has been suggested that theta-frequency neuronal activity modulated by the medial mammillary nuclei would be transmitted back to the hippocampus through a return-loop comprising the anteroventral thalamic nuclei, subicular, retrosplenial and entorhinal cortices (Kirk & Mackay, 2003). Gudden's ventral tegmental nucleus also has neurones that fire at theta rhythm and this rhythmicity in facts precedes theta activity in the hippocampus (Bassant & Poindessous-Jazat, 2001); this had led to the suggestion that, via its connections with the mammillary bodies, the ventral tegmental nucleus of Gudden may modulate the frequency of hippocampal theta (Kocsis, Di Prisco, & Vertes, 2001).

1.1.7.3 The "feed-forward" system (anteromedial thalamic nuclei)

As previously mentioned (see Figure 1-4), the anteromedial thalamic nuclei are reciprocally connected with both the anterior cingulate and the prelimbic cortices, and also send their input forward to the infralimbic cortex. No head-direction cells have been reported in the anteromedial thalamic nuclei, and the number of theta-frequency firing neurones is less than 6% (Albo, Di Prisco, & Vertes, 2003). Thus, given their anatomical connections, it is possible that these thalamic nuclei have a role in conveying the signal integrated from the hippocampal formation, the medial

mammillary nuclei and the dysgranular retrosplenial cortex onto prefrontal areas (Aggleton et al., 2010).

1.2 Diencephalic amnesia in humans

This thesis will focus on the effects of diencephalic lesions in rats. However, it is important to mention studies in patients in order to appreciate the importance that the diencephalon and other connected structures of the Papez circuit have in supporting episodic memory. Thus, if not otherwise specified, the following sections will report results from clinical patients with lesions within the different components of the Papez circuit.

1.2.1 Diencephalic amnesia

Diencephalic amnesia is a memory impairment associated with medial diencephalic damage, and the core feature is a severe anterograde amnesia (Graff-Radford, Tranel, Van Hoesen, & Brandt, 1990; Kopelman, 2015; Winocur, Oxbury, Roberts, Agnetti, & Davis, 1984); anterograde amnesia reflects an inability to acquire new memories and episodic (i.e. event) memories are the most commonly compromised. The memory impairment is typically selective and other components of learning and memory, such as short-term memory (i.e. digit span), procedural learning and priming appear normal (Graff-Radford et al., 1990; Warrington & Weiskrantz, 1982). While anterograde amnesia is always present there is less consistency in terms of whether memories prior to the onset of amnesia are affected (Graff-Radford et al., 1990). Studies involving patients with diencephalic amnesia have attempted to identify the critical sites of pathology within the medial diencephalon, however, as damage typically spreads across more than one nucleus and can also involve white matter pathways, there is still some degree of uncertainty.

Diencephalic amnesia can be associated with different pathologies. The two main ones are Korsakoff's syndrome and lacunar infarcts in the thalamus, although suprasellar tumours (e.g. Naggara, Varlet, Page, Oppenheim, & Meder, 2005) and intranasal penetrating injuries (e.g. Dusoir, Kapur, Byrnes, McKinstry, & Hoare, 1990) can also be a cause of diencephalic amnesia.

Korsakoff's syndrome was first described by the Russian clinician S.S. Korsakoff in 1887 as a disturbance associated with alcoholism (Victor & Yakovlev, 1955). Subsequently, it was established that the syndrome is caused by nutritional

deficiency, in particular the lack of thiamine or vitamin B1 (Kopelman, 2002). Korsakoff's syndrome is associated with a severe anterograde amnesia, and often retrograde memory impairments and confusion in reporting temporal sequences of events. This amnestic disorder is usually preceded by Wernicke's encephalopathy, the symptoms of which are confusion, ataxia, nystagmus and ophtalmoplegia; at this stage the condition is still reversible if the patient is treated early with a high-dose of thiamine. The atrophy of the mammillary bodies, and more specifically the medial mammillary nuclei, characterises patients affected by Wernicke's encephalopathy (Sheedy, Lara, Garrick, & Harper, 1999) and/or Korsakoff's syndrome (Mair, Warrington, & Weiskrantz, 1979; Mayes, Meudell, Mann, & Pickering, 1988). However, as there are cases with Wernicke's encephalopathy without anterograde amnesia (Davila, Shear, Lane, Sullivan, & Pfefferbaum, 1994; Harding, Halliday, Caine, & Kril, 2000) the argument has been that lesions of the mammillary bodies are not sufficient to account for the memory impairments typical of Korsakoff's syndrome. Some studies have reported other components of the diencephalon to be consistently associated with the syndrome, most notably the anterior thalamic nuclei (Harding et al., 2000) or the medial dorsal thalamic nucleus (Victor, Adams, & Collins, 1989), even if the involvement of the latter structure has not always been confirmed (Mair et al., 1979; Mayes et al., 1988). There is additional complexity in localising the critical sites of pathology in Korsakoff's syndrome because in many patients there is damage beyond the medial diencephalon, affecting both grey and white matter structures; for example the frontal lobes have been reported to be atrophic (Colchester et al., 2001) and this could account for the frontal symptoms exhibited by some patients (Kopelman, 1991).

Diencephalic vascular amnesia is usually caused by the occlusion of the tuberothalamic and/or the paramedian arteries, which supply blood to the anterior and medial portions of the thalamus (Schmahmann, 2003). Clinical studies have found that the mammillothalamic tract is the structure where damage is most consistently associated with vascular diencephalic amnesia (Carlesimo, Lombardi, & Caltagirone, 2011; Graff-Radford et al., 1990; Mori, Yamadori, & Mitani, 1986; Van der Werf et al., 2000; von Cramon, Hebel, & Schuri, 1985).

1.2.2 Comparison with medial temporal lobe amnesia

The more well-known cause of anterograde amnesia is the pathology within the medial temporal lobes, most typically involving the hippocampus and surrounding parahippocampal regions; this is referred to as temporal lobe amnesia (Insausti, Annese, Amaral, & Squire, 2013; Scoville & Milner, 1957). Diencephalic and temporal lobe amnesias are considered by some to be the same dysfunction caused by damage to a common system, the Papez circuit, which includes both the medial diencephalon and the hippocampal formation (e.g. Aggleton & Saunders, 1997; Aggleton, 2008), while others have suggested they are two different forms of amnesias caused by damage to anatomically distinct brain structures (Parkin, 1984; Squire, 1981). Support for this last view arises from two observations of qualitative differences between diencephalic and temporal lobe amnesia. The first observation is that some patients with temporal lobe amnesia have faster forgetting rates than those with diencephalic amnesia, suggesting that hippocampal lesions cause a deficit in memory consolidation/retention, while diencephalic damage disrupts memory acquisition (Huppert & Piercy, 1979; Squire, 1981). However, further studies have systematically failed to replicate this finding in other patients with temporal lobe amnesia (Freed, Corkin, & Cohen, 1987; McKee & Squire, 1992). The second observation is that some patients affected by diencephalic amnesia appear worse than patients with temporal lobe amnesia in using temporal contextual information (Hunkin & Parkin, 1993; Kopelman, Stanhope, & Kingsley, 1997; Parkin, Leng, & Hunkin, 1990). All those diencephalic patients, however, were affected by Korsakoff's syndrome, thus, as already mentioned, with a high probability of having prefrontal in addition to diencephalic damage (Colchester et al., 2001; Kopelman, 2015). Damage to prefrontal areas is sufficient to cause impairments in temporal contextual tasks (Kopelman et al., 1997), thus it is not possible to conclude that the deficit was caused by diencephalic damage *per se*. Profound temporal memory impairments have also been reported in a patient with more selective mammillary body pathology (Hildebrandt, Müller, Bussmann-Mork, Goebel, & Eilers, 2001) but further research is needed to assess whether these dissociations between diencephalic and temporal anterograde amnesia do, in fact, exist.

Finally, a further indication that the medial diencephalon and the hippocampal formation work as an integrated circuit in supporting episodic memory is provided by studies of patients with lesions of the fornix, one of the main connections between the

two structures. After some initial reports suggesting the fornix is not crucial for supporting memory (Garcia-Bengochea & Friedman, 1987; Woolsey & Nelson, 1975), many subsequent studies have instead shown fornix lesions to be associated with anterograde amnesia (Aggleton et al., 2000; D'Esposito, Verfaellie, Alexander, & Katz, 1995; Gaffan & Gaffan, 1991; Gaffan, Gaffan, & Hodges, 1991; Hodges & Carpenter, 1991; Poreh et al., 2006; Tsivilis et al., 2008; Vann et al., 2008). However, as previously discussed (Section 1.1.1.1), the fornix carries numerous projections in addition to those between the hippocampus and medial diencephalon, and it is not clear from these studies which projections are key in supporting memory function.

1.2.3 Theories of diencephalic amnesia

There have been different accounts proposed as to why damage to the diencephalic region results in memory impairments (Vann & Albasser, 2009):

(1) Medial diencephalic damage disconnects the hippocampal formation from the frontal cortex (Warrington & Weiskrantz, 1982).

(2) Medial diencephalic damage disconnects the hippocampal formation from the cingulate cortex (Aggleton & Brown, 1999; Delay & Brion, 1969). This theory is supported by the marked cingulate hypoactivity observed in patients with diencephalic damage (see Section 1.2.4).

(3) Medial diencephalic damage disconnects the hippocampal formation from both the frontal cortex and the cingulate cortex, with a widespread effect on cortical activity (Mair et al., 1979; Paller, 1997; Vann & Aggleton, 2004b), i.e. a combination of both (1) and (2).

(4) Medial diencephalic damage disconnects the ascending projections from the midbrain from reaching cortical and medial temporal lobe regions (Kocsis et al., 2001; Vann & Nelson, 2015; Vann, 2009).

(5) Medial diencephalic damage causes amnesia independently from the disconnection of the hippocampal formation (Parkin, 1984; Squire, 1981). From this hypothesis it is assumed that diencephalic and medial temporal lobe amnesia are substantially different memory disorders (even if they both give rise to a severe anterograde amnesia).

As already discussed in Section 1.2.2, there has been limited support for Theory (5) as no consistent differences have been found between the profiles of medial diencephalic and medial temporal lobe amnesia. Furthermore, the finding that the integrity of the fornix (the major tract connecting the hippocampal formation to the medial diencephalon) is necessary for supporting episodic memory in humans (Aggleton et al., 2000; D'Esposito, Verfaellie, Alexander, & Katz, 1995; Gaffan & Gaffan, 1991; Gaffan, Gaffan, & Hodges, 1991; Hodges & Carpenter, 1991; Poreh et al., 2006; Tsivilis et al., 2008; Vann et al., 2008) and spatial memory in rats (Aggleton, Neave, Nagle, & Hunt, 1995; Aggleton, Neave, Nagle, & Sahgal, 1995; Aggleton, Poirier, Aggleton, Vann, & Pearce, 2009; Becker, Walker, & Olton, 1980; Bussey, Duck, Muir, & Aggleton, 2000; Cassel et al., 1998; Markowska, Olton, Murray, & Gaffan, 1989; Neave, Nagle, & Aggleton, 1997; Shaw & Aggleton, 1993; Vann et al., 2011; Sziklas & Petrides, 2002; Warburton, Baird, & Aggleton, 1997; Warburton et al., 2000; Warburton, Aggleton, & Muir, 1998; Warburton & Aggleton, 1999) has been taken as evidence against this theory. Finally, cross-lesions of the anterior thalamic nuclei and either the fornix or the hippocampus produce memory impairments, again suggesting these regions works together to support memory (Henry, Petrides, St-Laurent, & Sziklas, 2004; Warburton, Baird, Morgan, Muir, & Aggleton, 2000, 2001) (see Section 1.3.4.7).

Theories (1), (2) and (3) consider diencephalic amnesia to be a disconnection syndrome due to the loss of indirect hippocampal efferents to the rest of the brain. However, as reported in Section 1.2.1, damage to the mammillothalamic tract has been most consistently associated with vascular diencephalic amnesia. Even in the presence of mammillothalamic tract damage, the direct hippocampal projections to the anterior thalamic nuclei are still intact as well as the direct projections from the hippocampal formation to the frontal and cingulate cortices.

Evidence for the most recent Theory (4) comes from studies in rats that showed the most important mammillary body inputs, in terms of supporting spatial memory, arose from the midbrain rather than the hippocampal formation (Vann, 2013) (see Section 1.3.3.3). This provides a role for the medial diencephalon that is independent of its hippocampal inputs and, in contrast to earlier models, it highlights the importance of the projections from the medial diencephalon to the hippocampal formation.

1.2.4 Diaschisis of the retrosplenial cortex in humans after damage of the medial diencephalon or the hippocampal formation

Diaschisis (from Greek διάσχισις meaning "shocked throughout") is when a brain region becomes functionally impaired as the result of a loss of afferents when a distal, connected brain structure has been damaged. The net result is a greater clinical deficit than would be expected only on the basis of the primary pathology. The concept was first introduced by Von Monakov in 1902 (Engelhordt & Da Mota Gomes, 2013) to describe the transient depressive effects that focal brain lesions can have on connected brain areas, and he distinguished it from the more global effects of oedema or general circulatory changes that are associated with a traumatic lesion (Finger, Koehler, & Jagella, 2014). This distal dysfunctionality has been measured in patients mainly in terms of cerebral oxygen metabolic rate, glucose utilisation and cerebral blood flow (Feeney & Baron, 1986) and it usually gradually recovers after the onset of the primary pathology. However, even if the dysfunctionality in the structures affected by diaschisis seems transient, studies on animals have demonstrated that the loss of neuronal connections can cause a re-organisation of their deafferented post-synaptic neurones (Jones, Manger, & Woods, 1997; Witte, 1998). Furthermore, studies of crossed-cerebellar diaschisis in patients have shown that the dysfunction can also be long-term (Pantano et al., 1986; Yamauchi, Fukuyama, Nagahama, Nishizawa, & Konishi, 1999).

Different experiments have reported that damage to either the medial diencephalon or the hippocampal formation in patients can result not only in anterograde amnesia but also in hypofunctionality in the posterior cingulate cortex (which in humans includes the retrosplenial cortex). One study reported that lesions of the left anterior thalamic nuclei and mammillothalamic tract caused global amnesia and glucose hypometabolism in the ipsilateral posterior cingulate cortex (Clarke et al., 1994). Another experiment found bilateral retrosplenial hypometabolism in four amnestic patients with medial temporal damage due to acute hypoxia (Reed et al., 1999). Korsakoff's syndrome has also been repeatedly associated with posterior cingulate hypoactivity measured through FDG-PET (Fazio et al., 1992; Paller et al., 1997; Reed et al., 2003). Furthermore, retrosplenial hypometabolism is present early on in Alzheimer's disease (Minoshima et al., 1997; Nestor, Fryer, Smielewski, & Hodges, 2003; Villain et al., 2008), a disease in which pathology initially affects both the medial

temporal lobe and thalamus and which is characterised by episodic memory loss (Serrano-Pozo, Frosch, Masliah, & Hyman, 2011).

In conclusion, all of these studies suggest that diencephalic amnesia and temporal amnesia could have in common an additional hypofunctionality observed at the level of the retrosplenial cortex, which could exacerbate the memory impairments due to the primary pathology (Aggleton, 2008). Interestingly, a study on 11 cases with different amnestic etiologies reported hypoactivity, measured through PET, not only in the cingulate cortex but also in the thalamus, hippocampal formation, and frontal basal regions (Fazio et al., 1992); this hypoactivity was present even when the patients' brains looked structurally normal or had pathology restricted to the medial diencephalon (in the two Korsakoff cases of the group the mammillary bodies were atrophic, while in the two cerebrovascular cases there were thalamic lesions). These findings strengthen the view that the structures within the Papez circuit work as a system and that their integrated activity supports episodic memory.

1.3 The effects of lesions in the Papez circuit on spatial memory in rodents

In this thesis, the distal effects of either lesioning the medial diencephalon or knocking down the expression of specific immediate early genes in either the dorsal hippocampus or the retrosplenial cortex were investigated in rats. It is, therefore, important to understand how the interconnected structures within the Papez circuit contribute to memory examining the effects of lesions within the Papez circuit on spatial memory behaviour of rodents.

As mentioned in the previous section (1.2), the identification of the critical sites of pathology for diencephalic amnesia has been problematic from patient studies as there is often co-occurring damage to a number of sites; this makes it difficult to disentangle the contribution of each of these sites to normal memory processes. An alternative approach is using animal models, in which lesions can be experimentally induced with high spatial precision and the subsequent effects on memory-dependent tasks can be assessed. Given that episodic memory is disproportionately affected in both diencephalic and temporal lobe amnesia, ideally one would want to assess episodic memory in the animal models, although whether this is possible is still a matter of debate. Some have argued that episodic memory is uniquely human as it

requires the conscious recollection of personal experiences through subjective mental time travel (Roberts, 2002; Suddendorf & Busby, 2003; Tulving, 2002). Since all animals (except humans) lack the use of verbal language (or at least a sophisticated verbal competence; e.g. Menzel, 1999), even if they can show through their behaviour that they have formed mental representations of their past, it is extremely hard to unequivocally demonstrate that they are aware of these representations. However, according to other authors, animals could still have an "episodic-like" memory, defined as the ability to retrieve information about something ("what") associated with the spatio-temporal context ("where" and "when") in which this information was acquired, but without assuming this retrieval is conscious (Clayton, Griffiths, Emery, & Dickinson, 2001; Clayton, Salwiczek, & Dickinson, 2007). While several rodent memory tests have been devised that combine all three components of episodic-like memory (e.g. Babb & Crystal, 2005; Dere, Huston, & De Souza Silva, 2005; Iordanova, Good, & Honey, 2008), this piece of work will focus on memory tasks testing the "where" component of episodic-like memory (i.e. spatial memory). Structures within the Papez circuit appear to be of particular importance for spatial memory, in both rodents and humans. Furthermore, rats are naturally adept at spatial memory tasks, many of which exploit aspects of natural behaviours, such as foraging and navigating. The following discussion will be mainly centred on two specific behavioural tasks, the T-maze task and the radial arm maze task, which have been designed to tax allocentric spatial memory in rats (i.e. the use of distal cues to guide spatial orientation and navigation) and which were used in the experiments reported in this body of work.

1.3.1 T-maze alternation

T-maze alternation requires animals to make a binary choice between the two goal arms of a T-shaped maze. It makes use of rats' innate preference to "alternate", i.e. not re-visit a previously visited location. This effect is particularly pronounced when a food supply has been depleted at that location (Douglas, 1966), however, rats, will also spontaneously alternate even without a reward. Rats can use multiple strategies to solve the T-maze task (Dudchenko, 2001): in order to alternate, and, therefore, remember which arm they visited most recently, they can rely on allocentric/extramaze cues (external landmarks and their relative positions; e.g. Aggleton et al., 1996), intramaze cues (mainly odour trails; e.g. Douglas, 1966), directional cues (i.e. positional alternation with respect to a specific bearing or heading, probably dependent on head direction cells; e.g. Dudchenko & Davidson, 2002) or egocentric/idiothetic cues (i.e. an internal representation of the last body

turn). Rats preferentially rely on extramaze cues if present (e.g. Dudchenko, 2001), otherwise they use the remaining strategies to guide alternation in the maze. However, rats seem unable to use egocentric cues to solve tasks requiring the use of working memory, like T-maze alternation (e.g. Baird, Futter, Muir, & Aggleton, 2004; Futter & Aggleton, 2006; Pothuizen, Aggleton, & Vann, 2008).

Different manipulations allow the experimenter to limit the types of cue available to solve the task (e.g. Nelson, Powell, Holmes, Vann, & Aggleton, 2015; Pothuizen et al., 2008), in order to probe different aspects of spatial memory. For example, intramaze cues can be removed (e.g. using a double T-maze) or put in conflict with extramaze cues; visual spatial cues can be removed by running the task in the dark. T-maze alternation can also be used to assess sensitivity to proactive interference by increasing the number of trials within a session (e.g. Vann & Aggleton, 2003); by manipulating the inter-trial delay it is also possible to obtain a measure of forgetting rates (e.g. Tako, Beracochea, & Jaffard, 1988; Vann & Aggleton, 2003).

1.3.2 The radial arm maze task

The radial arm maze task was first described by Olton & Samuelson (1976) and is run in a maze with a number of arms (typically eight) radiating from a small central platform. The task requires rats to run up and down arms of the maze to retrieve food rewards. It can be used as a measure of spatial memory, as animals need to remember which arms they have entered so they do not re-enter previously visited arms, which is counted as an error (and not rewarded). In the standard working memory version of the radial arm maze task, all arms are baited and the animal has to retrieve all the pellets from the maze. Some studies have introduced a modification to the standard working memory version of the task, in order to prevent animals from using intramaze cues, such as odour trails (Hunt & Aggleton, 1998; Pothuizen et al., 2008; Vann & Aggleton, 2002, 2004a). This modification involves stopping the task after the first four arm choices, rotating the maze by 45 º, moving the remaining four food rewards at the end of each arm so to match the same positions they were in before maze rotation relative to distal room cues, and finally re-starting the task, i.e. allowing the animal to continue exploring the maze arms. In this way, the animals cannot rely on intramaze cues to find the remaining four reward pellets, but they need to orientate themselves using other available cues, such as visual extramaze cues (e.g. visual stimuli on the walls around the maze). There is also a reference/working memory version of the radial arm maze task, in which only four arms are constantly

baited at the beginning of each session and the animal has to learn across sessions which arms should be visited and which should be avoided (e.g. He, Yamada, & Nabeshima, 2002); working memory in this task is a measure of how well the animals are able to keep track of their arm choices within a session, so they are less likely to revisit any previously visited arms.

1.3.3 Spatial memory impairments after discrete lesions within the Papez circuit

In this section, the effects of lesions to structures within or connected to the Papez circuit will be reported. The focus will be on standard spatial memory tasks (mainly the T-maze and radial arm maze tasks). If not otherwise specified, the results will refer to lesion studies in rats. A general overview is reported in Table 1-1 (T-maze task), and Table 1-2 (radial arm maze task).

lesioned area	REINFORCED STANDARD T-MAZE TASK
HIPPOCAMPUS	**impairment** (Aggleton et al, 1986; Bannerman et al, 1999; Dudchenko et al, 2000)
FORNIX	**impairment** (Aggleton, Neave, Nagle, & Hunt, 1995; Aggleton, Neave, Nagle, & Sahgal, 1995; Aggleton et al, 2009; Bussey et al, 2000; Markowska et al, 1989; Neave et al, 1997; Shaw & Aggleton, 1993; Vann et al, 2011; Warburton et al, 1997, 1998, 2000; Warburton & Aggleton, 1999)
ANTERIOR THALAMIC NUCLEI	**impairment** (Aggleton, Neave, Nagle, & Hunt, 1995; Aggleton et al, 1996; Aggleton et al, 2009; Harland et al, 2014; Jenkins, Dias, Amin, Brown, & Aggleton, 2002; Warburton & Aggleton, 1999; Warburton et al, 1997)
MAMMILLARY BODIES	**mild impairment** (Aggleton et al, 1990; Aggleton, Neave, Nagle, & Hunt, 1995; Neave et al, 1997*; Vann & Aggleton, 2003)
MAMMILLOTHALAMIC TRACT	**mild impairment** (Thomas & Gash, 1985; Vann & Aggleton, 2003) **no impairment** (Vann, 2013)
DESCENDING COLUMNS OF THE POSTCOMMISSURAL FORNIX	**mild impairment** (Vann et al, 2011) **no impairment** (Vann, 2013)
GUDDEN'S VENTRAL TEGEMENTAL NUCLEI	**impairment** (Vann, 2009, 2013)
RETROSPLENIAL CORTEX	**mild impairment** (Nelson et al, 2015) **no impairment** (Pothuizen et al, 2008, 2010)
CINGULUM BUNDLE	**impairment** [Aggleton, Neave, Nagle, & Sahgal, 1995) **mild impairment** (Neave et al, 1996, 1997; Warburton et al, 1998)
MEDIAL PREFRONTAL CORTEX	**no impairment** (Aggleton, Neave, Nagle, & Sahgal, 1995; Warburton et al., 1998)

Table 1-1. Effects of lesions within the Papez circuit, or in connected brain structures, on the reinforced T-maze alternation task. Only the experiments in which the retrosplenial cortex was completely lesioned are reported. * = lesion extending into the supramammillary nucleus.

	RADIAL ARM MAZE TASK	
lesioned area	STANDARD WORKING MEMORY VERSION	MODIFIED VERSION WITH MAZE ROTATION AFTER THE FIRST FOUR ARM CHOICES
HIPPOCAMPUS	**impairment** (Cassel et al, 1998; Li et al, 1999: Sziklas & Petrides, 2002)	
FORNIX	**impairment** [Becker et al, 1980; Cassel et al, 1998; Neave et al, 1997; Sziklas & Petrides, 2002]	
ANTERIOR THALAMIC NUCLEI	**impairment** (Aggleton et al, 1996; Sziklas & Petrides, 1999)	**impairment** (Aggleton et al, 1996)
MAMMILLARY BODIES	**mild impairment** (Vann & Aggleton, 2003)	**impairment** (Vann & Aggleton, 2003)
MAMMILLOTHALAMIC TRACT	**mild impairment** (Nelson & Vann 2014; Vann, 2013; Vann & Aggleton, 2003)	**impairment** (Nelson & Vann 2014; Vann, 2013; Vann & Aggleton, 2003)
DESCENDING COLUMNS OF THE POSTCOMMISSURAL FORNIX	**no impairment** (Vann et al, 2011; Vann, 2013)	**no impairment** (Vann et al, 2011; Vann, 2013)
GUDDEN'S VENTRAL TEGMENTAL NUCLEI	**impairment** (Vann, 2009, 2013)	**impairment** (Vann, 2009, 2013)
RETROSPLENIAL CORTEX	**mild impairment** (Pothuizen et al, 2010; Vann & Aggleton, 2002, 2004a) **no impairment** (Pothuizen et al, 2008)	**impairment** (Pothuizen et al, 2008, 2010; Vann & Aggleton, 2002, 2004a)
CINGULUM BUNDLE	**mild impairment** (Neave et al, 1997)	
MEDIAL PREFRONTAL CORTEX	**impairment with prelimbic cortex lesions** (Fritts et al, 1998) **no impairment with anterior cingulate cortex lesions** (Fritts et al, 1998)	

Table 1-2. Effects of lesions within the Papez circuit, or in connected brain structures, on the standard working memory version of the radial arm maze task and on the modified variant with maze rotation. Only experiments in which the retrosplenial cortex was completely lesioned are reported.

1.3.3.1 Hippocampal lesions

Hippocampal lesions in rats cause marked impairments on standard spatial memory tasks, such as T-maze alternation (Aggleton et al., 1986; Bannerman et al., 1999; Dudchenko, Wood, & Eichenbaum, 2000) and the radial arm maze task (Cassel et al., 1998; Li, Matsumoto, & Watanabe, 1999; Sziklas & Petrides, 2002).

Dorsal versus ventral hippocampal lesions

In terms of spatial memory involvement, differences have been found along the dorso-ventral axis of the hippocampus. Specifically, only lesions in the dorsal portion of the hippocampus have been associated with deficits on spatial memory tasks, such as the reinforced standard T-maze task (Bannerman et al., 1999; Potvin, Allen, Thibaudeau, Doré, & Goulet, 2006) and the standard working memory version of the radial arm maze task (Potvin et al., 2006); lesions in the ventral portion of the hippocampus did not affect performance on those same spatial memory tasks (Bannerman et al., 1999; Potvin et al., 2006). A higher number of place cells (neurones that discharge when the animal is in a specific position in the environment; e.g. O'Keefe, 1976) has been recorded in the dorsal hippocampus compared to the ventral hippocampus and this could account for the greater involvement of the dorsal hippocampus in supporting spatial memory (Jung, Wiener, & McNaughton, 1994). The ventral subdivision of the hippocampus, instead, has been implicated in processing of emotions and anxiety; selective ventral hippocampal lesions reduced the amount of freezing behaviour in comparison to control levels in tests of fear conditioning (Rogers, Hunsaker, & Kesner, 2006; Trivedi & Coover, 2004) and decreased the anxiety levels measured in the elevated T-maze test of anxiety (Trivedi & Coover, 2004).

Fornix lesions

Lesions of the fornix cause spatial memory deficits similar to those observed after hippocampal lesions, as fornix-lesioned rats are impaired on T-maze alternation (Aggleton, Neave, Nagle, & Hunt, 1995; Aggleton, Neave, Nagle, & Sahgal, 1995; Aggleton, Poirier, Aggleton, Vann, & Pearce, 2009; Bussey, Duck, Muir, & Aggleton, 2000; Markowska, Olton, Murray, & Gaffan, 1989; Neave, Nagle, & Aggleton, 1997; Shaw & Aggleton, 1993; Vann et al., 2011; Warburton, Baird, & Aggleton, 1997; Warburton et al., 2000; Warburton, Aggleton, & Muir, 1998; Warburton & Aggleton, 1999) and on the standard radial arm maze task (Becker, Walker, & Olton, 1980; Cassel et al., 1998; Neave et al., 1997; Sziklas & Petrides, 2002).

1.3.3.2 Anterior thalamic nuclei lesions

Lesions of the anterior thalamic nuclei in rodents severely disrupt performance on spatial memory tasks including T-maze alternation (Aggleton et al., 1996, 2009; Aggleton, Neave, Nagle, & Hunt, 1995; Célérier, Ognard, Decorte, & Beracochea, 2000; Harland, Collings, McNaughton, Abraham, & Dalrymple-Alford, 2014; Jenkins, Dias, Amin, Brown, & Aggleton, 2002; Warburton & Aggleton, 1999; Warburton et al., 1997) and the radial arm maze task (Aggleton et al., 1996; Mitchell & Dalrymple-Alford, 2006; Sziklas & Petrides, 1999). The impairments are often persistent, with animals showing little improvement over training. However, due to the location of the anterior thalamic nuclei, it is difficult to restrict the lesions to the three nuclei of interest and sometimes the lesions encroach into the overlying hippocampus or adjacent thalamic nuclei. This makes it difficult, in some cases, to assess the specific contribution of the anterior thalamic nuclei.

Selective lesions within the anterior thalamic nuclei

It has been shown that more selective lesions within the anterior thalamic nuclei, i.e. lesions targeting the specific sub-nuclei, have far less disruptive effects on tests of spatial memory. Combined anterodorsal/anteroventral lesions and selective anteromedial lesions were less disruptive than lesions of all three nuclei together on T-maze alternation and on a radial arm maze task (Aggleton et al., 2006). Furthermore, neither anteromedial or anteroventral thalamic lesions impaired performance of an automated version of the continuous alternation T-maze task, despite this task being sensitive to mammillary body lesions (Greene & Naranjo, 1986). None of the studies, to date, have found a consistent dissociation between the types of impairment reported following the different sub-nuclei lesions (Byatt & Dalrymple-Alford, 1996) although only a limited array of tasks have been assessed. The mild effects found after selective lesions of the anterior thalamic nuclei suggest that the intact nuclei are able to support some aspects of spatial learning and memory.

1.3.3.3 Mammillary body lesions

The findings from mammillary body lesions' studies sometimes appear inconsistent. This is in part due to the fact that in some studies the lesions extended into regions adjacent to the mammillary bodies while in other studies there was some tissue sparing (Vann & Aggleton, 2003). Some experiments have been particularly careful to target only the lateral and the medial mammillary nuclei (Aggleton, Hunt, & Shaw, 1990; Aggleton, Neave, Nagle, & Hunt, 1995; Vann & Aggleton, 2003), but others have also included adjacent brain structures, like the supramammillary nucleus

(Neave et al., 1997; Sutherland & Rodriguez, 1989; Sziklas & Petrides, 2000), the premammillary nuclei and the medial ventral tegmental area (Sziklas, Petrides, & Leri, 1996); the results obtained in these latter studies would need to be interpreted with caution.

Lesions of the mammillary bodies delayed the acquisition of both the reinforced standard T-maze task and the standard working memory version of the radial arm maze task in comparison to control levels (Aggleton et al., 1990; Aggleton, Neave, Nagle, & Hunt, 1995; Neave et al., 1997; Vann & Aggleton, 2003). Other studies using the standard radial arm maze task as well showed a more pronounced impairment, but in these cases the lesions were also extended into sites adjacent to the mammillary area (Neave et al., 1997; Sziklas et al., 1996; Sziklas & Petrides, 2000). However, more apparent deficits emerged when animals were no longer able to rely on the use of intramaze cues. For example, mammillary-lesioned animals showed clear impairments on a modified version of the standard T-maze task in which the start arms for sample and choices phases are opposite in space (Neave et al., 1997) and on the modified radial arm maze task with maze rotation after the first four arm choices (Vann & Aggleton, 2003). These findings suggest that the overreliance on the use of intramaze cues by mammillary-lesioned rats can mask a more severe impairment.

Lesions of the lateral mammillary nuclei versus lesions of the medial mammillary nuclei

Both anatomical connectivity (Section 1.1.3.1) and electrophysiological properties (Section 1.1.7) suggest the presence of at least two parallel circuits involving either the medial or the lateral mammillary nuclei. A few lesion studies have selectively targeted the lateral and medial mammillary nuclei and measured the effects on spatial memory performance in behavioural tasks. Lesions of the lateral mammillary nuclei did not impair the acquisition of the standard T-maze task or the continuous alternation variant of the task (Vann, 2005, 2011); however, these animals were impaired when the sample and choice phases of the standard T-maze task were run in two parallel mazes, removing the possibility of using intramaze cues (with this task manipulation animals mostly rely on allocentric cues; e.g. Vann et al., 2011). Lesions of the medial mammillary nuclei, instead, impaired performance on the continuous alternation T-maze task (Field, Rosenstock, King, & Greene, 1978; Greene & Naranjo, 1986; Rosenstock, Field, & Greene, 1977). From these results it seems that lesions of the lateral mammillary nuclei are not able to produce the complete deficits exhibited

after complete mammillary lesions, while, instead, lesions of the medial mammillary nuclei give a pattern of deficit highly similar to complete lesions. As reported in Section 1.1.7.1, the lateral mammillary nuclei contain head-direction neurones, and their loss could explain the mild impairment observed on the modified T-maze task as well as a geometric task in the water maze (Vann et al., 2011); however, as impairments are milder than those found after complete mammillary lesions, it appears that loss of head-direction information cannot solely account for the impairments found after mammillary body lesions.

Lesions of the mammillothalamic tract

In general, lesions of the mammillothalamic tract give rise to the same pattern of spatial memory impairments as lesions of the mammillary bodies; this suggests that the mammillary bodies principally have their effect via their projections to the anterior thalamic nuclei (Vann & Aggleton, 2003). Mammillothalamic tract lesions either mildly impair the acquisition of standard T-maze and radial arm maze task (Thomas & Gash, 1985; Vann & Aggleton, 2003) or produce no impairment at all (Vann, 2013). However, as with mammillary body lesion rats, these mild effects appear to be due to the animals performing the task abnormally and being over-reliant on intramaze cues. When the animals were no longer able to make use of intramaze cues, a marked impairment appeared on both the T-maze and radial arm maze tasks (Nelson & Vann, 2014; Vann & Aggleton, 2003; Vann, 2013).

Why do mammillary body lesions disrupt spatial memory tasks?

Different hypotheses have been proposed to explain why damage to the mammillary bodies is detrimental for the performance in some behavioural tasks taxing spatial memory (Vann & Aggleton, 2004b; Vann, 2010):

(1) The mammillary bodies enable the use of contextual cues to facilitate discrimination between similar events. According to this hypothesis, mammillary body lesions would cause an increase in sensitivity to proactive interference (Aggleton, Neave, Nagle, & Hunt, 1995; Beracochea & Jaffard, 1987; Beracochea & Jaffard, 1990). Studies have looked at the effect of proactive interference on animals with either mammillary bodies or mammillothalamic tract lesions using the continuous alternation T-maze task: rats with these lesions were impaired on the rewarded version of the task (Aggleton, Neave, Nagle, & Hunt, 1995; Field et al., 1978; Krieckhaus & Randall, 1967); also studies on mammillary-lesioned mice found a deficit in the variant of the continuous alternation T-maze task relying on spontaneous

alternations (Beracochea & Jaffard, 1987; Beracochea & Jaffard, 1990). However, further experiments with the rewarded continuous alternation T-maze task did not confirm any difference in performance between animals lesioned either in the mammillary bodies or the mammillothalamic tract and controls (Beracochea & Jaffard, 1990; Vann & Aggleton, 2003). Also studies employing another task with a high degree of proactive interference (like the delayed non-matching to sample lever task) failed to find any effect of mammillary body lesions on performance (Aggleton, Keith, & Sahgal, 1991; Harper, McLean, & Dalrymple-Alford, 1994).

(2) The mammillary bodies support the stability and long-term storage of spatial memories (Beracochea & Jaffard, 1990; Rosenstock et al., 1977; Sziklas & Petrides, 1998) and as such, damage to the mammillary bodies would result in faster forgetting. Some studies using the T-maze task imposed a time-delay between the first and the second goal-arm choices (animals should alternate in the second one) to test this hypothesis. Some experiments on rats and on mice with mammillary body lesions have found a detrimental effect of time delays of ten or more seconds (Aggleton, Neave, Nagle, & Hunt, 1995; Beracochea & Jaffard, 1990). However, this finding was not replicated in other studies with animals lesioned either in the mammillary bodies or in the mammillothalamic tract (Aggleton et al., 1990; Vann & Aggleton, 2003). Studies using the delayed non-matching to sample lever task tested this hypothesis as well, introducing delays up to about one minute between sample and test choice, but did not find any deficit in mammillary-lesioned animals (Aggleton et al., 1991; Harper et al., 1994).

(3) The mammillary bodies are involved in the rapid encoding of new spatial distal cues. This last hypothesis is supported by the finding that animals lesioned in the mammillary bodies or mammillothalamic tract are impaired when they need to rely mainly on allocentric spatial cues to solve spatial memory tasks, for example when the access to intramaze cues has been precluded or is not reliable (such as in the working memory version with maze rotation of the radial arm maze task) or during the early stages of spatial memory task acquisition (Neave et al., 1997; Nelson & Vann, 2014; Vann & Aggleton, 2003; Vann, 2013). Further support for this hypothesis was found in another study where mammillothalamic tract-lesioned animals were severely impaired on the

object-in-place task which requires the rapid encoding of a spatial array of objects (Nelson & Vann, 2014).

The role of hippocampal and midbrain inputs to the mammillary bodies in sustaining spatial memory

The mammillary bodies have often been considered a passive relay of the information coming from the hippocampal formation to the anterior thalamic nuclei (Aggleton & Brown, 1999; Papez, 1937). This assumption, however, does overlook the importance of non-hippocampal midbrain inputs to the mammillary bodies, in particular those sent via the mammillary peduncle from the tegmental nuclei of Gudden (Section 1.1.3.1). A few studies have assessed the effects of lesions to the separate mammillary inputs on tests of allocentric spatial memory. Rats received lesions to either the descending columns of the postcommissural fornix (i.e. that portion of the fornix that connects the hippocampal formation to the mammillary bodies) or to the ventral tegmental nucleus of Gudden (which is reciprocally connected with the medial mammillary nuclei). Lesions of the descending columns of the postcommissural fornix caused a mild impairment in the standard T-maze task (Vann et al., 2011); however, this finding was not replicated in a subsequent study (Vann, 2013). A mild deficit was observed on the continuous alternation version of the task (Vann et al., 2011), but not on the variant in which the sample and choice phases are run in two parallel mazes to exclude the possibility of using intramaze cues (Vann, 2013). Lesioning the fornical afferents to the mammillary bodies also did not cause any impairment either on the working memory version of the radial arm maze task, or on its variant with maze rotation (which exclude the possibility of relying on intramaze cues) (Vann et al., 2011; Vann, 2013). Conversely, lesions of the ventral tegmental nucleus of Gudden caused a significant deficit on all those same spatial memory tasks (Vann, 2009, 2013). Furthermore, lesions of the dorsal tegmental nucleus of Gudden also have a detrimental effect on the performance of tests of allocentric spatial navigation and memory, including a water maze task (Clark et al., 2013), a water T-maze task and a food-foraging task (Dwyer et al., 2013). These results highlight the importance of the midbrain input to the mammillary bodies, compared to the fornix input, in supporting allocentric spatial memory in rodents.

1.3.3.4 Retrosplenial cortex lesions

As with the mammillary bodies, the effects of retrosplenial cortex lesions in rats have sometimes appeared inconsistent. Initial studies found an impairment after complete cingulate lesions (which included both the anterior cingulate and retrosplenial cortex) on T-maze alternation (Markowska et al., 1989). However this finding was criticised as the cingulate cortex was lesioned through aspiration, thus likely damaging the proximal fibre tracts (e.g. the cingulum bundle and the corpus callosum). Subsequent experiments used excitotoxins to selectively lesion the cell bodies within retrosplenial cortex while leaving the fibres intact. Some of these experiments did not find any effect of retrosplenial lesions on tests of spatial memory, such as the reinforced standard T-maze task (Neave, Lloyd, Sahgal, & Aggleton, 1994). It is important to notice that in this last studies the most caudal portion of the retrosplenial cortex was spared; the caudal retrosplenial cortex has been found important for solving the radial arm maze task with maze rotation (Vann, Wilton, Muir, & Aggleton, 2003). However, even if excitotoxic lesions are made that encompass the entire rostral-caudal extent of the retrosplenial cortex, the lesion effects still appear inconsistent and mild in some cases. For example, these lesions result in either a mild or no impairment on both the standard T-maze task (Nelson et al., 2015; Pothuizen et al., 2008; Pothuizen, Davies, Aggleton, & Vann, 2010) and radial arm maze task (Pothuizen et al., 2008; Pothuizen, Davies, Aggleton, & Vann, 2010; Vann & Aggleton, 2002, 2004a). More obvious deficits emerged when intramaze and extramaze cues were put in conflict, as when a maze rotation was interposed between the sample and choice phase in the T-maze task (Nelson et al., 2015) or after the first four arm choices in the radial arm maze task (Pothuizen et al., 2008, 2010; Vann & Aggleton, 2002, 2004a). However, no impairment was present in the performance in the T-maze task when the sample and the choice phase were run into two parallel mazes (intramaze cues unavailable, extramaze, directional and egocentric cues available; Nelson et al., 2015; Pothuizen et al., 2008, 2010). Retrosplenial-lesioned animals were, instead, significantly impaired, compared to controls, when the same double T-maze manipulation was run in the dark (both intramaze and extramaze cues unavailable, directional and egocentric cues available; Nelson et al., 2015; Pothuizen et al., 2008, but in Pothuizen et al, 2010 the effect was only borderline). As it has been shown that rats cannot rely on egocentric cues to solve the T-maze task (Baird et al., 2004; Futter & Aggleton, 2006; Pothuizen et al., 2008), these results suggest the importance of the retrosplenial cortex in supporting spatial memory based on directional cues and in switching among

different spatial strategies (for example when intramaze and allocentric cues are in contraposition).

Effects of lesioning specific retrosplenial subregions

Selective lesions of the dysgranular retrosplenial cortex (Rdg) impaired animals' ability to use allocentric visual cues to solve the radial arm maze task. While seemingly unimpaired on the standard radial arm maze task, the lesioned rats were performing the task abnormally and adopted a sequential response strategy to solve the task. Consistent with this, the lesion rats were subsequently impaired when the maze was rotated mid-way through the task, thus preventing the use of intramaze cues (Vann & Aggleton, 2005).

Selective lesions have also been made within the subdivisions of granular retrosplenial cortex. After complete lesions of the granular retrosplenial region (Rga + Rgb), animals were unimpaired on the standard T-maze and radial arm maze tasks, but impaired when the tasks were modified so animals could not rely on intramaze cues (Pothuizen et al., 2010).

Cingulum bundle lesions

Cingulum bundle lesions disrupt performance on the same spatial memory tasks affected by hippocampal or anterior thalamic lesions, however the deficits appear less severe. Specifically, damage to the cingulum bundle causes a significant or mild impairment on T-maze alternation (Aggleton, Neave, Nagle, & Sahgal, 1995; Neave et al., 1997; Neave, Nagle, Sahgal, & Aggleton, 1996; Warburton et al., 1998), and a mild deficit on the radial arm maze task (Neave et al., 1997). However, as the cingulum bundle connects a number of different regions, it is not clear from these studies which are the key connections for spatial memory.

1.3.3.5 Medial prefrontal cortex lesions

Some studies have investigated the effects of medial prefrontal cortex lesions on spatial memory. Lesions of the prelimbic, infralimbic and anterior cingulate cortex had no effect on the standard T-maze task (Aggleton, Neave, Nagle, & Sahgal, 1995; Warburton et al., 1998); lesions of the prelimbic cortex (but not anterior cingulate cortex) impaired performance of the radial arm maze task (Fritts, Asbury, Horton, & Isaac, 1998). It has been suggested that the different areas within the medial prefrontal cortex (Vertes, 2004) support different cognitive processes: in particular, the prelimbic cortex would support spatial working memory, given its inputs from the

hippocampal formation (Fritts, Asbury, Horton, & Isaac, 1998); in contrast, the anterior cingulate cortex would mainly be involved in sustaining attentional processes, so its lesions would not necessarily affect spatial performance (Newman & McGaughy, 2011).

1.3.3.6 Comparison of spatial memory effects following lesions within the Papez circuit

It is evident that lesions of either the hippocampus, fornix or anterior thalamic nuclei cause a severe impairment on spatial memory tasks. The deficits caused by mammillary lesions or retrosplenial cortex lesions appear milder. However, it is difficult to make direct comparisons across studies with different cohorts of rats and experimental procedures; the strongest evidence comes from direct comparisons within the same study. Several studies have compared anterior thalamic, fornix and mammillary body lesions on tasks including T-maze alternation, and a delayed non-matching-to-position task (Aggleton et al., 1991; Aggleton, Neave, Nagle, & Hunt, 1995; Sutherland & Rodriguez, 1989). The mammillary body lesion effects were milder across all tasks. For the mammillary bodies, it appears that lesion-induced spatial memory deficits only emerge with specific task manipulations that either force the animals to use non-intramaze cues (Vann & Aggleton, 2003) or that increase proactive interference (Aggleton, Neave, Nagle, & Hunt, 1995).

While both anterior thalamic lesions and fornix lesions can result in pronounced deficits on spatial memory tasks, direct comparisons of the two lesions have found differences. In both a water maze task and a geometric discrimination test, anterior thalamic lesions were found to be more disruptive than fornix lesions (Aggleton et al., 2009; Warburton & Aggleton, 1999). Interestingly, damage to the lateral mammillary nuclei also caused a mild impairment on the same geometric discrimination test (Vann, 2011) where fornix lesions were found to be unimpaired (Aggleton et al., 2009). These results highlight the importance of non-hippocampal inputs for at least some aspects of anterior thalamic function. For the geometric discrimination task, performance most likely depends on the ascending head direction information from the dorsal tegmental nucleus of Gudden via the lateral mammillary nuclei (Section 1.1.7.1).

1.3.3.7 Crossed-lesion experiments

The similar profile of deficits following lesions to structures within the Papez circuit has been taken as evidence that these regions work together to support spatial memory. However, more convincing evidence can be found from cross-lesion studies, i.e. where unilateral lesions of two different structures are made in contralateral hemispheres (crossed-lesion). The rationale is that when two structures are connected via unilateral projections, a crossed-lesion would effectively disconnect the two structures from each other. Animals with crossed-lesions of the hippocampus and anterior thalamic nuclei were significantly impaired on T-maze alternation, the radial arm maze task, a water maze task and on visual-spatial conditional learning; animals with both lesions in the same hemisphere were unimpaired (Henry et al., 2004; Warburton et al., 2001). Furthermore, disconnection studies involving the retrosplenial cortex showed the importance of this structure in supporting spatial memory. Crossed-lesions of the retrosplenial cortex and either the anterior thalamic nuclei or hippocampus impaired animals' performance on memory in a water maze task; again, unilateral lesions of the same structures in the same hemisphere had no effect (Sutherland & Hoesing, 1993). Finally, crossed anterior thalamic and fornix lesions disrupted performance of an object location task, while again animals with unilateral lesions in the same hemisphere were unimpaired (Warburton et al., 2000). However, in contrast to the finding from crossed anterior thalamic and hippocampal lesions, these animals were only mildly impaired on the standard version of the T-maze task and not impaired on the radial arm maze task or in a water maze task. These mild effects were attributed to intact non-fornical routes by which the hippocampus could project to the controlateral anterior thalamic nuclei: for example via the hippocampal commissure (Gottlieb & Cowan, 1973), internal capsule and indirectly through the retrosplenial cortex (Section 1.1.4.1). In the same study, crossed anterior thalamic/fornix lesions were combined with the transection of the hippocampal commissure; these lesions impaired performance on the T-maze task, radial arm maze task and a water maze task, suggesting a more complete disconnection of the hippocampus and anterior thalamic nuclei.

1.3.4 Covert pathology caused by lesions in the Papez circuit in rodents

When considering the effects of lesions to particular brain structures one should always take into account that other sites connected to those structures will also be affected. This phenomenon is called diaschisis and has already been introduced in Section 1.2.4 in relation to studies on patients. The phenomenon has also been reported in animal studies, in which the lesion of brain structures not only causes overt pathology in the disconnected areas (e.g. lesions of the dorsomedial prefrontal cortex in monkeys causes retrograde fibre degeneration and associated cell loss and gliosis in the connected medial dorsal thalamic nucleus; Tanaka, 1976), but also functional "covert pathology" not detectable at the gross morphological level using standard histological techniques. Furthermore, this covert pathology caused by disconnection can also affect areas only indirectly connected to the lesioned brain site.

Similar to the findings in patients, covert pathology has been reported following lesions within the Papez circuit in animals. While anterior thalamic lesions do not cause obvious structural changes in the hippocampus or retrosplenial cortex that can be detected through conventional histological techniques (Jenkins, Vann, Amin, & Aggleton, 2004; Poirier & Aggleton, 2009; Poirier, Shires, et al., 2008), more detailed analysis has shown changes at the dendritic level. Anterior thalamic lesions reduced dendritic spine density and arbor complexity in the hippocampus and in the retrosplenial cortex (Harland, Collings, McNaughton, Abraham, & Dalrymple-Alford, 2014; Harland, 2013). They caused a shortening of apical dendritic length in CA1 pyramidal neurones and a loss of dendritic spines in both CA1 pyramidal neurones and in superficial (layers II - III) neurones of the retrosplenial subregion Rgb (Harland et al., 2014; Harland 2013).

In addition to these structural changes, functional changes in the hippocampus have also been found following lesions to structures within the Papez circuit.

Hippocampal function has been assessed in terms of cholinergic activity, which normally increases (and correlates with performance) when the animals are engaged on spatial memory tasks (Fadda, Cocco, & Stancampiano, 2000). Studies on rats using the pyrithiamine-induced thiamine deficiency model of Wernicke-Korsakoff's syndrome (which causes damage to the medial diencephalon) found significantly lower levels of acetylcholine release in the hippocampus in comparison to control (Roland & Savage, 2007; Savage, Chang, & Gold, 2003). A similar decrease was

observed also after discrete lesions of either the anterior thalamic nuclei in rats (Savage, Hall, & Vetreno, 2011), or the mammillary bodies in mice (Beracochea, Micheau, & Jaffard, 1995). Decreased acetylcholinesterase staining in the hippocampus has also been found after mammillothalamic tract lesions in rats (Winter et al., 2011). It has been suggested that the medial diencephalon exerts its effect on hippocampal cholinergic activity indirectly through the retrosplenial cortex, which in turn interacts not only with the hippocampus but with the septal nuclei (see section 1.1.4.1), the main source of hippocampal cholinergic innervation (Woolf, 1991).

The retrosplenial cortex has been repeatedly found to be functionally affected by distal lesions to structures within the Papez circuit. An electrophysiological study showed that anterior thalamic lesions suppressed the excitatory neuronal discharge normally developed in the retrosplenial cortex when rabbits learned to discriminate the conditioned stimulus in a differential avoidance conditioning task (Gabriel et al., 1983). Furthermore, unilateral lesions of the anterior thalamic nuclei caused a disruption in plasticity in the superficial layers of the granular retrosplenial cortex, measured as a loss of long-term depression after artificial electrical stimulation in brain slices (Garden et al., 2009); since both hemispheres received the identical stimulation protocol, the loss of synaptic plasticity observed unilaterally cannot be interpreted as a mere loss of inputs but rather as a change in retrosplenial functional properties due to the unilateral anterior thalamic nuclei lesions. The disruption of long term depression in the retrosplenial cortex was associated with a decrease in $GABA_A$ transmission (Garden et al., 2009). Consistent with this, an analysis of the transcriptome of granular retrosplenial cortex after unilateral anterior thalamic lesions found a decrease in expression of genes implicated in energy metabolism, synaptic plasticity and neurotransmission, including GABAergic-related gene expression, in the retrosplenial cortex ipsilateral to the lesion (Poirier, Shires, et al., 2008). Anterior thalamic lesions also appear to disrupt metabolic activity within the retrosplenial cortex. For example, Mendez-Lopez et al. (2013), found a decrease in cytochrome oxidase levels (a marker of cellular metabolic activity; e.g. Sakata, Crews, & Gonzalez-Lima, 2005) within the superficial layers of the granular retrosplenial cortex and part of the anterior cingulate cortex (but not in the hippocampus) in rats with anterior thalamic lesions. This finding seems to be at least partially in contrast with the results of another study of transcriptional levels of markers of retrosplenial functionality (Amin et al., 2010); specifically, a trend was found for an increase in the expression of *cox6b* (which encodes for subunit 6b of cytochrome c oxidase protein complex; e.g. Little, Kocha, Lougheed, & Moyes, 2010) in layer II of retrosplenial subregion Rgb of rats with

anterior thalamic lesions. This same experiment also detected a decrease in the level of transcription of genes *5ht2rc*, *kcnab2*, *c-fos*, and *zif268*; the last two are immediate early genes which have been used in several studies for showing the effects of lesions within the Papez circuit on the rest of the system, and they will be the focus of the next section.

1.4 Using c-Fos and Zif268 immediate early gene imaging to study the Papez circuit

One of the experiments described in this thesis involved the use of immediate early gene imaging in the Papez circuit after medial diencephalic lesions, while other experiments verified the effect on spatial memory of knocking-down immediate early genes into either the dorsal hippocampus or the retrosplenial cortex. The following section describes immediate early genes, with a particular focus on c-Fos and Zif268, as they are most relevant in this body of work.

1.4.1 What are the immediate early genes?

Immediate early gene is a term created in virology during the late 1960s and the early 1970s to describe those viral genes whose transcription is induced, after a virus has infected a host-cell, without requiring the synthesis of any other protein (hence the "early" definition); this is due to the virus being able to exploit the transcription machinery already present in the host cell (Davis, Bozon, & Laroche, 2003). Subsequently, it was reported that extracellular stimuli (e.g. growth factors and mitogens) can also trigger gene regulation with no protein synthesis, leading to the discovery of "cellular" immediate early genes (simply "immediate early genes" in the rest of the text), normally present in cells (Herrera & Robertson, 1996). As for their viral counterparts, protein inhibitors cannot prevent their expression and their induction in the cell is transient and occurs within minutes after stimulation (Tischmeyer & Grimm, 1999).

Immediate early genes can be divided into two categories (Guzowski, Setlow, Wagner, & McGaugh, 2001):

- "Regulatory" immediate early genes encode for transcription factors at the top of intracellular pathways initiated after cellular stimulation (Aggleton & Brown, 2005; Tischmeyer & Grimm, 1999). Their transcripts get translated into

proteins within the cytosol and then return to the nucleus where they bind to specific promoter regions in the genome and regulate the expression of downstream genes (called “late-response” genes; e.g. Chaudhuri, 1997), which are finally responsible for the long-term modifications of the cell’s phenotype. They have also been defined as “inducible” transcription factors, in order to distinguish them from the “constitutively” expressed transcription factors (e.g. CREB). Constitutive transcription factors are also present in quiescent neurones, they are regulated by post-translational modifications (Davis et al., 2003) and in turn regulate the transcription of the inducible transcription factors (Herdegen & Leah, 1998).

- “Effector” immediate early genes encode for proteins with a more direct functional role in the cell, e.g. structural or enzymatic. They are expressed and exert their functions mainly in the cytosol, but they can also be secreted extracellularly (Clayton, 2000).

1.4.2 Immediate early gene expression in neurones

In neurones, immediate early gene induction is triggered by a variety of stimuli, such as neurotransmitters, neuropeptides, growth factors, depolarisation, seizures, brain injury, ischaemia, and sensory stimulation (Tischmeyer & Grimm, 1999). The signal is conveyed from cell surface receptors (which are activated, for example, by synaptic stimulation) to the nucleus, through activation within the cytoplasm of second messengers, intracellular signal transduction pathways and constitutive transcription factors; these enter the nucleus and bind to the DNA activating the transcription of the immediate early genes (Figure 1-13).

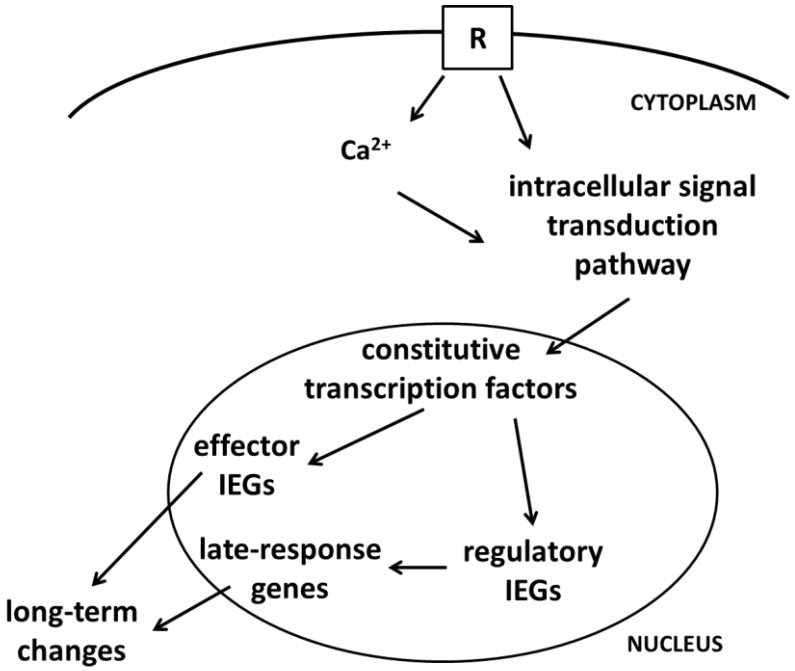

Figure 1-13. Simplified diagram of activation of immediate early genes (IEGs) within the cell. R = receptor.

It has been suggested that immediate early genes could be important in initiating long-term memory consolidation processes as they are able to convert neuronal activity into long-lasting changes inside the cell (Herrera & Robertson, 1996).

The neuronal activation and function of two immediate early genes, c-Fos and Zif268, both belonging to the class of inducible transcription factors, will be described in the following sections.

1.4.2.1 c-Fos

c-fos is a proto-oncogene, i.e. a gene that if mutated can become an oncogene, able to induce cancer (Sassone-Corsi, Sisson, & Verma, 1988). It was first identified as the homologue of the retroviral oncogene *v-fos*, whose DNA sequence was originally isolated from a murine sarcoma virus (the name "*fos*" derives from FBJ murine OsteoSarcoma virus). *c-fos* gene belongs to a multigene family (also comprising genes *fra-1*, *fra-2* and *fosB*; e.g. Gass, Herdegen, Bravo, & Kiessling, 1992) and it encodes for a 56 kDa protein (380 aminoacids), c-Fos, which exerts its activity in the nucleus as regulatory immediate early gene (Herrera & Robertson, 1996). Protein c-Fos, binds non-covalently to members of the Jun family of immediate early genes (c-Jun, JunB and JunD) through a leucine zipper domain (Ransone, Visvader, Sassone-Corsi, & Verma, 1989), forming the heterodimer AP-1 which binds to the AP-1 binding site on DNA and regulates the transcription of late-response genes that bear the AP-1 consensus site 5'-TGAG/CTCA-3' (Alberini, 2009; Mechta-Grigoriou, Gerald, & Yaniv, 2001). Basal levels of Fos are low in most cell types, including neurones (Chaudhuri, 1997; Gass et al., 1992; Herrera & Robertson, 1996). However, c-Fos expression can be markedly and transiently stimulated by a variety of stimuli, including some linked to cell division (e.g. serum and polypeptides) and others specific for neuronal activation, such as neurotransmitters, depolarising stimuli and seizures (Herrera & Robertson, 1996).

c-Fos expression regulation

c-fos has different *cis*-acting regulatory elements located close to its transcription active site; the main ones are the Ca^{2+}/cAMP responsive element (Ca/CRE) and the serum response element (SRE), located 60 and 310 nucleotides 5' to the transcription start site, respectively (Vanhoutte et al., 1999). Neuronal excitation, leads to either the influx of Ca^{2+} inside the neuron (for example through voltage-sensitive calcium channels or NMDA receptors; e.g. Ginty, 1997) and/or the activation of cAMP (e.g. Sheng & Greenberg, 1990). Both Ca^{2+} and cAMP act as second messengers and lead to the activation of protein kinases (e.g. protein kinase A and calcium/calmodulin-dependent kinases) able to phosphorylate and activate the constitutive transcription factor CREB (c-AMP responsive element binding protein). Phosphorylated CREB enters in the nucleus and binds to the Ca/CRE element, triggering *c-fos* transcription. Ca^{2+} influx into neurones also leads to the activation of the serum response factor (SRF) and the ternary complex factor (TCF), which bind to the SRE element and increase *c-fos* transcriptional levels (Flavell & Greenberg, 2008).

c-Fos and synaptic plasticity

Some studies have found that c-Fos expression levels increased in the hippocampus after long term potentiation (LTP) and long term depression (LTD). LTP and LTD are two forms of synaptic plasticity important for memory processes involved in consolidation (Martin, Grimwood, & Morris, 2000) ; hippocampal LTP and LTD have been associated with spatial learning (Goh & Manahan-Vaughan, 2013; Moser, Krobert, Moser, & Morris, 1998) and novel space exploration (Kemp & Manahan-Vaughan, 2004). However, even though c-Fos expression levels were increased in the dentate gyrus after LTP, this increase was not found to correlate with levels of either LTP induction (Dragunow et al., 1989) or maintenance (Jeffery, Abraham, Dragunow, & Mason, 1990). Instead, it has been shown that the protein expression of *c-fos* in the CA1 subfield is essential for the induction of LTD associated with spatial learning (Kemp, Tischmeyer, & Manahan-Vaughan, 2013).

1.4.2.2 Zif268

The *zif268* gene (also known as *krox24*, *NGFI-A*, *egr-1*, *TZS8* and *zenk*) is part of a family of inducible regulatory transcription factors, the EGR family, which also includes *egr-2* (*krox20*), *egr-3* (*pilot*) and *Egr-4*. They all share three zinc finger sequences in their DNA-binding domain, able to bind to GC-rich response elements in the DNA and regulate the expression of late-response genes (Bozon et al., 2003; Davis et al., 2003). *zif268* encodes for Zif268, a 75 kDa protein (Lonergan, Gafford, Jarome, & Helmstetter, 2010) which in the rodent brain is constitutively expressed in the neocortex (at maximum levels in layers IV and VI), primary olfactory and entorhinal cortices, hippocampus (mainly in CA1, while it is almost absent in dentate gyrus and CA3; e.g. Richardson et al., 1992), amygdala, nucleus accumbens, striatum and cerebellum (Davis et al., 2003). Similarly to c-Fos, different stimuli are able to increase Zif268 expression levels in cells, for example growth factors, serum, neurotransmitters, depolarisation and seizures (Bozon et al., 2003; Gass et al., 1992).

Zif268 expression regulation

Different transcription regulatory regions are located close to the *zif268* promoter, including CRE and SRE responsive elements, AP-1 like motifs, and a GSG box. The constitutively expressed transcription factors CREB and Elk-1, once phosphorylated, bind to CRE and SRE sites respectively; the inducible transcription heterodimer AP-1 binds to the AP-1 site; members of the same EGR family are able to bind to the GSG box, providing an autoregulatory mechanism for Zif268 expression (Davis et al.,

2003). CREB and Elk-1 are phosphorylated by the MAPK/ERK (mitogen-activated protein kinase/extracellular signal-regulated kinase) pathway, which in turn is activated by receptor signalling, such as tyrosin kinase, dopamine, adrenergic and NMDA receptors. Furthermore, the activation of NMDA receptors increases the influx of Ca^{2+} inside neurones, which can both activate the MAPK/ERK pathway and calcium-dependent kinases able to directly phosphorylate CREB (Davis et al., 2003).

Zif268 and synaptic plasticity

Zif268 expression is necessary for LTP in the dentate gyrus, and in particular, its levels are correlated with LTP maintenance rather than induction (Richardson et al., 1992; Richter-Levin, Thomas, Hunt, & Bliss, 1998). This was confirmed by an experiment that created mutant mice not expressing Zif268 (Jones et al., 2001); the animals exhibited normal early LTP in the dentate gyrus but did not show the late phase of LTP. Conversely, in mice in which Zif268 was overexpressed in the forebrain the LTP was enhanced in the dentate gyrus and this was paralleled by a better performance than wild-type controls in an object-place task requiring long-term memory (Penke et al., 2014). Interestingly, one of the late-response genes activated by Zif268 transcription factor encodes for the pre-synaptic protein synapsin I (Thiel, Schoch, & Petersohn, 1994) the levels of which increased during LTP in the dentate gyrus (Sato, Morimoto, Suemaru, Sato, & Yamada, 2000). However, the role of Zif268 in LTP maintenance has only been established in the dentate gyrus so far; in the CA1 subfield Zif268 expression levels have not been correlated to LTP (French et al., 2001).

1.4.3 Time course of c-Fos and Zif268 expression

Some studies have investigated the expression time courses of *c-Fos* and *Zif268* RNA messengers (mRNAs) and c-Fos and Zif268 proteins. An experiment was performed triggering immediate early gene expression through light stimulation in the primary visual cortex of dark-reared rats (Zangenehpour & Chaudhuri, 2002). Both *c-Fos* and *Zif268* transcripts reached their peak after 30 minutes of light stimulation; however, *c-Fos* levels started to rapidly decline, reaching baseline levels after two hours of light stimulation, while *Zif268* levels remained sustained for the whole time the light stimulation was present. This was mirrored by protein peak levels: both c-Fos and Zif268 levels reached their maximum after two hours of light stimulation, but while c-

Fos levels went back to basal levels after six hours of light stimulation, Zif268 protein levels remained plateaued until the light stimulation was removed.

Other studies on rats found partially similar results. For example, c-Fos reached its level peak in the hippocampus and neocortex two to four hours after the induction of seizures and returned to basal levels eight hours afterwards (Dragunow & Faull, 1989; Gass et al., 1992). In an experiment in which LTP was induced in the dentate gyrus, *Zif268* transcript level reached its peak 20 minutes post-tetanisation and was back to basal levels after two hours, while Zif268 protein level reached its maximum two hours after LTP induction and fell to baseline after eight hours (Richardson et al., 1992). The lack of a difference in the time of return to basal levels between c-Fos and Zif268 (at about eight hours after stimulation for both) appears in contrast with what found by Zangenehpour & Chaudhuri (2002). However, it is important to consider that the light stimulation was continuous in the latter study and this could explain the persistent high expression levels of Zif268. It has been suggested that c-Fos expression appears to be more unstable and transient in comparison to Zif268, because c-Fos is able to bind to a repressor region in the gene promoter, thus auto-regulating its own expression through a negative feedback loop (Sassone-Corsi et al., 1988). Thus c-Fos expression could be particularly suitable to track recent neural activity, for example related to novelty detection via the sensory systems (Chaudhuri, 1997).

Interestingly, some studies have shown the presence of a second wave of increase in inducible transcription factor levels after the same cellular stimulation (Herdegen & Leah, 1998). For example, the application of a noxious stimulus to rats' hindpaws caused a first increase in c-Fos expression levels in thalamus and hypothalamus 1 hour after stimulation, and then a second wave 6 hours after stimulation (Redburn & Leah, 1997). Furthermore, an experiment on c-Fos expression in the dorsal hippocampus after inhibitory avoidance training showed that there are also two waves of expression, 1 and 24 hours after training; the former wave was related to long-term memory consolidation processes and the second to long-term memory persistence (Katche et al., 2010).

1.4.4 Immediate early gene imaging

Accumulation of immediate early genes in neurones indicates a previous state of activity, regardless of their specific function. For this reason, measurement of immediate early gene expression levels in the brain has been interpreted as an index

of metabolic activity of those areas in which it has been recorded, allowing the creation of functional activity maps (Chaudhuri, 1997). The main advantage of using immediate early gene imaging is the ability to compare neuronal activity with a high level of spatial resolution (i.e. at a cellular level), simultaneously across a number of brain areas (Aggleton & Brown, 2005), thus offering a complementary research tool to brain lesion and electrophysiological studies.

There are, however, some limitations to this technique, which are important to consider when evaluating the outcomes of experiments using immediate early gene imaging:

- There is sometimes very little correlation with metabolic neuronal activity (Chaudhuri, 1997; Clayton, 2000; Jorgensen, Deckert, Wright, & Gehlert, 1989). For example, c-Fos expression levels do not correlate with 2-deoxy-D-glucose levels, a commonly used marker for studying brain metabolism (Nasrallah, Pagès, Kuchel, Golay, & Chuang, 2013), at the level of striatum (Sagar, Sharp, & Curran, 1988), cerebellum and substantia nigra (Dragunow & Faull, 1989). The reason could be associated to the fact that metabolic activity increases with both neuronal activation and inhibition, while c-Fos expression levels rise only with neuronal activation (Bullitt, 1990). Moreover, it has been shown that *c-fos* expression is not induced in some neurones after depolarisation (Bullitt, 1990; Hunt, Pini, & Evan, 1987), thus c-Fos expression levels cannot be considered representative of neuronal electrical activity.
- Immediate early genes are expressed only by specific neuronal types, so they cannot be used to monitor the whole brain's activity (Chaudhuri, 1997); for example, c-Fos is not expressed by the neurones of substantia nigra (Dragunow & Faull, 1989).

1.4.5 Expression of c-Fos and Zif268 in the Papez circuit during spatial tasks

Expression levels of c-Fos and Zif268 have been used to visualise the activation of different areas in the Papez circuit during spatial tasks. They do not provide completely overlapping information as they are expressed at different levels and in different structures in the nervous system in basal conditions; furthermore, they have been associated with different processes of synaptic plasticity, so they can provide complementary results on the functionality of the brain regions under investigation.

1.4.5.1 Exposure to a novel environment

Studies in which rats were exposed to a novel environment showed a rise (in comparison to animals in a familiar environment) in c-Fos levels in a number of structures within the Papez circuit (the hippocampus, parasubiculum, anteroventral and anteromedial thalamic nuclei and retrosplenial cortex) and connected to it (the prelimbic, postrhinal and perirhinal cortices) (Jenkins, Dias, Amin, Brown, et al., 2002; VanElzakker, Fevurly, Breindel, & Spencer, 2008; Zhu, McCabe, Aggleton, & Brown, 1997). Another experiment, where animals explored a novel training apparatus, detected an increase of *c-Fos* mRNA levels in the visual cortex, olfactory cortex and hippocampus (especially subfield CA1) of the rats (Hess, Lynch, & Gall, 1995). Finally, Zif268 levels appeared higher in both dentate gyrus and CA1 when animals explored a novel environment (Gheidi, Azzopardi, Adams, & Marrone, 2013; Hall, Thomas, & Everitt, 2000).

1.4.5.2 Execution of a spatial memory task

A number of studies have measured c-Fos and Zif268 expression levels within the Papez circuit (and connected areas) in rats engaged in tasks requiring spatial memory. Some of these studies will be discussed below with a particular focus on those that were carried out in the radial arm maze.

In animals that performed the radial arm maze task in comparison to sensory and motor matched-controls (which were forced to run up and down a single arm of the maze, so removing the memory demand from the task) there was an increase of c-Fos levels in the hippocampus, subiculum, entorhinal and postrhinal cortices, postsubiculum, presubiculum, parasubiculum, anterior thalamic nuclei, retrosplenial cortex, prelimbic cortex and caudal portion of the anterior cingulate cortex (Vann, Brown, & Aggleton, 2000; Vann, Brown, Erichsen, & Aggleton, 2000a). Another experiment measured Zif268 levels after the radial arm maze task and found an increase in the anterodorsal thalamic nuclei, ventral subiculum, postsubiculum, presubiculum, parasubiculum, entorhinal, anterior, postrhinal and perirhinal cortices (Jenkins, Amin, Brown, & Aggleton, 2006); it is important to notice, though, that in this last experiment the levels refer to the intact hemisphere of animals with unilateral hippocampal lesions which were compared to home-cage naïve controls. Performing the radial arm maze task in a novel room further increased c-Fos expression levels in comparison to animals tested in a familiar room: c-Fos levels were increased in the

hippocampus, subiculum, entorhinal and postrhinal cortices (Vann, Brown, Erichsen, et al., 2000a), in the postsubiculum, presubiculum, parasubiculum, anterior thalamic nuclei and prelimbic cortex (Vann, Brown, & Aggleton, 2000); however, no change was detected in the anterior cingulate cortex and retrosplenial cortex.

One experiment focused on measuring both c-Fos and Zif268 expression levels in the retrosplenial cortex after a modified version of the radial arm maze task sensitive to retrosplenial lesions, during either dark or light conditions (Pothuizen et al., 2009). Performing the task in the light increased both c-Fos and Zif268 levels in the whole retrosplenial cortex, while performing the task in the dark increased their levels only in the granular retrosplenial cortex, while in Rdg there was a decrease in c-Fos levels and no change in Zif268 levels.

A study by Poirier et al. (2008) assessed whether expression levels of Zif268 within the hippocampus were affected by performance and/or training levels on a radial arm maze task. Rats initially acquired the task and then were trained for a further two or five days on the same task but in a novel room. Zif268 levels in the dentate gyrus correlated negatively with performance but only for the group trained for two days; in the group trained for five days, instead, Zif268 levels in CA1 were positively correlated with performance, while Zif268 levels in CA3 were negatively correlated.

An experiment using the a water maze task found a peak of increase of both *c-Fos* and *Zif268* mRNA levels in the dorsal hippocampus at 30 minutes after the end of the task training; however, a similar increase was found also in a non-spatial version of the water maze task (cued-water task), even if *c-Fos* and *Zif268* mRNA levels showed a trend in correlating with animals' performance only in the spatial variant of the task (Guzowski et al., 2001).

Finally, using an object-place recognition task, an increase in expression levels of both c-Fos and Zif268 was recorded in the hippocampus (Mendez, Arias, Uceda, & Arias, 2015; Soulé et al., 2008); moreover, Mendez et al. (2015) showed that the increase of c-Fos in CA1 was positively correlated with memory performance in the task.

1.4.6 The distal effect of lesions within Papez circuit on c-Fos and Zif268 expression

Different studies have combined immediate early gene imaging and lesions techniques to analyse interactions among structures in the Papez circuit (for an overview see Table 1-3, table 1-4, table 1-5 and Table 1-6).

		RETROSPLENIAL CORTEX		
		Rdg	Rgb	Rga
lesioned area	HIPPOCAMPUS	**c-Fos level decrease** (Albasser et al, 2007) **Zif268 level decrease** (Albasser et al, 2007)	**c-Fos level decrease** (Albasser et al, 2007) **Zif268 level decrease** (Albasser et al, 2007)	**c-Fos level decrease** (Albasser et al, 2007) **Zif268 level decrease** (Albasser et al, 2007)
	FORNIX		**c-Fos level decrease** (Vann, Brown, Erichsen, & Aggleton, 2000b)	**c-Fos level decrease** (Vann, Brown, Erichsen, & Aggleton, 2000b)
	ANTERIOR THALAMIC NUCLEI	**c-Fos level decrease** (Jenkins et al, 2004; Poirier & Aggleton, 2009) **Zif268 level decrease** (Jenkins et al, 2004; Dumont et al, 2012)	**c-Fos level decrease** (Jenkins, Dias, Amin, & Aggleton, 2002; Jenkins, Dias, Amin, Brown, et al, 2002; Jenkins et al, 2004; Poirier & Aggleton, 2009) **Zif268 level decrease** (Dumont et al, 2012; Jenkins et al, 2004; Poirier & Aggleton, 2009)	**c-Fos level decrease** (Jenkins, Dias, Amin, & Aggleton, 2002; Jenkins, Dias, Amin, Brown, et al, 2002; Jenkins et al, 2004) **Zif268 level decrease** (Dumont et al, 2012; Jenkins et al, 2004)
	LATERODORSAL THALAMIC NUCLEI	**no change in c-Fos levels** (Poirier & Aggleton, 2009) **no change in Zif268 levels** (Poirier & Aggleton, 2009)	**no change in c-Fos levels** (Poirier & Aggleton, 2009) **no change in Zif268 levels** (Poirier & Aggleton, 2009)	
	MAMMILLOTHALAMIC TRACT	**c-Fos level decrease** (Vann & Albasser, 2009; Vann, 2013)	**c-Fos level decrease** (Vann & Albasser, 2009; Vann, 2013)	**c-Fos level decrease** (Vann & Albasser, 2009; Vann, 2013)
	DESCENDING COLUMNS OF THE POSTCOMMISSURAL FORNIX		**no change in c-Fos level** (Vann, 2013)	**no change in c-Fos level** (Vann, 2013)
	GUDDEN'S VENTRAL TEGEMENTAL NUCLEI		**c-Fos level decrease** (Vann, 2013)	**c-Fos level decrease** (Vann, 2013)

Table 1-3. Effects of lesions within the Papez circuit and connected areas on c-Fos and Zif268 levels in the retrosplenial cortex.

		HIPPOCAMPAL FORMATION				
		HIPPOCAMPUS	**SUBICULUM**	**PRESUBICULUM**	**PARASUBICULUM**	**POST-SUBICULUM**
lesioned area	**HIPPOCAMPUS**		**no change in c-Fos level** (Jenkins et al, 2006) **Zif268 level decrease** (Jenkins et al, 2006)	**c-Fos level decrease** (Jenkins et al, 2006) **Zif268 level decrease** (Jenkins et al, 2006)	**no change in c-Fos level** (Jenkins et al, 2006) **Zif268 level decrease** (Jenkins et al, 2006)	**c-Fos level decrease** (Jenkins et al, 2006) **no change in Zif268 level** (Jenkins et al, 2006)
	FORNIX	**c-Fos level decrease** (Vann, Brown, Erichsen, & Aggleton, 2000b)	**c-Fos level decrease** (Vann, Brown, Erichsen, & Aggleton, 2000b)	**c-Fos level decrease** (Vann, Brown, Erichsen, & Aggleton, 2000b)	**c-Fos level decrease** (Vann, Brown, Erichsen, & Aggleton, 2000b)	**c-Fos level decrease** (Vann, Brown, Erichsen, & Aggleton, 2000b)
	ANTERIOR THALAMIC NUCLEI	**c-Fos level decrease** (Jenkins, Dias, Amin, & Aggleton, 2002; Jenkins, Dias, Amin, Brown, et al, 2002) **no change in Zif268 level** (Dumont et al, 2012)	**no change in c-Fos level** (Jenkins, Dias, Amin, & Aggleton, 2002; Jenkins, Dias, Amin, Brown, et al, 2002) **no change in Zif268 level** (Dumont et al, 2012)	**c-Fos level decrease** (Jenkins, Dias, Amin, & Aggleton, 2002) **no change in c-Fos level** (Jenkins, Dias, Amin, Brown, et al, 2002) **no change in Zif268 level** (Dumont et al, 2012)	**no change in c-Fos level** (Jenkins, Dias, Amin, & Aggleton, 2002; Jenkins, Dias, Amin, Brown, et al, 2002)	**c-Fos level decrease** (Jenkins, Dias, Amin, & Aggleton, 2002) **no change in c-Fos level** (Jenkins, Dias, Amin, Brown, et al, 2002) **no change in Zif268 level** (Dumont et al, 2012)
	MAMMILLOTHALAMIC TRACT	**c-Fos level decrease** (Vann & Albasser, 2009; Vann, 2013)	**no change in c-Fos level** (Vann & Albasser, 2009)	**no change in c-Fos level** (Vann & Albasser, 2009)	**c-Fos level increase** (Vann & Albasser, 2009)	**c-Fos level decrease** (Vann & Albasser, 2009)
	DESCENDING COLUMNS OF THE POSTCOMMISSURAL FORNIX	**no change in c-Fos level** (Vann, 2013)				
	GUDDEN'S VENTRAL TEGEMENTAL NUCLEI	**c-Fos level decrease** (Vann, 2013)				

Table 1-4. Effects of lesions within the Papez circuit and connected areas on c-Fos and Zif268 levels in the hippocampal formation.

		PREFRONTAL CORTICES		
		ANTERIOR CINGULATE CORTEX	**INFRALIMBIC CORTEX**	**PRELIMBIC CORTEX**
lesioned area	**HIPPOCAMPUS**	**no change in c-Fos level** (Jenkins et al, 2006) **no change in Zif268 level** (Jenkins et al, 2006)	**no change in c-Fos level** (Jenkins et al, 2006) **no change in Zif268 level** (Jenkins et al, 2006)	**no change in c-Fos level** (Jenkins et al, 2006) **no change in Zif268 level** (Jenkins et al, 2006)
	FORNIX	**c-Fos level decrease** (Vann, Brown, Erichsen, & Aggleton, 2000b)		**c-Fos level increase** (Vann, Brown, Erichsen, & Aggleton, 2000b)
	ANTERIOR THALAMIC NUCLEI	**c-Fos level decrease** (Jenkins, Dias, Amin, Brown, et al., 2002) **no change in c-Fos level** (Jenkins, Dias, Amin, & Aggleton, 2002)	**no change in Zif268 level** (Dumont et al, 2012)	**c-Fos level decrease** (Jenkins, Dias, Amin, Brown, et al., 2002) **no change in c-Fos level** (Jenkins, Dias, Amin, & Aggleton, 2002) **no change in Zif268 level** (Dumont et al, 2012)
	MAMMILLOTHALAMIC TRACT	**no change in c-Fos level** (Vann & Albasser, 2009)	**no change in c-Fos level** (Vann & Albasser, 2009; Vann, 2013)	**c-Fos level decrease** (Vann & Albasser, 2009; Vann, 2013)
	DESCENDING COLUMNS OF THE POSTCOMMISSURAL FORNIX		**no change in c-Fos level** (Vann, 2013)	**no change in c-Fos level** (Vann, 2013)
	GUDDEN'S VENTRAL TEGEMENTAL NUCLEI		**no change in c-Fos level** (Vann, 2013)	**c-Fos level decrease** (Vann, 2013)

Table 1-5. Effects of lesions within the Papez circuit and connected areas on c-Fos and Zif268 levels in the prefrontal cortices.

		ANTERIOR THALAMIC NUCLEI		
		ANTEROVENTRAL	ANTEROMEDIAL	ANTERODORSAL
lesioned area	HIPPOCAMPUS	**c-Fos level decrease** (Jenkins et al, 2006) **Zif268 level decrease** (Jenkins et al, 2006)	**c-Fos level decrease** (Jenkins et al, 2006) **Zif268 level decrease** (Jenkins et al, 2006)	**c-Fos level decrease** (Jenkins et al, 2006) **Zif268 level decrease** (Jenkins et al, 2006)
	FORNIX	**c-Fos level decrease** (Vann, Brown, Erichsen, & Aggleton, 2000b)	**c-Fos level decrease** (Vann, Brown, Erichsen, & Aggleton, 2000b)	**c-Fos level decrease** (Vann, Brown, Erichsen, & Aggleton, 2000b)

Table 1-6. Effects of lesions within the Papez circuit and connected areas on c-Fos and Zif268 levels in the anterior thalamic nuclei.

1.4.6.1 Anterior thalamic nuclei lesions

The effects of anterior thalamic lesions have been extensively analysed in combination with *c-fos* and *zif268* imaging. In these experiments, in order to elicit the expression of these immediate early genes, rats were either exposed to a novel environment or were engaged in the radial arm maze task. In the former case, the rats were previously lesioned in the anterior thalamic nuclei either unilaterally (Poirier & Aggleton, 2009) or bilaterally (Dumont, Amin, Poirier, Albasser, & Aggleton, 2012; Jenkins, Dias, Amin, Brown, et al., 2002; Jenkins et al., 2004; Poirier & Aggleton, 2009), while in the latter case only unilateral-lesioned rats were assessed (Jenkins, Dias, Amin, & Aggleton, 2002) as bilateral lesions would impair performance (Section 1.3.4.2). Animals with bilateral lesions were compared to a matched control group, while in animals with unilateral lesions comparisons were made between lesioned and not-lesioned hemisphere in each animal.

Retrosplenial cortex c-Fos and Zif268 expression levels

The most prominent and consistent change in immediate early gene expression after anterior thalamic lesions was found in the granular portion of the retrosplenial cortex, with a massive decrease, in comparison to controls, of both c-Fos (Jenkins, Dias, Amin, & Aggleton, 2002; Jenkins, Dias, Amin, Brown, et al., 2002; Jenkins et al., 2004; Poirier & Aggleton, 2009) and Zif268 (Dumont et al., 2012; Jenkins et al., 2004; Poirier & Aggleton, 2009) expression levels (Table 1-3). The robustness of this effect was confirmed in different rat strains (both Lister Hooded: Poirier & Aggleton, 2009; and Dark Agouti: Dumont et al., 2012; Jenkins, Dias, Amin, & Aggleton, 2002; Jenkins, Dias, Amin, Brown, et al., 2002; Jenkins et al., 2004; Poirier & Aggleton, 2009) and was replicated using different lesioning procedures (both excitotoxic lesions: Dumont et al., 2012; Jenkins, Dias, Amin, & Aggleton, 2002; Jenkins, Dias, Amin, Brown, et al., 2002; Jenkins et al., 2004; Poirier & Aggleton, 2009; and lesions made using radiofrequency: Jenkins et al., 2004). The reduction was evident at early post-surgical stages for both c-Fos and Zif268, from 1 week after anterior thalamic lesions (Poirier & Aggleton, 2009) in the superficial laminae (comprising layers II and upper III) of the granular retrosplenial cortex; the effect was confirmed to be persistent for c-Fos up to 1 year after anterior thalamic lesions (Poirier & Aggleton, 2009) and for Zif2668 up to 10 months after lesion (Jenkins et al., 2004). Reduction in number of positive-stained nuclei extended to granular retrosplenial cortex deep laminae (deep III – VI layers) for c-Fos from 8 weeks and for Zif268 from 4 weeks after anterior thalamic lesions (Poirier & Aggleton, 2009); this effect was persistent for both immediate early genes up to 10 months post-surgery (Jenkins et al., 2004).

In the dysgranular portion of the retrosplenial cortex, decreased levels of both c-Fos and Zif268 were found from 4 weeks after anterior thalamic lesions (Dumont et al., 2012; Poirier & Aggleton, 2009), and persisted up to 1 year after surgery for c-Fos (Poirier & Aggleton, 2009) and 10 months for Zif268 (Jenkins et al., 2004) (Table 1-3)

Interestingly, in one of these experiments in which a decrease of Zif268 protein levels was observed, pCREB levels also appeared reduced in the retrosplenial subregion Rgb, when rats with bilateral anterior thalamic lesions were compared to controls after having explored a radial arm maze in a novel room. As already mentioned (Sections 1.4.2.1 and 1.4.2.2), CREB protein is a constitutively expressed transcription factors that, once activated through phosphorylation, enters the nucleus where it is responsible for the increase of both *c-fos* and *zif268* transcription levels.

In order to verify the specificity of the effect of anterior thalamic lesions on c-Fos and Zif268 levels in the retrosplenial cortex, Poirier & Aggleton (2009) lesioned the laterodorsal thalamic nuclei unilaterally and compared the number of c-Fos and Zif268-positive cells between the lesioned and the intact hemisphere. Similar to the anterior thalamic nuclei, the laterodorsal thalamic nuclei are connected with all three retrosplenial subregions (see Section 1.1.4.1), but no effect was found either in the dysgranular or granular retrosplenial cortex (Table 1-3).

Hippocampal c-Fos and Zif268 expression levels

Anterior thalamic nuclei lesions reduced c-Fos levels both in the dorsal hippocampus (Jenkins, Dias, Amin, & Aggleton, 2002; Jenkins, Dias, Amin, Brown, et al., 2002) and ventral hippocampus (Jenkins, Dias, Amin, Brown, et al., 2002). In contrast, Zif268 levels were unaffected by the lesion (Dumont et al., 2012) (Table 1-4).

Considering the subicular complex, lesions of the anterior thalamic nuclei were associated in one study with a reduction of c-Fos levels in the postsubiculum and presubiculum (Jenkins, Dias, Amin, & Aggleton, 2002), but this was not confirmed in another experiment (Jenkins, Dias, Amin, Brown, et al., 2002). No changes were found in the parasubiculum and subiculum (Jenkins, Dias, Amin, & Aggleton, 2002; Jenkins, Dias, Amin, Brown, et al., 2002). The lesions also caused a decrease of Zif268 levels in the postsubiculum, but no changes were detected in the dorsal subiculum (Dumont et al., 2012) (Table 1-4).

Prefrontal cortex c-Fos and Zif268 expression levels

After anterior thalamic lesions, decreased levels of c-Fos were detected in the prelimbic cortex and caudal anterior cingulate cortex (Jenkins, Dias, Amin, Brown, et al., 2002), but this result was not replicated in another study (Jenkins, Dias, Amin, & Aggleton, 2002). No changes in Zif268 levels were found in the prelimbic and infralimbic cortices (Dumont et al., 2012) (Table 1-5).

1.4.6.2 Hippocampal lesions

The effect of unilateral hippocampal lesions on c-Fos and Zif268 expression levels in rats that performed a radial arm maze task has also been investigated; comparisons were made across the lesioned and non-lesioned hemispheres (Jenkins et al., 2006). In the lesioned hemisphere, c-Fos and Zif268 levels were reduced in the entorhinal, perirhinal and postrhinal cortices, presubiculum and anterior thalamic nuclei, but not in the prelimbic, infralimbic and anterior cingulate cortices. c-Fos levels were also significantly decreased in the postsubiculum, while Zif268 levels were reduced in the ventral subiculum and parasubiculum (Table 1-4, Table 1-5 and Table 1-6).

The levels in the retrosplenial cortex after hippocampal lesions were not measured in Jenkins et al. (2006) experiment, as they were analysed in a subsequent study (Albasser, Poirier, Warburton, & Aggleton, 2007). That study was divided into different smaller experiments that tested the impact on immediate early gene expression of different types of lesioning techniques (through radiofrequency or excitotoxic lesions with NMDA or ibotenic acid), different rat strains (Lister Hooded or Dark Agouti), different kinds of behavioural procedures (exploration of a novel environment or visual exposure to a novel spatial arrangement of familiar visual stimuli) and either bilateral or unilateral hippocampal lesions. The lesions were associated with a marked decrease of c-Fos and Zif268 levels in all three retrosplenial subregions (Rdg, Rgb and Rga), in both superficial and deep layers (the experiments were run from 1 month to 8 months after surgery) (Table 1-3).

To verify the specificity of these results, Albasser et al. (2007) lesioned the entorhinal cortex (which, like the hippocampus, is connected with the retrosplenial cortex, see Section 1.1.4.1), but no change in c-Fos levels were detected in Rgb retrosplenial subregion (Zif268 levels and the other retrosplenial subregions were not analysed).

1.4.6.3 Fornix lesions

Rats with unilateral fornix lesions performed the radial arm maze task. After the task, changes in the levels of c-Fos were measured in several brain structures. In the lesioned hemisphere, compared to the non-lesioned hemisphere, there was a significant decrease of c-Fos-positive nuclei in the hippocampus, ventral subiculum, presubiculum, parasubiculum, postsubiculum, entorhinal cortex, anterior thalamic nuclei, anterior cingulate cortex, granular retrosplenial cortex (but less pronounced than after either anterior thalamic or hippocampal lesions) and postrhinal cortex; in contrast, an increase was detected in the prelimbic cortex (Vann, Brown, Erichsen, & Aggleton, 2000b) (Table 1-3, Table 1-4, Table 1-5 and Table 1-6).

1.4.6.4 Mammillothalamic tract lesions

Transection of the mammillothalamic tract caused, in comparison to controls, a decrease in c-Fos levels (elicited by exploration of a novel environment) especially pronounced in all retrosplenial subregions (excluding the deep layer of Rga), and also present in the dorsal hippocampus, postsubiculum and prelimbic cortex; an increase was detected at the level of the parasubiculum, while no change was measured in the subiculum, presubiculum, anterior cingulate cortex, infralimbic cortex and entorhinal, perirhinal and postrhinal cortices (Vann & Albasser, 2009; Vann, 2013). The effect on Zif268 levels were not investigated in those experiments (Table 1-3, Table 1-4 and Table 1-5).

1.4.6.5 Lesions of the inputs to the mammillary bodies

To verify if the effects of mammillothalamic lesions were more influenced by the fornix or the midbrain inputs to the mammillary bodies, a study directly compared c-Fos levels in different structures of the Papez circuit after lesions to either the descending columns of the postcommissural fornix or to the ventral tegmental nucleus of Gudden (Vann, 2013) (Table 1-3, Table 1-4 and Table 1-5).

Lesions of the postcommissural fornix did not give rise to any c-Fos level change in the granular retrosplenial cortex, hippocampus, prelimbic and infralimbic cortices. Conversely, a significant decrease in c-Fos levels was detected after lesion of the Gudden's ventral tegmental nucleus in granular retrosplenial cortex, hippocampus and prelimbic cortex. These results confirm the greater importance of the midbrain

input, in comparison to the hippocampal input, to the mammillary bodies in determining their influence on c-Fos expression in other structures of the Papez circuit, and parallels what was found measuring spatial memory behavior (Section 1.3.4.3).

1.4.7 The use of antisense oligodeoxynucleotides to knock-down c-Fos and Zif268 expression levels

Antisense oligodeoxynucleotides (ODNs) are short (usually 13-25 base pairs in length) single strands of deoxyribonucleic acid, designed to be complementary to a specific target mRNA via Watson-Crick base-pair hybridisation (Dias & Stein, 2002). Once hybridised with their target mRNA, they are able to inhibit its transcription due to several mechanisms (Figure 1-14). Usually the antisense ODN/mRNA heteroduplex triggers the activity of the RNase H endonuclease enzyme, which is able to hydrolise the RNA strands present in RNA/DNA hybrids (Wu et al., 2004); thus the mRNA gets degraded, while the antisense ODN remains intact. Another mechanism by which antisense ODNs have their effect is by blocking mRNA translation by sterical hindrance of ribosomal activity (Lecosnier, Cordier, Simon, François, & Saison-Behmoaras, 2011). Finally, antisense ODNs can also work by destabilising pre-mRNA in the nucleus or by stopping mRNA maturation via splicing inhibition (Chan, Lim, & Wong, 2006).

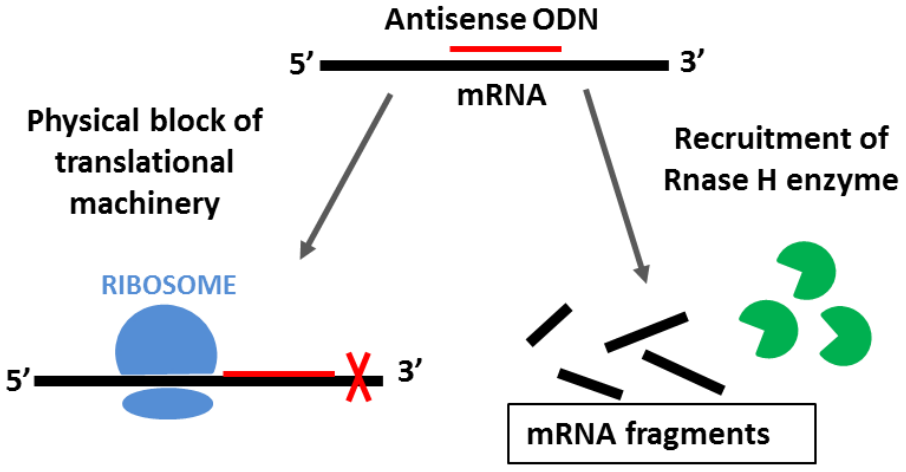

Figure 1-14. Main mechanisms of inhibition of mRNA transcription by the antisense ODNs.

Antisense ODNs have been infused into a number of different brain sites to assess the effect of inhibiting the functionality of specific molecules with a high degree of spatial and temporal precision (Guzowski, 2002). Antisense ODNs are taken up by a large number of neurons approximately 15-30 minutes post-infusion (Ogawa, Brown, Okano, & Pfaff, 1995; Sommer et al., 1998; Yee, Ericson, Reis, & Wahlestedt, 1994). Antisense ODNs levels within the neurons starts to decline from four hours post-infusion and they are almost absent 24 hours post-infusion (Ogawa et al., 1995). The uptake of antisense ODNs by glial cells appears to be very inefficient (Ogawa et al., 1995; Sommer et al., 1998).

Antisense ODNs are negatively charged hydrophilic macromolecules, which are not able to passively diffuse into the cellular membrane (Sommer et al., 1998); instead, an active mechanism of receptor-mediated endocytosis mediates their uptake into the cells (Loke et al., 1989). Once in the cell they move inside the nucleus using passive diffusion (Leonetti, Mechti, Degols, Gagnor, & Lebleu, 1991).

The unmodified antisense ODNs have a phosphorodiester backbone; their degradation within the cell by nucleases is very rapid (Wickstrom, 1986) and gives rise to toxic mononucleotides (Vaerman et al., 1997). In order to overcome these limitations, different chemical modifications have been created that increase resistance to nucleases and decrease the non-sequence-specific toxicity (Dias & Stein, 2002). The most widely used are the phosphorothioated ODNs, and they will be the focus of the next section as they are most relevant to this body of work.

1.4.7.1 Phosphorothioated antisense ODNs

In the modified phosphorothioated version of the antisense ODNs, a sulphur atom replaces one of the non-bridging oxygen atoms in the phosphodiester bond in the backbone of the ODN strand (Chan et al., 2006) (Figure 1-15).

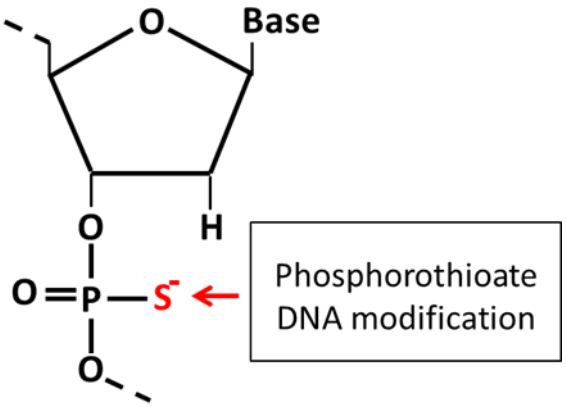

Figure 1-15. Chemical modification in phosphorothioated ODNs.

The phosphorothioate modification increases the molecular resistance of the ODN strands to nuclease attack, improving their bioavailability, as they are still able to exert their effect up to 10-15 hours after infusion, while after 24 hours they are almost absent in the cell (Cirelli, Pompeiano, & Tononi, 1995; Lee, Everitt, & Thomas, 2004). Furthermore, this modification also enhances the absorption of the ODN molecule into the cell via endocytosis and promotes the action of RNase H on the target mRNA (Bonham et al., 1995; Chan et al., 2006; Dias & Stein, 2002). However there are some drawbacks in the use of the phosphorothioated antisense ODNs: for example, their affinity to their target mRNA decreases (in comparison to a non-modified antisense ODN) because the melting temperature of the phosphorothioated antisense ODN/mRNA heteroduplex increases by about 0.5 °C/nucleotide (Chan et al, 2006; Sommer et al, 1998). Furthermore, the phosphorothioated antisense ODNs can bind to some neurotrophic factors (e.g. PDGF and VEGF) and inhibit their biological activity, thus resulting in neurotoxicity (Chiasson, Armstrong, Hooper, Murphy, & Robertson, 1994). In order to maintain the benefits of using the phosphorothioated antisense ODNs, but at the same time reducing their limitations, partial modifications can be used (Cirelli et al., 1995), such as antisense ODN stretches with phosphorothioate substitutions only at the extremities (“end-capped”).

Specific end-capped phosphorothioated antisense ODNs targeting either *c-Fos* or *Zif268* mRNAs have been designed and infused in different sites in the rat brain. Their efficacy has been verified experimentally by analysing animals' post-infusion performance on different behavioural tasks. Using this method, a number of studies have identified a role for c-Fos and Zif268 expression in supporting different forms of long-term memory (Countryman, Kaban, & Colombo, 2005; Katche et al., 2010, 2013; Lee et al., 2004; Malkani, Wallace, Donley, & Rosen, 2004; Seoane, Tinsley, & Brown, 2012; Tolliver, Sganga, & Sharp, 2000).

1.5 What this thesis will cover

The overall aims of this body of work are to try and uncover why damage to the medial diencephalon, and mammillothalamic tract in particular, results in memory impairments. The main focus will be on distal effects, within the Papez circuit, that are brought about by mammillothalamic tract lesions and whether these changes contribute to the profile of memory impairments seen.

Analysis of the expression of immediate early genes can be used to assess the functionality of different brain areas simultaneously. This technique can be used to compare brain activity in the intact brain and in the lesioned brain. As already mentioned (Section 1.4.6.4), a previous study found an effect of mammillothalamic tract lesions on c-Fos protein expression levels on a number of distal brain regions (Vann & Albasser, 2009). Chapter 2 will extend these findings by measuring expression levels of protein Zif268 in the Papez circuit (specifically in the retrosplenial cortex, hippocampus and subicular complex) and connected areas (the medial prefrontal cortex, specifically the anterior cingulate, prelimbic and infralimbic cortices) in animals that had received mammillothalamic tract lesions. As previously mentioned, c-Fos and Zif268 exert a different role in the cell, and possibly in memory processes (the former being implicated in long term depression and the second in long term potentiation; see Sections 1.4.2.1 and 1.4.2.2). Thus the results of this experiment could contribute to a better understanding of the role of retrosplenial hypofunctionality after medial diencephalic lesions.

The loss of immediate early gene expression at the level of the retrosplenial cortex, after either medial diencephalic or hippocampal lesions has been described as "covert pathology", as the retrosplenial neurones, even if dysfunctional, are neither decreased in number nor exhibit consistent changes in the morphology of their somata (Albasser

et al., 2007; Jenkins et al., 2004; Poirier & Aggleton, 2009; Poirier, Shires, et al., 2008). However, a recent study found a decrease in spine density in the apical dendritic arbors of superficial fusiform pyramidal neurones in Rgb after anterior thalamic lesions (Harland et al., 2014). Chapter 3 aimed to investigate a possible microstructural correlate of the loss of immediate early gene expression in the retrosplenial cortex after mammillothalamic tract lesions. I examined whether lesioning the mammillothalamic tract caused any change in the dendritic microstructure of neurones located in Rgb, as this area presents the most dramatic decrease in immediate early gene expression after medial diencephalon lesions. Specifically, lesioned and control animals were compared in terms of dendritic complexity and dendritic apical spine density measured at the level of the small pyramidal neurones located in layers II and upper III of Rgb, which receive most of the anterior thalamic input (Wyss, Groen, & Sripanidkulchai, 1990). Visualisation of dendritic arbors was obtained using Golgi staining.

The functional effect of the loss of immediate early gene expression in certain areas of the Papez circuit after medial diencephalic or hippocampal lesions is still uncertain. It is not clear whether this decrease contributes to the spatial memory impairments found in the lesioned animals or it is simply an indicator of a disruption within the system. Chapters 4, 5 and 6 describe a series of interconnected experiments aimed at evaluating the impact on spatial memory of knocking down immediate early gene expression in selected regions of the Papez circuit. The final goal was to infuse antisense ODNs, targeting either c-Fos or Zif268 expression, into either the dorsal hippocampus or retrosplenial cortex and subsequently testing animals on tasks that tax spatial memory. If these immediate early genes are necessary for supporting the memory process, the knocking down of their expression through the infusion of specific ODNs will impair performance on spatial memory tasks. This would support the hypothesis that a loss of immediate early genes in the Papez circuit after medial diencephalic lesions is not just a secondary effect of the lesion but has a functional effect that can be appreciated at the behavioural level.

Specifically, Chapter 4 will describe the development of a spatial memory task (a 3-hour delay with maze rotation variant of the radial arm maze task) designed to test rats after antisense ODN infusion. In the same chapter, two additional experiments will be described, aimed at verifying the efficacy of cannulae implantation into the dorsal hippocampus and of the infusion technique by infusing muscimol (a GABAergic agonist) and looking at the effects on spatial memory using a reinforced T-maze alternation and a radial arm maze task.

Chapter 5 verified the effect on spatial memory of infusing antisense ODNs specific for either c-Fos or Zif268 or both in the dorsal hippocampus; spatial memory performance was evaluated using two different spatial memory tasks: the modified radial arm maze task described in Chapter 3 and the object-in-place task with 3 hours of delay between the sample and the test phase. Furthermore, in Chapter 5, the effect of infusing antisense ODNs into the dorsal hippocampus in reducing the levels of c-Fos and Zif268 proteins will be measured using the Western blot technique.

Chapter 6 comprises two experiments. In the first experiment, the efficacy of cannulation surgery and infusion procedure in the retrosplenial cortex was evaluated by infusing the animals with muscimol and subsequently testing them in the object-in-place task. In the second experiment, animals' performance in the object-in-place task was tested after infusion into the retrosplenial cortex of antisense ODNs knocking down Zif268 expression; in this experiment, the effect of the antisense ODN infusions was evaluated also at the histological level using immunohistochemistry.

Chapter 2 Zif268 levels in selected areas of the Papez circuit and medial prefrontal cortex after mammillothalamic tract lesions

2.1 Introduction

Mammillothalamic tract damage has been consistently linked to diencephalic amnesia in humans (Carlesimo et al., 2007; Van der Werf et al., 2000; Yoneoka et al., 2004) and spatial memory deficits in animals (Field et al., 1978; Krieckhaus & Randall, 1967; Thomas & Gash, 1985; Vann & Aggleton, 2003; Vann, Honey, & Aggleton, 2003). Mammillothalamic tract lesions disconnect the anterior thalamic nuclei from their mammillary body inputs. The underlying mechanism as to why damage to this specific structure results in memory impairments is still uncertain.

Studies on rats have shown that anterior thalamic lesions give rise to a widespread immediate early gene (c-Fos and Zif268) hypoactivity in the rest of the Papez circuit and connected areas when animals are engaged in activities taxing spatial memory (Dumont et al., 2012; Jenkins, Dias, Amin, & Aggleton, 2002; Jenkins, Dias, Amin, Brown, et al., 2002; Jenkins et al., 2004; Poirier & Aggleton, 2009; Poirier, Shires, et al., 2008). It is unknown if this hypoactivity has a functional effect on memory function or is just a secondary effect of the anterior thalamic lesions.

Given the dense connections from the mammillary bodies to the anterior thalamic nuclei via the mammillothalamic tract, one study (Vann & Albasser, 2009) investigated if lesioning the tract also caused hypoactivity (measured as a change in c-Fos expression levels) in the other structures of Papez circuit (retrosplenial cortex, in all its subdivisions: rostral Rdg, rostral Rgb and Rga, in both superficial and deep layers; hippocampal system: ventral and dorsal hippocampus; subicular complex; parahippocampal regions) and connected medial prefrontal areas (prelimbic, infralimbic and anterior cingulate cortices) in the brain of rats exploring a novel environment, a task able to trigger immediate early gene expression in these brain structures (Hess et al., 1995; Jenkins, Dias, Amin, Brown, et al., 2002; Vann, Brown,

& Aggleton, 2000; Vann, Brown, Erichsen, et al., 2000a; Zhu et al., 1997). The main results of this experiment have been summarised in Figure 2-1. In short, lesioning the mammillothalamic tract gave rise to a significant decrease of c-Fos expression in retrosplenial cortex (rostral portion of both Rdg and Rgb, in both superficial and deep layers, and in superficial layers of Rga), dorsal hippocampus (all three main subfields: dentate gyrus, CA1 and CA3), postsubiculum and prelimbic cortex; a significant increase was found in parasubiculum; no other relevant change was found in the remaining regions. These findings were replicated in another study (Vann, 2013) and are particularly interesting as the mammillothalamic tract does not directly target any of the regions where a c-Fos change was detected unlike the anterior thalamic nuclei (Conde' et al., 1990; Shibata, 1993a, 1993b; Van Groen & Wyss, 1995; Wyss, Swanson, & Cowan, 1979). Furthermore, these effects were specific to mammillothalamic tract transections, and not just caused by generic brain damage/deafferentation, as lesions of the amygdala, which directly innervates the hippocampal formation (Pitkänen, Pikkarainen, Nurminen, & Ylinen, 2006), resulted in a completely different pattern of c-Fos changes, i.e., an increase rather than a decrease in c-Fos levels in the retrosplenial subregions; an increase in c-Fos levels in the dorsal CA3 subdfield and a decrease in the ventral hippocampus (Vann & Albasser, 2009).

To expand on the Vann & Albasser (2009) study, the present experiment used brain sections from the same animals to verify if Zif268 expression levels were also affected by mammillothalamic tract lesions, in order to evaluate if the effect is more general or if it is specific to the c-Fos immediate early gene. This new analysis included all the regions where a significant change in c-Fos was detected and also included the caudal (posterior to splenium) portions of Rdg and Rgb.

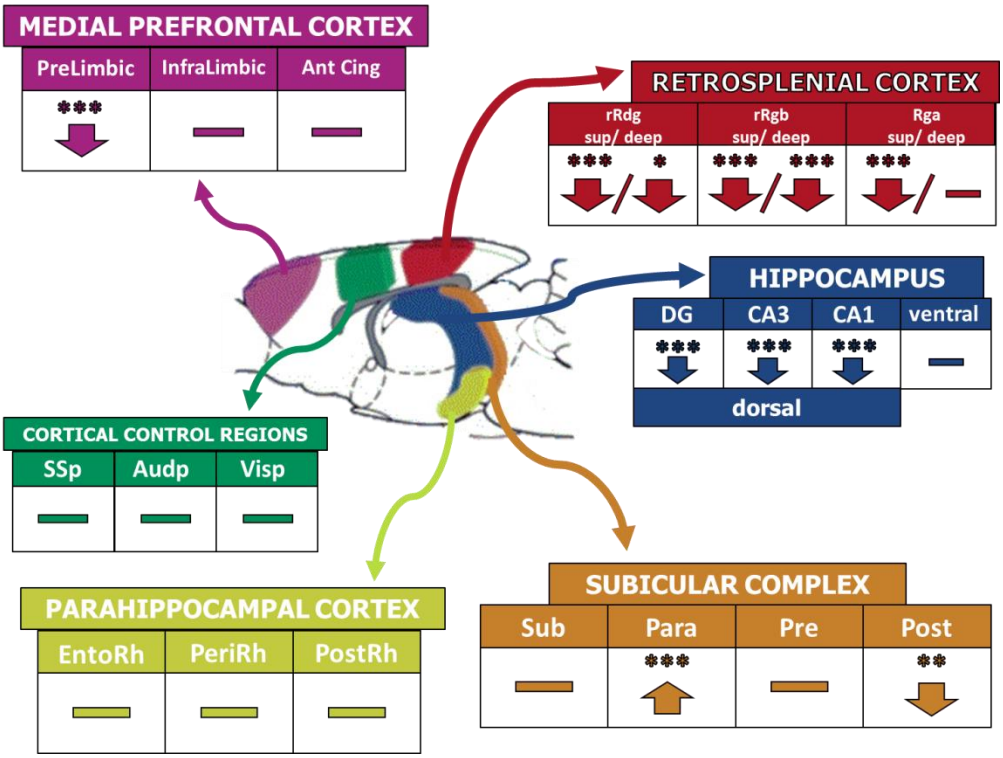

Figure 2-1. Summary of results for c-Fos expression levels after mammillothalamic tract lesions (MTT lesions) in the Papez circuit and connected structures (figure adapted from Vann & Albasser, 2009). A down arrow indicates a decrease in immediate early gene levels in the mammillothalamic tract-lesioned animals compared to the surgical/behavioural controls, an up arrow indicates an increase, while the horizontal bar indicates no significant change. Significance levels of difference in comparison to control levels are expressed with asterisks: * $p < 0.05$, ** $p < 0.01$, *** $p < 0.001$. The areas analysed are: anterior cingulate cortex (Ant Cing), auditory primary cortex (Audp), CA3 (dorsal hippocampus), CA1 (dorsal hippocampus), dentate gyrus (DG, in dorsal hippocampus), entorhinal cortex (EntoRh), infralimbic cortex, parasubiculum (Para), perirhinal cortex (PeriRh), postsubiculum (Post), postrhinal cortex (PostRh), presubiculum (Pre), prelimbic cortex, rostral Rdg superficial layers (rRdg sup), rostral Rdg deep layers (rRdg deep), Rga superficial layers (Rga sup), Rga deep layers (Rga deep), rostral Rgb superficial layers (rRgb sup), rostral Rgb deep layers (rRdg deep), somatosensory primary cortex (SSp), subiculum (Sub), ventral hippocampus (ventral), visual primary cortex (Visp).

2.2 Methods

Animal handling, surgery, behavioural testing and immunohistochemical procedure had already been performed for a published study (Vann & Albasser, 2009). My contribution was performing cell counting and statistical analysis. In the next section, all the methods will be reported for clarity.

2.2.1 Subjects

Subjects were 20 male naïve Dark Agouti rats (Harlan, UK), weighing 215-250 grams at the time of surgery. Rats were housed in pairs under diurnal light conditions (14 h light/10 h dark) and testing was carried out during the light phase at a regular time. They were given free access to water throughout the experiments. During the behavioural test period the animals were food deprived, but their body weight did not fall below 85% of free feeding weight. Animals were thoroughly handled before the study began in order to habituate them to the handling procedure. The experiment was carried out in accordance with UK Animals (Scientific Procedures) Act, 1986 and associated guidelines.

2.2.2 Behavioural procedure

2.2.2.1 Forced-runs in a radial arm maze

Apparatus

An eight-arm radial maze was used for behavioural testing, consisting of a wooden central platform (diameter 34 cm) and eight equally spaced wooden radial arms (each long 87 cm and 10 cm wide); the walls of the arms were made of clear Perspex panels (height 12 cm). A clear Perspex guillotine door (height 24 cm) attached to a pulley system was placed at the beginning of each arm, at the conjunction with the central platform, so that the access to each arm could be controlled by the experimenter. There were food wells at the end of each arm into which the sucrose reward pellets (45 mg; Noyes Purified Rodent Diet, Lancaster, NH, US) could be placed.

Two identical radial arm mazes (one for the training and the other for the final test day) were placed in two rooms easily discriminable for size (one 295 cm x 295 cm x 260 cm, the other 255 cm x 330 cm x 260 cm), shape, lighting and with distinct visual cues on the walls to help animals to orientate in the maze (e.g. high-contrast stimuli and geometric shapes)

Post-surgery behavioural procedure

A forced-run version of the radial arm maze task was used because mammillothalamic tract-lesioned rats are normally impaired in the standard working memory version (Vann & Aggleton, 2003); in this way, lesioned and control animals could be matched for motor responses and number of rewards received, so they experienced similar environmental stimulations.

Rats were trained in matched pairs (one mammillothalamic tract-lesioned animal and one yoked control) to retrieve sucrose pellets for running down pre-selected arms of the radial arm maze. All arms were baited at the beginning of each trial (a trial comprises a visit to all eight arms), and their access was controlled by the experimenter through the pulley system operating the guillotine doors. At the end of one trial (when all eight arms were visited) the rat was placed in a holding box for approximately 2 minutes, and during this time all the arms were re-baited. Every day, for 11 consecutive days, rats had one session of this behavioural task, lasting 20 minutes in total and consisting of multiple trials; within each session, the arm sequences were different and randomised for consecutive trials. Matched pairs of animals (one mammillothalamic tract-lesioned animal and its yoked control) completed the same number of trials and visited the same arms in the same order. On day 12 (the final day of test), animals performed the same task but in a novel room; each animal was placed in a dark and quiet room 30 minutes before the beginning of the session and 90 minutes after, before being perfused; it has been shown that about 90 minutes is the time required for *c-fos* and *zif268* genes to be expressed as proteins after neuronal stimulation (Zangenehpour & Chaudhuri, 2002).

2.2.3 Surgical procedure

Animals were divided into two groups, one receiving bilateral mammillothalamic tract lesions (n = 10, MTT-lesioned) and the other were their matched surgical control (n = 10, controls). Animals were deeply anesthetized by intraperitoneal injection of sodium pentobarbital (60 mg/kg) and then positioned in a stereotaxic head-holder (David Kopf instruments, California, US). The position of the incisor bar of the stereotaxic frame set at +5.0 mm to the interaural line, to maintain the skull flat on the horizontal plane. A midline incision was made on the top of the scalp to expose the dorsal skull, which was drilled at the point of the lesion. An electrode (0.7-mm tip length, 0.25-mm

diameter; Radionics TCZ, Radionics, US) was lowered vertically and its tip temperature was raised to 60°C for 15 seconds using a RFG4-A Lesion Maker (Radionics, US). The stereotaxic coordinates were: antero-posterior (AP) +4.2 mm (relative to bregma), lateral-medial (LM) ±0.9 mm (relative to bregma), and dorso-ventral (DV) -6.9 mm (from top of the cortex). For the surgical controls the electrode was positioned at the same AP and LM but only lowered to DV +1.0 mm above the lesion site to avoid damaging the tract; the electrode's tip temperature was not raised. After surgery, the skin was sutured, an antibiotic powder applied (Acramide: Dales Pharmaceuticals, UK) and animals received 5 ml of glucose saline subcutaneously. They were then placed in a temperature-controlled recovery box until they awoke from the anaesthetic. All animals were allowed three weeks to recover after surgery before starting the behavioural procedure.

2.2.4 Zif268-positive cells immunohistochemistry

Rats were anaesthetised with sodium pentobarbital (60 mg/kg, Euthatal, Rhone Merieux, UK) 90 minutes after they have completed the final test session in the radial arm maze, and then transcardially perfused with 0.1 M phosphate buffer saline (PBS) followed by 4% paraformaldehyde in PBS (PFA). The brains were then extracted and postfixed in 4% PFA for 4 hours, and then transferred to 25% sucrose in distilled water overnight. On the following day, brains were cut in the coronal plane using a freezing microtome (40 µm slice thickness), and three series (1:3) of sections were collected: two series were collected in PBS for Zif268 and c-Fos staining (c-Fos staining has been described in Vann & Albasser, 2009). The third series was mounted directly onto gelatin-coated slides and stained using cresyl violet, a Nissl stain, for verification of the lesion location and size.

For Zif28 staining, sections were transferred to 10-mM citrate buffer (pH 6.0) dissolved in deionized H_2O, and then incubated in water bath at 70°C for 30 min. Subsequently, sections were incubated for 10 minutes on a shaker in a solution of 0.3% hydrogen peroxidase (Fisher Scientific, US) in PBST (0.2% Triton in PBS), in order to block endogenous peroxidase activity. Then they were washed four times (10 minutes each) with PBST. Next, sections were incubated with primary Zif268 antibody (Egr-1 (C19): Sc-189; Santa Cruz Biotechnology, Texas, US) diluted 1:3000 in PBST: they were stirred on the shaker in the primary antibody solution for 10 minutes at room temperature and then they were incubated in the same primary antibody solution for

48 hours at +4°C (at the end of the first 24 hours the sections in the primary antibody solution were stirred again for another 10 minutes at room temperature and then returned to the fridge). Sections were then rinsed again four times (10 minutes each) in PBST, and then incubated in biotinylated goat secondary antibody (diluted 1:200 in PBST; Vectastain, Vector Laboratories, Burlingame, USA) and 1.5% normal goat serum, and left on the shaker for 2 hours at room temperature. After this, sections were washed four times (10 minutes each) in PBST and processed with avidin-biotinylated horseradish peroxidase complex in PBST (Vectastain Elite ABC kit PK-6100, Vector Laboratories, UK) for 1 hour at room temperature, again with constant rotation on the shaker. Sections were then rinsed four times (10 minutes each) in PBST, and then washed two times (10 minutes each) in 0.05 M Tris buffer (pH 7.4, prepared diluting Trizma base in distilled water). Finally, sections were incubated with 3.3'-diaminobenzidine (DAB Substrate Kit, Vector Laboratories, UK) until a brown stain was obtained (requiring usually no more than few minutes); the reaction was stopped in cold PBS. Sections were mounted on gelatin-coated slides, dehydrated through a graded series of alcohols and cover-slipped (DPX, Thermoscientific, UK). Sections from each behaviourally matched pair of animals (MTT-lesioned and yoked surgical control) were processed simultaneously.

2.2.5 Zif268-positive cell counts

Counting procedures were carried out without knowledge of group assignment. Images were viewed on a Leica microscope (5X magnification) and photographed using an Olympus DP70 camera. The program ImageJ (1.46r version, NIH, US) was used to grey-scale the images and to count the number of Zif268-positive neuronal nuclei above threshold (the threshold value was set manually for each picture). For each group of regions, counts were made in a frame area comprising all laminae under investigation. This counting procedure is not stereological, and so it does not provide a precise account of absolute Zif268-positive cell numbers; however, it provides account of relative numbers, allowing group comparisons. All nuclei above threshold and between 10-100 μm^2 in area size were counted. For each brain region analysed, Zif268-positive cell counts were taken from an average of six sections (consecutive if possible) per brain (see Table 2-1 for details of the number of sections obtained in each region; the variability in these numbers was due to different qualities of staining and different extensions on the antero-posterior axis of the regions of interest), and a mean was calculated for each animal.

	AREA	GROUP	NUMBER OF SECTIONS
RETROSPLENIAL CORTEX	rRgb superficial layer	CONTROL	105
		MTT-LESIONED	98
	rRgb deep layer	CONTROL	103
		MTT-LESIONED	92
	rRdg superficial layer	CONTROL	107
		MTT-LESIONED	93
	rRdg deep layer	CONTROL	109
		MTT-LESIONED	98
	cRgb superficial layer	CONTROL	55
		MTT-LESIONED	53
	cRgb deep layer	CONTROL	57
		MTT-LESIONED	54
	cRdg superficial layer	CONTROL	56
		MTT-LESIONED	54
	cRdg deep layer	CONTROL	56
		MTT-LESIONED	55
	Rga superficial layer	CONTROL	58
		MTT-LESIONED	53
	Rga deep layer	CONTROL	58
		MTT-LESIONED	50
DORSAL HIPPOCAMPUS	DG	CONTROL	77
		MTT-LESIONED	68
	CA3	CONTROL	75
		MTT-LESIONED	66
	CA1	CONTROL	78
		MTT-LESIONED	66
SUBICULAR COMPLEX	Parasubiculum	CONTROL	41
		MTT-LESIONED	36
	Presubiculum	CONTROL	41
		MTT-LESIONED	36
	Postsubiculum	CONTROL	42
		MTT-LESIONED	36
PREFRONTAL CORTEX	Infralimbic cortex	CONTROL	76
		MTT-LESIONED	74
	Prelimbic cortex	CONTROL	75
		MTT-LESIONED	74
	Anterior cingulate cortex	CONTROL	74
		MTT-LESIONED	75

Table 2-1. Number of sections used for each region of interest, subdivided by Lesion group (MTT = mammillothalamic tract). DG = dentate gyrus, rRgb = rostral Rgb, rRdg = rostral Rdg, cRgb = caudal Rgb, cRdg = caudal Rdg.

2.2.6 Regions of interest

The regions of interest were identified in coronal sections, using the nomenclature adopted by Wyss & Van Groen (1992) (Figure 2-2). These were the same regions in which Vann & Albasser (2009) found significant changes in c-Fos expression after mammillothalamic tract lesions; this choice was made in order to verify if these changes could also be extended to Zif268.

In the dorsal hippocampus, separate counts were made in its three main subfields: dentate gyrus, CA1, and CA3. In the retrosplenial cortex, counts were made in its three main subregions: granular b (Rgb), granular a (Rga), and dysgranular cortex (Rdg), keeping separated the superficial (II and upper III) and deep (lower III to VI) layers; the border between superficial and deep layers is signalled by an abrupt change in cell size and packaging density (Jenkins et al., 2004; Vann & Albasser, 2009). Furthermore, for Rgb and Rdg, counts were taken at both rostral (- 2.56 mm from bregma) and caudal (- 6.04 mm from bregma) levels. In the subicular complex, cell counts were performed in the parasubiculum, the presubiculum, and the postsubiculum. In the medial prefrontal cortex, counts were made in the infralimbic cortex, the prelimbic cortex and the anterior cingulate cortex.

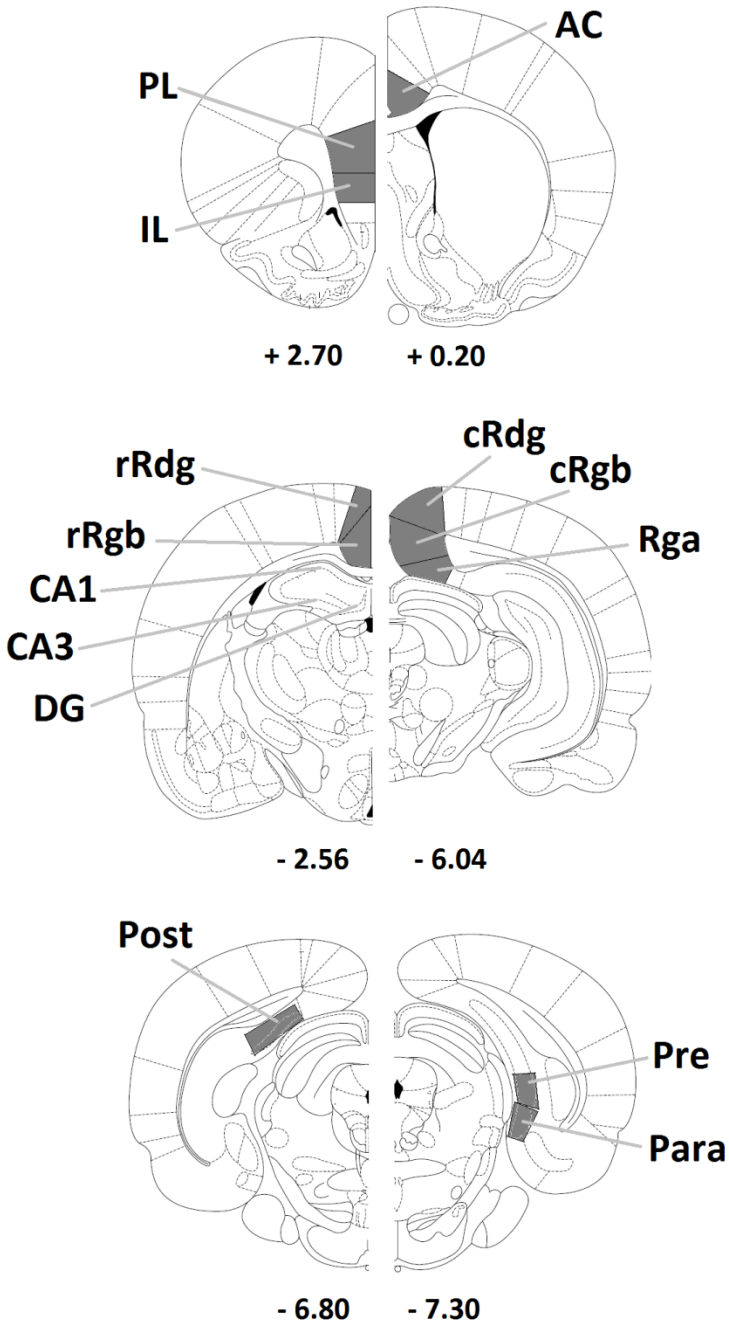

Figure 2-2. Location in coronal schematic sections of the regions of interest where cell counting was performed. Numbers under each section refer to their distance from bregma, referring to the brain atlas Paxinos & Watson (1998). Pictures were adapted from a digital version of the atlas. AC (anterior cingulate cortex), CA1, CA3, cRdg (caudal dysgranular retrosplenial cortex), cRgb (caudal granular b retrosplenial cortex), DG (dentate gyrus), IL (infralimbic cortex), Para (parasubiculum), PL (prelimbic cortex), Post (postsubiculum), Pre (presubiculum), Rga (granular a retrosplenial cortex), rRdg (rostral dysgranular retrosplenial cortex), rRgb (rostral granular b retrosplenial cortex).

2.2.7 Statistics

Analyses were carried out on mean raw counts which were derived by averaging the values obtained for all the sections for each region of interest in each brain.

A mixed ANOVA design was used to analyse the results; different anatomical areas were grouped together for the analysis of the variance, so that each ANOVA comprised related brain areas:

- Two different ANOVAs were performed for analysing the cell counts of the retrosplenial cortex, grouping the subdivisions on the basis of their rostro-caudal location. Analysis of the rostral retrosplenial cortex was carried out with Lesion as between-subject factor (two levels: MTT-lesioned / controls), while Region (two levels: rostral Rgb / rostral Rdg) and Layer (two levels: superficial / deep) were the within-subject factors. Similarly, analysis of the caudal retrosplenial cortex was carried out with Lesion as between-subject factor (two levels: MTT-lesioned / controls), while Region (three levels: caudal Rgb / caudal Rdg / Rga) and Layer (two levels: superficial / deep) were the within-subject factors.
- Analysis of the dorsal hippocampus was carried out with Lesion as between-subject factor (two levels: MTT-lesioned / controls), and Region (three levels:
- dentate gyrus / CA3 / CA1) as within-subject factor.
- Analysis of the parasubicular, presubicular and postsubicular cortices was carried out with Lesion as between-subject factor (two levels: MTT-lesioned / controls), and Region (three levels: parasubiculum / presubiculum / postsubiculum) as within-subject factor.
- Analysis of the medial prefrontal cortex was carried out with Lesion as between-subject factor (two levels: MTT-lesioned / controls), and Region (three levels: prelimbic cortex / infralimbic cortex / anterior cingulate cortex) as within-subject factor.

When the sphericity assumption was violated, Greenhouse-Geisser correction was applied to the degrees of freedom. When significant interactions were found, the simple effects for each brain region were analysed as recommended by Winer (1971) using the pooled error term.

The main effect of Region (and of Layer in the case of the retrosplenial cortex) was not considered because all regions of interest are different in size, thus the comparison would be meaningless. SPSS software (version 20, IBM Corporation) was used to carry out statistical analyses. The threshold for significance was set at $p < 0.05$

2.3 Results

2.3.1 Lesion histology

Looking at the MTT-lesioned brains, nine out of ten rats had discrete and complete bilateral lesions (Figure 2-3); one rat had some sparing of the tract in the left hemisphere. The transection of the mammillothalamic tract in this experiment disconnected medial but not lateral mammillary nuclei from the anterior thalamic nuclei; this was confirmed in another study (Vann & Albasser, 2009) by using retrograde tracer injections in the anterior thalamic nuclei of additional animals that received equivalent mammillothalamic tract lesions. Given that connections between the medial mammillary nuclei and the anterior thalamic nuclei are only unilateral (Hayakawa & Zyo, 1989), cell counting was performed only in the right hemisphere of the case with partial sparing of the left mammillothalamic tract.

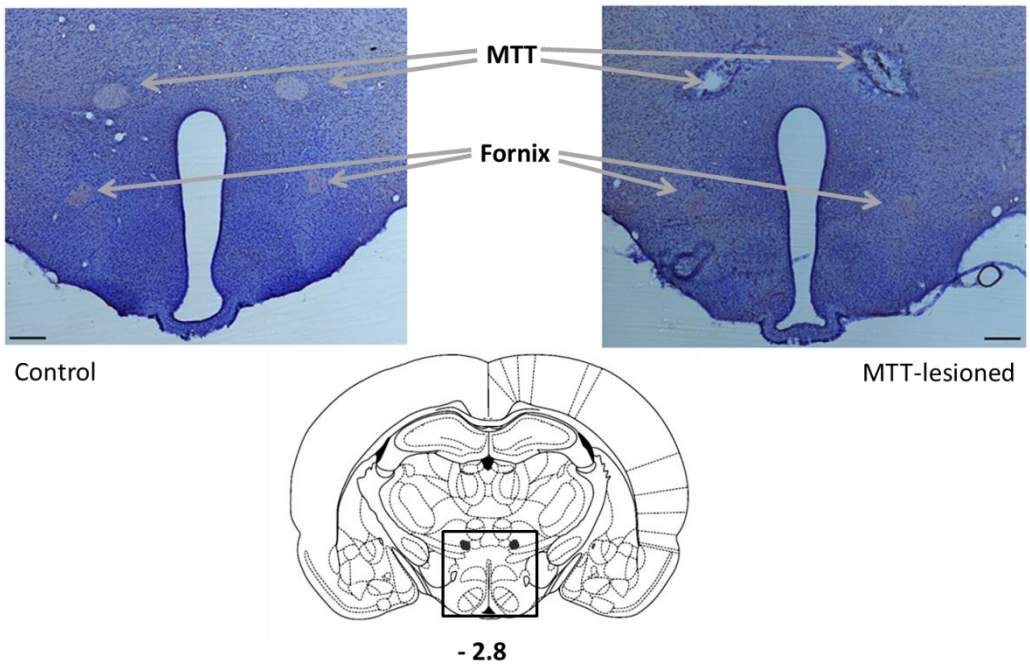

Figure 2-3. Representative coronal sections from a control animal (left) and a mammillothalamic tract (MTT)-lesioned animal (right). Bilateral lesions of the mammillothalamic tract are evident. In all cases the fornix was intact. Scale bar 200 µm. The lesion location is also visible in the schematic section adapted from Paxinos & Watson atlas (1998), with the number indicating distance from bregma (in mm).

2.3.2 Behaviour

These results were collected and analysed as part of a previous experiment (Vann & Albasser, 2009) but are reported for clarity.

On the final test day, animals performed 20 minutes of forced-runs in the radial arm maze in a novel room. Animals completed 4.1 ± 0.5 (mean ± SEM) trials; this number was significantly smaller than the number of trials completed on the last day of training in the familiar room (mean ± SEM: 4.6 ± 0.8; Wilcoxon $T = 247$, $p < 0.01$), and probably was due to the effect of spatial novelty on rats' exploratory activity. MTT-lesioned animals were yoked to their respective controls in respect of number of trials executed in all sessions, including the test session.

2.3.3 Counting of Zif268*-positive cells*

2.3.3.1 Retrosplenial cortex

Looking at Zif268 expression levels in the rostral part of retrosplenial cortex (comprising rostral Rgb and rostral Rdg), statistical analysis revealed a significant main effect of Lesion ($F_{1,18} = 7.4$, $p < 0.05$); the interactions of Lesion factor with either Region or Layer or both factors were not significant (Lesion x Region: $F < 1$; Lesion x Layer: $F_{1,18} = 2.4$, $p = 0.14$; Lesion x Region x Layer: $F < 1$) (Figure 2-4; histological representative example Figure 2-5).

.

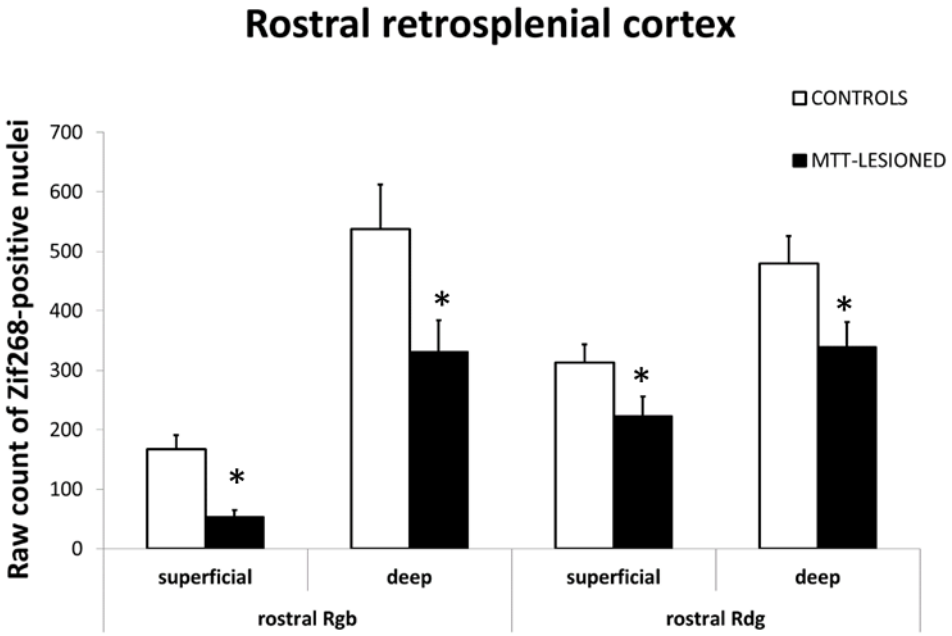

Figure 2-4. Raw counts (mean ± SEM) of Zif268-positive nuclei in the rostral retrosplenial cortex (rostral Rgb and rostral Rdg) after bilateral mammillothalamic tract lesions and in controls. Level of significance: * $p<0.05$.

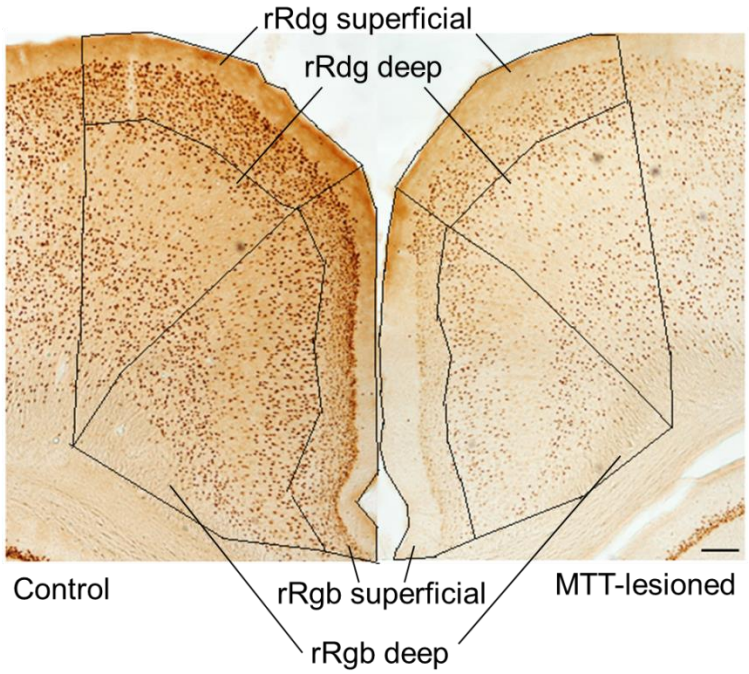

Figure 2-5. Representative coronal sections of the rostral portion of the retrosplenial cortex. The section on the left is from a control animal, the section on the right is from a mammillothalamic tract (MTT)-lesioned animal. The different retrosplenial subdivisions are reported: rRdg = rostral Rdg; rRgb = rostral Rgb. It is evident the decrease in the number of Zif268-positive nuclei in the lesioned animal. Scale bar 100 µm.

Also in the caudal part of retrosplenial cortex (which includes Rga, as it is located caudally) there was a Lesion main effect ($F_{1,18} = 5.7$, $p < 0.05$); among the interactions of Lesion factor with Region and Layer factors, only Lesion x Region was significant ($F_{2,36} = 6.0$, $p < 0.01$; Lesion x Layer: $F_{1,18} = 2.7$, $p = 0.12$; Lesion x Region x Layer: $F_{2,36} = 1.9$, $p = 0.17$). In order to further explore the interaction Lesion x Region, simple effects were calculated: a significant difference between MTT-lesioned and control animals was present in both caudal Rgb and caudal Rdg (both $p < 0.05$), but not in Rga ($p = 0.72$) (Figure 2-6; histological representative example Figure 2-7).

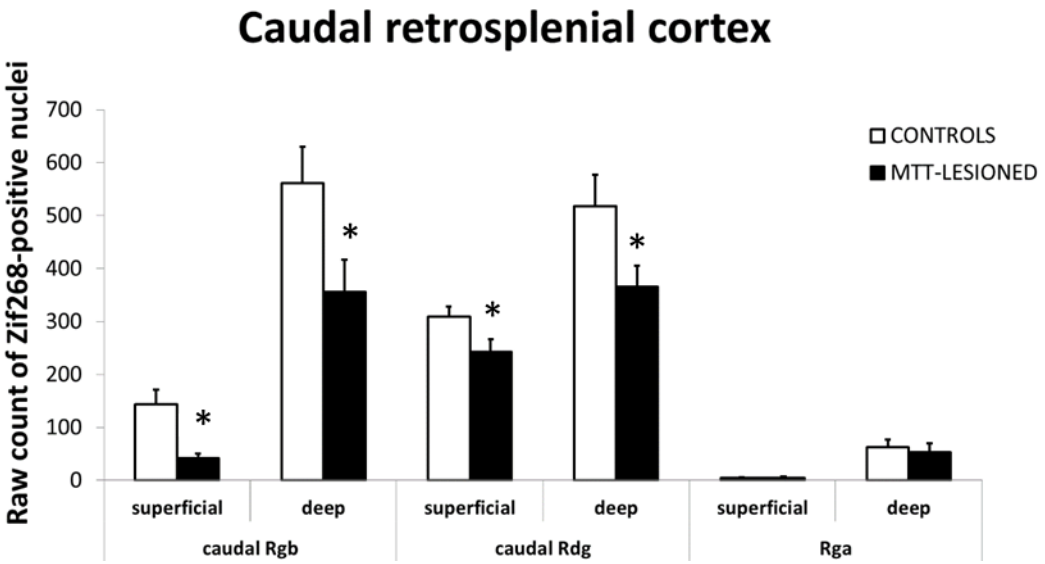

Figure 2-6. Raw counts (mean ± SEM) of Zif268-positive nuclei in the caudal retrosplenial cortex (caudal Rgb, caudal Rdg and Rga, which is present only at caudal level) after bilateral mammillothalamic tract lesions and in controls. Level of significance: * $p<0.05$.

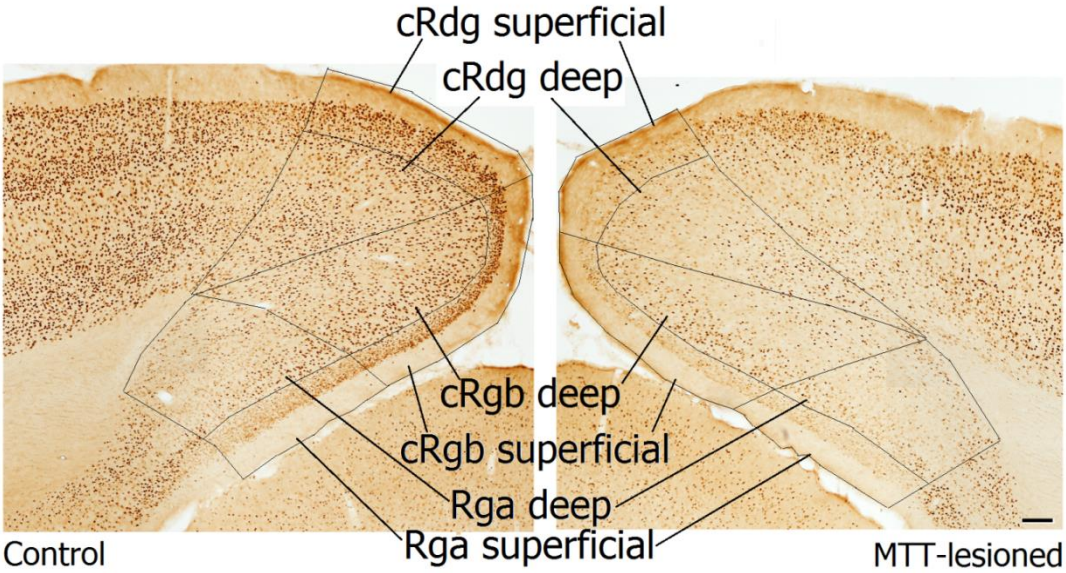

Figure 2-7. Representative coronal sections of the caudal portion of the retrosplenial cortex. The section on the left is from a control animal, the one on the right is from a mammillothalamic tract (MTT)-lesioned animal. The different retrosplenial subdivisions are reported. It is evident the decrease in the number of Zif268-positive nuclei in the lesioned animal. Scale bar 100 µm.

2.3.3.2 Dorsal hippocampus

The mammillothalamic tract lesions had no effect on Zif268 expression levels in the dorsal hippocampus, reflected by a lack of main effect of Lesion factor ($F<1$); furthermore, the Lesion x Region interaction was not significant ($F<1$) (Figure 2-8).

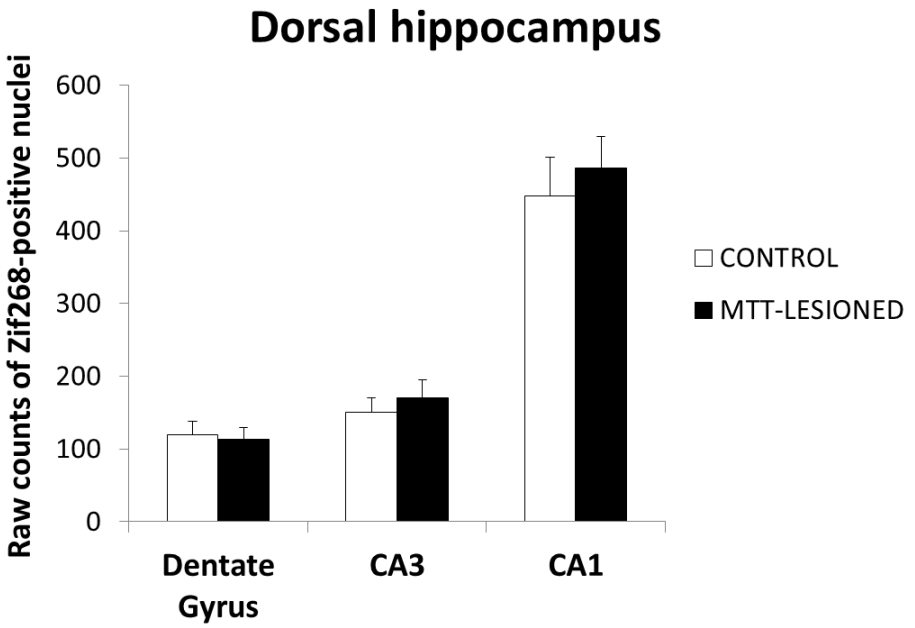

Figure 2-8. Raw counts (mean ± SEM) of Zif268-positive nuclei into the three main subfields (dentate gyrus, CA3 and CA1) of the dorsal hippocampus after bilateral mammillothalamic tract lesions and in controls.

2.3.3.3 Parasubiculum, presubiculum and postsubiculum

The statistical analysis did not reveal a significant main effect of the Lesion factor ($F < 1$). The interaction Lesion x Region was significant ($F_{1,18} = 5.6$, $p < 0.05$), but an analysis of simple main effects revealed no significant differences in any of the regions under inspection (parasubiculum: $p = 0.10$; presubiculum: $p = 0.34$; postsubiculum: $p = 0.57$) (Figure 2-9).

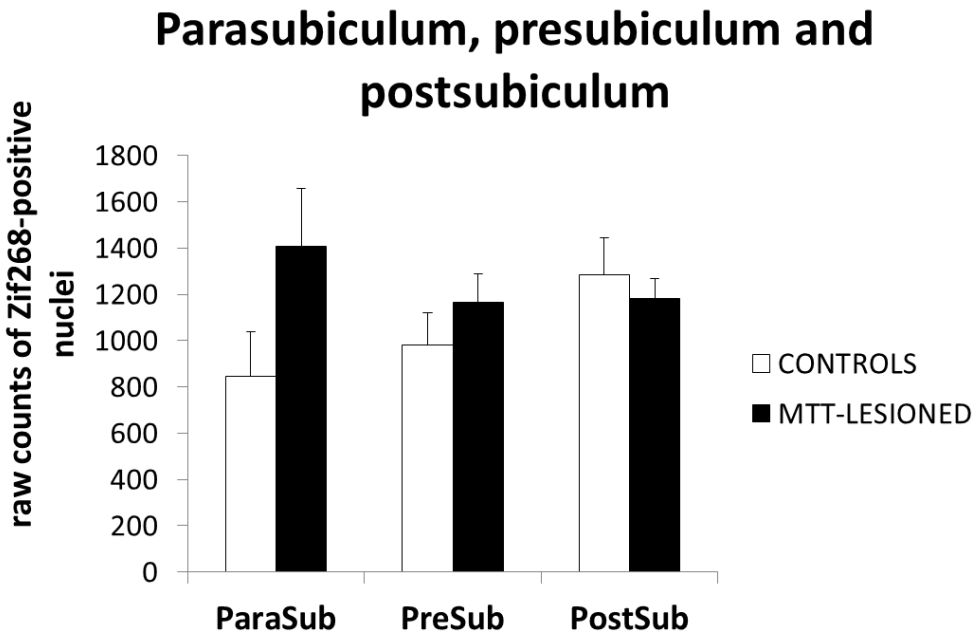

Figure 2-9. Raw counts (mean ± SEM) of Zif268-positive nuclei in the parasubiculum (ParaSub), presubiculum (PreSub) and postsubiculum (PostSub) after bilateral mammillothalamic tract lesions and in controls.

2.3.3.4 Medial prefrontal cortex

No significant effect of the Lesion factor was found in the medial prefrontal cortex regions (comprising infralimbic, prelimbic and anterior cingulate cortex) ($F < 1$); also the interaction Lesion x Region did not reach statistical significance ($F < 1$) (Figure 2-10).

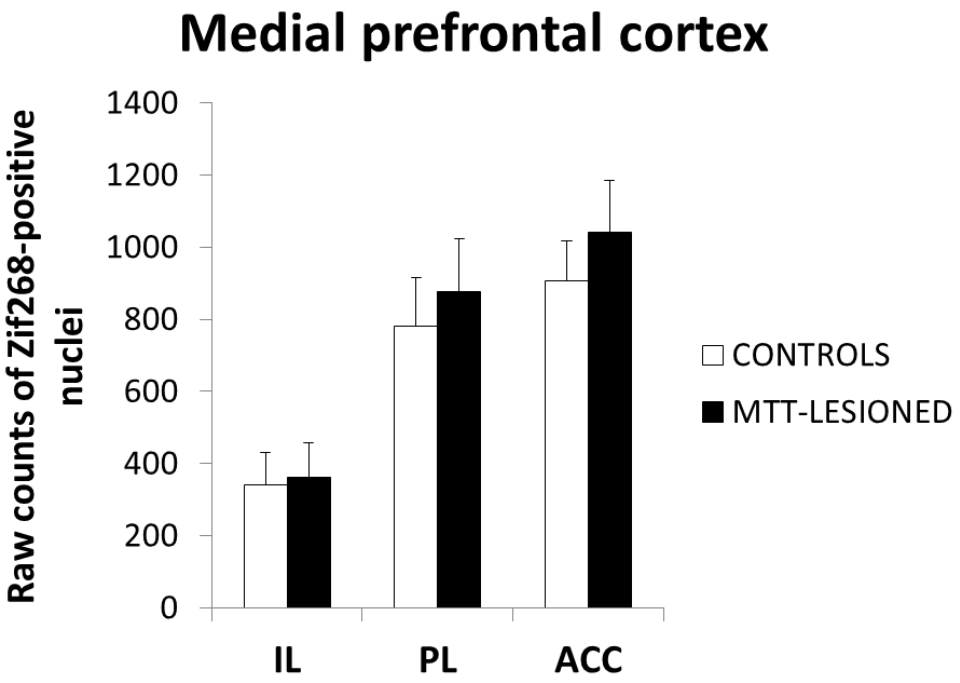

Figure 2-10. Raw counts (mean ± SEM) of Zif268-positive nuclei in areas within the medial prefrontal cortex: infralimbic (IL), prelimbic (PL) and anterior cingulate (ACC) cortices after bilateral mammillothalamic tract lesions and in controls.

2.4 Discussion

An analysis of the effects of mammillothalamic tract lesions on distal expression of Zif268 was carried out in animals that had previously performed a spatial behavioural task engaging the Papez circuit (forced runs in the radial arm maze; Vann & Albasser, 2009). A significant decrease in the number of neurones expressing Zif268 was detected at the level of the retrosplenial cortex (both in its rostral and caudal portion) in mammillothalamic tract-lesioned animals in comparison to controls. In contrast, no significant change was detected at the level of dorsal hippocampus, parasubiculum, presubiculum, postsubiculum and medial prefrontal cortex (infralimbic, prelimbic and anterior cingulate cortex).

The mammillothalamic tract is the only white matter tract that conveys information entirely inside the Papez circuit, connecting the mammillary bodies to the anterior thalamic nuclei. Thus its lesion provides important clues on the functionality of the circuit itself, as the damage is confined within the Papez circuit and does not affect the connections with other brain areas. In this particular experiment, only the fibres connecting medial mammillary nuclei to the anterior thalamic nuclei were lesioned, transecting the efferents to the anteromedial and anteroventral thalamic nuclei. It is likely that the bilateral connections of the lateral mammillary nuclei to the anterodorsal thalamic nuclei were instead spared; this was verified through a parallel tractography experiment which used the same surgical coordinates (Vann & Albasser, 2009). It has been shown that loss of the lateral mammillary nuclei had a small impact on rats' performance on spatial memory tasks (Vann, 2005, 2011), while loss of the whole mammillary structure caused a significant impairment (Vann & Aggleton, 2003), suggesting a major involvement of the medial mammillary nuclei in supporting spatial memory (Field et al., 1978). It is then reasonable to expect that removing the input from the medial mammillary nuclei to the anterior thalamic nuclei would have an impact (in terms of changes in Zif268 expression levels) on other structures connected to the anterior thalamic nuclei and implicated in spatial memory, even if the lateral mammillary connections are still intact (see Section 1.3.4.3).

This study has shown that transection of the mammillothalamic tract causes a significant reduction of Zif268 expression levels in Rdg and Rgb subregions of the retrosplenial cortex. Interestingly, immediate early gene expression (c-Fos and Zif268) in the retrosplenial cortex is also significantly reduced after anterior thalamic lesions (Dumont et al., 2012; Jenkins, Dias, Amin, & Aggleton, 2002; Jenkins, Dias,

Amin, Brown, et al., 2002; Jenkins et al., 2004; Poirier & Aggleton, 2009; Poirier, Shires, et al., 2008), hippocampal lesions (Albasser et al., 2007), fornix lesions (Vann, Brown, Erichsen, et al., 2000b) and lesions of Gudden's ventral tegmental nucleus (Vann, 2013). These findings suggest that retrosplenial functional hypoactivity could be a constant when another structure within the Papez circuit is damaged. The present result partially overlaps with that for c-Fos expression levels after mammillothalamic tract lesions, which, in contrast to Zif268, also appeared to be reduced in the superficial layers of rostral Rdg and of Rga (Vann & Albasser, 2009). Another study (Vann, 2013), employing mammillothalamic tract lesions and looking at c-Fos expression levels, found a significant decrease in both caudal Rdg and caudal Rgb (no distinction was made between superficial and deep layers).

In the current experiment both rostral and caudal portions of Rdg and Rgb were examined in order to verify if mammillothalamic tract lesions affect differently Zif268 expression at different antero-posterior levels in the retrosplenial cortex. Different anatomical studies have shown that connections between the retrosplenial cortex and other structures of the Papez circuit and the visual cortices are topographically organised along the rostro-caudal axis (Shibata, 1998; Van Groen & Wyss, 2003, 1992; Wyss & Van Groen, 1992). For example, retrosplenial rostral (anterior to splenium) subregions Rdg and Rgb are mainly connected with the caudal portion of the anterior thalamic nuclei; conversely, retrosplenial caudal (posterior to splenium) subregions Rdg, Rgb and Rga are densely connected with the rostral part of the anterior thalamic nuclei (Shibata, 1998; Sripanidkulchai & Wyss, 1986; Van Groen & Wyss, 2003). Furthermore, a study employing immediate early gene imaging (of both c-Fos and Zif268) after rats performed a radial arm maze task, found a different involvement of the retrosplenial rostral and caudal subregions (Pothuizen et al., 2009): the task caused an increment in the expression levels of both c-Fos and Zif268 in caudal Rgb in comparison to rostral Rgb, and of c-Fos in caudal Rdg in comparison to rostral Rdg. The authors hypothesised that this difference was due to the fact that the rostral portion of the retrosplenial cortex projects to the retrosplenial caudal portion, but not the other way around (Shibata, Honda, Sasaki, & Naito, 2009), thus the change of immediate early gene expression levels could be amplified caudally. In the present experiment, however, the pattern of decrease for Zif268 expression levels was very similar for both rostral and caudal Rgb and Rdg subregions (Figure 2-8).

No effect was found in the other regions under investigation. The study of Vann & Albasser (2009), instead, showed a change of c-Fos expression after

mammillothalamic tract lesions in additional areas: a significant decrease in the dorsal hippocampus (in the dentate gyrus, CA3 and CA1 subfields), postsubiculum and prelimbic cortex (confirmed also in Vann, 2013), and a significant increase in the parasubiculum (Figure 2-1). In the parasubiculum and postsubiculum, the direction of Zif268 expression level change was similar to c-Fos (an increase in the parasubiculum and a decrease in the postsubiculum), but it did not reach statistical significance. Overall, the reason for these differences between the c-Fos and Zif268 findings could reflect the functional differences between these two immediate early genes. Both c-Fos and Zif268 have been widely used for gene imaging in the Papez circuit, and their activation in these areas has been related to exploration of a novel environment (Hess et al., 1995; Jenkins, Dias, Amin, Brown, et al., 2002; Zhu et al., 1997) and spatial memory (Pothuizen et al., 2009; Vann, Brown, & Aggleton, 2000; Vann, Brown, Erichsen, et al., 2000a). However, their role in synaptic plasticity is only partially overlapping: for example, while Zif268 expression has been shown to be essential for long term potentiation in the dentate gyrus (Davis et al., 2003; Richardson et al., 1992; Richter-Levin et al., 1998; Wisden et al., 1990), c-Fos expression is necessary for induction of long term depression in CA1 (Kemp et al., 2013). Thus it is possible that the different pattern of change of expression of c-Fos and Zif268 after mammillothalamic tract lesion is due to their different roles in the Papez circuit.

It is worth comparing changes in c-Fos and Zif268 expression levels after mammillothalamic tract and anterior thalamic lesions (Table 2-2) as the mammillothalamic lesions are most likely having their effects via the anterior thalamic nuclei given that the anterior thalamic nuclei are the only direct target of the mammillothalamic tract. After anterior thalamic lesions, the most noticeable decrease in expression levels of both c-Fos and Zif268 has been detected in the retrosplenial cortex, both in its granular (Jenkins, Dias, Amin, & Aggleton, 2002; Jenkins, Dias, Amin, Brown, et al., 2002; Jenkins et al., 2004; Poirier & Aggleton, 2009; Poirier, Shires, et al., 2008) and dysgranular (Dumont et al., 2012; Jenkins et al., 2004; Poirier & Aggleton, 2009) subdivisions. Regarding dorsal hippocampal expression levels, anterior thalamic lesions caused a reduction of c-Fos levels (Jenkins, Dias, Amin, & Aggleton, 2002), but not of Zif268 levels (Dumont et al., 2012). In the subicular complex, anterior thalamic lesions resulted in a decrease of both c-Fos and Zif268 levels in the postsubiculum (Dumont et al., 2012; Jenkins, Dias, Amin, & Aggleton, 2002) and of only c-Fos in the presubiculum (Jenkins, Dias, Amin, & Aggleton, 2002). In the medial prefrontal areas, only c-Fos levels appeared to decrease in the prelimbic and anterior cingulate cortex after anterior thalamic damage (Jenkins, Dias, Amin,

Brown, et al., 2002). While in the subicular complex and medial prefrontal cortex the effects of mammillothalamic tract and anterior thalamic lesions only partially overlap, in the retrosplenial cortex and dorsal hippocampus the overall pattern of change in immediate early gene expression is very similar (a significant decrease of both c-Fos and Zif268 in the former case and a significant decrease of c-Fos but no change in Zif268 in the latter case). This consistency of findings supports the hypothesis that the mammillary input to the anterior thalamic nuclei, via the mammillothalamic tract, is important in influencing the anterior thalamic nuclei input to the retrosplenial cortex and the dorsal hippocampus, as lesions of either the mammillothalamic tract or the anterior thalamic nuclei are associated with the same pattern of change of c-Fos and Zif268 in those regions.

It has been shown that a significant reduction of c-Fos levels in the parasubiculum, postsubiculum and caudal retrosplenial cortex is also present in home-cage control rats with anterior thalamic lesions in comparison to home-cage control rats with sham surgery (Jenkins, Dias, Amin, Brown, et al., 2002), i.e. these distal changes are present even at baseline levels. It would, therefore, be interesting to verify whether the changes in c-Fos and Zif268 expression detected after mammillothalamic tract lesions are also present in home-cage control animals.

Finally, the animals in the present study were not tested on a spatial memory task; the behavioural task (the forced runs in the radial arm maze) had no memory component so that it was possible to match lesioned animals' and controls' behaviour during the task (otherwise, the mammillothalamic tract-lesioned animals would be impaired in solving the radial arm maze task and the two groups could not have been properly matched). This, however, means that it was not possible to assess whether the Zif268 levels correlated with any spatial memory impairment in this experiment. Combining an experiment of Zif268 imaging with a task that provides a measure of spatial memory would therefore be a valuable next step. An alternative approach to assess whether there is an association between levels of Zif268 and spatial memory performance would be to artificially manipulate the levels of Zif268 in specific areas of the Papez circuit and then test the animals in a relevant spatial memory task. The experiments reported in Chapter 5 and 6 of this thesis have explored this possibility.

ROI / LESION	Retrosplenial cortex	Dorsal hippocampus	Parasubiculum	Presubiculum	Postsubiculum	Infralimbic cortex	Prelimbic cortex	Anterior cingulate cortex
Anterior thalamic nuclei	c-Fos ↓	c-Fos ↓	c-Fos –	c-Fos ↓ –	c-Fos ↓ –	c-Fos ?	c-Fos ↓ –	c-Fos ↓ –
	Zif268 ↓	Zif268 –	Zif268 ?	Zif268 ?	Zif268 ↓	Zif268 –	Zif268 –	Zif268 ?
Mammillo-thalamic tract	c-Fos ↓	c-Fos ↓	c-Fos ↑	c-Fos –	c-Fos ↓	c-Fos –	c-Fos ↓	c-Fos –
	Zif268 ↓	Zif268 –	Zif268 –	Zif268 –	Zif268 –	Zif268 –	Zif268 –	Zif268 –

Table 2-2. Comparison of the effects on immediate early gene expression levels (c-Fos and Zif268) of either anterior thalamic or mammillothalamic tract lesions in the regions of interest (ROI) analysed in the current experiment. A down arrow indicates a decrease in immediate early gene levels in lesioned animals compared to controls, an up arrow indicates an increase, while the horizontal bar indicates no significant change. If both the up arrow and the horizontal bar are present in the same cell, it means that different studies have detected a different effect. A question mark indicates lack of data for that specific case. The studies from which the table data have been extracted are the following, Anterior thalamic lesions: Dumont et al., 2012; Dupire et al., 2013; Jenkins, Dias, Amin, & Aggleton, 2002; Jenkins, Dias, Amin, Brown, et al., 2002; Jenkins et al., 2004; Poirier & Aggleton, 2009; Poirier et al., 2008. Mammillothalamic tract lesions: Vann & Albasser, 2009; Vann, 2013; and the current study.

Chapter 3 : Analysis of dendritic complexity and apical density in pyramidal neurones of superficial layers of Rgb after mammillothalamic tract lesions

3.1 Introduction

Lesions in structures belonging to the Papez circuit, such as the hippocampus (Albasser et al., 2007), the anterior thalamic nuclei (Dumont et al., 2012; Jenkins, Dias, Amin, & Aggleton, 2002; Jenkins, Dias, Amin, Brown, et al., 2002; Jenkins et al., 2004; Poirier & Aggleton, 2009; Poirier, Shires, et al., 2008) and the mammillothalamic tract (Vann & Albasser, 2009; see also results in Chapter 2), produce a marked decrease in c-Fos and Zif268 expression levels in the retrosplenial cortex, especially in the superficial layers of the granular subdivision. This neuronal dysfunction has also been confirmed using other molecular markers (e.g. cytochrome oxidase; Mendez-Lopez et al, 2013) and by assessing the electrophysiological properties of the retrosplenial neurones (Garden et al., 2009) (see Section 1.3.4).

However, some of those previously mentioned immediate early gene studies have also shown that hippocampal (Albasser et al., 2007) and anterior thalamic (Jenkins et al., 2004; Poirier & Aggleton, 2009; Poirier, Shires, et al., 2008) lesions do not affect the number of neurones in the retrosplenial cortex. Moreover, some studies have investigated more subtle morphological changes in retrosplenial neuronal bodies (looking at their area and sphericity), after either anterior thalamic (Harland, 2013; Poirier & Aggleton, 2009) or hippocampal (Albasser et al., 2007) lesions, but did not detect any consistent change. For these reasons, this immediate early gene expression loss within the retrosplenial cortex has been defined as “covert pathology” (Aggleton, 2008), because retrosplenial areas appear morphologically intact when examined with standard histological techniques, but their neurones instead are dysfunctional.

Dendrites are specialised neuronal processes that typically receive the cell's synaptic inputs (Sjöström, Rancz, Roth, & Häusser, 2008). Thus, it is expected that synaptic functionality for a specific neuron is at least partially related to the properties of its dendrites. It has been shown that dendritic arbor morphology influences the passive and active electrical properties of the neuron (Sjöström et al., 2008) and determines its pattern of connectivity within neuronal networks (Kalisman, Silberberg, & Markram, 2003).

Furthermore, the majority of excitatory synapses target dendritic spines (Hering & Sheng, 2001), which are tiny protrusions (usually long 0.5-2 μm) located on the branches of dendritic arbors. The dendritic spines are able to influence the neuronal response to synaptic inputs; they not only increase the post-synaptic surface area but also act as biochemical compartments able to isolate ions and molecules from the rest of the dendrite (Sjöström et al., 2008). Generic spine shape comprises a bulbous tip extremity, called "head", sprouting from the "neck" which connects it to the dendritic shaft (Bourne & Harris, 2007). Many specific variations in spine morphology have been identified so far, with the most common shapes described as thin, mushroom and stubby (Tashiro & Yuste, 2003; Figure 3-1).

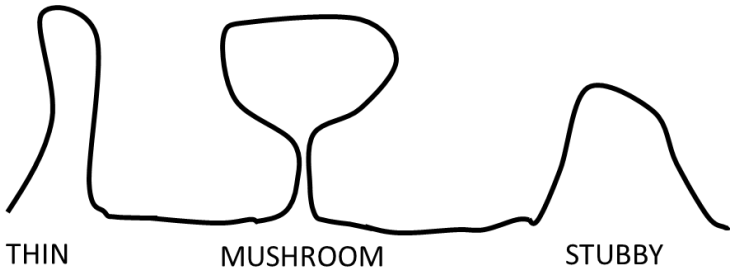

Figure 3-1. Main categories of dendritic spine shape.

Thin spines are the most abundant type in the brain and have a narrow and long neck terminating in a small spherical head. Mushroom spines have a very prominent head and a thin neck. Stubby spines have a very large neck and their head is not well defined; they have been described as an intermediate stage in the process of the dendritic shaft protruding into a proper spine (Fiala, Feinberg, Popov, & Harris, 1998). Less common shapes are branched spines (with a neck dividing into multiple heads) and filopodial spines (without a head, very motile and most commonly present during early developmental stages of the nervous system, representing the precursors of proper mature spines; e.g. Fiala et al., 1998). Spines are very dynamic structures,

able to change size and shape in a very short time (within minutes; e.g. Hering & Sheng, 2001). Different functionalities have been attributed to spine shape, with thin spines considered as “learning” spines as they are able to convert to mushroom “memory” spines, which are instead larger and more stable; long term potentiation, in particular, seems to enhance this transformation, while long term depression facilitates the opposite conversion from mushroom to thin spines (Bourne & Harris, 2007).

Given the importance of dendritic arbor and spines for neuronal function, examining the fine dendritic structure of the retrosplenial neurones (i.e. measuring their dendritic arbor complexity and their dendritic spine density and shape) could help to shed light on possible microstructural changes associated with the “covert pathology” shown by the retrosplenial cortex after lesions within the Papez circuit.

Some studies have shown that lesions located either in the diencephalon or in the hippocampal formation are associated with a change in dendritic complexity and spine density in connected brain areas. Lesions of the subiculum were associated with a decrease in dendritic complexity of both apical and basal dendritic arbors of hippocampal pyramidal neurones (in both CA1 and CA3 subfields; e.g. Shankaranarayana, Govindaiah, Laxmi, Meti, & Raju, 2001). Lesions of hippocampus produced, instead, a decrease in spine density in neurones of medial prefrontal cortex (Marquis, Goulet, & Dore’, 2008). Regarding diencephalic areas, lesions of either the thalamic reticular nucleus or the subthalamic nucleus were associated with a reduction in spine density in neurones of the CA1 subfield and prefrontal cortex, and with a decrease in total dendritic length of medium spiny neurones of nucleus accumbens (Camacho-Abrego et al., 2014; Torres-García et al., 2012). Lesions of the medial dorsal thalamic nucleus were followed by a decrease in dendritic spine density in neurones of the anterior cingulate, prelimbic and dorsolateral prefrontal cortices (Marmolejo, Paez, Levitt, & Jones, 2012).

Recently, the effects of anterior thalamic lesions on both dendritic complexity and spine density in the Papez circuit have been investigated (Harland, Collings, McNaughton, Abraham, & Dalrymple-Alford, 2014; Harland, 2013). Anterior thalamic lesions produced a decrease in spine density (thin and mushroom spines) in both the apical and basal arbors of dorsal CA1 pyramidal neurones and in density of thin spines protruding from the apical arbors of the neurones located in the superficial layers (II and III) of Rgb. Furthermore, dorsal CA1 pyramidal neurones in the lesioned

animals exhibited a reduction in complexity and length of basal dendritic arbors and a reduced length of apical dendritic arbors (Rgb dendritic arbor complexity was not analysed in those experiments).

In the experiment presented in this chapter, I verified if mammillothalamic tract lesions had an impact on the dendritic complexity and spine density of Rgb neurones; three main reasons justify this analysis:

(1) The reduction in spine density in Rgb neurones after anterior thalamic lesions (Harland et al., 2014).
(2) The consistent decrease in immediate early gene expression observed in Rgb after both anterior thalamic (Dumont et al., 2012; Jenkins et al., 2004; Poirier & Aggleton, 2009) and mammillothalamic tract lesions (Vann & Albasser, 2009; Vann, 2013; Chapter 2 of this thesis).
(3) The massive input that the anterior thalamic nuclei receive from the mammillary bodies through the mammillothalamic tract (Cruce, 1975; Shibata, 1992), suggesting a strong influence of the mammillary input on the anterior thalamic output, which, in turn, targets Rgb (Wright et al., 2013).

Dendritic complexity and apical dendritic spine density/shape were investigated in neurones of the retrosplenial Rgb subregion of rats lesioned in the mammillothalamic tract and in controls, 3 months after surgery. During this time period, the efficacy of the surgery was verified by testing the rats on a reinforced T-maze alternation task. As already reported in Section 1.3.1, animals with mammillothalamic tract lesions only exhibit a mild impairment or no deficit at all on the standard version of the T-maze task (Vann & Aggleton, 2003; Vann, 2013). However, the task can be manipulated in order to selectively remove the type of cues available to the animals, making the task more difficult to solve (Pothuizen et al., 2008; Vann, 2013). For example, it is possible to remove all the intramaze cues by running the sample and the choice phases of the task in two distinct mazes, obtaining a spatial memory task on which mammillothalamic tract lesioned rats are impaired (Baird et al., 2004; Pothuizen et al., 2008; Vann, 2013). Thus, a double T-maze task was used in this experiment in order to verify the efficacy of the mammillothalamic tract lesion surgeries.

Rgb was chosen among other subdivisions of the retrosplenial cortex because it is where the loss of c-Fos and Zif268 expression levels is the most consistent after lesion of other components of the Papez circuit (Albasser et al., 2007; Dumont et al., 2012; Jenkins, Dias, Amin, & Aggleton, 2002; Jenkins, Dias, Amin, Brown, et al.,

2002; Jenkins et al., 2004; Poirier & Aggleton, 2009; Poirier, Shires, et al., 2008; Vann & Albasser, 2009), and it enables comparisons to be made with the earlier studies by Harland et al. (2013, 2014).

The cytoarchitecture within the Rgb retrosplenial subregion has been studied in detail by Vogt & Peters (1981), who identified different types of neurones in the area divided by layer. Rgb consists of six layers, with layers II and III that cannot be differentiated but are merged as a dense band of neuronal cell bodies (Figure 3-2).

Unique to granular retrosplenial cortex is the presence of fusiform pyramidal neurones (e.g., Figure 3-2, neurones “a” and “b”), whose oval (about 8 x 12 µm of minor/major diameter) cell body is located in layer II-III. Their apical dendritic arbors branch out and form a tuft in layer I, while their basal dendritic arbors extend in layer IV. Both apical and basal dendritic arbors are covered by a moderate number of dendritic spines. The distal branches of the apical arbors are covered with many cell spines, while the primary apical branch has only few (Wyss et al., 1990).

In addition, canonical pyramidal neurones (small, medium and large in size) have been described in Rgb, and their somata are located in layers II-VI.

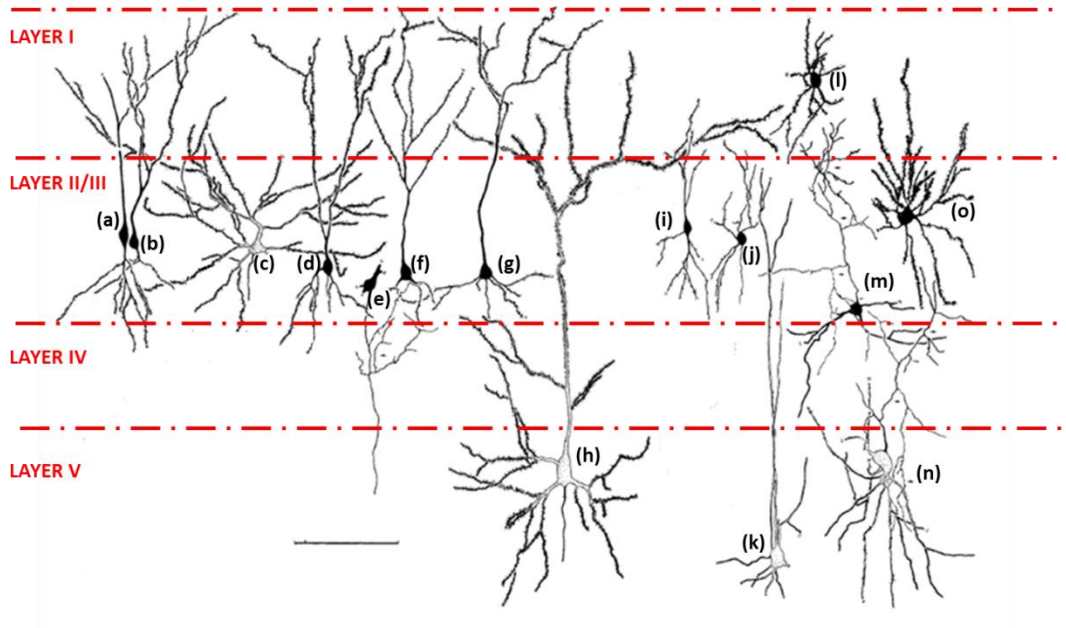

Figure 3-2. Adapted from Vogt & Peters (1981). Neurones in layers I-V of the Rgb subregion of the retrosplenial cortex subdivision (layer VI is not reported in this image). Layer subdivision is represented as red dashed lines. Types of neurones: (a) and (b) fusiform pyramids; (c) medium pyramid; (d), (e), (f) and (g) small pyramids; (h) large pyramid with apical branching in layer I; (i) small bipolar cell; (j) and (l) small multipolar cells; (m) medium multipolar cell; (k), (n) and (o) large multipolar cells. Scale bar = 100 µm, with a 10 µm division.

Small pyramidal cells are usually located in layers II and III, and they have a round/slightly oval soma. Their basal dendritic arbors protrude as a “skirt” from their soma, while their apical dendritic arbors either form a tuft (e.g., Figure 3-2, neuron “g”) or branch out more evenly (e.g., Figure 3-2, neuron “f”) in layer I. Their dendrites are densely covered by spines, especially the distal branches of the apical arbors (Wyss et al., 1990).
Pyramidal neurones, whose cell body is located in layer V or VI, are usually larger. Some of layer V neurones (e.g., Figure 3-2, neuron “h”) have an apical arbor that branches out in layer I; layer VI neurones’ apical dendritic arbors, instead, usually terminate before layer I.

It has been shown (Wyss et al., 1990) that small pyramidal neurones (both fusiform and canonical ones), whose cell body is located in layer II-III of Rgb, give rise to apical dendritic arbors that form bundles in the inferior portion of layer I and then spread out in the upper portion. Most of the inputs reaching Rgb from the anteroventral thalamic nucleus make contact with the bundles in layer I, while the spaces interposed between

one bundle and the other (where dendrites from the deeper pyramidal neurones are found) are targeted by cortical inputs.

The analysis performed in this experiment focused on the dendritic arbors of small pyramidal neurones (both fusiform and canonical) whose cell body is located in superficial layers II-III of Rgb, as they receive most of the anterior thalamic input (Wyss et al., 1990) and exhibit the most impressive loss of *c-fos* and *zif268* expression after anterior thalamic lesions (Jenkins et al., 2004; Poirier & Aggleton, 2009). Dendritic arbor complexity was measured in both apical and basal arbors, while spine density/shape was analysed only in the apical arbors, due to time constraints and because they were easier to analyse with the available techniques.

Dendritic arbors were visualised using the Golgi method, a staining technique invented by Golgi (1873) which allows the visualisation of neurones in their entirety through silver impregnation. This is possible because the staining is quite “capricious” and stains, for still unknown reasons, only a very small fraction of the cells (1-10%) in any preparations (Shankaranarayana & Raju, 2004); thus the processes of the neurones can be completely traced with relatively small overlap from neighbouring cells. As the original Golgi method is very time consuming (requiring several months), different variants have been developed, e.g. the Rapid Golgi method, the Golgi-Kopsch method and the Golgi-Cox method (Koyama, 2013). All of them, as the original technique, are based on cytoplasmic impregnation with a metallic salt, but are much quicker (Shankaranarayana & Raju, 2004). In this experiment the Golgi-Cox method was used, which involves the substitution of silver nitrate with mercury chloride (Levine et al., 2013) and requires less than 3 weeks for each preparation; background staining is less intense than with the other variants of Golgi staining, thus it is particularly suitable for the analysis of dendritic morphology (e.g. Koyama, 2013; Figure 3-3).

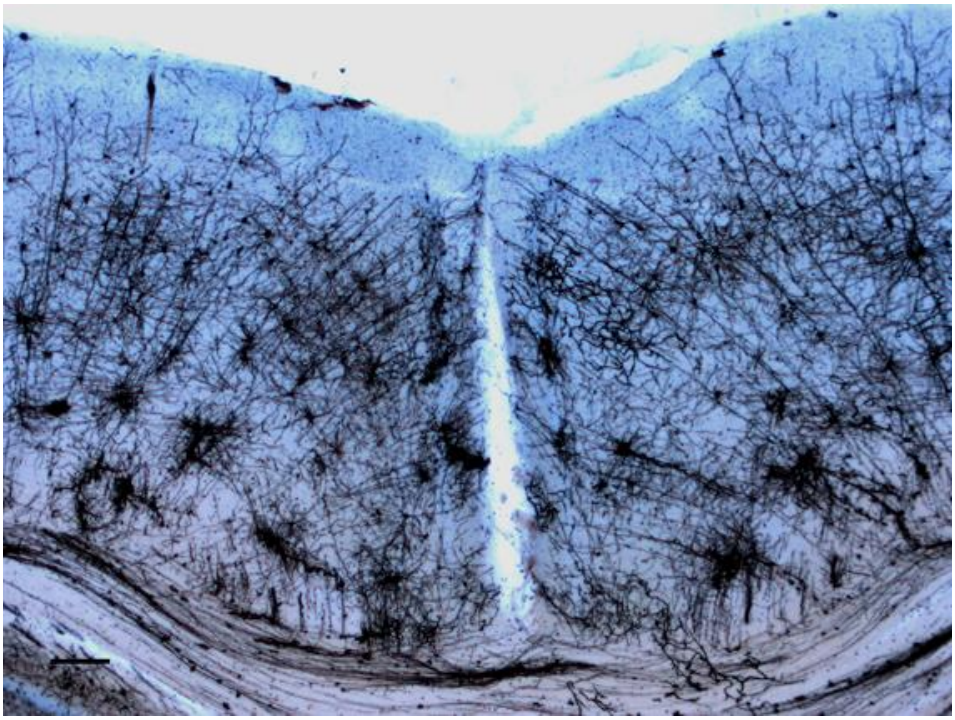

Figure 3-3. Representative coronal section of the rostral portion of the retrosplenial cortex stained with Golgi staining. Scalebar 100 µm.

3.2 Methods

3.2.1 Subjects

Subjects were 26 male naïve Lister Hooded rats (Harlan, UK) weighing 230-300 grams at the time of surgery. Rats were housed in pairs under diurnal light conditions (14 h light/10 h dark) and testing was carried out during the light phase at a regular time. They were given free access to water throughout the experiments. During the behavioural test period the animals were food deprived, but their body weight did not fall below 85% of free feeding weight. Animals were thoroughly handled before the study began in order to habituate them to the handling procedure. The experiment was carried out in accordance with UK Animals (Scientific Procedures) Act, 1986 and associated guidelines.

3.2.2 Surgical procedure

The surgeries for the experiment reported in this chapter were performed by Dr A. J. D. Nelson.

Animals were divided into two groups, one receiving bilateral mammillothalamic tract lesions (n = 14, MTT-lesioned animals) and the other was its matched surgical control group (n = 12, control animals). Surgery was performed under an isoflurane-oxygen mixture (2-2.5% isoflurane). Once the animals were anaesthetised, they were positioned in a stereotaxic head-holder (David Kopf instruments, California, US). The position of the incisor bar of the stereotaxic frame was set at -3.3 mm below the intra-aural line, to maintain the skull flat on the horizontal plane. The scalp was incised longitudinally in order to expose the skull, which then was drilled at the lesion point. A thermocouple radiofrequency electrode (0.7-mm tip length, 0.25-mm diameter; Diros Technology Inc., Canada) was lowered vertically and its tip temperature was raised to 70°C for 33 s using an OWL Universal RF System URF-3AP lesion maker (Diros Technology Inc., Canada). The stereotaxic coordinates were: antero-posterior (AP) -2.5 mm (relative to bregma), lateral-medial (LM) ±0.9 mm (relative to bregma), and dorso-ventral (DV) -6.9 mm (from top of the cortex). For the surgical controls the probe was positioned at the same AP and LM but only lowered to DV +1.0 mm above the lesion site. To avoid damaging the tract, the tip temperature of the electrode was not raised. After surgery, the skin was sutured, an antibiotic powder applied (Acramide: Dales Pharmaceuticals, UK), and animals received 5 ml of glucose saline subcutaneously. They were then placed in a temperature-controlled recovery box until they awoke from the anaesthetic. All animals were allowed at least 10 days of recovery after surgery before starting the behavioural procedure.

3.2.3 Behavioural procedure

3.2.3.1 T-maze task

Apparatus

Testing was performed in two cross-shaped mazes (“A” and “B”). One of the arms in each maze could be blocked off to form a T-shaped maze, with a stem (start arm) ending in a transversal crosspiece. The floor of both cross-mazes was made of painted white wood. The crosspiece was divided into two goal arms (left and right), 91 cm in total and 12 cm wide, with side walls (32.5 cm high) made of black Perspex;

at the end of each goal arm was a sunken food well (2 cm in diameter and 0.75 cm deep) to contain reward pellets. Access to a goal arm could be prevented by placing an aluminium barrier at its entrance. The two cross-mazes were identical and placed parallel side-by-side on a table (74 cm high) in the same experimental room with salient visual cues on the walls. Lighting was provided by overhead lights.

Pre-training

Before being trained, all animals were given 2 days of habituation to both mazes. On the first day, home-cage pairs of rats were placed together for 5 minutes in each maze, with sucrose reward pellets (5TUT/1811251 45 mg, TestDiet, St Louis, Missouri, US) scattered down each arm and two in each food well. On the second day, four pellets were placed in each food well and individually each rat was allowed to explore each maze for 5 minutes. In order to encourage the rats to explore the maze, reward pellets were continuously replaced during the habituation sessions.

Stage 1: Standard T-maze task

Testing in the standard T-maze task started the day after the last pre-training session. Rats received ten sessions of training in total, one each day, with eight trials in each session. Training was performed in the two distinct mazes on alternating days, so five sessions in total were performed in maze “A” and five sessions in total in maze “B”. Each trial consisted of a forced ‘sample’ phase followed by a ‘choice’ phase. During the forced sample phase, one of the goal arms of the T-maze was blocked by an aluminium barrier. After the rat turned into the pre-selected goal arm, it was allowed to eat one reward pellet, which had been previously placed in the food well. The rat was then picked up from the maze and immediately returned to the beginning of the start arm, where it was kept for 10 seconds using another aluminium barrier. Then, the choice phase began. The rat was now allowed to run up the start arm and given a free choice to enter either the left or the right goal arm. The rat received one reward pellet only if it turned in the direction opposite to the forced choice in the sample run (i.e. non-matching to sample choice; Figure 3-4a). Left/right allocations for the sample runs were pseudo-randomised over daily trials, sessions and rats, with no more than three consecutive sample runs to the same side in each session. The start arm was kept constant for the whole procedure.

At the beginning of each session, rats were taken from the holding room to the experimental room, each one transported in a separate compartment of an enclosed, opaque aluminium carry-box. Animals were tested in groups of either three or four, each one having one trial in turn (the inter-trial interval was about 3 minutes).

Stage 2: Double T-maze task

Testing in the double T-maze task started the day after the last session of standard T-maze task. Double T-maze training was very similar to standard T-maze training, except sample and choice phases were now conducted in the two distinct mazes in order to prevent the use of intra-maze cues. Rats received ten sessions of training in total, one each day, with eight trials in each session. Trials were divided into two types: in the different place trials (Figure 3-4b) the goal arm to choose in one maze was opposite to the arm visited in the sample phase in the other maze (this type of trial was very similar to trials performed in the standard T-maze task); in the same place trials (Figure 3-4c) the goal arm to choose in the choice phase in one maze was located very close to the arm visited in the sample phase in the other maze (this manipulation makes the allocentric cues potentially interfere with the identification of the correct goal arm). The eight trials per session were equally divided across these two distinct trial types, and sample phases balanced between maze “A” and “B”. As for the previous task, left/right allocations for the sample runs were pseudo-randomised over daily trials, sessions and rats, with no more than three consecutive sample runs to the same side in each session. The start arm was kept constant for the whole procedure. At the beginning of each session, rats were taken from the holding room to the experimental room, each one transported in a separate compartment of an enclosed, opaque aluminium carry-box. Animals were tested in groups of either three or four, each one having one trial in turn (the inter-trial interval was about 3 minutes).

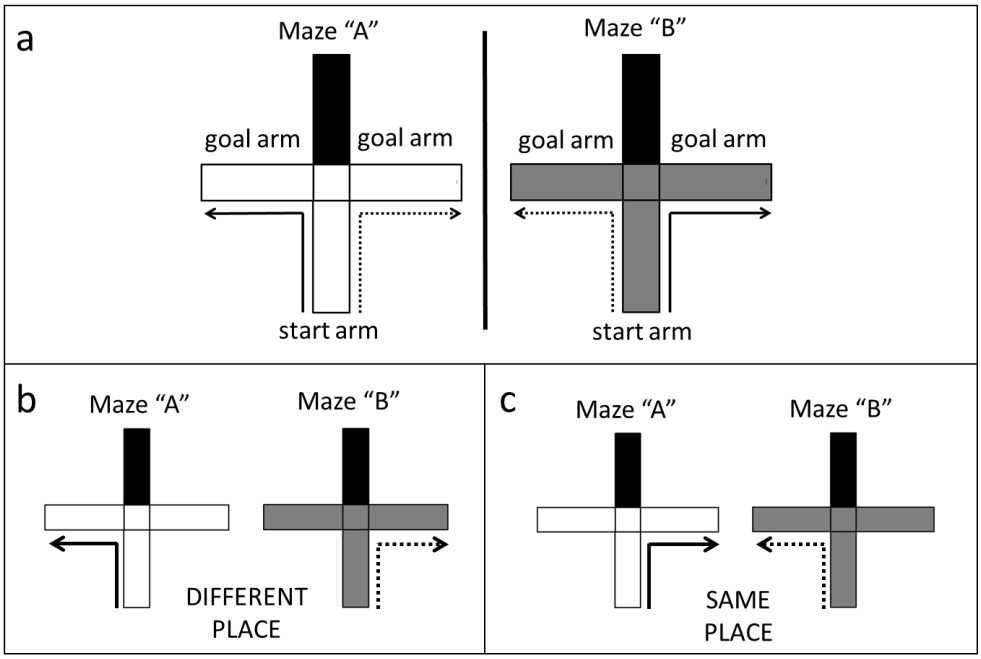

Figure 3-4. Test protocols used in the two variants of the reinforced alternation T-maze task. Both cross mazes were transformed into T-mazes by placing an aluminium barrier at the entrance of the Northern arm (here depicted as black). "Start arm" was always the Southern arm for both sample and choice phases. The two mazes A and B were identical (white floor and black side walls) but they have been assigned different colours in this picture in order to facilitate the protocol explanation. Solid arrows indicate the forced choice in the sample phase, while dashed arrows indicate the correct choice in the choice phase. (a) Standard T-maze (Stage 1): rats performed both the sample and the choice phases in the same maze, but half of the sessions were performed in maze A and the other half in maze B, on alternating days. Only two of the four possible combinations of forced choice /correct choice are illustrated. (b) & (c) Double T-maze (Stage 2): rats performed the sample phase in one maze and the choice phase in the other maze. Only the two possible cases in which the sample phase is performed in maze A are reported.

3.2.4 Golgi staining

The following procedure was carried out with the help of Dr. C. M. Dillingham.

Golgi staining was carried out 3 months after surgery using the FD Rapid GolgiStain Kit™ (FD NeuroTechnologies, Inc., Columbia, MD, US), based on the Golgi-Cox impregnation technique, using the same Golgi staining kit used in Harland (2013) and Harland et al. (2014) experiments. Rats were terminally anaesthetised with sodium pentobarbital (60 mg⁄kg, Euthatal, Rhone Merieux, Harlow, UK) and transcardially perfused with 0.1 M phosphate buffer saline (PBS) followed by 4% paraformaldehyde

in 0.1 M PBS (PFA). The brains were quickly removed from the skull and rinsed in distilled water. The brains were then immersed in an impregnation solution containing mercuric chloride, potassium dichromate and potassium chromate (kit solutions A +B), and stored in the dark at room temperature for about 2 weeks. The brains were then transferred into another kit solution (C) at 4°C for about 1 week, and then cut with a cryostat (thickness 150 µm). All slices were mounted on subbed microscope slides and stored in the dark at room temperature for no more than 3 days. After that, sections were rinsed in distilled water two times (2 minutes each), and then placed for 8 minutes in a mixture of kit Solution D, Solution E and distilled water (with these proportions 1:1:2). For counterstaining sections were first rinsed in distilled water (4 minutes), then immersed in cresyl violet staining (for about 8 minutes), rinsed again in distilled water for 30 seconds, and then dehydrated in ethanol at different concentration (70% ethanol for 4 minutes, 90% ethanol for 4 minutes and 100% ethanol for 8 minutes). Finally sections were cleared in xylene (for 4 minutes) and coverslipped (in DPX mounting medium; Thermoscientific, UK).

The number of arbors and dendritic branches imaged per animal was relative to the quality of Golgi staining. A set of rules was implemented in order to select the neurones suitable for either Sholl analysis or spine density analysis (see Sections 3.2.5 & 3.2.6).

3.2.5 Sholl analysis

All slides were re-coded, so both imaging and tracing were performed blind to group assignment (controls versus mammillothalamic tract-lesioned animals).

Image stacks from Golgi impregnated slices were obtained with a Zeiss LSM 510 confocal microscope (Carl Zeiss Ltd, UK) using a 20x apochromat objective to allow the capture of the entire dendritic arbor in a single image. A Helium-Neon laser (633 nm) was used to image the slices at high resolution (1024 x 1024 pixels). The microscope took images at pre-set intervals (0.5 µm) on the Z-plane, so generating image stacks (about 120-140 images per stack) that allowed the analysis of neuronal dendritic arbors in three-dimensions.

Sholl analysis was performed on dendritic arbors of small fusiform and canonical pyramidal neurones whose somata were positioned in superficial layers II-III of the rostral portion of Rgb, extending 2.80 – 5.70 mm posterior to bregma (Paxinos & Watson, 1998). For a more detailed analysis, the Rgb rostral portion was further

divided into an anterior (extending from 2.80 mm to 4.05 mm posterior from bregma) and a posterior subdivision (extending from 4.20 mm to 5.70 mm posterior from bregma).

Pyramidal neurones comprise two distinct dendritic arbors, the apical and the basal arbor. The former is characterised by a very long primary apical branch that divides into smaller and thinner branches, while the latter presents a more uniform distribution of branches around the soma. Given their different geometrical properties, apical and basal branches have been analysed separately. Eligibility criteria were adapted from Harland (2013) and used in order to select those arbors suitable for tracing: arbors needed to be intact and clearly visible (no staining artefacts obscuring them), and isolated, as much as possible, from the rest of the other stained neurones. For basal arbors the whole neuronal cell body needed to be clearly visible, while for apical arbors being able to identify the portion of the cell body from which the primary apical branch emerged was sufficient.

ImageJ software (1.48a Fiji version; Schindelin et al., 2012) and its free segmentation plugin Simple Neurite Tracer (Longair, Baker, & Armstrong, 2011) were used to trace the dendritic arbors in a semi-automatic way and to execute Sholl analysis (Figure 3-5).

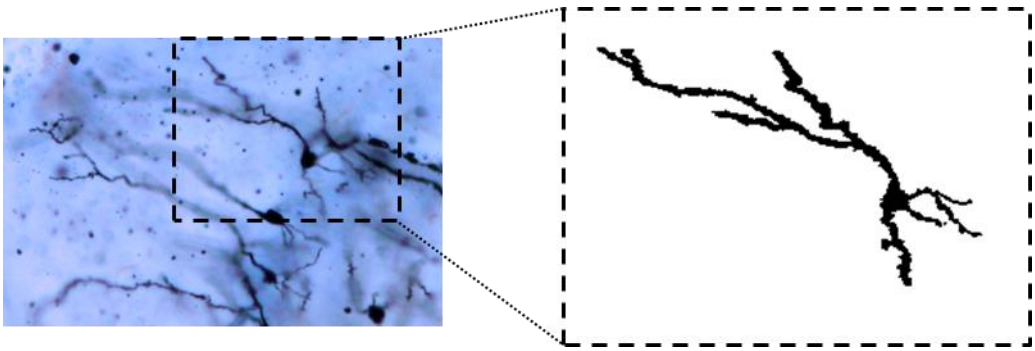

Figure 3-5. Example of a small pyramidal neuron in the superficial layers of Rgb traced with the Simple Neurite Tracer plugin of ImageJ.

A total of 350 dendritic arbors were traced, 158 from control brains and 192 from MTT-lesioned brains. For just eight of these neurones (seven from the MTT-lesioned group and one from the control group) it was possible to trace both basal and apical dendritic arbors, while either only apical or only basal arbors were traced for the remaining neurones (for these cells, staining artefacts or the overlap of other neurones/dendrites made either the apical or basal arbor ineligible to be traced), specifically 82 basal

arbors and 74 apical arbors for the control group, and 86 basal arbors and 92 apical arbors for the MTT-lesioned group (at least six arbors of each kind per animal).

Sholl analysis (Sholl, 1953) allows quantification of dendritic complexity by measuring the number of dendritic branches relative to distance from the cell's soma. It is accomplished by drawing concentric equidistant circles of increasing radius centred on the perikaryon (Figure 3-6), and by counting the number of intersections of the dendritic arbor with each circle. These data can be visualised on a plot, with distance from cell body (in steps of 5 µm in this experiment) on the X-axis and number of intersections on the Y-axis.

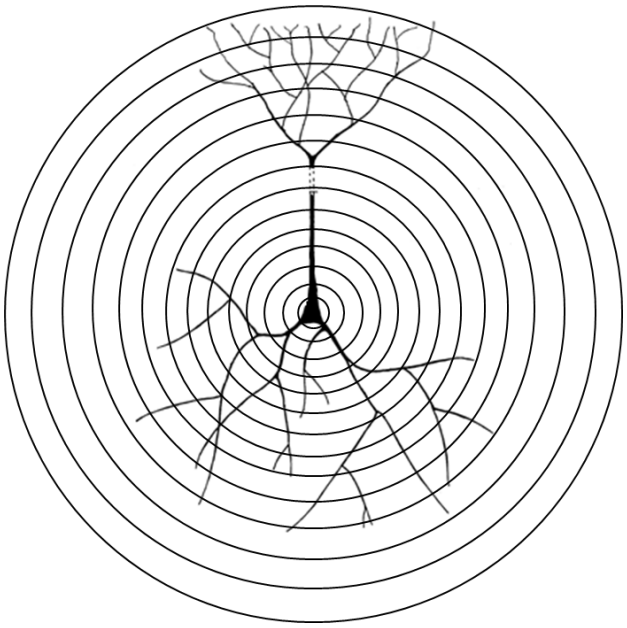

Figure 3-6. Diagram of a pyramidal cell with Sholl circles overlapped. Adapted from Sholl (1953).

A further analysis involved the calculation of a Sholl regression coefficient (k) for each arbor (using the Simple Neurite Tracer plug-in), which was used as an indicator of the rate of decay of the number of branches with increasing distance from the cell body (Sholl, 1953). The determination of the Sholl coefficient involved the logarithmic transformation of either the number of dendritic intersections (semi-log transformation, only the Y-axis; Figure 3-7), or of both the number of dendritic intersections and the distance from the cell body (log-log transformation, both the X-axis and the Y-axis; Figure 3-8). In all cases, before being transformed, the number of dendritic intersections was normalised by the circle's area.

$$\log_{10}(N/S) = -k * r + m$$

Figure 3-7. In the semi-log Sholl method, the logarithms of the number of intersections normalised per circle's area are plotted against the radius increments. "N" = number of dendritic crossings per circle of radius "r"; "S" = area of the circle of radius "r"; "k" = Sholl regression coefficient; "m" = intercept of the regression line.

$$\log_{10}(N/S) = -k * \log_{10}(r) + m$$

Figure 3-8. In the log-log Sholl method, the logarithms of the number of intersections normalised per circle's area are plotted against the logarithms of radius increments. "N" = number of dendritic crossings per circle of radius "r"; "S" = area of the circle of radius "r"; "k" = Sholl regression coefficient; "m" = intercept of the regression line.

Milosević & Ristanović (2007) have shown that a different transformation needs to be employed if the dendritic arbor is either apical or basal. For basal dendritic arbors, k was calculated using the semi-log Sholl method, while for apical dendritic arbors k was calculated using the log-log Sholl method. When the correct method is used, Sholl data plotted on the transformed cartesian axis should approximately lie on a straight line, whose equation can be inferred and whose regression coefficient is represented by k; in other words, k constitutes the rate of change in density of dendritic crossings as a function of the distance from the cell body.

3.2.6 Dendritic spine counting

Dendritic segments belonging to apical dendritic branches of neurones (small fusiform and canonical pyramids) located in layers II-III of Rgb were imaged without being aware of group assignments (the slides were re-coded for blind analysis). The region of interest was the rostral Rgb portion located 2.80 – 5.70 mm posterior to bregma (Paxinos & Watson, 1998). For the control group a total of 72 segments and 825 spines were analysed, while for the MTT-lesioned group, a total of 84 segments and 973 spines were analysed.

Pictures were acquired using a Leica DM5000B microscope with a 100x oil-immersion objective (Leica, Germany), attached to a Leica DFC310FX digital camera; microscope and camera settings were adjusted using the Leica Application Suite image acquisition software.

Six apical dendritic segments were analysed for each brain. They were chosen using the following criteria, adapted from Harland et al. (2014):

- They did not belong to the primary apical dendritic branch, but they were selected from either the II or III order branches.
- They were 25 µm in length and their starting and ending extremities were at least 10 µm away from any dendritic branching point or terminal.
- They had to be unobscured by other dendrites or staining artefacts.
- They had to be in one focal plane as much as possible (as this criterion was particularly difficult to meet, image Z-stacks for each segment were manually collected, so that most of the spines were in focus at different levels of the Z-axis).
- The beginning of a segment had to start from a point equidistant between two spines.

ImageJ software was used to process the Z-stacks in order to obtain a single image for each segment on which spine density analysis was performed. Z-stacks were projected onto a single image using a median type transformation (which converted pixels' intensities into their median value on the grey scale); these single images were then converted to black and white (through "binary" transformation, so that spine black contour stood out from a homogenous white background; Figure 3-9).

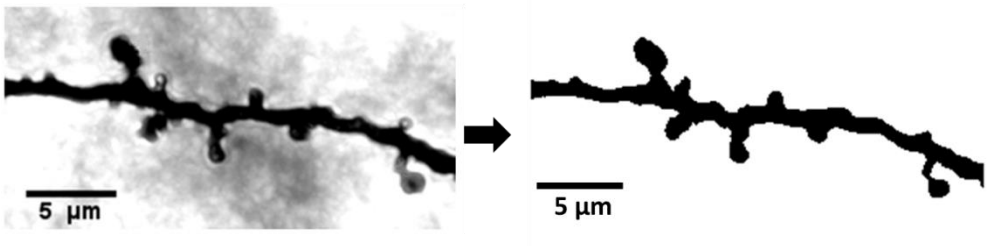

Figure 3-9. On the left, representative image of a dendritic segment obtained projecting a Z-stack of microscopy images on one plane. On the right, image transformation using a binary function in ImageJ, to better delineate the dendritic spine contours.

Spine counting was then performed and spines were classified into four different categories, on the basis of their shape (Harland et al., 2014; Figure 3-10):

- "Thin" if their total length was greater than the neck diameter, and the head diameter was less than three times the neck diameter.
- "Mushroom" if their head diameter was at least three times their neck diameter.
- "Stubby" if their neck diameter was equal or larger than spine total length.

- “Other” was the category for all the spines that could not be classified using the previous criteria (e.g. branched spines).

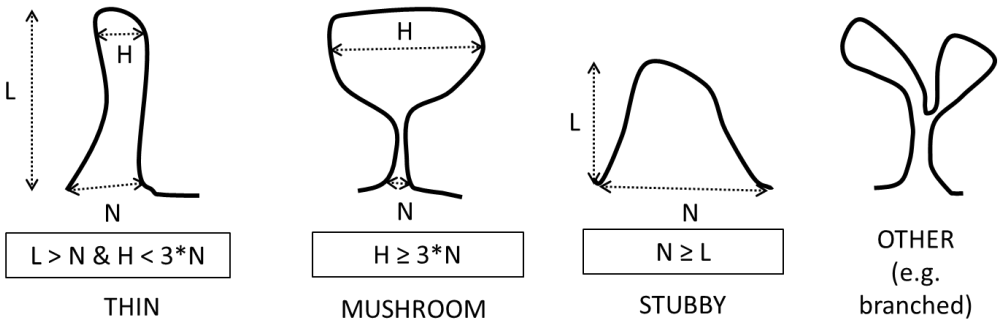

Figure 3-10. Assignment criteria for dendritic spine shape

3.2.7 Statistics

SPSS software (version 20, IBM Corporation) was used to carry out statistical analyses. The threshold for significance was set at $p < 0.05$.

3.2.7.1 T-maze data analysis

For both variants of the T-maze task used (standard and double), the number of correct choices per session was noted. For the double T-maze task, the number of correct choices per Trial type (different place versus same place) was noted as well. In both cases measurements were transformed into percentages. For both T-maze tasks, a mixed ANOVA, with Lesion (control group versus MTT-lesioned group) as between-subjects factor and Session (from 1 to 10) as the within-subjects factor, was used to compare groups’ performance in each task. To evaluate if the two lesion groups (controls and MTT-lesioned animals) were performing the task above chance level, overall mean percentages were compared against 50% using one-sample t-test.

To investigate if Trial type (different place versus same place) had any impact on the groups’ performances in the double T-maze task, a mixed ANOVA was performed on overall mean percentages across all 10 sessions; the between-subject factor was Lesion (control group versus MTT-lesioned group) and the within-subject factor was Trial type.

Finally, to evaluate if animals were significantly more impaired in the double T-maze task compared to the standard T-maze task, a mixed ANOVA was performed with

Lesion as the between-subjects factor and Task type (standard T-maze task versus double T-maze task) as the within-subjects factor.

3.2.7.2 Sholl analysis

The statistical analysis was performed separately for apical and basal dendritic arbors using a mixed ANOVA design, with Lesion (control group versus MTT-lesioned group) as between-subjects factor, and incrementing Radius as within-subjects factor (radius was incremented in 5 µm-steps, starting from 0 µm and reaching a maximum of 220 µm for the apical arbors and 155 µm for the basal arbors). Additional covariates were introduced to verify if they had any impact on the analysis: number of traced arbors (as this varied from brain to brain), percentage of arbors from the left hemisphere and percentage of arbors from the anterior subdivision of the region of interest.

Further analysis was carried out on Sholl regression coefficients “k”, separately for apical (log-log “k”) and basal (semi-log “k”) dendritic arbors, comparing the control group and the MTT-lesioned group using independent sample t-tests; the impact of covariates (number of traced arbors, percentage of arbors from the left hemisphere and percentage of arbors from anterior subdivision) on Sholl regression coefficients was verified re-running the analysis as a one-way ANOVA.

3.2.7.3 Spine density counting

General spine density was analysed using a one-way ANOVA with Lesion (control group versus MTT-lesioned group) as between-subjects factor. An additional analysis of variance was performed entering Branch order (analysed segment located in either II-order or III-order branches), Location (analysed segment located either in the anterior or posterior subdivision of the region of interest) and Hemisphere (analysed segment located either in the left or the right hemisphere) as extra fixed factors, in order to verify if they had any direct impact on the results or gave rise to any interaction with the Lesion factor.

Further investigation looked at spines divided on the basis of their shape using ANOVA with Lesion and Spine shape (thin versus stubby versus mushroom versus other) as between-subjects factors.

3.3 Results

3.3.1 Lesion histology

All fourteen lesioned animals had a discrete and bilateral lesion of the mammillothalamic tract and were, therefore, all included in subsequent analyses (Figure 3-11).

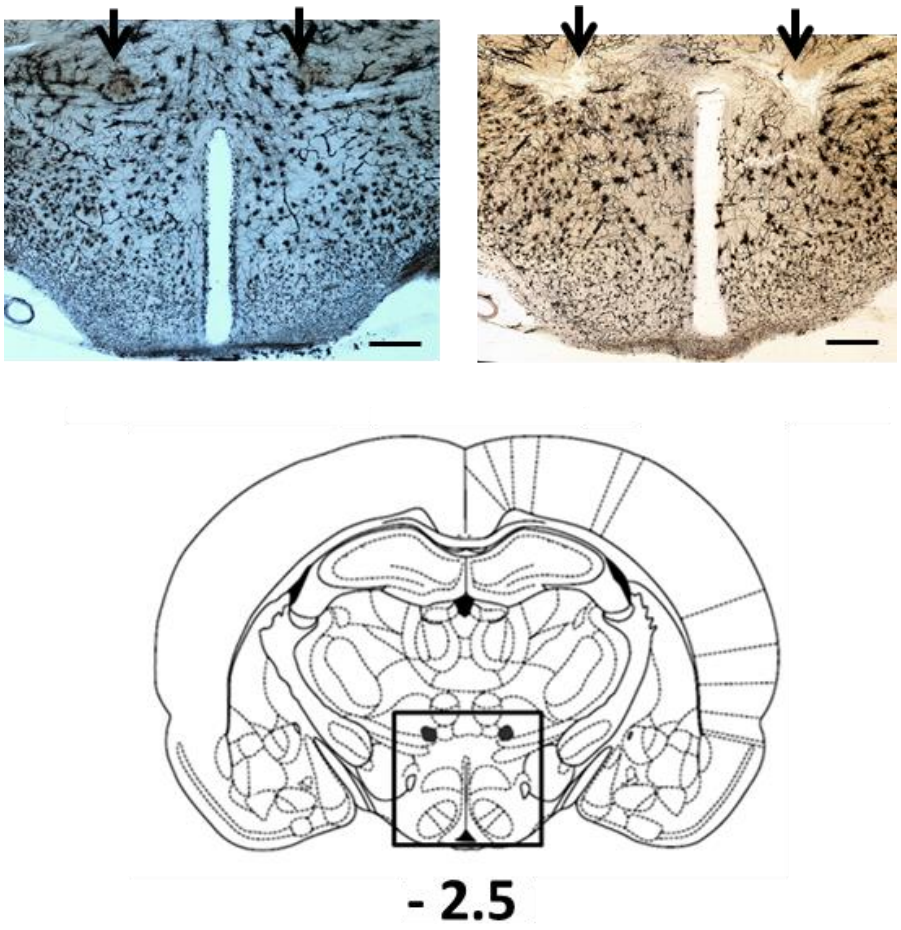

Figure 3-11. Representative coronal sections from a control animal (left) and a mammillothalamic tract (MTT)-lesioned animal (right). Bilateral lesions of the mammillothalamic tract (pointed by an arrow) are evident. In all cases, the fornix was intact. Scale bar 200 µm. The lesion location is also visible in the schematic section adapted from Paxinos & Watson atlas (1998), with the number indicating distance from bregma (in mm).

3.3.2 Behaviour

3.3.2.1 Standard T-maze task

Performance on the standard T-maze task was analysed over the ten sessions (Figure 3-12). Analysis of variance revealed a significant main effect of Lesion factor ($F_{1,24}$ = 6.9, $p < 0.05$), but no effect of Session main effect ($F_{9,216}$ = 1.7, $p = 0.08$) or Lesion x Session interaction ($F_{9,216}$ = 1.2, $p = 0.30$). Overall, MTT-lesioned animals appeared to have a mild impairment in the acquisition of the forced-choice alternation rule in the standard T-maze, but by the last sessions their performance was visually comparable to controls' performance.

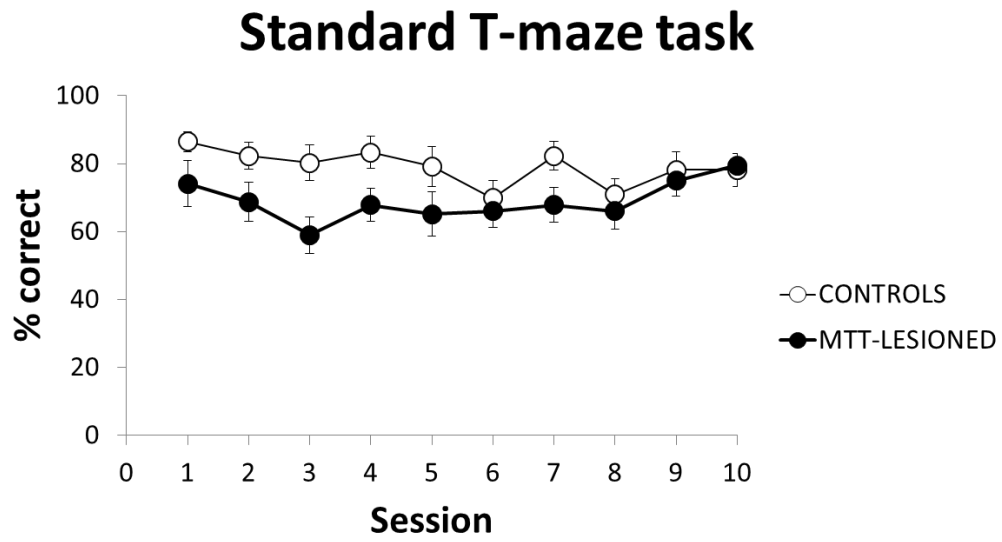

Figure 3-12. Performance on the standard T-maze task for the mammillothalamic tract (MTT) lesioned animals and the controls. Data are presented as mean ± SEM across the ten sessions of training.

In order to establish if performance was above chance levels in the standard T-maze task, scores were averaged across the ten sessions for each group and compared to 50% random choice level. Both the control group (t_{11}= 17.0, $p < 0.001$) and the MTT-lesioned group (t_{13} = 5.8, $p < 0.001$) were able to perform the standard T-maze task above chance levels.

3.3.2.2 Double T-maze task

After the acquisition of the standard T-maze task, rats were trained in its double maze variant, in which sample and choice phases were run in two identical but distinct mazes, place side by side, in order to exclude the use of intramaze cues to solve the task.

Performances over the ten sessions were compared between the two lesion groups (Figure 3-13). Again, the main effect of Lesion was significant ($F_{1, 24} = 14.9$, $p < 0.01$), as well as the main effect of Session ($F_{9, 216} = 3.2$, $p < 0.01$); however, there was no Lesion x Session interaction ($F_{9, 216} = 1.0$, $p = 0.46$).

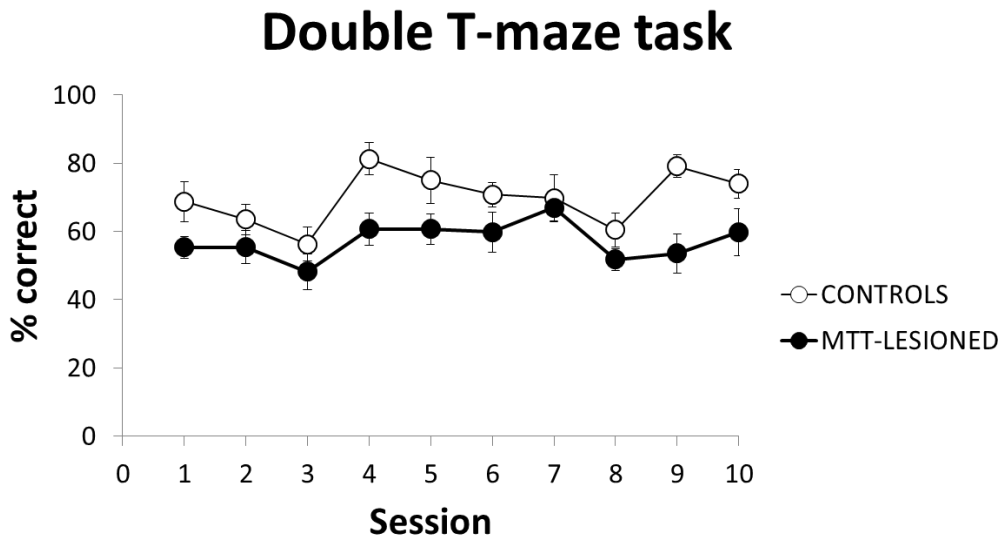

Figure 3-13. Performance on the standard T-maze task for the mammillothalamic tract (MTT) lesioned animals and the controls. Data are presented as mean ± SEM across the ten sessions of training.

The groups' performance across the ten session was compared against chance level (50%); the analysis revealed that performance of both the control group ($t_{11} = 10.2$, $p < 0.001$) and the MTT-lesioned group ($t_{13} = 2.8$, $p < 0.05$) animals was above chance.

In the double T-maze task, the trial types can be subdivided into different place type or same place type, depending on the relative positions of the "sample" and "choice" arms in the two mazes (see Figure 3-4). Same place trials are more difficult than different place trials because the position of the "sample" and "choice" arms is very

close in relation to extramaze cues, so animals may be reluctant to return to the same absolute location. We verified if this trial type factor (different place versus same place) had any impact on performances of the two groups in the double T-maze task. Analysis of variance revealed a significant effect of the Trial type factor ($F_{1, 24}$ = 29.2, $p < 0.001$) and a significant effect of the Lesion factor ($F_{1, 24}$ = 13.3, $p < 0.01$), but not a Lesion x Trial type interaction ($F_{1, 24}$ = 1.4, $p = 0.25$) because both animal groups performed worse in the same place trials in comparison to different place trials (Figure 3-14).

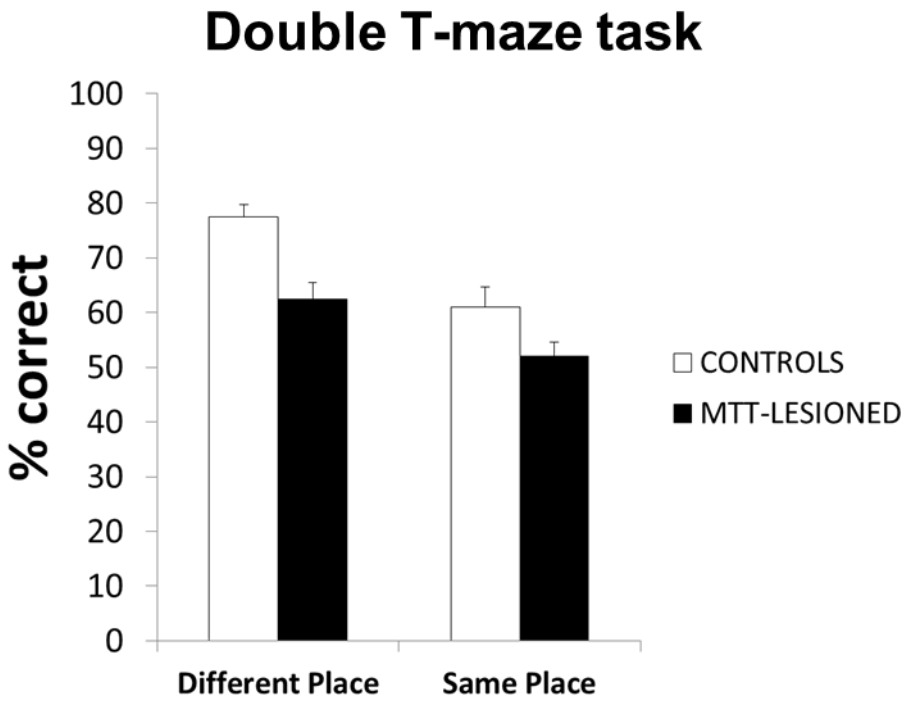

Figure 3-14. Performance on the double T-maze task, separated by trial type (different or same place). Histograms represent the percentage of correct choices (mean ± SEM) across the ten sessions.

Finally, groups' performance across the ten sessions was compared between the two variants of the T-maze task (standard T-maze task versus double T-maze task; Figure

3-15). Analysis of variance revealed a significant main effect of Task type factor ($F_{1, 24} = 30.0$, $p < 0.001$), and also of Lesion factor ($F_{1, 24} = 14.2$, $p < 0.001$), but not a significant interaction ($F < 1$).

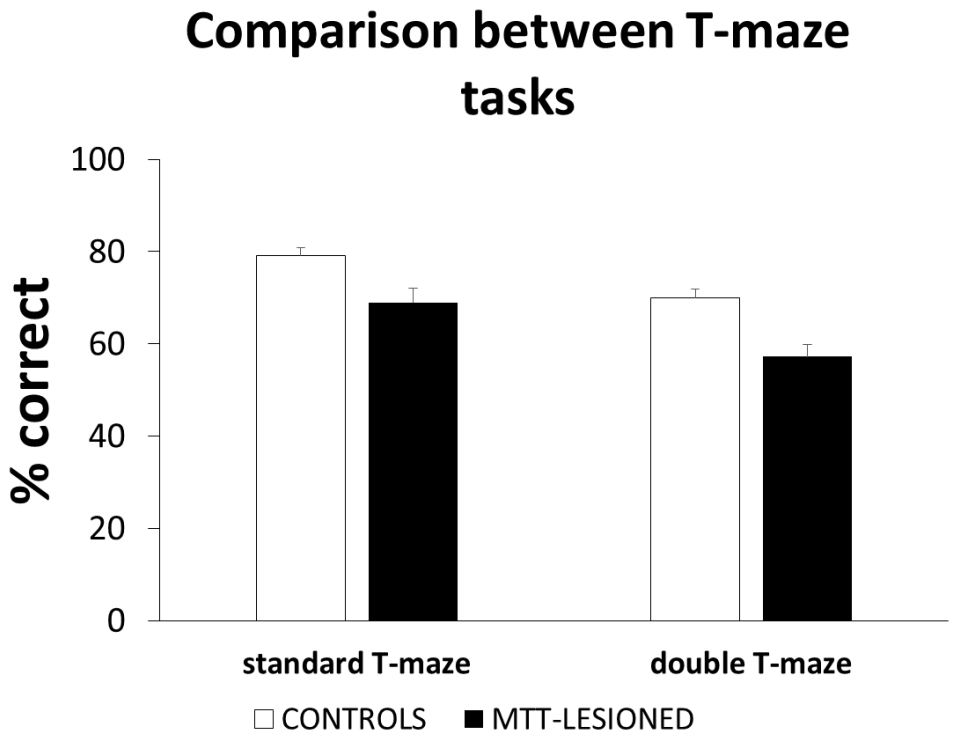

Figure 3-15. The groups' performance across T-maze task types. Histograms represent the percentage of correct choices (mean ± SEM) across the ten sessions.

3.3.3 Sholl analysis

Statistical analysis of apical arbors' Sholl data showed neither a main effect of Lesion factor ($F < 1$) on the number of dendritic intersections with Sholl circles, nor a significant interaction of Lesion x Radius ($F < 1$) (Figure 3-16). There was however a significant main effect of Radius factor ($F_{44,1056} = 81.8$, $p < 0.001$), as the number of dendritic intersections varied with radial distance from the cell body: the maximum number of intersections was (mean ± SEM) 2.4 ± 0.1 for the control group, and 2.3 ± 0.2 for the MTT-lesioned group, reached in both cases at 100 µm of distance from the cell body. The addition of extra factors as covariates (Number of traced arbors, Percentage of arbors from the left hemisphere, and Percentage of arbors from the anterior subdivision) did not have any relevant impact on the model (Table 3-1).

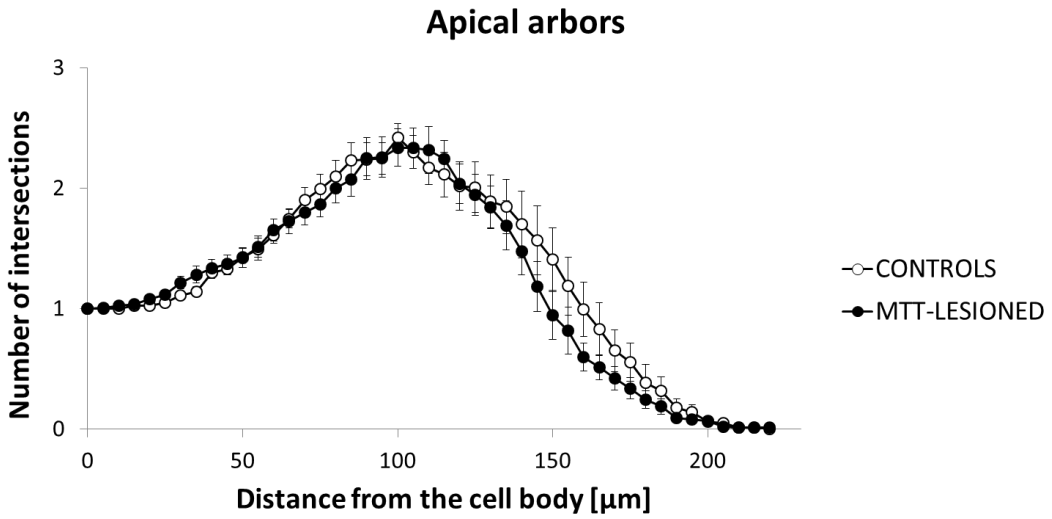

Figure 3-16. Number of dendritic intersections per Sholl circle (radius increasing in steps of 5 µm) for the apical dendritic arbors of Rgb superficial (layer II-III) small pyramidal neurones. Each white/black circle represents the number of intersections (mean ± SEM).

APICAL ARBORS

EXTRA FACTORS	LESION GROUP	
	CONTROL	MTT-LESIONED
NUMBER OF ARBORS	6.25 ± 0.3	7.07 ± 0.4
% ARBORS FROM LEFT HEMISPHERE	60.48 ± 9.1	56.87 ± 4.5
% ARBORS FROM ANTERIOR SUBDIVISION	26.39 ± 7.9	24.56 ± 7.9

Table 3-1. Data in the cells are represented as mean ±SEM.

Statistical analysis performed on Sholl data of basal branches did not reveal either a significant main effect of Lesion factor ($F_{1,24} = 1.7$, $p = 0.20$) or a significant interaction Lesion x Radius ($F < 1$) on the number of dendritic intersections with Sholl circles (Figure 3-17). Again, the main effect of Radius was significant ($F_{31,744} = 306.6$, $p < 0.001$), as the number of dendritic intersections varied with radial distance from the cell body: the maximum number of intersections was (mean ± SEM) 4.3 ± 0.2 for both the control and the MTT-lesioned group, reached in both cases at 25 µm of distance from the cell body. Introduction of the covariates (Number of traced arbors, Percentage of arbors from the left hemisphere, and Percentage of arbors from anterior subdivision) did not affect the statistical model (Table 3-2).

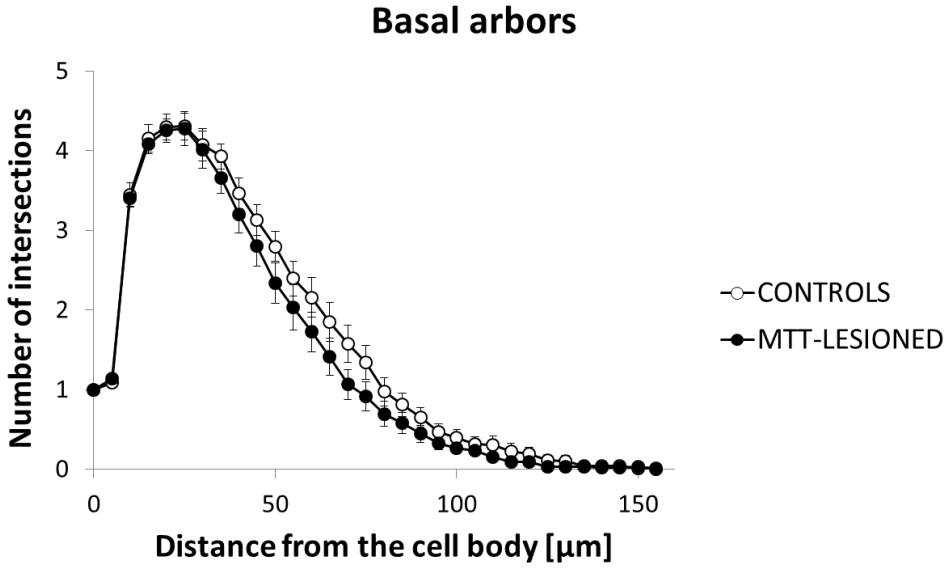

Figure 3-17. Number of dendritic intersections per Sholl circle (radius increasing in steps of 5 µm) for the basal dendritic arbors of Rgb superficial (layer II-III) small pyramidal neurones. Each white/black circle represents the number of intersections (mean ± SEM).

BASAL ARBORS

EXTRA FACTORS	LESION GROUP	
	CONTROL	MTT-LESIONED
NUMBER OF ARBORS	6.92 ± 0.4	6.64 ± 0.2
% ARBORS FROM LEFT HEMISPHERE	58.99 ± 6.5	61.16 ± 4.5
% ARBORS FROM ANTERIOR SUBDIVISION	17.28 ± 7.0	26.69 ± 7.6

Table 3-2. Data in the cells are represented as mean ± SEM.

Analysis of the Sholl regression coefficients did not reveal any significant difference between controls and MTT-lesioned animals, for either apical (t_{24} = -1.0, p = 0.33; Figure 3-18) or basal dendritic arbors (t_{24} = -1.5, p = 0.15; Figure 3-19). The additional covariates (Number of traced arbors, Percentage of arbors from the left hemisphere, and Percentage of arbors from anterior subdivision) did not alter the result.

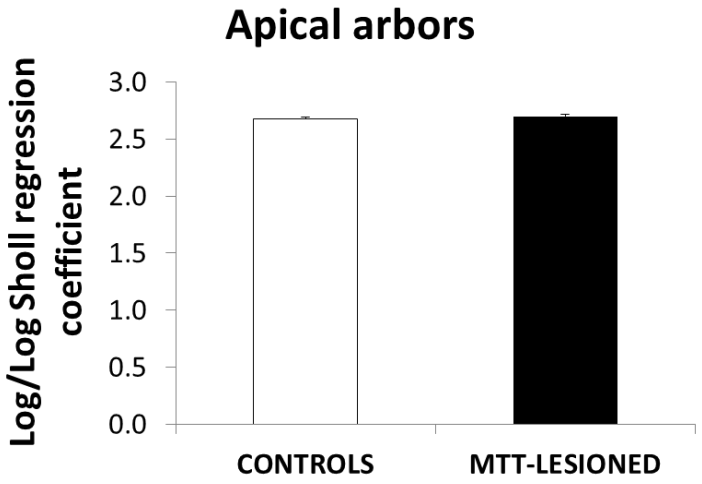

Figure 3-18. Log-log Sholl regression coefficient "k" (mean ± SEM) for apical dendritic arbors of Rgb superficial (layer II-III) small pyramidal neurones.

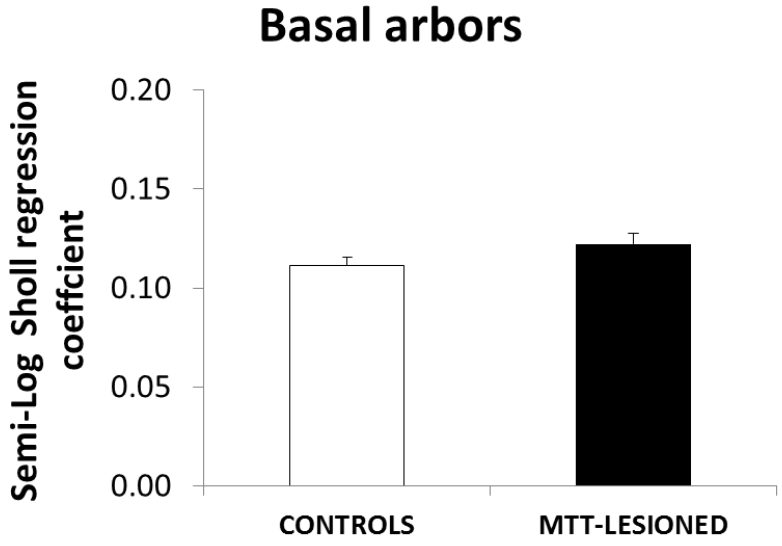

Figure 3-19. Semi-log Sholl regression coefficient "k" (mean ± SEM) for basal dendritic arbors of Rgb superficial (layer II-III) small pyramidal neurones.

3.3.4 Spine density analysis

General spine density for the apical dendritic branches of the small pyramidal neurones located in superficial layers II-III of Rgb was compared between the controls and the MTT-lesioned animals (Figure 3-20). Analysis of variance did not reveal any significant main effect of Lesion factor ($F < 1$).

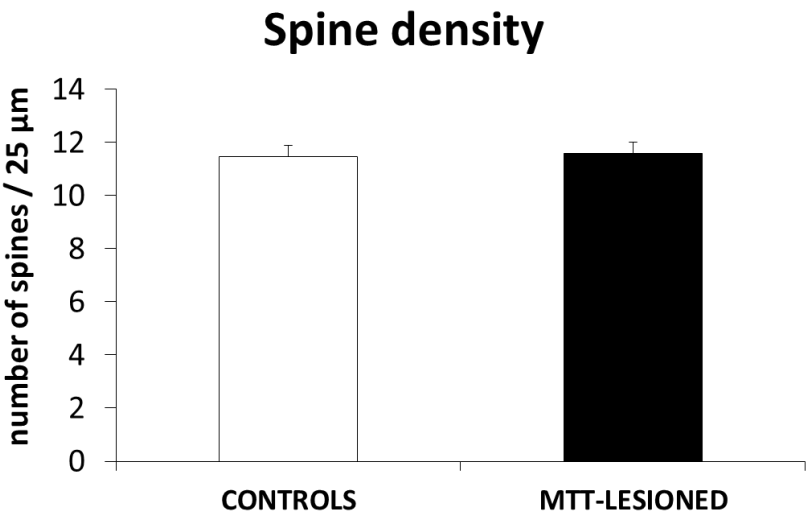

Figure 3-20. Spine densities (mean ± SEM) calculated in 25 µm-long segments selected from dendritic apical branches of small pyramidal neurones located in layers II-III of Rgb.

Furthermore, the addition of the extra factors Branch order (II-order vs III-order branches, 82.1% and 17.9% of total branches, respectively), Location (anterior vs posterior, 41.7% and 58.3% of total branches, respectively) and Hemisphere (left vs right, 57.7% and 42.3% of total branches, respectively) did not have any impact on the analysis of variance, as they did not give rise to any significant main effect or interaction ($F < 1$ in all cases; Table 3-3).

EXTRA FACTORS	LESION GROUP	
	CONTROL	MTT-LESIONED
BRANCH ORDER I	11.5 ± 0.5	11.5 ± 0.5
BRANCH ORDER II	11.4 ± 0.9	12.0 ± 0.2
LOCATION: ANTERIOR	12.0 ± 0.7	12.2 ± 0.7
LOCATION: POSTERIOR	11.0 ± 0.6	11.3 ± 0.6
HEMISPHERE: LEFT	11.4 ± 0.6	11.0 ± 0.6
HEMISPHERE: RIGHT	11.5 ± 0.7	12.4 ± 0.7

Table 3-3. Spine densities (mean ± SEM) in 25 µm-long segments selected from dendritic apical branches of small pyramidal neurones located in layers II-III of Rgb. The means have been subdivided on the basis of the lesion group and some extra factors (branch order, antero-posterior location, and hemisphere).

Further analysis showed no significant effect of Lesion factor on spine density when spines were subdivided on the basis of their shapes ($F<1$; Figure 3-21). A significant effect was obtained for Spine shape factor ($F_{3,616} = 329.8$, $p <0.001$) as thin and stubby spines were more abundant than the other two types (41.8% and 51.9% of total spines, respectively, while the mushroom type and the other spine type constituted 4.2% and 2.1%, respectively), but the Lesion x Spine shape interaction was not significant ($F<1$).

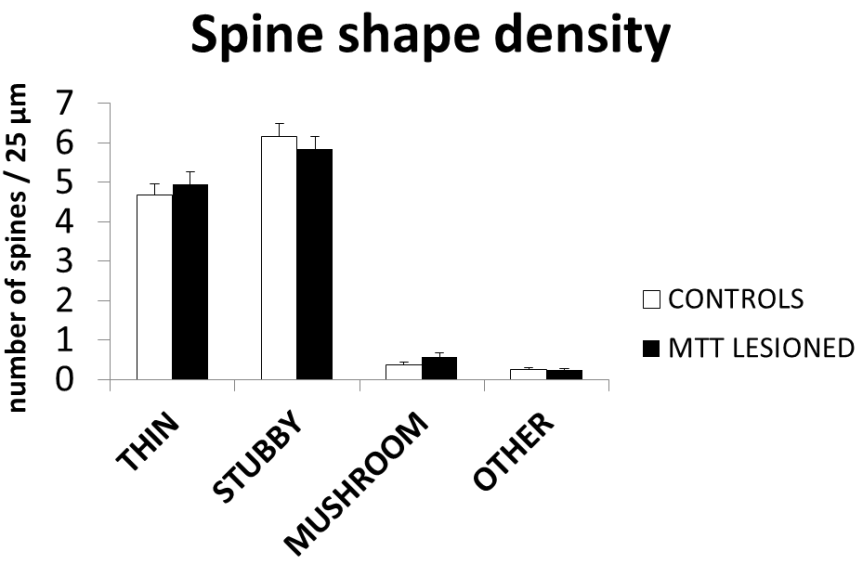

Figure 3-21. Spine densities (mean ± SEM) calculated in 25 µm-long segments selected from dendritic apical branches of small pyramidal neurones located in layers II-III of Rgb. Distinction was made among four different spine shapes.

Again, the additional factors Branch order (II-order vs III-order branches), Location (anterior vs posterior) and Hemisphere (left vs right) did not give rise to any significant main effect or interaction in the analysis ($F < 1$ in all cases; Table 3-4).

EXTRA FACTORS	DENDRITIC SPINE SHAPE			
	THIN		STUBBY	
	CONTROL	MTT-LESIONED	CONTROL	MTT-LESIONED
BRANCH ORDER I	4.6 ± 0.3	4.8 ± 0.4	6.3 ± 0.4	5.9 ± 0.3
BRANCH ORDER II	4.9 ± 0.5	5.8 ± 0.9	5.6 ± 0.8	5.4 ± 0.9
LOCATION: ANTERIOR	5.3 ± 0.4	4.8 ± 0.5	5.9 ± 0.4	6.5 ± 0.5
LOCATION: POSTERIOR	4.1 ± 0.3	5.0 ± 0.5	6.4 ± 0.5	5.5 ± 0.4
HEMISPHERE: LEFT	4.6 ± 0.4	4.5 ± 0.4	6.2 ± 0.5	5.6 ± 0.4
HEMISPHERE: RIGHT	4.8 ± 0.4	5.6 ± 0.5	6.1 ± 0.5	6.2 ± 0.6
EXTRA FACTORS	MUSHROOM		OTHER SHAPE	
	CONTROL	MTT-LESIONED	CONTROL	MTT-LESIONED
BRANCH ORDER I	0.4 ± 0.1	0.6 ± 0.1	0.2 ± 0.1	0.2 ± 0.1
BRANCH ORDER II	0.4 ± 0.1	0.6 ± 0.3	0.4 ± 0.2	0.3 ± 0.1
LOCATION: ANTERIOR	0.4 ± 0.1	0.8 ± 0.2	0.3 ± 0.1	0.1 ± 0.1
LOCATION: POSTERIOR	0.3 ± 0.1	0.4 ± 0.1	0.2 ± 0.1	0.3 ± 0.1
HEMISPHERE: LEFT	0.4 ± 0.1	0.7 ± 0.2	0.3 ± 0.1	0.3 ± 0.1
HEMISPHERE: RIGHT	0.4 ± 0.1	0.4 ± 0.1	0.2 ± 0.1	0.2 ± 0.1

Table 3-4. Spine densities (mean ± SEM) subdivided by spine shape, measured in 25 µm-long segments selected from dendritic apical branches of small pyramidal neurones located in layers II-III of Rgb. The means have been subdivided on the basis of lesion group, spine shape and extra factors (branch order, antero-posterior location, and hemisphere).

3.4 Discussion

The aim of this experiment was to assess whether the loss of immediate early gene expression observed in the retrosplenial cortex after medial diencephalic lesions, as shown in Chapter 2, was also associated with a structural modification. The first main outcome was that lesions of the mammillothalamic tract did not affect the dendritic complexity of either apical or basal arbors of small and fusiform pyramidal neurones located in the superficial layers of retrosplenial cortex subregion Rgb. The second main outcome was that mammillothalamic tract lesions did not affect the density of dendritic spines located on the branches of the apical arbors of those same type of neurones.

With respect of the analysis of dendritic arbor complexity, inspecting the Sholl analysis graphs, a subtle decrease in dendritic complexity is visible for the MTT-lesioned group in the final portion of the apical dendritic arbors (Figure 3-16) and in the middle portion of the basal dendritic arbors (Figure 3-17), but this difference did not reach statistical significance.

Thus, although mammillothalamic tract lesions result in a loss of immediate early gene expression in the retrosplenial cortex, these changes do not seem to reflect significant structural changes at the dendritic level. This negative outcome is different from the results obtained in another study using anterior thalamic lesions (Harland et al., 2014); that study found a decrease in the number of thin spines in the small fusiform pyramidal neurones located in the superficial layers of Rgb. Harland et al. did not assess retrosplenial dendritic complexity in their study. A possible explanation for these different outcomes could rely on the fact that the mammillothalamic tract lesions do not directly de-afferent the retrosplenial cortex, unlike the anterior thalamic lesions. However, it must be noted that in Harland (2013) and Harland et al. (2014) experiments, the dendritic microstructure of neurones located in area CA1 appears also to be affected. Their lesions involved the anteroventral and anteromedial thalamic nuclei, which do not directly innervate the CA1 subfield. So it is possible to observe dendritic changes in the hippocampus without direct deafferentation, but it is not known if it is also the case for the retrosplenial cortex.

There are a number of possible methodological reasons why no significant lesion effects were found in the present experiment. It is necessary to consider the limits of the experimental protocol, for example, by re-evaluating the number of subjects, the time inserted between surgery and Golgi staining, the type of morphological analysis

employed, the neuronal area chosen to be studied, the staining method, the microscopy technique, and any possible effect of the behavioural training that could have had an impact on the results.

For the Sholl analysis, an average of thirteen cells per animal were used, while for the spine density analysis six dendritic branches per animal were analysed; it is possible that an effect could be detected by increasing this number. However, the number of animals per group and the number of dendritic branches per animal analysed were almost identical to those used in Harland (2013) and Harland et al. (2014) studies, while the number of dendritic arbors per animal for Sholl analysis was greater in this experiment in comparison to those other studies. Thus the number of animals, dendritic arbors and dendritic branches used in this experiment appears reasonable.

The time delay interposed between surgery and Golgi staining could also have had an impact on the outcome. Three months were chosen for two main reasons. First, both Harland (2013) and Harland et al. (2014) experiments used approximately the same amount of time and so maintaining the same delay would provide a closer comparison with previously published findings. Second, immediate early gene imaging studies have shown retrosplenial dysfunction ranging from 2 weeks (Vann & Albasser, 2009) 10 months (Vann, 2013) after mammillothalamic tract lesion, thus structural changes might also be expected within a 3 month frame. It is possible, however, that a longer time delay would increase the magnitude of the change, and that 3 months after surgery the change is still extremely small. For example, a subtle difference was detected in the present experiment between the two groups (MTT-lesioned versus controls) when looking at the complexity in the distal part of their apical dendritic arbors and in the middle part of their basal arbors, with the MTT-lesioned group's arbors appearing less complex than the arbors of controls (Figure 3-16 and Figure 3-17). Maybe these differences could have been exacerbated waiting inserting a longer time-delay between surgery and Golgi staining.

Another possible improvement in the experimental analysis would be categorising the type of neurones imaged. In this experiment, small pyramidal neurones located in layers II-III of Rgb were analysed. It was difficult to morphologically distinguish between small canonical pyramidal neurones and small fusiform pyramidal neurones, especially for the apical dendritic arbor Sholl analysis and spine density analyses, because for the majority of cases their basal arbors/complete somata were not visible (mainly because other neurones or staining artefacts were obscuring them) and the two types of neuron (fusiform and canonical pyramids) are very similar in their apical

portion. However, it could be the case that these two types of neurones are differentially affected by the mammillothalamic tract lesions, so their subdivision could be important; in the study of Harland et al. (2014) only the fusiform pyramidal type was analysed. A possible refinement of the experiment could be trying to re-analyse the data, selecting a subset in which the small canonical pyramidal neurones and small fusiform pyramidal neurones are clearly discernible.

Regarding the analyses of the dendritic arbor complexity, additional parameters could be measured, as they may be differentially affected by the lesions: for example comparing the total dendritic length and the mean length of each branch order (as in the studies of Torres-García et al., 2012; and Harland, 2013], with the expectation that dendrites in the MTT-lesioned group would be possibly shrunken and their length reduced in comparison to controls.

Finally, as the analysis of this study was limited to the superficial layers II-III of Rgb, it could be interesting to extend it also to other areas where a loss in immediate early gene expression was found, such as the deep layers of Rgb, the retrosplenial subregion Rdg and the hippocampus. As already mentioned, the study carried out by Harland (2013) showed a decrease in spine density and dendritic complexity for pyramidal neurones of the CA1 subfield after anterior thalamic lesions, making this region potentially interesting.

Regarding the staining technique, the Golgi method, as already mentioned, is quite unpredictable as it stains only a small percentage of the total neurones present in the brain; the mechanisms behind this apparently random staining are still unknown. It has been suggested that the selectivity of the staining could be related to the metabolic activity and pH levels of the cells, but the exact mechanisms are not clear (Shankaranarayana & Raju, 2004). It is then possible that the stained neurones are not representative of the whole population of cells and this could have biased the interpretation of the results reported here. A possible alternative technique to Golgi staining, which allows staining without selection bias (i.e. regardless of the physiological status of the cell), is DiOlistic labelling (Gan, Grutzendler, Wong, Wong, & Lichtman, 2000); this involves in propelling lipophilic dye-coated particles (which are usually made either of tungsten or gold, while the dye is mostly fluorescent) into the cells using a high-pressure ballistic particle delivery system (a high pressure helium device also called “gene gun”, as the technique was originally used for the delivery of DNA constructs into the cells; e.g. Lo, McAllister, & Katz, 1994). Once the

dye-coated particle is “shot” into the neuron, the cell membrane incorporates the dye, giving rise to a fluorescent Golgi-like staining. As the dye-coated particles are dispersed across the tissue sample, the labelled neurones should be separated enough to be completely visualised on normal background tissue. Furthermore, the density of the staining (which was a particularly relevant issue in this experiment, giving rise to many artefacts) can be controlled by choosing the appropriate amount of dye on each delivery particle (Staffend & Meisel, 2011). This technique has been used to visualise dendritic morphology (Williams et al., 2013; Wu, Reilly, Young, Morrison, & Bloom, 2004), dendritic spine density (Ji et al., 2003; Smith, Pozueta, Gong, Arancio, & Shelanski, 2009; Williams et al., 2013; Wu et al., 2004) and dendritic spine shapes (Smith et al., 2009).

Another limit of the experiment concerns the visualisation of dendritic spine morphology using bright field microscopy, as with this technique dendritic spine shapes can be correctly recognised only if they are properly oriented. As an alternative, confocal microscopy (Bulley, Drew, & Morton, 2012) could be considered for imaging dendritic spines, as it improves the image quality by reducing background noise and allowing the reconstruction of three-dimensional pictures (in two-dimensional images the number of spines is often underestimated). However, all conventional light microscopy techniques (included confocal microscopy) offer a limited resolution that never gets over the theoretical limit of 200 nm (Abbe diffraction limit), due to the diffraction properties of light. The main problem with dendritic spines is that, apart from spine length, the other spine dimensions are usually smaller than this limit. In order to correctly visualise dendritic spine details it is possible to use super resolution microscopy, for example stimulated emission depletion imaging (Tønnesen, Katona, Rózsa, & Nägerl, 2014) or serial electron microscopy (Dhanrajan et al., 2004; Harris & Stevens, 1989); however, super resolution microscopy is not always easily accessible and is technically demanding. A more affordable possibility would be using deconvolution image processing techniques able to improve the resolution of digital images acquired through confocal microscopy (Dumitriu, Rodriguez, & Morrison, 2013; Heck, Betuing, Vanhoutte, & Caboche, 2012).

When considering the behavioural component of the experiment, the lesioned animals were impaired on the double T-maze task in comparison to control levels, consistent with previous findings (Vann, 2013); this impairment confirmed the efficacy of the mammillothalamic tract lesions in this experiment. It has been shown that lesions of different components of the Papez circuit make animals more reliant on specific

strategies to solve the T-maze task. As already described in Section 1.3.4, rats are impaired on the standard version of the T-maze (in which all types of cues are available) after anterior thalamic nuclei lesions (Aggleton et al., 1996; Aggleton, Neave, Nagle, & Hunt, 1995; Warburton, Baird, & Aggleton, 1997), fornix lesions (Aggleton, Neave, Nagle, & Hunt, 1995; Aggleton, Neave, Nagle, & Sahgal, 1995; Baird et al., 2004; Harland et al., 2014; Markowska, Olton, Murray, & Gaffan, 1989; Neave, Lloyd, Sahgal, & Aggleton, 1994; Neave, Nagle, & Aggleton, 1997; Shaw & Aggleton, 1993; Vann, Erichsen, O'Mara, & Aggleton, 2011; Warburton et al., 1997; Warburton, Aggleton, & Muir, 1998) and hippocampal lesions (Aggleton et al., 1986; Bannerman et al., 1999; Dudchenko et al., 2000; Racine & Kimble, 1965). However, after mammillary body lesions the deficit on the standard T-maze task appear milder and gradually disappear with training (Aggleton et al., 1990; Aggleton, Neave, Nagle, & Hunt, 1995; Neave et al., 1997; Vann & Aggleton, 2003). Similarly, after mammillothalamic tract lesions, animals show only transitory deficits (Vann & Aggleton, 2003) or no impairment at all (Vann, 2013). However, an impairment after mammillary and mammillothalamic tract lesions has been shown to emerge when animals are forced to rely on extramaze cues to solve the task, as in the double version of the T-maze task (Vann, 2011, 2013), reflecting a deficit in extramaze cue processing after these two kinds of lesions. In the present study, MTT-lesioned animals were impaired not only in the double version of the T-maze task (as expected), but also in its standard variant. However, examining their performance on each trial, MTT-lesioned animals seemed to have reached control' performance levels by the last sessions of the standard T-maze (Figure 3-12), while in the double T-maze task they were still impaired in the last sessions in comparison to the control group (Figure 3-13). This is probably due to the fact that in the standard T-maze task MTT-lesioned animals learned to use intramaze cues to solve the task by the end of training, while in the double T-maze task those cues were no longer available and the animals were impaired in using alternative strategies.

As found in previous studies (Pothuizen et al., 2008; Vann, 2013), in the double T-maze task the same place trials were more difficult to solve than the different place trials, and the control animals showed the biggest drop in performance (see Figure 3-14), probably because they were relying more on the use of extramaze cues, which were misleading in the same place trials.

A further factor to consider is that the spatial memory training employed to verify the behavioural efficacy of the lesions could have had some impact on the dendritic

morphology and spine density results. Some experiments have found that spatial learning can affect dendritic morphology and spine density in the brain. Standard T-maze training was associated with an increase in spine density and branch order in pyramidal neurones of the anterior cingulate cortex (Comeau, McDonald, & Kolb, 2010; Kolb, Cioe, & Comeau, 2008). In Harland (2013) and Harland et al. (2014) experiments, environmentally-enriched rats trained both on reinforced T-maze alternation and on the radial arm maze task showed an increase of thin and mushroom spine density in the basal dendritic arbors and an increase in dendritic complexity and length of apical dendritic arbors of CA1 pyramidal neurones, in comparison to yoked pseudo-trained controls. Harland et al. (2014) also looked at apical dendritic spine density of fusiform pyramidal cells of Rgb but they did not find any significant effect of spatial memory training on their number; however, they did not look at Rgb dendritic arbor complexity. Moreover, a study by Tronel et al. (2010) found an increase, in the granule cells of the dentate gyrus, of dendritic arbor complexity and mushroom spine density after rats were trained for 6 days on the water maze task; these changes were still present 3 months after training. Thus, it appears that dendritic changes related to spatial learning can be persistent for a period of time comparable to that used in this experiment (3 months), even when the behavioural training was only lasted a few days. In the present experiment, both lesioned and non-lesioned groups received pre-training and training on the standard and double T-maze task for a total of 22 days starting 1 week after surgery. In order to clarify if this behavioural training had affected dendritic complexity and spine density, it would be worth adding two control home-cage groups of rats, which received either mammillothalamic tract lesion or sham surgery but were behaviourally naïve at the time of perfusion.

In conclusion, lesions of the mammillothalamic tract produced a behavioural impairment yet had no effect on spine density measured at the level of the apical arbors of superficial small pyramidal neurones of Rgb. A subtle effect on dendritic arbor complexity (analysing separately the apical and the basal arbors) was visible, as in the MTT-lesioned group the apical arbors and the basal arbors gave rise to a smaller number of Sholl intersections in comparison to controls in either their distal or middle part, respectively. However, this difference did not reach statistical significance. Complementary approaches to assess dendritic plasticity may be needed to investigate this trend further given some limitations of the Golgi staining

and the analysis, e.g. using a different staining technique and/or analysing the data with more powerful statistical tests.

Chapter 4 Methods development for infusion of antisense *c-Fos* and *Zif268* oligodeoxynucleotides into either the dorsal hippocampus or the retrosplenial cortex.

4.1 INTRODUCTION

Performing spatial memory tasks increases expression of c-Fos and Zif268 in the dorsal hippocampus (He et al., 2002; Vann, Brown, Erichsen, et al., 2000a) and in the retrosplenial cortex (Pothuizen, Davies, Albasser, Aggleton, & Vann, 2009; Vann, Brown, & Aggleton, 2000) of rats. However, it is not known whether these changes are functionally important for task performance. Furthermore, c-Fos and Zif268 expression has been reported to be disrupted in the same regions following lesions of the anterior thalamic nuclei and mammillothalamic tract (Dumont et al., 2012; Jenkins, Dias, Amin, & Aggleton, 2002; Jenkins, Dias, Amin, Brown, et al., 2002; Jenkins et al., 2004; Poirier & Aggleton, 2009; Poirier, Shires, et al., 2008; Vann & Albasser, 2009; Vann, 2013), but again it is uncertain whether these immediate early gene changes contribute to the spatial memory impairments observed. In order to specifically test this, it is necessary to disrupt immediate early gene expression and assess the behavioural consequences. For this purpose, it is necessary to develop a behavioural task that might be sensitive to disruption of immediate-early gene expression and that is dependent on the key brain structures under investigation, i.e. the hippocampus and the retrosplenial cortex. To disrupt immediate-early gene expression, specific antisense oligodeoxynucleotides (ODNs) can be infused into the area under consideration before animals are tested on the task. Therefore, it is also necessary to be sure that all aspects of cannulation and infusion are robust and effective. This chapter focuses on developing these methodological components with the ultimate aim of assessing the effects of antisense ODN infusions into either the dorsal hippocampus or the retrosplenial cortex on spatial memory in rats.

The aim of Experiment 1 of this chapter was to develop a behavioural task that could be subsequently used to test the effect of immediate early gene disruption by infusion

of antisense ODNs. The task chosen was a variant of the standard working memory radial arm maze task and included the insertion of a maze rotation and a 3-hour delay in the middle of the task. Rats trained in this task received also dorsal hippocampal cannulation surgery and were then challenged in the task with infusion of muscimol, a GABAergic agonist, in order to verify that the performance in the modified task was dependent on dorsal hippocampal activity.

All rats acquired this modified radial arm maze task, but half of them were not impaired after muscimol infusions, mainly because of cannulae misplacement and infusion microinjectors blockage. Two further experiments (Experiments 2 and 3) were then carried out, which focused on task development in order to optimise cannulation surgery and infusion procedure in the dorsal hippocampus. These experiments used muscimol infusions as the behavioural effects of these infusions into the hippocampus are well-described. Three different spatial tasks were used in Experiments 2 and 3, the 1-minute delay with maze rotation variant of the radial arm maze task, the standard T-maze task and the continuous alternation T-maze task; they were chosen because they all tax spatial memory and were therefore expected to be dependent on the dorsal hippocampus. A further factor was that those tasks were relatively quick to acquire. Muscimol infusions were administered before the tasks in order to produce a spatial memory impairment.

4.2 EXPERIMENT 1: modification of a radial arm maze task to be used after *c-Fos* and *Zif268* antisense oligodeoxynucleotide infusion

A radial arm maze task was chosen as an increased immediate early gene expression in normal animals (Section 1.4.5.2) and a decreased expression in lesioned animals (Section 1.4.6) was found in the Papez circuit following performance on this task.

Other possible spatial memory tasks, such as the water maze task and the T-maze task were not considered to be suitable: the former because it has been shown to highly increase stress levels in the animals (Holscher, 1999), thus adding a confounding factor to the experiment for which it is difficult to obtain suitable control; furthermore, given that the rats will have cannulae protruding from their heads and attached with cementum, it was not the best option to use a behavioural task that requires animal to spend time in the water. Considering the T-maze task, instead, a main issue was that the retrosplenial cortex (which, with the dorsal hippocampus, was one of the brain areas under investigation) does not seem to be necessary to support it, as its lesions did not cause any impairment in the standard T-maze task (Nelson et al., 2015; Pothuizen et al., 2008; Pothuizen, Davies, Aggleton, & Vann, 2010).

The performance on the standard version of the radial arm maze task is highly reliant on the integrity of the hippocampal system as lesions of either the whole hippocampus (Cassel et al., 1998; Li et al., 1999; Sziklas & Petrides, 2002), the dorsal hippocampus (Potvin et al., 2006; Winocur, 1982), or of the main hippocampal efferent pathway, the fornix (Becker et al., 1980; Cassel et al., 1998; Neave et al., 1997; Sziklas & Petrides, 2002) highly disrupt performance on this task. Varying results have been found regarding the effects of retrosplenial lesions on the standard radial arm maze task, with two studies detecting just a mild deficit (Vann & Aggleton, 2002, 2004a) and a third study no deficit at all (Pothuizen et al., 2008). However, impairments are consistently observed after retrosplenial lesions in a modified version of the task which removes the possibility of using intramaze cues for its solution (Pothuizen et al., 2008; Vann & Aggleton, 2002, 2004a). In this modified version, after the first four arm choices, the task is stopped and the maze is rotated of 45 º (either clockwise or anticlockwise). The remaining four food rewards at the end of each arm are moved

so that they are placed in the same position relative to distal room cues in which they were in before maze rotation. The task is then re-started, allowing the animal to explore all the maze arms. As the four remaining food rewards have been re-positioned, animals cannot rely anymore on intramaze cues, but need to use the other cues available, such as the visual distal cues present in the room surrounding the maze. It has been suggested that retrosplenial-lesioned animals are impaired in solving the task when extramaze cues are put in conflict with intramaze cues, a phenomenon which has also been confirmed using the standard T-maze task (Nelson et al., 2015).

I modified the standard working memory protocol taking into account two requirements. Because the final goal was testing the effect of disrupting *zif268* and *c-fos* expression on spatial memory in both the dorsal hippocampus and in the retrosplenial cortex, the behavioural task to be employed needed to be sensitive to lesions of both structures. The second requirement was to design the task so that increased expression of *c-fos* and *zif268* could have a functional effect on the task. Many immediate early gene studies have shown that increased protein levels are typically found 90-120 minutes after neuronal activation (see Section 1.4.3 and Vann, Brown, & Aggleton, 2000; Vann, Brown, Erichsen, et al., 2000a); these increased levels might not be expected to have an effect on a previously performed task but instead might affect consolidation of this task. The modified radial arm maze task with rotation appeared suitable for these aims; not only it relies on both hippocampal and retrosplenial functionality, but it also can be divided into two phases, one before the rotation (the “sample” phase, during which the animals explore four arms and retrieve the first four food rewards) and the other after the rotation (the “test” phase, during which the animals need to remember which arms are still unexplored so they can retrieve the remaining food rewards), and a variable time delay can be inserted between the two. The hypothesis was that animals would have learned the spatial positions of the four visited arms during the sample phase and spatial learning and consolidation memory process would have increased *c-fos* and *zif268* expression levels in the Papez circuit during and immediately after the sample phase. If this immediate early gene increase was functional to spatial learning and was experimentally disrupted during the time delay between the sample and test phase, the animals should not remember which arms they had visited in the sample phase, resulting in them making more errors.

In previous experiments which used radial arm maze task with maze rotation, the time delay inserted in the middle of the task was usually minimal, about 60 seconds (Nelson & Vann, 2014; Pothuizen et al., 2008; Vann & Aggleton, 2002, 2004a, 2005), and only one study employed a longer delay of 20 minutes (Vann & Aggleton, 2003). As already mentioned, *c-fos* and *zif268* reach their peak of protein expression at about 2 hours after stimulation; thus, for this experiment a time delay of 3 hours was inserted between the sample and test phase, in order to allow for the protein expression of these two immediate early genes after the sample phase. Two studies employing a time delay after the first four choices in the standard radial arm maze task (but without maze rotation) showed that animals' performance was still similar to no delay levels when interposing a time delay of up to 4 (Yoshihara & Ichitani, 2004) - 6 hours (Galani et al., 2002) between the sample and the test phase of the task. Furthermore, an experiment using a different modification of the radial arm maze task has shown that rats are able to retain spatial memories for at least 4 hours if they are gradually habituated to the delay (Saito, Okada, et al., 2010).

In the present experiment (see schematic behavioural protocol Figure 4-1) a group of rats was first trained on the standard working memory version of the radial arm maze task, then introduced to the maze rotation variant with a 1-minute delay between the two phases of the task, and then gradually habituated to longer time delays, up to 3 hours. The gradual increase of the delay seemed essential as rats found it very difficult to solve the task if the 3-hour time delay was introduced immediately after the 1-minute delay task (personal observation). After the gradual task acquisition, the same group of animals received cannulation surgery aimed at the dorsal hippocampus. The animals were then re-trained on the 3-hour delay with rotation variant of the radial arm maze task and were finally tested after infusion of muscimol. Muscimol is a powerful GABAergic agonist of neuronal ionotropic receptors (specifically it is agonist of $GABA_A$ receptors and partial agonist of $GABA_C$ receptors) and it is extracted from Amanita Muscaria mushrooms (Johnston, 2014). Due to its properties, muscimol can temporarily impair brain activity locally (through neuronal hyperpolarization) yet spares fibres of passage (Edeline, Hars, Hennevin, & Cotillon, 2002), thus inducing a "reversible" lesion. Animals were infused with muscimol in order to verify at the behavioural level the efficacy of the surgeries and of the infusion technique; given the importance of the dorsal hippocampus for the task, they were expected to be impaired. Muscimol has already been shown to disrupt spatial memory performance when infused in the dorsal hippocampus of rats subsequently tested with a variety of tasks: a variant of the radial arm maze task (Saito, Okada, et al., 2010),

standard T-maze alternation (McHugh, Niewoehner, Rawlins, & Bannerman, 2008) and continuous T-maze alternation (Czerniawski, Yoon, & Otto, 2009; Hallock, Arreola, Shaw, & Griffin, 2013), the reference memory version of the water maze task (Moser & Moser, 1998), a spontaneous alternation task in the Y-maze (Krebs-Kraft & Parent, 2009), a spatial discrimination task (Kim & Lee, 2011) and a conditioned place preference task (Holahan, 2005). The behavioural impairment caused by muscimol is reversible: effects typically reach their peak at about 30 minutes - 1 hour and a half post infusion, gradually disappear in the following 5 hours and a half (Arikan et al., 2002) and are completely absent 24 hours after the infusion (McHugh et al., 2008); thus, animals can be tested more than once on different days. In this experiment, animals were infused with muscimol and 30 minutes later they were engaged in the modified radial arm maze task; given the highly disruptive effect of muscimol on neuronal activity, the animals were expected to show a deficit in their performance after the dorsal hippocampal infusions.

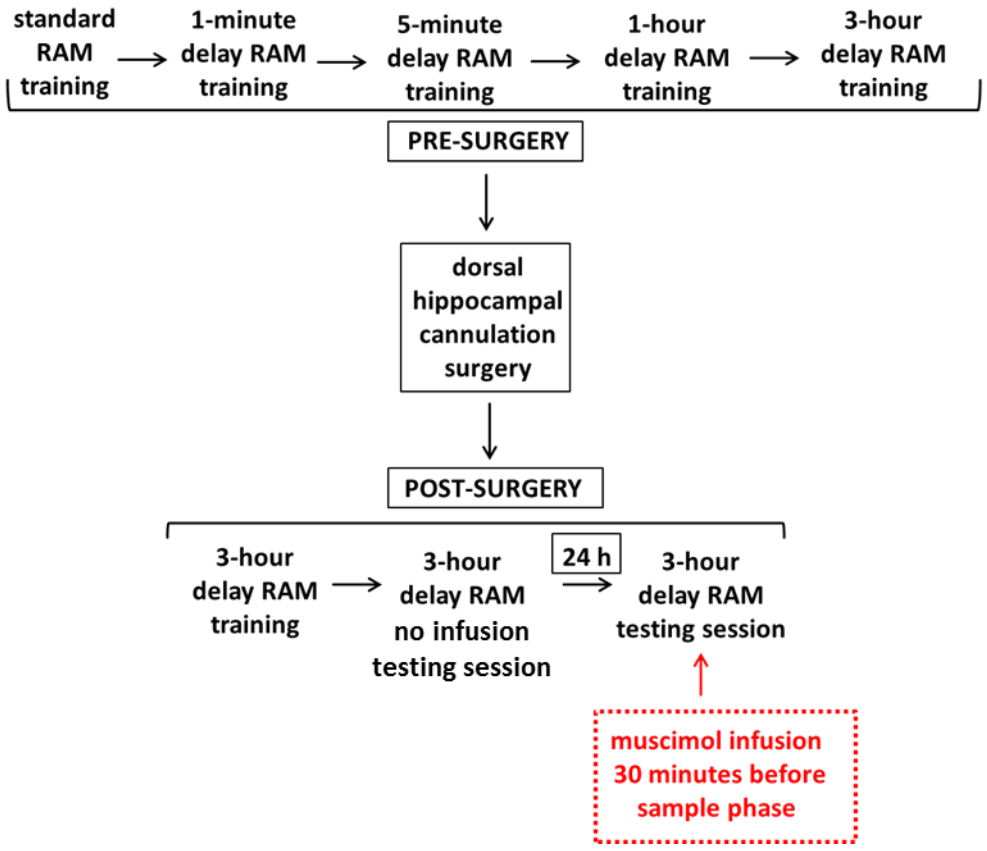

Figure 4-1. Schematic behavioural protocol. RAM = radial arm maze. All the delayed radial arm maze tasks involved also a maze rotation (45° either clockwise or anticlockwise) between the sample and test phase of the task.

4.2.1 Methods

4.2.1.1 Subjects

Subjects were seven male naïve Lister Hooded rats (Charles River, UK), weighing 387-406 g at the time of surgery. Rats were initially housed in pairs under diurnal light conditions (14 h light/10 h dark) and testing was carried out during the light phase. After surgery, the animals were housed individually due to the implanted cannulae. Rats were given free access to water throughout the experiments. During the behavioural test period the animals were food deprived, but their body weight did not fall below 85% of free feeding weight. Animals were thoroughly handled before the study began in order to habituate them to the handling procedure. The experiment was carried out in accordance with UK Animals (Scientific Procedures) Act, 1986 and associated guidelines.

4.2.1.2 Behavioural procedure

Radial Arm Maze Task

Apparatus

Testing was carried out in an eight-arm radial maze. The maze consisted of an octagonal central platform (34 cm in diameter) with eight equally spaced arms (87 cm long, 10 cm wide). The floor of the central platform and the floors of the eight arms were made of wood, and the walls of the arms (24 cm high) were made of clear Perspex. Close to the furthest end of each arm was a food well (2 cm in diameter and 0.5 cm deep). At the start of each arm was a clear Perspex guillotine door (12 cm high) that controlled access to and from the central platform. Each door was attached to a pulley system that enabled the experimenter to control access to the arms. The maze was in a rectangular room that contained salient visual cues such as geometric shapes and high-contrast stimuli on the walls. Lighting was provided by overhead lights.

Pre-surgery behavioural procedure

One day before the beginning of training, the rats were familiarised with the sucrose reward pellets (5TUT/1811251 45 mg, TestDiet, St Louis, Missouri, US) in their home cage. Rats were brought to the testing room individually in an aluminium carrying box, with a lid on the top to prevent them from seeing outside the box. Rats first underwent three habituation sessions where they were allowed to freely explore the maze for 5 minutes. All guillotine doors were raised and reward pellets were scattered down the

arms. In the first habituation session rats were placed in the maze in home-cage pairs, then singularly for the remaining two sessions. This was followed by formal training. Formal training consisted of two stages.

Stage 1 was the standard working memory version of the radial arm maze task (Figure 4-2). At the start of a session, each of the eight arms was baited with a single reward pellet. The rat would then make an arm choice, eat the pellet from the end of the arm and then return to the central platform. All the doors were then closed for about 10 seconds before being opened again, allowing the rat to make another choice. This continued until all eight arms were visited or a time limit of 10 minutes was reached. The rats' optimal strategy was to retrieve the reward pellets from all eight arms without re-entering any previously visited arm. If a rat re-entered a previously visited arm it was considered an error. The training continued until the rats were performing the task well, making no more than one error per session for at least two consecutive sessions.

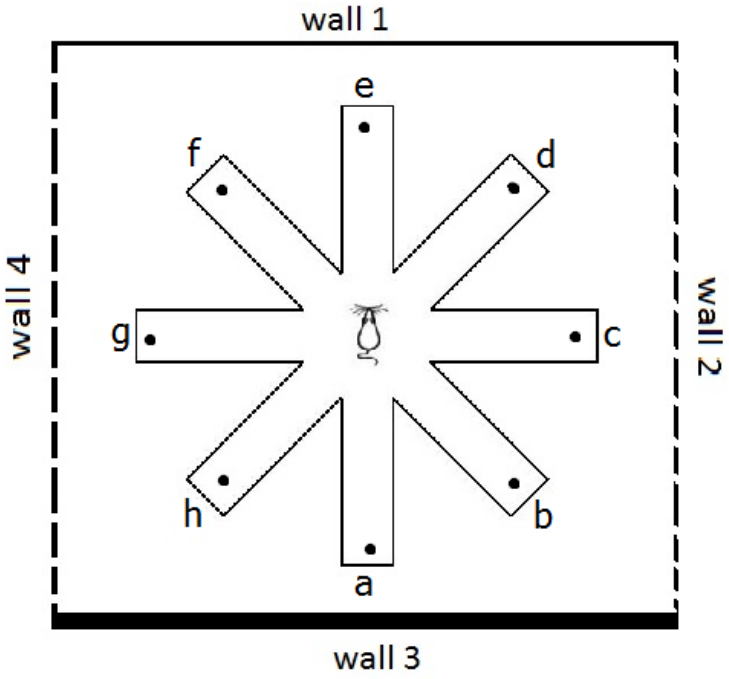

Figure 4-2. Apparatus for the radial arm maze task. The different line patterns around the maze represent different visual extramaze cues on each wall of the testing room

In Stage 2, a modification to the standard working memory task was introduced, inserting a maze rotation and gradually increasing time delays in the middle of the task. The start of the session (sample phase) was identical to the standard version of the task. However, after the animal made four correct choices, it was removed from

the maze for a variable time delay during which the maze was rotated by 45° (either clockwise or anticlockwise, on alternating days) and the remaining food pellets were moved, so that they were still in the same position in relation to the extramaze cues, but they were now placed in different arms (different position referring to the intramaze cues) (Figure 4-3). After that, the rat was returned to the central platform of the maze and the session continued until all the remaining four reward pellets were retrieved or 10 minutes were passed (test phase). The time delay between the sample and the test phase was gradually increased, starting from 1 minute, to 5 minutes, 1 hour and finally 3 hours. During the delay, the rat was placed in an enclosed aluminum carry-box (10 cm wide x 10 cm high x 26 cm long, also located in the testing room) in the case of the 1-minute delay, or in a cage in a separate dark and quiet room for longer delays. Each time-delay increment was introduced after the rat was able to perform the task at the criterion level (no more than one error and all arms visited for at least two consecutive sessions). The animals received one training session per day. After the animals reached criterion for the 3-hour delay task, they underwent surgery (Section 4.2.1.3).

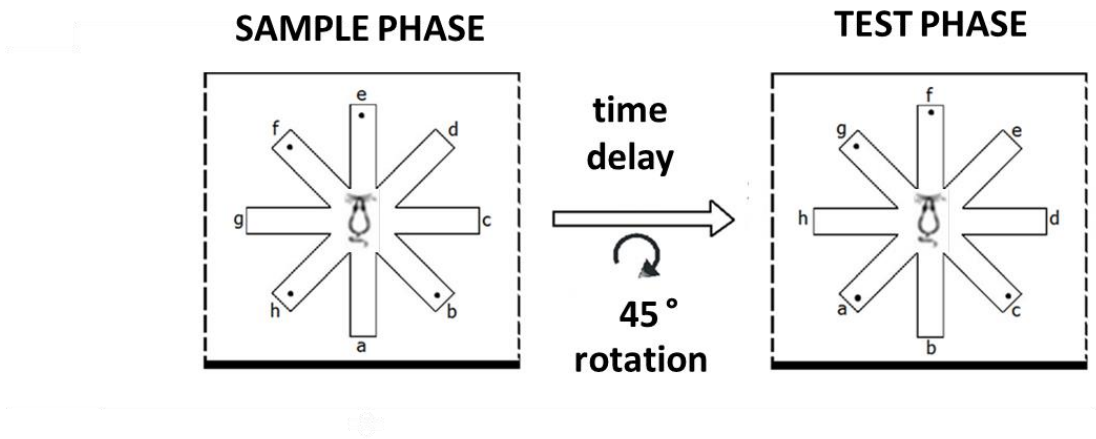

Figure 4-3. Modified version of the radial arm maze task with maze rotation and a time delay between the sample and the test phase. The different line patterns around the maze represent different visual extramaze cues on each wall of the testing room. Maze rotation was 45° either clockwise or anticlockwise.

Post-surgery behavioural procedure

After animals had recovered from surgery, they were re-trained on the 3-hour delay version of the radial arm maze task. Once they reached the criterion level, they

received a test sessions without any infusion; then, they received a final test session after receiving a muscimol infusion (muscimol administered 30 minutes before the sample phase, see Section 4.2.1.4).

4.2.1.3 Surgical procedure

Once animals could reliably perform the modified version of the radial arm maze task with maze rotation and a 3-hour delay, they were implanted with bilateral chronic indwelling guide cannulae targeting the dorsal hippocampus.

Each animal was deeply anaesthetised with 4% isofluorane (Teva UK Limited) in O_2 in a transparent Plexiglas induction chamber; once anaesthetised, the rat was placed in a stereotaxic frame (David Kopf Instruments, Tujunga, CA) with a specialised mask for continuous anaesthetic flow (1-2 % isofluorane in O_2). The position of the incisor bar of the stereotaxic frame was adjusted for each rat (approximately -3.5/-3.0 mm to the interaural line), to maintain the skull flat on the horizontal plane. The incision site was sterilised with surgical scrub (Videne, Ecolab, UK). A midline incision was made on the top of the scalp to expose the dorsal skull. Lidocaine (2% w/v, B. Braun, Germany) was topically applied to the skin to act as a local anaesthetic. Bregma was identified, and antero-posterior (AP) and medio-lateral (ML) coordinates were taken. Four bone micro screws (Bilaney, United Kingdom) were fitted into four small burr holes in the skull that were made using a handheld drill (Bilaney, United Kingdom), two positioned in the posterior part of the frontal bone and two positioned in the posterior part of the parietal bone. Two circular holes were made using a drill to target the dorsal hippocampus (coordinates: -3.5 mm AP, ± 1.9 mm ML) for the implantation of bilateral stainless steel guide cannulae (21 gauge, 3.8 mm centre-to-centre, cut to 3 mm below the plastic supporting pedestal; PlasticsOne, Virginia, United States). The guide cannulae were lowered such that the plastic pedestal rested on the skull surface and was adhered to the skull and to the four bone screws using dental acrylic cement (Kemdent, United Kingdom). Two stainless steel stylets (to protrude 1 mm beyond the guide cannulae, PlasticsOne, Virginia, United States) were inserted to maintain cannula patency during recovery and prevent infection. To reduce post-operative pain, all animals received a subcutaneous injection of 0.06 ml Metacam (5 mg/ml; Boehringer Ingelheim, Berkshire, UK) before the end of the surgery. On completion of surgery, the skin was loosely sutured around the cannulae and antibiotic powder (Clindamycin Hydrochloride; Pharmacia, Sandwich, United Kingdom) was topically applied on the wound site. Finally, animals received subcutaneous injections of 5 ml glucose saline and were placed in a temperature-controlled recovery box until

they awoke from surgery. Rats were allowed to recover for 7 days before undergoing any further procedures; during this time their recovery was carefully monitored and their weights daily checked.

4.2.1.4 Infusions

General infusion procedure

Each rat was gently wrapped in a soft towel whilst awake and the stylets were manually removed before dual microinjectors (28 gauge, 3.8 mm centre-to-centre, 1.25 mm projection beyond the tip of the guide cannulae; PlasticsOne, Virginia United States) were inserted slowly into the surgically implanted guide cannulae. The microinjectors were connected via polyethylene tubings (PE 0.38x0.355 mm; Scientific Laboratory Supplies, United Kingdom) to two 5 µl syringes (800 Series, Cemented Needle; Hamilton, United States) fixed in a microinjection pump (model 11 plus, dual syringe pump; Harvard Apparatus, United Kingdom). At the end of each infusion, the microinjectors were kept in place inside the brain for further 2 minutes to allow any solution to diffuse away from the microinjector tip. The microinjectors were then gently removed and the stylets replaced.

To habituate the rats to the infusion procedure and to test cannula patency, they received an infusion of sterile phosphate buffered saline (PBS, 0.1 M pH 7.4; 0.5 µl/infusion site at a rate of 0.5 µl/minute) into the dorsal hippocampus at least 3 days before any testing infusion.

Infusion procedure specific for the experiment

Each animal was infused with 0.5 µl/infusion site of muscimol (diluted in sterile PBS at a concentration of 1 µg/µl; M1523, Sigma-Aldrich, UK) at a rate of 0.5 µl/minute. This volume and dose of muscimol have been effective in other studies (Corcoran, Desmond, Frey, & Maren, 2005; Corcoran & Maren, 2001; Holt & Maren, 1999; Lee & Kesner, 2003; Matus-Amat, Higgins, Barrientos, & Rudy, 2004). Muscimol spread after intracortical infusion (1 µl / infusion site) overlaps with an area with radius 1.7 mm from the infusion site (Martin, 1991). Previous studies have shown that muscimol has an effect on behaviour starting from 20-30 minutes after infusion (Corcoran et al., 2005; Corcoran & Maren, 2001; Czerniawski et al., 2009; Lee & Kesner, 2003; Sang & Lee, 2011; Yoon, Okada, Jung, & Kim, 2008). For this experiment muscimol was infused 30 minutes before the modified radial arm maze task.

4.2.1.5 Histology

Nissl staining for checking cannulae placement

On completion of the experiment, the animals were irreversibly anaesthetised with sodium pentobarbital (60 mg⁄kg, Euthatal, Rhone Merieux, Harlow, UK) and perfused transcardially with 0.1 M PBS followed by 10% formol-saline. The brains were removed and post-fixed in 10% formol-saline for 4 hours and then transferred to 25% sucrose (in 0.1 M PBS) overnight. Sections were cut at 40 µm on a freezing microtome in the coronal plane, and a one-in-three series of sections was mounted onto gelatin-coated slides and stained with cresyl violet, a Nissl stain.

4.2.1.6 Statistical analysis of behavioural data

SPSS software (version 20, IBM Corporation) was used to carry out statistical analyses. The threshold for significance was set at $p < 0.05$ for all statistical tests.

The number of correct arm entries in the first eight arm choices and the total number of errors were recorded for each radial arm maze task session.

For pre-surgery behavioural analysis, performance on the sessions of the modified radial arm maze task with maze rotation and time-delay was compared over time delays (1 minute, 5 minutes, 1 hour and 3 hours) using repeated measures ANOVA. Sphericity of data was checked using Mauchly's sphericity test and degree of freedom corrections were applied when necessary. When significant main effects were found, Bonferroni post hoc tests were run in order to identify which sessions differed from each other.

For post-surgery behavioural analysis both the number of correct entries in the first eight arm choices and the total number of errors after the last no infusion session were then compared to the values obtained in the test session after muscimol infusion using paired samples t-test.

4.2.2 Results

4.2.2.1 Cannulae placement histology

Histological analysis showed that in half of the animals the cannulae were not ideally placed, as they were very asymmetric along the medio-lateral axis. Furthermore, the tracts of the cannulae tips appeared very superficial, located at the extreme top of the dorsal hippocampus (Figure 4-4). Given the limited number of animals, post-surgical behavioural analysis was intially performed on all animals. However, because of the high variability in the behavioural performance, further analysis was performed just on a subset of three animals with the most symmetric cannulae placement (shown on Figure 4-4 and Figure 4-5).

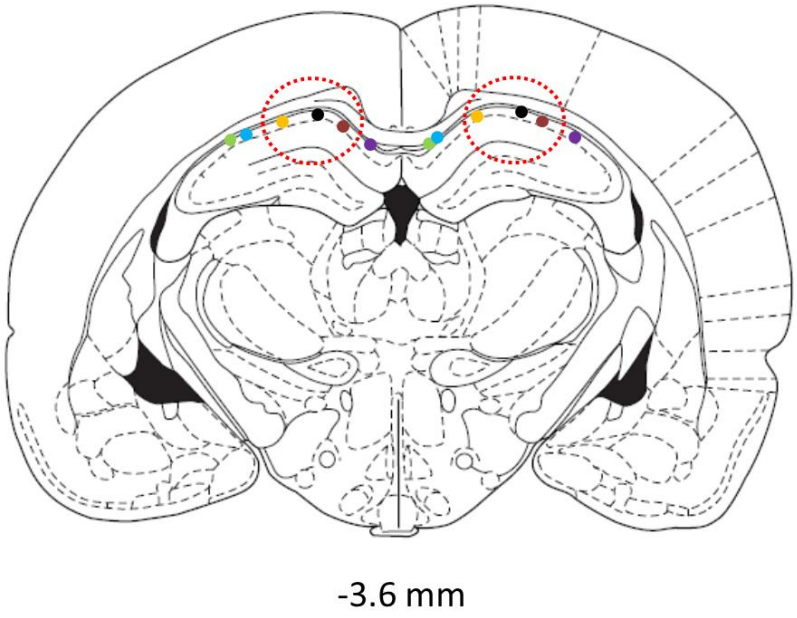

Figure 4-4. Cannulae placement into the dorsal hippocampus (coronal view). Each point represents the position of the tip of the cannula. A different colour has been used to identify cannulae placement for each animal. The red circles enclose the most symmetric cannulae placements (three animals). The distance in mm from bregma is reported. Figure adapted from Paxinos & Watson (1998).

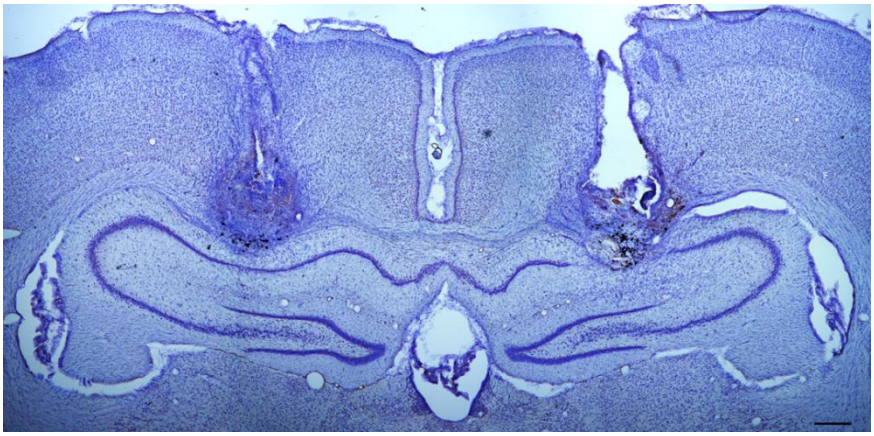

Figure 4-5. Coronal section of the dorsal hippocampus showing cannulae placement. This case was from the subset with the best cannulae placement (i.e. symmetric to the midline). Tissue stained with cresyl violet staining. Scale bar 200 µm.

4.2.2.2 Behaviour

Pre-surgery radial arm maze training

Animals were first trained on the standard working memory version of the radial-arm maze task. Subsequently, time delays of increasing length were inserted after the first four arm choices (1 minute, 5 minutes, 1 hour and finally 3 hours). The animals' performance is summarised in Table 4-1. All animals were able to reach the criterion level (no more than one error and all arms visited for at least two consecutive sessions) in both the standard task and in the variant with maze rotation with each of the delays inserted.

Statistical analysis was carried out comparing performance on the modified radial arm maze with rotation task over the different time delays (the performance on the standard radial arm maze task was not included in the analysis). The analysis did not reveal any significant differences among the different time delays when considering the number of correct entries in the first eight choices ($F_{3,18}$=2.0, p=0.15; Table 4-1).

A significant difference appeared when considering the total number of errors ($F_{3,18}$=3.4, $p<0.05$; Table 4-1), with Bonferroni post-hoc tests revealing a significant decrease in errors when the task was performed with the 3-hour delay in comparison to the 1-minute delay ($p<0.05$).

TIME DELAY INSERTED IN THE TASK	Mean NUMBER OF SESSIONS BEFORE REACHING CRITERION ± SEM	Mean NUMBER OF CORRECT ENTRIES (first eight choices) ± SEM	Mean TOTAL NUMBER OF ERRORS ± SEM
NO DELAY (STANDARD RAM task)	11.0 ± 0.9	5.4 ± 0.3	3.2 ± 0.4
1-MINUTE DELAY	5.6 ± 0.7	6.8 ± 0.1	2.2 ± 0.2
5-MINUTE DELAY	5.3 ± 0.7	7.2 ± 0.1	1.7 ± 0.3
1-HOUR DELAY	3.7 ± 0.5	7.1 ± 0.2	1.3 ± 0.4
3-HOUR DELAY	13.0 ± 1.8	7.2 ± 0.1	1.2 ± 0.1 *

Table 4-1. Summary of performance during pre-surgery behavioural training in the radial arm maze (RAM) task. *significant difference between the performance (evaluated as total number of errors) measured either with the 1-minute or the 3-hour delay variant of the radial arm maze task ($p < 0.05$).

Post-surgery radial arm maze training/testing

One animal died during surgery, thus only six rats contributed to the following analyses.

Following recovery from surgery, rats were trained on the 3-hour delay with maze rotation variant of the task until their performance again reached criterion (no more than one error and all arms visited for at least two consecutive sessions). The mean number of sessions (± SEM) required to reach criterion was 2.6 ± 1.1. During these trials the rats made 1.1 ± 0.2 errors and 7.3 ± 0.1 correct entries in the first eight arm maze choices.

The animals were then tested following muscimol infusion 30 minutes before the sample phase of the task. The performance in the muscimol infusion session was compared with performance after no infusion. No significant difference was found (correct entries during first eight choices: $t_5=1.5$, $p=0.20$; total number of errors: $t_5=-1.6$, $p=0.18$; Figures 4-6 & 4-7).

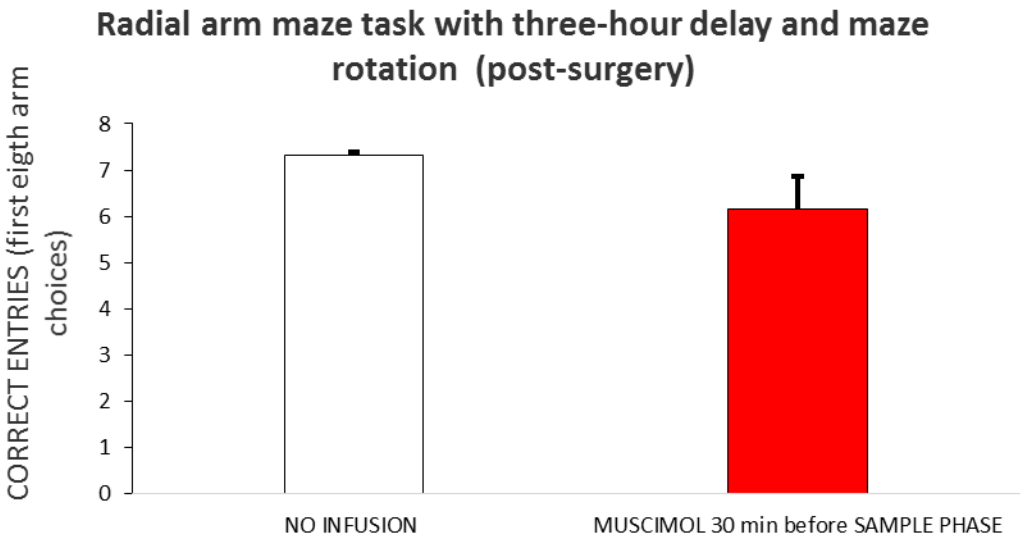

Figure 4-6. Correct entries (mean ± SEM) in the first eight arm choices in the 3-hour delay radial arm maze task with maze rotation after dorsal hippocampal cannulation surgery.

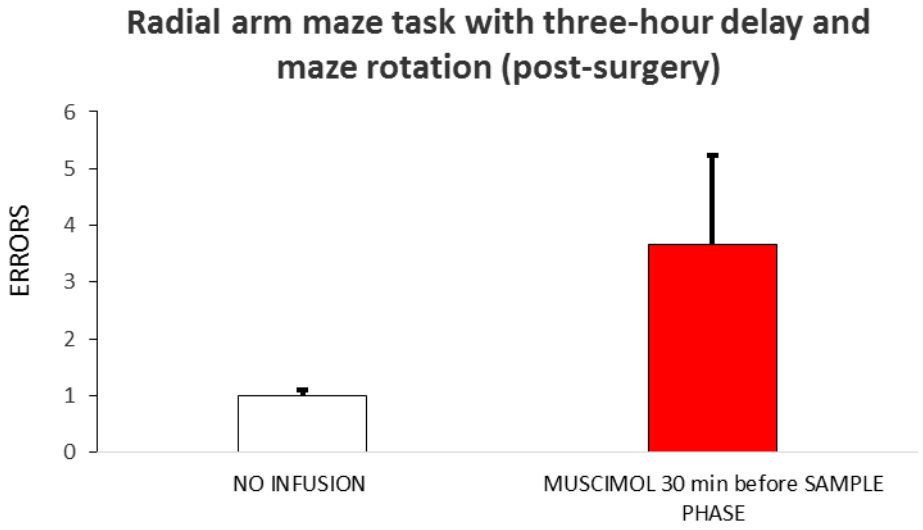

Figure 4-7. Total errors (mean ± SEM) in the 3-hour delay radial arm maze task with maze rotation after dorsal hippocampal cannulation surgery.

4.2.3 Interim discussion

Naïve animals were succesfully trained to acquire a modified version of the radial arm maze task (3-hour delay with maze rotation variant), developed to be used in subsequent experiments. The same animals were then implanted with infusion cannulae targeting the dorsal hippocampus. The animals were re-trained on the 3-hour delay with maze rotation variant of the radial arm maze task, and then tested in the task after receiving bilateral infusions of the GABAergic agonist muscimol; surprisingly, however, the infusions did not impair performance on the behavioural task. Subsequent histological inspection revealed that the cannulae position was not ideal, being too dorsal and asymmetric.

The aim of the present experiment was to develop a behavioural task that could subsequently be used to test the effects of antisense ODN infusions. A modified version of the radial arm maze task was used as it should be dependent on both the dorsal hippocampus and the retrosplenial cortex. In order to detect any behavioural impairments, it is important that animals perform the task well under normal conditions. Despite requiring a large number of training sessions, the animals were able to gradually learn the task with maze rotation and a 3-hour delay inserted in the middle and could perform it making a small number of errors. Furthermore, a significant decrease in the total number of errors was detected in the 3-hour delay task compared to the 1-minute delay task. However, this effect should not be interpreted as the rats' performance improving as a result of the increasing time delay; instead it most likely reflects the accumulated training, as the animals were more experienced on the task during the 3-hour delay training than during the 1-minute delay training. Finally, all animals were able to directly re-acquire the 3-hour delay task realtively quickly post-surgery. It, therefore, appears that this task may be suitable to test the effects of neuronal disruption after antisense ODN infusions.

To test whether performance on this behavioural task was dependent on the dorsal hippocampus, animals were infused with the GABAergic agonist muscimol 30 minutes before the sample phase of the task. When looking at the performance of all animals, there was no effect of infusion. There could be a number of reasons for this. For example an incorrect dose or time of administration of muscimol (even if both have been succesfully used in other experiments, see Section 4.2.1.4). Also blockage of the microinjectors or the guide cannulae during infusion could have contributed to the null results. There are contrasting findings to date as to whether both hippocampi are required to support spatial memory tasks. For example, unilateral hippocampal lesion

studies in rats did not find any impairment in the acquisition of spatial memory tasks like the radial arm maze task (Li et al., 1999; Warburton et al., 2001), the morris water maze task (Warburton et al., 2001) and the T-maze task (Warburton et al., 2001); however, two other studies reported a mild impairment in the acquisition (Fenton & Bures, 1993) and an evident impairment in memory consolidation (Cimadevilla, Miranda, López, & Arias, 2005) on the water maze task in animals unilaterally infused with tetrodotoxin in the hippocampus before the task. It is therefore not clear whether unilateral muscimol infusions into the dorsal hippocampus would be sufficient to induce a spatial memory impairment.

The placement of the cannulae appears critical for obtaining a significant spatial memory impairment. In this experiment, some of the cannulae were positioned asymmetrically and were potentially too superficial. This incorrect placement may have resulted in poor spread of muscimol into the dorsal hippocampus, thus not giving rise to any behavioural impairment in the radial arm maze task.

No control infusions were used in this experiment, as it was a pilot for developing the behavioural task and verifying the efficacy of the lesion and infusion procedures.

In the next experiments, small modifications to the protocol were introduced (e.g., different doses of muscimol to infuse and the extension of the length of the infusion microinjectors) in order to have the best conditions for infusing the antisense *c-Fos* and *Zif268* ODNs and verifying their impact on spatial memory.

4.3 EXPERIMENT 2: effects of muscimol infusions into the dorsal hippocampus on tests of spatial memory (I)

The main goal of this experiment was to optimise the experimental protocol in terms of cannulations and infusions. This principally involved making the cannulae placements more symmetrical. To test the efficacy of the infusion procedures, rats were tested on three behavioural tasks. All animals were trained on the standard and 1-minute delay with maze rotation variant of the radial arm maze task, before dorsal hippocampal cannulae implantation. The reason for choosing the 1-minute delay variant, rather than the 3-hour delay variant of the radial arm maze task, for this pilot experiment was so the animals would acquire the task more rapidly. This would provide a more time-efficient way in testing the efficacy of the surgery and of the infusion techniques on the animals. However, the 1-minute delay variant is not suitable for testing animals infused with the antisense ODNs targeting c-Fos and Zif268, and its use will be confined to the pilot experiments, combined with muscimol infusions, for verifying the efficacy of the surgery and infusion techniques.

After the surgery the rats were re-trained and tested with the 1-minute delay with maze rotation radial arm maze task and with two T-maze tasks (the continuous alternation T-maze task and standard T-maze task). All three types of behavioural tasks are sensitive to dorsal hippocampal dysfunction. Lesions of the dorsal hippocampus disrupt spatial memory performance on the standard radial arm maze task (Potvin et al., 2006; Winocur, 1982), and a deficit has also been reported after muscimol infusions (Saito, Okada, et al., 2010). Furthermore, studies using muscimol infusions into the dorsal hippocampus have shown impairments in the performance of both the standard (Hallock et al., 2013; McHugh et al., 2008) and the continuous alternation (Czerniawski et al., 2009) T-maze tasks.

For all experiments, testing was carried out 30 minutes after the animals were infused with muscimol (see schematic behavioural protocol, Figure 4-8).

Two different volumes of muscimol were used in order to identify the best parameters for future experiments.

After all behavioural procedures were completed, a final bilateral infusion of biotinylated solution was used to visually inspect the spread of the infusate into the dorsal hippocampus.

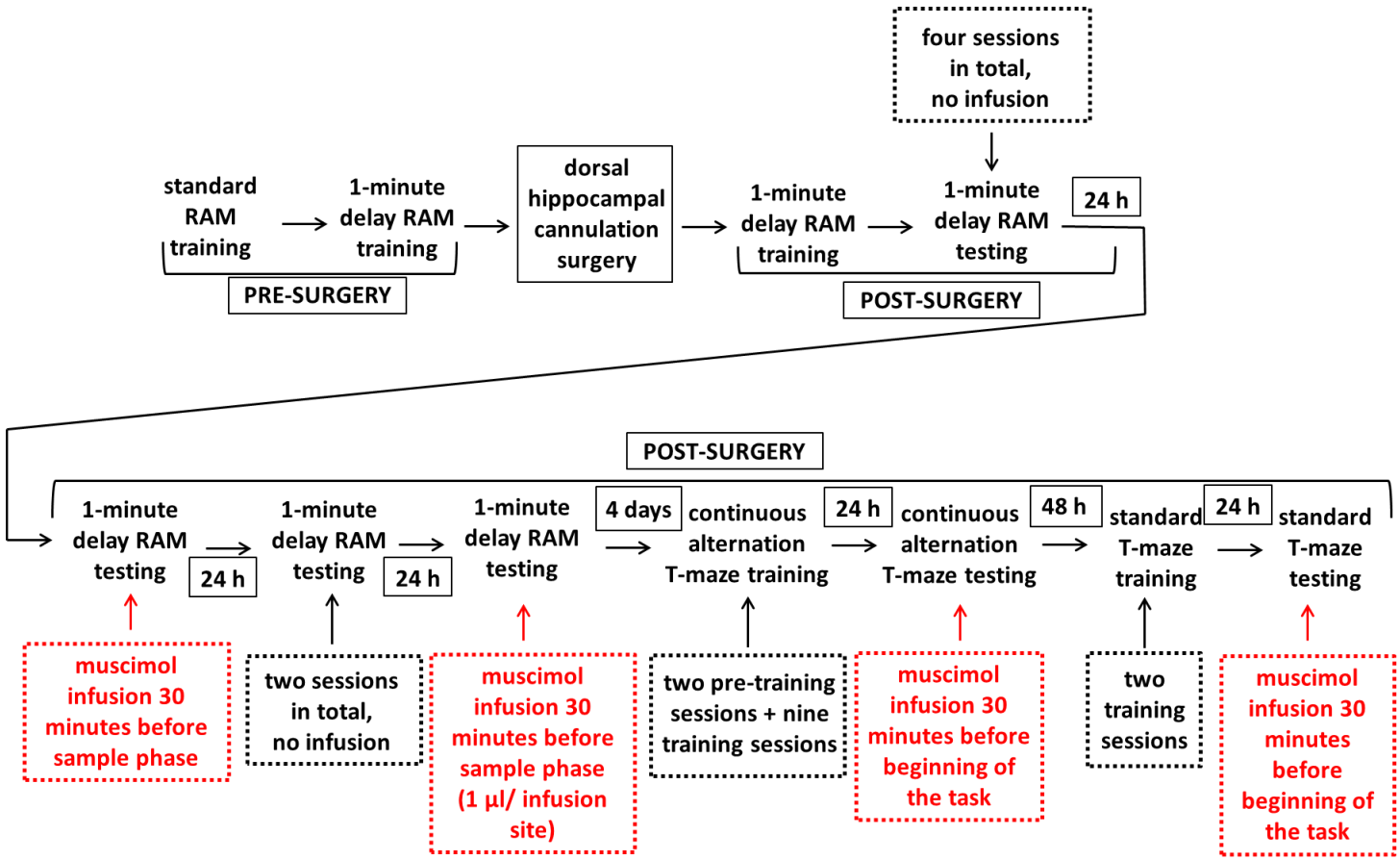

Figure 4-8. Schematic behavioural protocol. All the delayed radial arm maze (RAM) sessions involved also a maze rotation between the sample and the test phase of the task. If not otherwise specified, muscimol infusions were 0.5 µl/infusion site.

4.3.1 Methods

4.3.1.1 Subjects

Subjects were six male naïve Lister Hooded rats (Charles River, UK), weighing 284-326 g at the time of surgery. The housing, light, water access, diet restriction and handling conditions were kept identical to those used in Experiment 1 (Section 4.2.1.1). The experiment was carried out in accordance with UK Animals (Scientific Procedures) Act, 1986 and associated guidelines.

4.3.1.2 Behavioural procedures

Radial arm maze task

Apparatus

The apparatus was identical to that employed in Experiment 1 (Section 4.2.1.2).

Pre-surgery behavioural procedure

Animals were first trained on the standard working memory version of the radial arm maze task and after they reached the criterion level (no more than one error and all arms visited for at least two consecutive sessions) they were trained on the 1-minute delay with maze rotation variant of the task, as described in Experiment 1 (Section 4.2.1.2), until they reached the same criterion level. Then they underwent surgery (Section 4.3.1.3).

Post-surgery behavioural procedure

After animals had recovered from surgery, they were re-trained on the 1-minute delay with rotation variant of the radial arm maze task. Once they reached the criterion level they were tested for eight sessions in total with these specifications: in the first four test sessions animals were not infused; on the fifth test session animals were infused with muscimol before the task; on the following two test sessions animals were not infused; on the final eighth test session animals were again infused with muscimol before the task (see Figure 4-12, and Section 4.3.1.4 for muscimol infusion details).

T-maze task

Apparatus

Testing was performed in a modifiable four-arm (cross-shaped) maze. One of the arms could be blocked off to form a T-shaped maze, with a stem (start arm) ending in a transversal crosspiece. The floors of the T-maze were 10 cm wide and made of wood painted white. The crosspiece was divided into two goal arms (left and right) 140 cm long in total, and the end of each goal arm there was a food well 2 cm in diameter and 0.75 cm deep. The walls of the maze were 17 cm high and made of clear Perspex. The maze was supported on two stands 94 cm high. Access to a goal arm could be prevented by placing an aluminium barrier at its entrance. The maze was located in a room with salient visual cues on the walls. Lighting was provided by overhead lights.

Post-surgery behavioural procedure

Pre-training

Pre-training began post-surgery, 4 days after completion of the radial arm maze task. Each animal was given 2 days of pre-training (8 minutes/day) in order to run reliably down the stem of the maze to find sugar pellets in the food wells in both goal arms. Training began the day after the second pre-training session.

Continuous alternation T-maze task

This task required each animal to continuously alternate between the left and right goal arms to obtain a sugar pellet reward. Each session began with a forced-choice trial, during which the rat was forced to choose a specific baited goal arm (the other was kept inaccessible with a metal barrier). This first forced choice was followed by 20 consecutive free alternation trials, in which the metal barrier was removed. Between trials, the rat was held in the start arm of the T-maze for 10 seconds (during which the opposite goal arm was baited by the experimenter). After this time, the metal barrier was removed and the animal was free to explore the maze and choose to turn in one of the two goal arms. If the animal did not choose the opposite goal arm in comparison to the previous trial, it did not receive the sugar pellet reward. The first forced choice trial of each session (left or right goal arm) was pseudorandomised over sessions and animals. The rats were trained over nine sessions. A following test session 30 minutes after muscimol infusion was performed only for the animals that reached the criterion level (to make at least 75% of correct goal arm choices in one session) in the last training session.

Standard T-maze task

This task started 2 days after completion of the continuous alternation T-maze task (pre-training was not required because the animals were already familiar with the T-maze apparatus). The rats received in total two sessions of training, one per day, with twelve trials on the first day and fourteen on the second. Each trial consisted of a forced 'sample' phase followed by a free 'choice' phase. During the sample phase, one of the goal arms of the T-maze was blocked by an aluminium barrier. After the rat turned into the preselected goal arm, it was allowed to eat one reward pellet, which had previously placed in the food well. The rat was then picked up from the maze and immediately returned to the beginning of the start arm, where it was kept for 10 seconds using another aluminium barrier. Then, the choice phase began. The rat was now allowed to run up the start arm and given a free choice to enter either the left or the right goal arm. The rat received one reward pellet only if it turned in the direction opposite to the forced choice in the sample run (i.e. non-matching to sample choice). Between each trial, the animal was placed back in an aluminium carry-box for 90 seconds (during this time the experimenter prepared the maze for the next trial). The criterion was to make at least 80% of correct arm choices in one session. Left/right allocations for the sample and choice runs were pseudo-randomised over daily trials, sessions and rats, with no more than three consecutive sample runs to the same side in each session. On the third day, animals received a muscimol infusion and 30 minutes after they were tested on fourteen trials in total.

4.3.1.3 Surgical procedure

Once animals could reliably perform the modified version of the radial arm maze task with maze rotation and a 1-minute delay, they were implanted with bilateral chronic indwelling guide cannulae targeting the dorsal hippocampus. Anaesthesia, surgery and post-operation recovery were performed in the same way as described for Experiment 1 (Section 4.2.1.3).

4.3.1.4 Infusions

General infusion procedure

The infusion procedure was identical to that employed in Experiment 1 (Section 4.2.1.4).

Infusion procedure specific for the experiment

On two test sessions of the 1-minute delay with maze rotation variant of the radial arm maze task, rats were tested 30 minutes after having received muscimol infusion (diluted in sterile PBS at a concentration of 1 µg/µl; M1523, Sigma-Aldrich, UK). In the first session they received a dose of 0.5 µl/infusion site of muscimol at a rate of 0.5 µl/minute. After this first session, the animals were given two days of testing without any infusion. After these two no-infusion test sessions, a further session after muscimol infusion was carried out, with animals receiving an infusion of 1 µl/infusion site of muscimol, at a rate of 1 µl/minute (see Figure 4-12).

For both the continuous alternation T-maze task and the standard T-maze task, muscimol infusion dose was 0.5 µl/infusion site (infusion rate 0.5 µl/minute), administered 30 minutes before the beginning of the test.

On completion of the behavioural procedures, animals were infused with 1 µl/infusion site of biotinylated antisense *Zif268* ODNs (1 nmol/µl; Sigma-Genosys, Sigma-Aldrich, UK) at the rate of 0.167 µl/min. Biotinylated antisense *Zif268* ODNs were used as a generic infusate solution in order to visualise the spread of the infusate in the cannulated region.

4.3.1.5 Histology

Infusion of biotinylated antisense *Zif268* ODN and β-thionin counterstaining to verify infusate diffusion and cannulae placement

Ninety minutes after the infusion of the biotinylated antisense *Zif268* ODNs (Section 4.3.1.4), the animals were irreversibly anaesthetised with sodium pentobarbital (60 mg⁄kg, Euthatal, Rhone Merieux, Harlow, UK) and perfused transcardially with 0.1 M PBS followed by 4% paraformaldehyde in 0.1 M PBS (PFA). The brains were removed and post-fixed in 4% PFA for 2 hours and then transferred to 20% sucrose (in 0.1 M PBS) overnight. Sections were cut at 40 µm on a freezing microtome in the coronal plane, and a one-in-three series of sections was selected and quenched in 50:50 10%

methanol (Sigma-Aldrich, UK) and 10% H_2O_2 (Fisher Scientific, US). The sections were rinsed three times in PBS (15 minutes each) and permeabilised in 0.3% Triton overnight. The sections were then incubated in an avidin-biotidin complex (Vectastain Elite ABC kit PK-6100, Vector Laboratories, UK) for 2 hours and again rinsed three times in PBS (15 minutes each). Finally, the sections were exposed to DAB (DAB Peroxidase (HRP) Substrate Kit, 3,3'-diaminobenzidine, Vector Laboratories, UK) until visualization of biotinylated ODNs was complete (requiring about 1 minute), washed again in cold PBS and left at +4°C overnight. The day after they were mounted onto gelatin-coated slides and air dried before counterstaining with β-thionin (for histological assessment of cannulae placement). For counterstaining, the sections were immersed in β-thionin (diluted at a concentration of 1% in distilled water; Sigma-Aldrich T7029, UK) for 10 minutes, rinsed in distilled water for 1 minute, then gradually dehydrated in ethanol at increasing concentrations (5 minutes in 70% ethanol, 20 minutes in 90% ethanol and 20 minutes in 100% ethanol), and then immersed in Histoclear (National Diagnostics, UK) for at least 40 minutes. Finally the sections were coverslipped (Gurr DePeX mounting medium, BDH Laboratory Supplies, Poole, UK).

4.3.1.6 Statistical analysis of behavioural data

SPSS software (version 20, IBM Corporation) was used to carry out statistical analyses. The threshold for significance was set at $p < 0.05$ for all statistical tests.

For the 1-minute delay with maze rotation variant of the radial arm maze task, the number of correct arm entries in the first eight choices and the total number of errors were recorded for each radial arm maze post-surgery test session. In the six test sessions with no infusion these values were averaged and compared to those obtained during the two muscimol infusion test sessions using repeated measures ANOVA with Session as within-subject factor. Sphericity of data was checked using Mauchly's sphericity test and degree of freedom corrections were applied when necessary. When significant main effects were found, Bonferroni post hoc tests were run in order to identify which sessions differed.

For both the standard and the continuous alternation T-maze tasks, the percentage of correct alternation choices in each session was calculated and was compared between the no-infusion and muscimol infusion sessions using paired sample t-tests.

In addition, for the standard T-maze task, a comparison between the animals' performances and the random choice level of 50% correct alternation choices was performed using one sample t-test.

4.3.2 Results

4.3.2.1 Cannulae placement histology and spread of antisense Zif268 ODNs after infusion

Histological analysis showed that in most of the animals the cannulae were not ideally placed. In three out of six cases they were placed too anteriorly (the ideal position is 3.6 mm posterior to bregma; Figure 4-9). Furthermore, similar to the cases in Experiment 1, their tip position appeared very superficial, only slightly protruding inside the dorsal hippocampus.

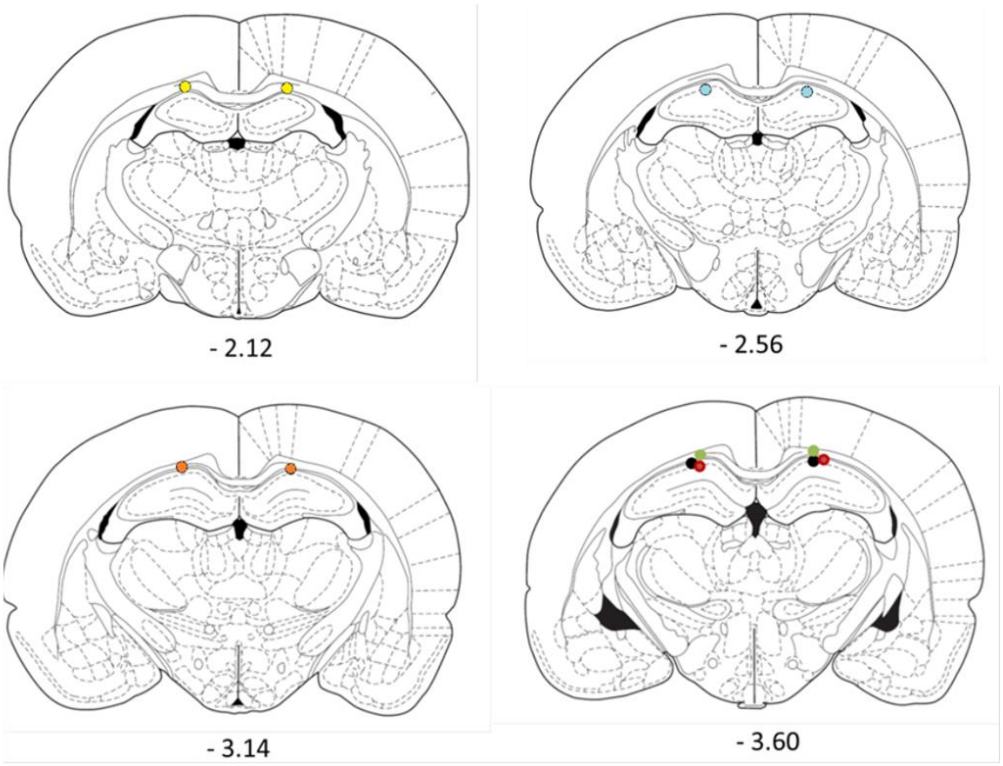

Figure 4-9. Cannulae placement into the dorsal hippocampus (coronal view). Each point represents the position of the tip of the cannula. A different colour has been used to identify cannulae placement for each animal. The distance in mm from bregma is reported. Figure adapted from Paxinos & Watson (1998).

Assessment of the spread of biotinylated *Zif268* antisense ODNs confirmed that infusions were too superficial (Figure 4-60); furthermore, in some cases the staining was unilateral, probably due to a blockage of one of the two cannulae during the infusion process.

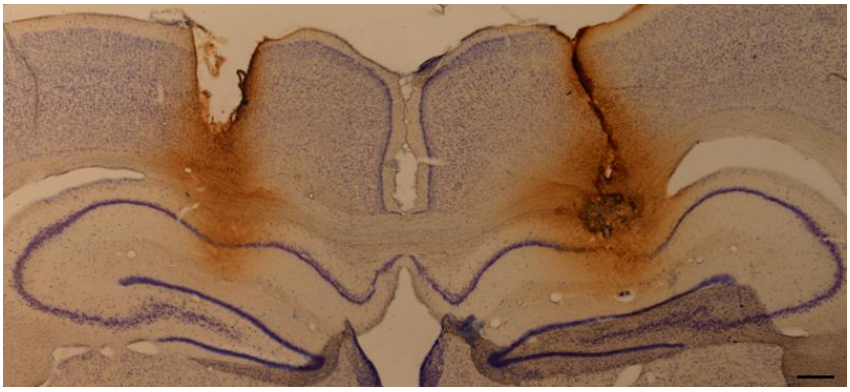

Figure 4-60. Representative section showing diffusion of biotinylated antisense *Zif268* ODN infused into the dorsal hippocampus. Scale bar 200 µm.

4.3.2.2 Behaviour

Pre-surgery radial arm maze training

Before surgery, animals were able to reach criterion (no more than one error and all arms visited in at least two consecutive trials) in the standard radial arm maze task in 10.5 ± 0.2 trials (mean ± SEM; correct entries in the first eight choices: 6.1 ± 0.3; total errors: 2.1 ± 0.5). They were then trained on the 1-minute delay with maze rotation variant of the radial arm maze task, reaching criterion after a mean of 9.0 ± 0.8 trials (correct entries in the first eight arm choices: 7.4 ± 0.1; total errors: 0.8 ± 0.2).

Post-surgery radial arm maze training/testing

After being implanted with cannulae targeting the dorsal hippocampus, rats were re-trained directly on the 1-minute delay with maze rotation variant of the radial arm maze task until they reached criterion (visiting all eight arms with no more than one error for at least two consecutive trials) in 5.8 ± 0.2 trials, making 7.6 ± 0.1 correct entries in the first eight choices and 0.6 ± 0.2 total errors. Then, a series of test sessions was carried out: four sessions with no infusion, followed by a session with muscimol infusion (0.5 µl/infusion site, 1 µg/µl, 30 minutes before the sample phase), then other two sessions with no infusion and finally a final session with muscimol infusion at a higher dose (1 µl/infusion site, 1 µg/µl, 30 minutes before the sample phase; Figure 4-71).

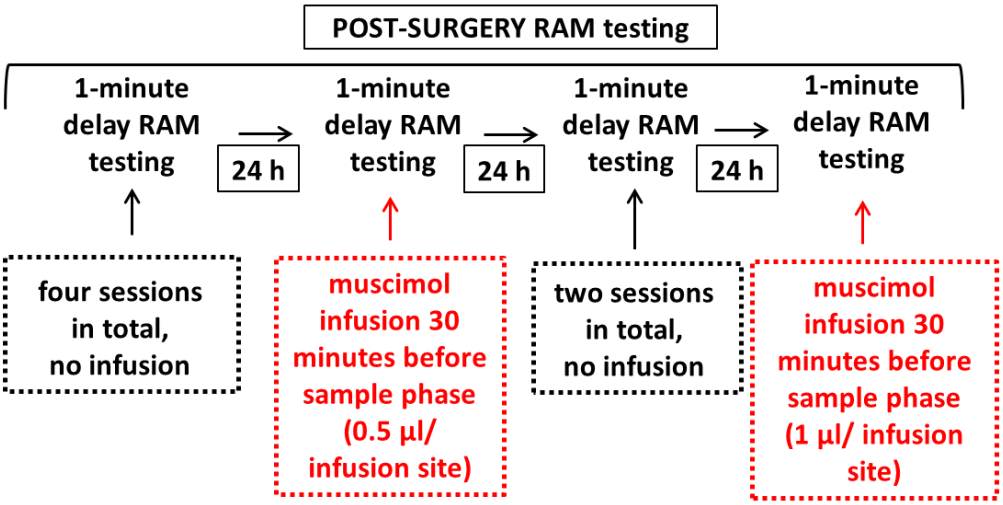

Figure 4-71. Schematic behavioural protocol for radial arm maze (RAM) testing in Experiment 1. A maze rotation was interposed between the sample and the test phase in all sessions.

Performance measures for the no-infusion test sessions were averaged across sessions as they were all very similar ($F < 1$ for both correct entries in the first eight arm choices and total errors comparing the six sessions using repeated measures ANOVA). These mean scores were compared to the scores obtained during the two muscimol test sessions with different drug dose (either 0.5 µl/infusion site or 1 µl/infusion site).

There was a significant main effect of test session on the number of correct entries in the first eight choices ($F_{2,10} = 8.8$, $p < 0.01$), and Bonferroni post hoc analysis revealed a significantly worse performance when animals were infused with muscimol 1 µl/infusion site in comparison to no infusion ($p<0.01$) (Figure 4-82).

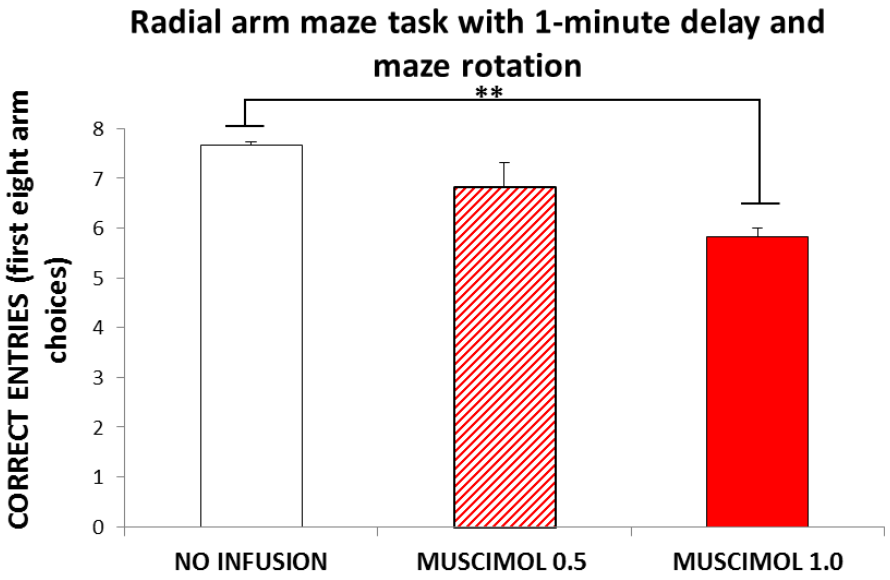

Figure 4-82. Correct entries (mean ± SEM) in the first eight arm choices in the 1-minute delay radial arm maze task with maze rotation after dorsal hippocampal cannulation surgery. Rats received either no infusion (in the graph mean of six no infusion sessions) or infusion of muscimol at two different doses (0.5 µl/infusion site or 1.0 µl/infusion site; concentration 1.0 µg/µl in both cases) 30 minute before the sample phase. Level of significance: ** $p<0.01$

Looking at total number of errors, instead, the main effect of test session was not significant ($F_{2,10}$ = 1.9, p = 0.20; Figure 4-93).

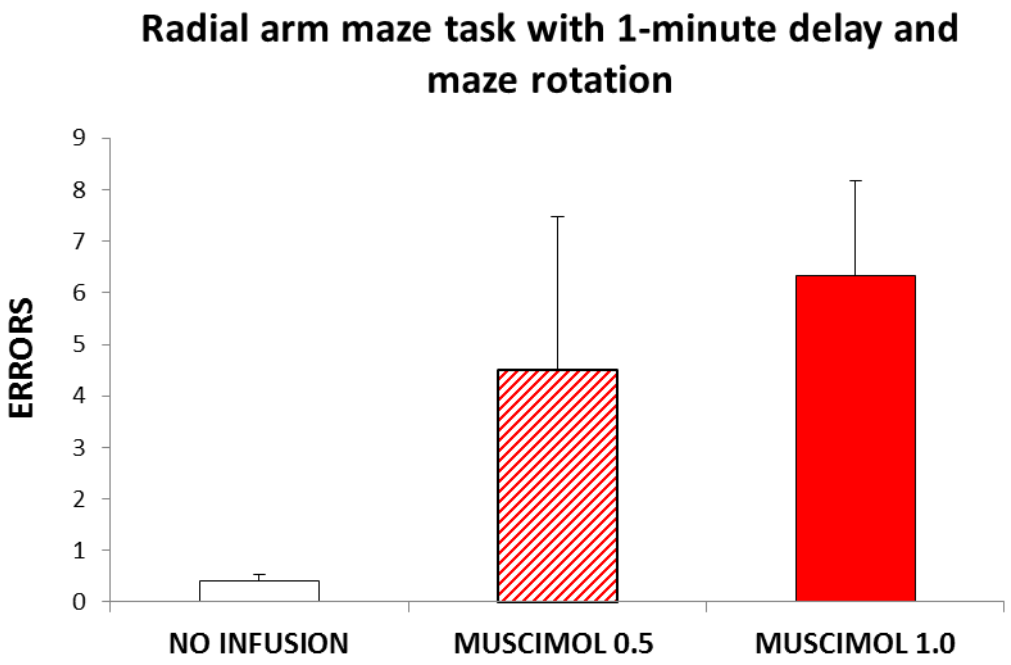

Figure 4-93. Total errors (mean ± SEM) in the 1-minute delay radial arm maze task with maze rotation after dorsal hippocampal cannulation surgery. Rats received either no infusion (in the graph mean of six no infusion sessions) or infusion of muscimol at two different doses (either 0.5 µl/infusion site or 1 µl/infusion site; concentration 1.0 µg/µl in both cases) 30 minute before the sample phase.

Post-surgery continuous alternation T-maze training/testing

After being tested on the 1-minute delay with maze rotation variant of the radial arm maze task, animals were trained on the continuous alternation T-maze task. Two out of six animals did not reach the criterion of 75% correct choices/session after nine days of training, so they were excluded from further analysis. The remaining animals underwent a test session 30 minutes after having been infused with muscimol (0.5 µl/infusion site).

Performance (percentage of correct alternation choices) during the last two sessions of training and the muscimol test session was compared but no significant difference was found ($t_3 = 1.4$, $p = 0.25$; Figure 4-14).

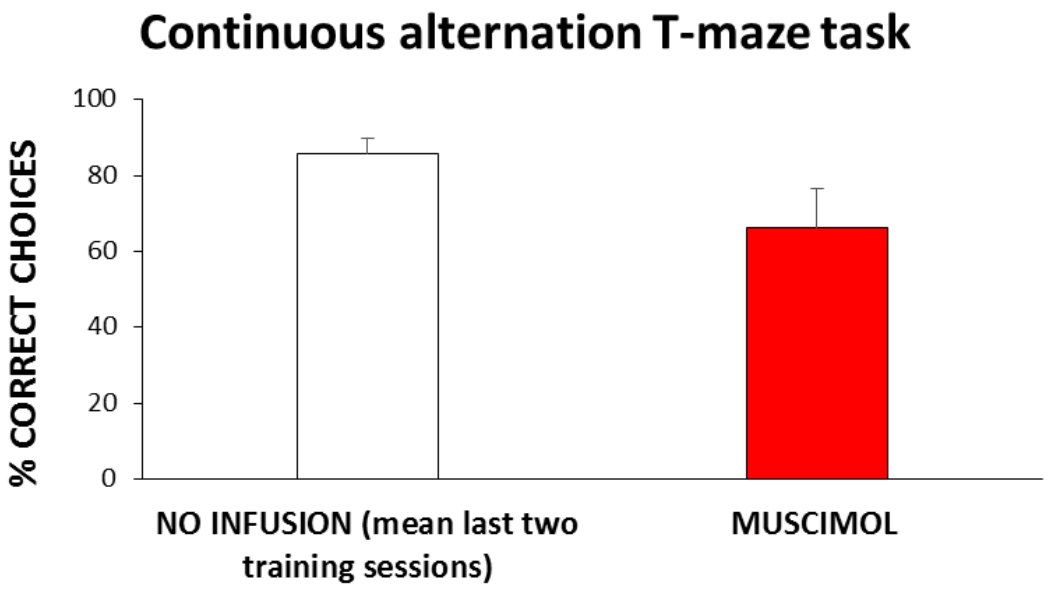

Figure 4-104. Percentage of correct alternation choices (mean ± SEM) in the continuous alternation T-maze task after dorsal hippocampal cannulation surgery. Rats received either no infusion or infusion of muscimol (0.5 µl/infusion site) 30 minute before the beginning of the task.

Post-surgery standard T-maze training/testing

Having completed the continuous alternation T-maze task, all six animals were trained on the standard T-maze task and reached criterion by the second day of training. Subsequently they underwent a test session 30 minutes after having been infused with muscimol (0.5 µl/infusion site). Performance (percentage of correct alternation choices) was compared during the training and the test sessions, but no significant

difference was found (t_5 = 1.7, p = 0.15; Figure 4-115). The alternation scores were also compared also against the chance probability level (50%). The rats performed above chance when they were not infused prior to testing (t_5 = 13.2, p<0.001), but not when they were infused with muscimol (t_5 = 1.9, p = 0.12).

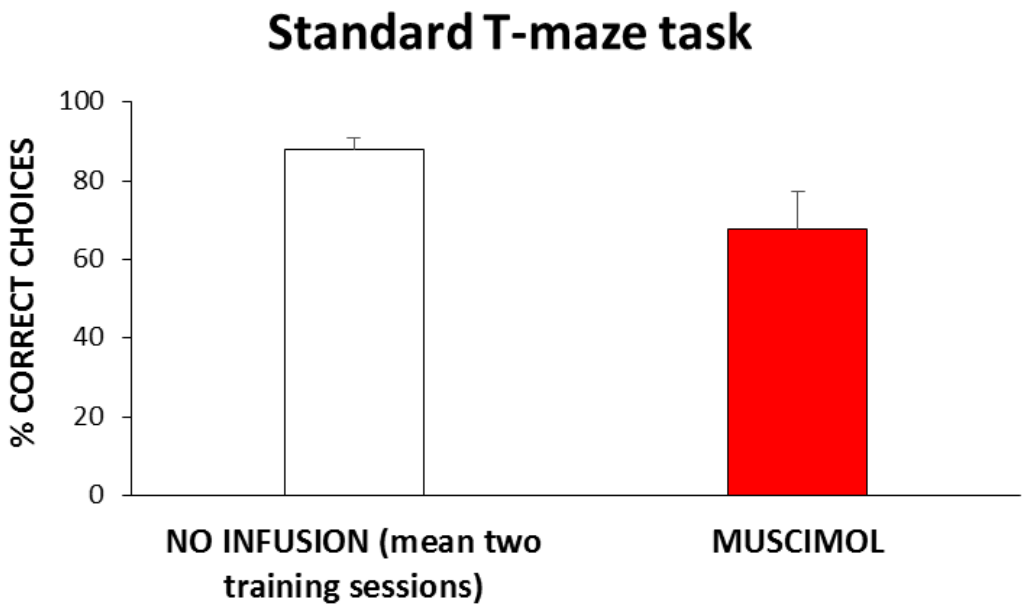

Figure 4-115. Percentage of correct alternation choices (mean ± SEM) in the standard T-maze task after dorsal hippocampal cannulation surgery. Rats received either no infusion or infusion of muscimol (0.5 µl/infusion site) 30 minute before the beginning of the task.

4.3.3 Interim discussion

Animals with a pair of cannulae in the dorsal hippocampus were tested in the 1-minute delay with maze rotation version of the radial arm maze task (acquired before surgery) and were challenged with muscimol infusions. Only the infusion of the higher dose of the drug (1 µg in 1 µl/infusion site) impaired performance (considering the number of correct entries in the first eight arm choices) in the spatial memory task, while the lower dose (0.5 µg in 0.5 µl/infusion site) wasn't. The animals were also tested in two T-maze tasks (the continuous alternation version and the standard variant), after infusions of the lower dose of muscimol (as the higher had caused motor problems in some of the animals): no difference in performance was detected when animals were either infused with muscimol or not infused. However, in the standard T-maze task, the performance reached chance level only after animals were infused with muscimol.

Histological inspection of cannulae placement revealed that for some animals the cannulae were placed too anteriorly and they were still too dorsal.

The experiment showed that infusing muscimol at a dose of 1 μg in 1 μl in each dorsal hippocampus was able to disrupt the performance in the modified radial arm maze task, decreasing the number of correct entries performed in the first eight arm choices, while the dose of 0.5 μg in 0.5 μl was not effective. However, when infused with the larger volume, some of the animals showed a general lack of motivation in completing the task (some rats did not eat most of the reward pellets when tested in the maze) and inability to move; this last finding is in contrast to what is observed after hippocampal lesions, which make animals hyperactive rather than hypoactive (Bannerman et al., 1999; Cassel et al., 1998; Good & Honey, 1997).

Inspection of cannulae placement histology and general infusate diffusion showed that some of the cannulae were not properly placed along the antero-posterior axis (with half of the cases being too anterior), although they did all now appear symmetrical to the midline, due to improvements in taking midline co-ordinates. Furthermore, the tracts of the injector tips appeared quite dorsal and it is possible that with the larger volume (1 μl/infusion site) some of the infusate had spread into the overlying cortex (which includes the motor cortex), causing the motor hypoactivity and motivational abnormalities. In order to avoid these collateral effects associated with the infusion of the larger volume of muscimol, only the smaller volume (0.5 μl/infusion site, which has been shown in literature to be effective when infused into dorsal hippocampus, e.g. Corcoran et al., 2005; Corcoran & Maren, 2001; Holt & Maren, 1999; Lee & Kesner, 2003; Matus-Amat et al., 2004) was infused for testing the animals on the T-maze tasks.

In contrast to previous studies (Czerniawski et al., 2009; Hallock et al., 2013; McHugh et al., 2008), in this experiment muscimol infusion had no significant behavioural effect on either the continuous alternation T-maze task or the standard T-maze task. However, on the standard T-maze task, the performance of animals after muscimol infusion did not differ from chance level, while it was significantly above chance when animals were tested without infusions. While this cannot be interpreted as a difference between the two infusion conditions, it suggests that animals cannot perform the task optimally following muscimol infusions. As with the findings from Experiment 1, the limited behavioural effects following muscimol infusions most likely reflected issues in cannulation surgery or infusion technique. A further pilot experiment was then carried out to rectify some of these issues.

4.4 EXPERIMENT 3: effects of muscimol infusions into the dorsal hippocampus on tests of spatial memory (II)

The goal of this experiment was to further optimise the surgical and infusion procedures in the dorsal hippocampus.

Animals were first trained on the standard T-maze task and, subsequently, underwent dorsal hippocampal cannulation surgery; they were then re-trained and tested on the task after muscimol infusions (Figure 4-16). Saline solution infusions were introduced as control infusions for each animal. As muscimol infusions produced a significant impairment in the performance of the standard T-maze task in comparison to control infusions, animals were further trained and tested on the 1-minute delay with maze rotation variant of the radial arm maze task, in order to employ a task more similar to the task that would be used with antisense ODN infusions. After all behavioural procedures were completed, a final bilateral infusion of biotinylated solution was used to visually inspect the spread of the infusate into the dorsal hippocampus.

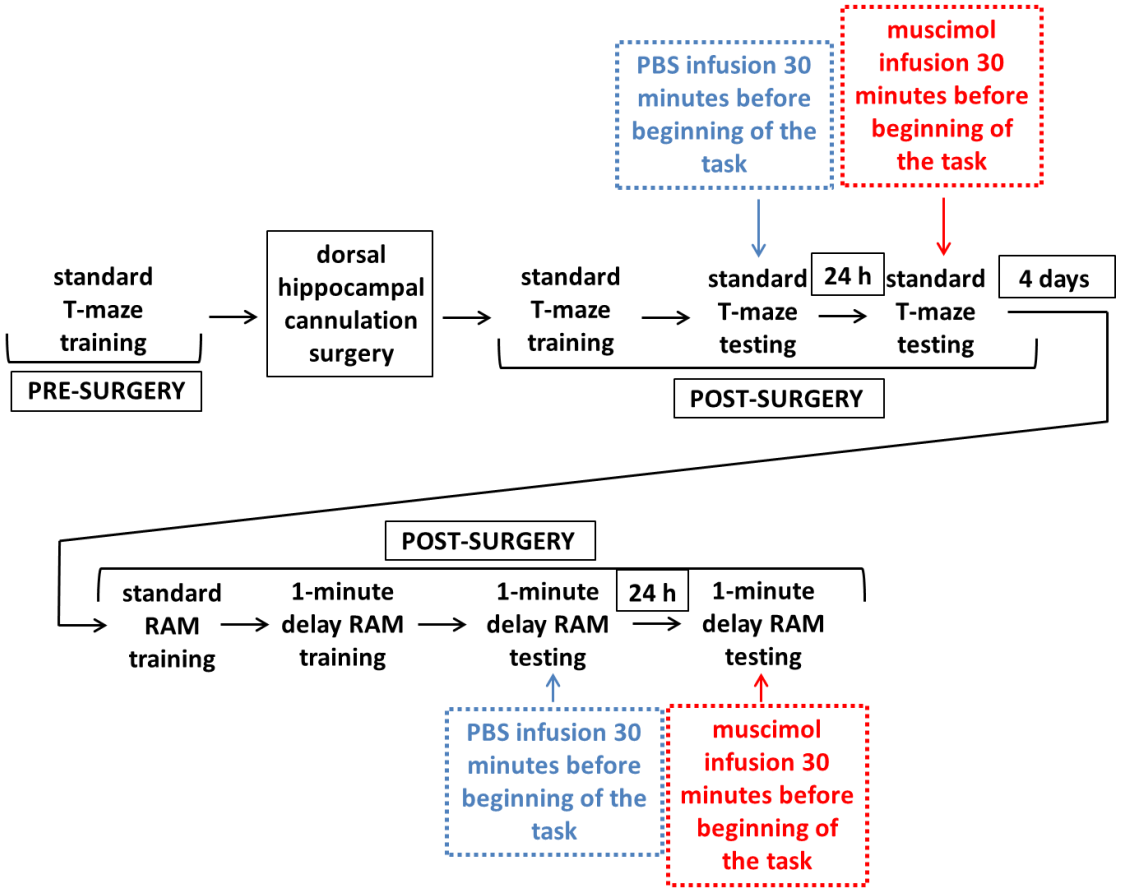

Figure 4-16. Schematic behavioural protocol for experiment 2. The delayed radial arm maze (RAM) tasks involved also a maze rotation between the sample and the test phase. PBS and muscimol infusions were 0.3 µl/infusion site.

4.4.1 Methods

4.4.1.1 Subjects

Subjects were ten male naïve Lister Hooded rats (Harlan, UK), weighing 264-310 g at the time of surgery. The housing, light, water access, diet restriction and handling conditions were kept identical to those used in Experiment 1 (Section 4.2.1.1). The experiment was carried out in accordance with UK Animals (Scientific Procedures) Act, 1986 and associated guidelines.

4.4.1.2 Behavioural procedures

Standard T-maze

Apparatus

Identical to that used in Experiment 2 (Section 4.3.1.2).

Pre-surgery behavioural procedure

The pre-training procedure was identical to that used in Experiment 2. Animals were trained (eight trials/session) until they reached the criterion level (at least 80% of correct arm choices in one session). Then they underwent surgery (Section 4.4.1.3).

Post-surgery behavioural procedure

After surgery, animals were re-trained (12 trials/session) until they reached the same criterion level. They then underwent two test sessions (consisting of 12 trials/session), the first one after control saline solution infusion, and the second one two days later, after muscimol infusion (Section 4.4.1.4).

Radial Arm Maze Task

Apparatus

Identical to that used in Experiment 1 (Section 4.2.1.2).

Post-surgery behavioural procedure

The behavioural training/testing procedures were identical to those employed in Experiment 2. Four days after completing the standard T-maze test, the animals were trained to the standard radial arm maze task. Once they acquired the task at criterion level (making no more than one error and exploring all maze arms for at least two

consecutive sessions), they were trained in the 1-minute delay with maze rotation variant of the task (as described in Experiment 2, Section 4.3.1.2); once they reached the criterion level they underwent two test sessions: the first one after control saline solution infusion and the second one two days later, after muscimol infusion (Section 4.4.1.4).

4.4.1.3 Surgical procedure

All animals were implanted with bilateral dorsal hippocampal cannulae after they were able to perform the standard T-maze task at criterion level (at least 80% of correct arm choices in one session). Anaesthesia, surgery and post-operation recovery were performed in the same way as described for Experiment 1 (Section 4.2.1.3). The only modification was the way in which AP and LM measurements were taken: in the previous experiments the measures were measured using the tip of the right cannula; in this experiment, instead, all measures were taken using the tip of a Hamilton syringe (whose diameter is much smaller in comparison to the cannula's tip), marking the point with a pencil marker and finally being sure that the centre of each cannula tip was overlapping the mark.

4.4.1.4 Infusions

General infusion procedure

The infusion procedure was identical to that employed in Experiment 1 (Section 4.2.1.4). The only modification was the verification that both before and after each animal's infusion the infusate was effectively being pumped out from both microinjectors; this was accomplished loading about 0.2 µl of infusate in excess for each infusion and activating the pump immediately before and after each animal was infused, verifying that the procedure was working correctly and repeating the infusion of the animal if necessary.

Infusion procedure specific for the experiment

In this experiment either saline control solution (phosphate buffered saline, PBS, pH 7.4) or muscimol (1 µg/µl) were administered before testing. The infusate volume was initially 0.5 µl/infusion site, however, this resulted in gross behavioural impairments (an inability to move) in some animals so it was reduced to 0.3 µl/infusion site (infusion rate 0.3 µl/minute). In all cases, the infusions were administered 30 minutes before

the beginning of the task. Forty-eight hours were interposed between PBS and muscimol infusion test sessions in both the standard T-maze task and the modified radial arm maze task.

On completion of the behavioural procedures, animals were infused with 1 µl/infusion site of biotinylated antisense *Zif268* ODNs (1 nmol/µl; Sigma-Genosys, Sigma-Aldrich, UK) at the rate of 0.167 µl/min.

4.4.1.5 Histology

Infusion of biotinylated antisense *Zif268* ODN and β-thionin counterstaining to verify infusate diffusion and cannulae placement

Tissue processing for the visualisation of the spread of biotinylated antisense *Zif268* ODNs (with β-thionin counterstaining) into the dorsal hippocampus was performed in the same way as described for Experiment 2 (Section 4.3.1.5).

4.4.1.6 Statistical analysis of behavioural data

SPSS software (version 20, IBM Corporation) was used to carry out statistical analyses. The threshold for significance was set at $p < 0.05$ for all statistical tests.

For the standard T-maze task, the percentage of correct trials in each post-surgery test session (after either PBS or muscimol infusion) was calculated; the percentage values were compared using paired sample t-tests. Furthermore, a comparison between the animals' performances and the random choice level of 50% correct choices was performed using one sample t-test.

For the modified radial arm maze task, the number of correct arm entries in the first eight choices and the total number of errors were recorded for each radial arm maze test session (after either PBS or muscimol infusions). Both measures were compared using paired sample t-test.

4.4.2 Results

4.4.2.1 Cannulae placement histology and spread of antisense Zif268 ODN after infusion

Histological analysis confirmed that all cannulae were well-placed at the correct antero-posterior level and symmetric to the midline for all ten subjects (Figure 4-17).

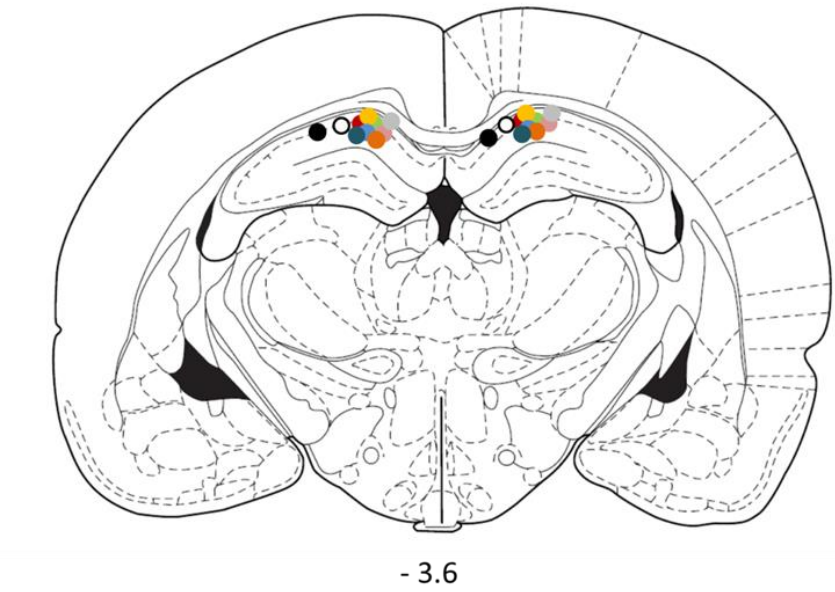

Figure 4-17. Cannulae placement into the dorsal hippocampus (coronal view).
Each point represents the position of the tip of the cannula. A different colour has been used to identify cannulae placement for each animal. The distance in mm from bregma is reported. Figure adapted from Paxinos & Watson (1998).

However, the staining of the spread of biotinylated antisense *Zif268* ODN showed that infusions were still too superficial (see representative section, Figure 4-18).

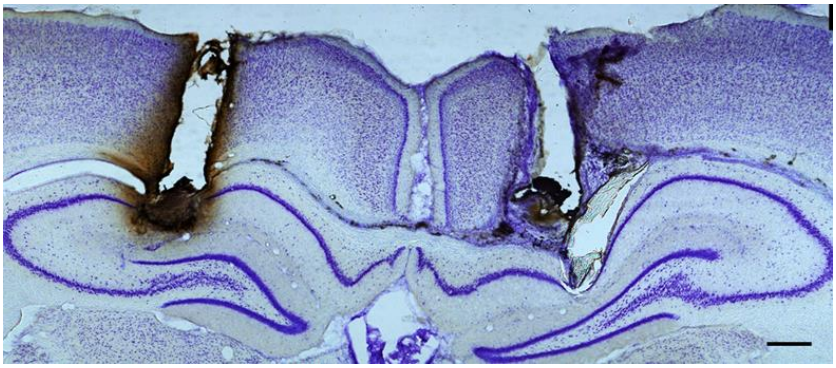

Figure 4-18. Representative section showing diffusion of biotinylated antisense *Zif268* ODNs infused into the dorsal hippocampus. Scale bar 200 µm.

4.4.2.2 Behaviour

Presurgery standard T-maze training

Before surgery, all animals reached criterion (80% correct trials in at least two consecutive sessions) in 2.8 ± 0.4 (mean ± SEM) sessions.

Post-surgery standard T-maze training/testing

After surgery, the animals were re-trained and reached the criterion in 4.8 ± 1.1 (mean ± SEM) sessions. Then they were tested for two sessions either after PBS or after muscimol infusions. One animal was excluded from the analysis as it was unable to perform the task following muscimol infusion. The statistical analysis revealed that animals' performance (measured as percentage of correct arm choices in one session) after muscimol infusion was significantly worse than after PBS infusion (t_8 = 3.0, $p < 0.05$; Figure 4-19). However, performance was above 50 % chance level after both PBS (t_8 = 7.4, $p < 0.001$) and muscimol (t_8 = 2.4, $p < 0.05$) infusions.

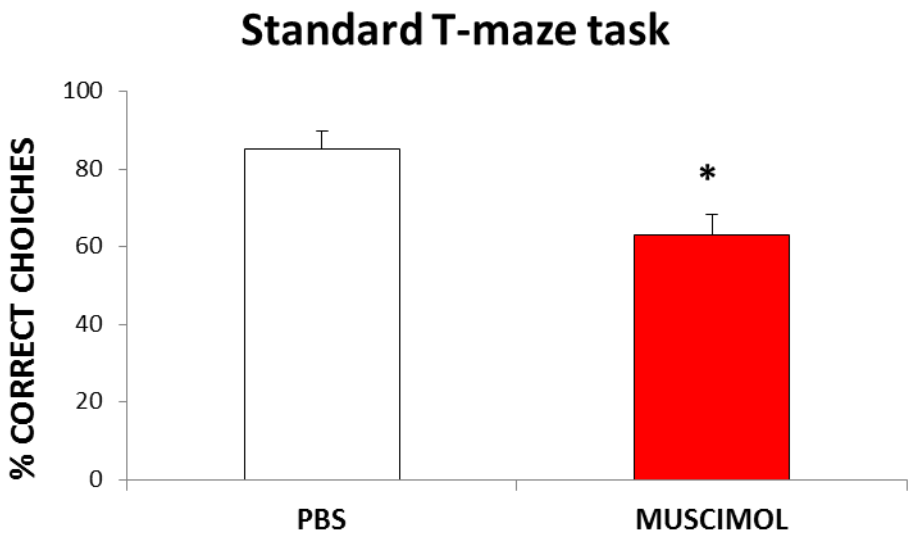

Figure 4-19. Percentage of correct alternation choices (mean ± SEM) in the standard T-maze task after dorsal hippocampal cannulation surgery. Rats received infusion of either PBS or muscimol (0.3 µl/infusion site) 30 minute before the beginning of the task. Level of significance: * $p < 0.05$.

Post-surgery radial arm maze training/testing

After surgery, the animals were able to reach the criterion level for the standard version of the radial arm maze task after 12.2 ± 1.4 (mean ± SEM) sessions, and the 1-minute delay with maze rotation variant of the task after a further 6.4 ± 1.2 (mean ± SEM) sessions.

There was a non-significant decrease in the number of correct entries following muscimol infusion in comparison to PBS infusion (t_9= 2.1, p = 0.07; Figure 4-120). Moreover, when the rats were infused with muscimol, they made a significantly greater number of errors compared to when they were infused with PBS (t_9= -2.3, p <0.05; Figure 4-131).

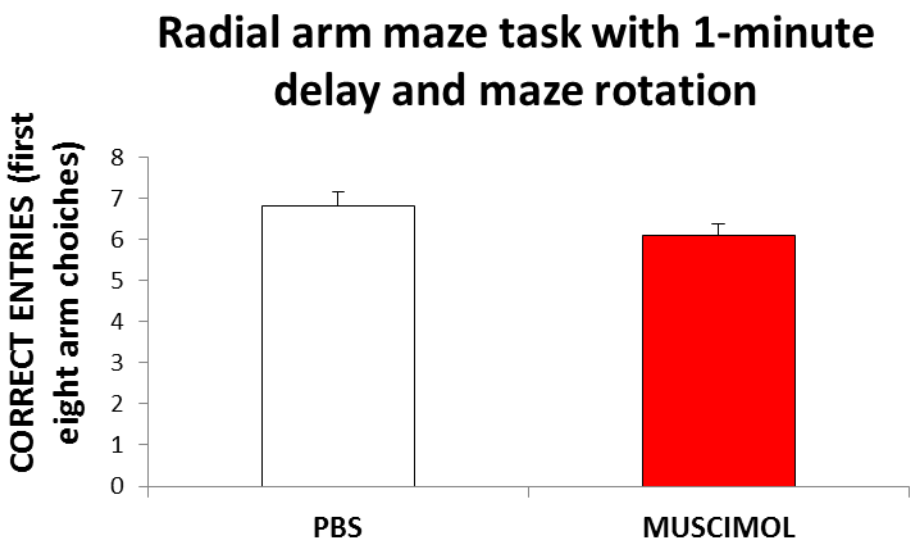

Figure 4-120. Correct entries (mean ± SEM) in the first eight arm choices in the 1-minute delay variant of the radial arm maze task with maze rotation after dorsal hippocampal cannulation surgery. Rats received infusion of either PBS or muscimol (0.3 µl/infusion site) 30 minute before the beginning of the task.

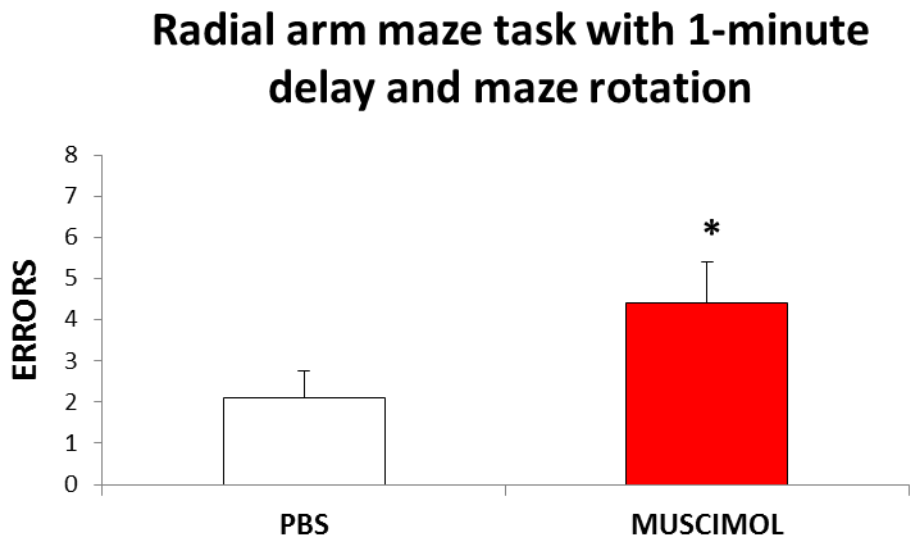

Figure 4-131. Total errors (mean ± SEM) in the 1-minute delay variant of the radial arm maze task with maze rotation after dorsal hippocampal cannulation surgery. Rats received infusion of either PBS or muscimol (0.3 µl/infusion site) 30 minute before the beginning of the task. Level of significance: * $p < 0.05$.

4.4.3 Interim discussion

To verify the improvement of cannulation surgery and infusion procedure, the animals from this group were trained after surgery with two spatial memory tasks that were relatively quick to acquire (the standard T-maze task and the 1-minute delay with maze rotation variant of the radial arm maze task) and then tested after either muscimol infusion or a control (PBS) infusion. Animals were impaired on both tasks after muscimol infusions in comparison to PBS infusions. This confirmed the validity of the protocols used for surgery and cannulation.

In this experiment, muscimol infusions into the dorsal hippocampus caused a significant impairment in the performance of two spatial memory tasks, T-maze alternation and the radial arm maze task. These positive results most likely reflect an improvement in the quality of the cannulation surgery (in this experiment the tracts of the cannulae were all properly located on the antero-posterior and on the medio-lateral axis) and in the infusion procedure (which was carefully controlled to avoid unilateral infusions). A further confirmation of the general improvement in surgery and infusion techniques was that muscimol infusions were effective given an infusate volume of 0.3 µl/infusion site, a smaller volume than the one used in the previous two experiments; this was a sign that most of the infusate was concentrated in the target region, the dorsal hippocampus.

We also used the 0.5 µl/infusion site dose of muscimol at the outset of the experiment, however, it produced gross behavioural effects in some of the animals (which had difficulties in moving and completely lacked any motivation in retrieving pellets in the maze), similar to those we observed using 1.0 µl/infusion site of muscimol in Experiment 2. For this reason the subsequent infusions were at a lower dose of 0.3 µl. This reaction to the 0.5 µl dose could be an indication that the infusate was not diffusing just into the dorsal hippocampus but was probably also affecting the overlying cortex. For example, the effect of muscimol on the motor cortex could explain the hypoactivity effect. Histological inspection of the placement of the cannulae tips confirmed this hypothesis, as they were located just on the dorsal border of the dorsal hippocampi. Ideally, the cannulae placements should be more ventral and more centrally placed within the hippocampus; this could be achieved by using longer infusion microinjectors. Furthermore, while the animals were impaired on the T-maze task following the muscimol infusions, they still were able to perform the task above chance level. Previous lesion and muscimol infusion experiments have shown a more marked deficit with animals' performance dropping to chance (Aggleton et al.,

1986; McHugh et al., 2008). It is likely that the milder effects seen in this experiment reflect the suboptimal placement on the cannulae and the likelihood that the infusions were slightly too dorsal.

4.5 GENERAL DISCUSSION

The main aim of this series of experiments was developing the skills for knocking down c-Fos and Zif268 expression in the dorsal hippocampus, and to develop a spatial memory behavioural task suitable for testing if this knocking down was associated to an impairment in spatial memory performance.

Immediate early gene imaging experiments have shown that the standard working memory version of the radial maze task elicits the increase of c-Fos and Zif268 expression levels in both the dorsal hippocampus and the retrosplenial cortex (Jenkins et al., 2006; Vann, Brown, & Aggleton, 2000; Vann, Brown, Erichsen, et al., 2000a). The total testing time used in these studies has never exceeded 30 minutes, and the immediate early gene expression level increase has been measured 90 minutes after the completion of the task. Given the c-Fos and Zif268 expression level increase occurs *after* completion of the task, it is unlikely to be having a retroactive effect on the spatial working memory task. Thus, from these experiments it is not clear whether this immediate early gene increase is functionally important (i.e. for memory consolidation) or if it simply reflects a 'neuronal activity marker'. To investigate this issue it is necessary to employ a behavioural task in which the increase of expression levels of c-Fos and Zif268 could be critical for the performance, i.e. they need to be expressed before the completion of the task. Furthermore, it is also necessary to experimentally block this increase, making it possible to compare the behavioural performance when the increase is present and when it is not.

The first part of Experiment 1 piloted a modified version of the standard working memory radial arm maze task. A 3-hour delay was introduced into the middle of the task (after the first four arm choices) so that it would be possible to block the increase of c-Fos and Zif268 expression levels elicited by the first part of the task (sample phase) and verify the effect on spatial memory during the final phase of the task (test phase). A further modification was the insertion between the sample and the test phase of a 45° maze rotation, in order to remove the use of intramaze cues to solve the task and making it dependent on the functionality of both the dorsal hippocampus and the retrosplenial cortex. Naïve animals were able to acquire this modified radial

arm maze task using a gradual increase in the time delay inserted between the sample and the test phase (from 1 minute, to 5 minutes, to 1 hour and finally to 3 hours).

Infusion of antisense ODNs targeting *c-Fos* and *Zif268* transcripts into either the dorsal hippocampus or the retrosplenial cortex is a technique for blocking the increase of their expression levels in a very specific manner (Section 1.4.7). The second part of Experiment 1 and Experiments 2 and 3 were aimed at acquiring the skills for cannulae implantation and solution delivery into the dorsal hippocampus. In order to verify at the behavioural level the efficacy of the surgery and the infusion techniques, the animals were tested after muscimol infusion on behavioural tasks that taxed spatial memory and were dependent on dorsal hippocampus (the radial arm maze task with 1-minute delay and maze rotation; the standard T-maze task; the continuous alternation T-maze task). The results of these tests showed a gradual improvement in surgical and infusion procedures. This was necessary to determine the best protocols for the subsequent experiment involving the infusion of antisense ODNs, targeting *c-Fos* and *Zif268* transcripts, into the dorsal hippocampus in rats subsequently tested in the 3-hour delay with maze rotation variant of the radial arm maze task.

Chapter 5 Antisense *c-Fos* and *Zif268* oligodeoxynucleotide infusions into the dorsal hippocampus

5.1 Introduction

Lesions within the Papez circuit reduce immediate-early gene expression in functionally related areas (Albasser et al., 2007; Dumont et al., 2012; Jenkins et al., 2006, 2004; Jenkins, Dias, Amin, & Aggleton, 2002; Jenkins, Dias, Amin, Brown, et al., 2002; Poirier & Aggleton, 2009; Poirier, Shires, et al., 2008; Vann & Albasser, 2009). However, it is not known whether these changes in immediate early gene expression, most typically c-Fos and Zif268, are functionally important and contribute to the spatial memory impairments seen following these lesions (Aggleton et al., 1996, 1986; Sziklas & Petrides, 2002; Vann & Aggleton, 2002, 2003). The following chapter attempted to address this issue. We investigated whether reducing the levels of c-Fos and/or Zif268 proteins in the dorsal hippocampus, by infusing antisense oligodeoxynucleotides (ODNs), affected spatial memory.

The antisense ODN sequences used in the following experiments target either *c-Fos* or *Zif268* transcripts and have been previously shown to affect rats' behaviour. It has been demonstrated that unilateral infusion of the antisense *c-Fos* ODN (sequence: 5'-GAA CAT CAT GGT CGT-3', which is complementary with a region overlapping the first codon on *c-Fos* mRNA; e.g. Chiasson et al., 1994; Grimm et al., 1997) into the striatum exerts an effect on locomotor behaviour, increasing the number of rotations ipsiversive to the infusion site in rats systemically injected with amphetamine after the infusion (Hebb & Robertson, 1997; Hooper, Chiasson, & Robertson, 1994). The same antisense sequence interferes with memory processes when infused in various brain areas. For example, infusions into the amygdala caused a deficit in extinction of a conditioned taste aversion memory (Lamprecht & Dudai, 1996), while infusions into the nucleus accumbens disrupted the acquisition of a morphine conditioned-place preference (Tolliver et al., 2000). More pertinent to the current investigation, infusions of the same antisense *c-Fos* ODN into the dorsal hippocampus or the anterior portion of the retrosplenial cortex (rostral to Rga) impaired the long-term retention of an

inhibitory avoidance response (Katche et al., 2010, 2013). In addition, infusion of this specific antisense *c-Fos* ODNs into the dorsal hippocampus caused an impairment in retention of a brightness discrimination memory (Grimm et al., 1997), a disruption of long-term memory of a socially-transmitted food preference (Countryman et al., 2005) and a deterioration in the performance in the reference/working memory version of the radial arm maze task (He et al., 2002). Finally, infusions of this same antisense *c-Fos* ODN sequence into the perirhinal cortex impaired the performance in both the one-trial object recognition and the object-in-place recognition tasks (Seoane et al., 2012).

Infusions of the antisense ODNs targeting *Zif268* mRNA (sequence: 5'-GGT AGT TGT CCA TGG TGG-3') are also behaviourally effective in rats. When infused into the striatum unilaterally, antisense *Zif268* ODN significantly increased the number of ipsilateral rotations when challenged with amphetamine (Hebb & Robertson, 1997). It also influenced memory processes, causing a deficit in the long-term retention of a contextual fear memory when infused into the amygdala (Malkani et al., 2004), or in reconsolidation when infused into the dorsal hippocampus (Lee, Everitt, & Thomas, 2004).

The main aim of the experiments presented in this chapter was to verify whether knocking down the expression of either c-Fos or Zif268 or both in the dorsal hippocampus of rats, through the use of specific antisense ODNs, had any impact on behavioural performance on specific spatial memory tasks. Furthermore, the effect of the antisense ODN infusion in decreasing the expression of c-Fos and Zif268 was also tested at the molecular level.

The experiments used three groups of animals:

The first group (Group 1) was used to address technical issues encountered with the dorsal hippocampal cannula placement. When assessing cannula placement using histology in Chapter 4, the cannulae tips consistently appeared too dorsal. Furthermore, the spread of biotinylated antisense *Zif268* ODNs in some of the animals confirmed this observation. Accordingly, the behavioural results following hippocampal infusions were somewhat inconsistent and milder than might have been expected. To be sure that subsequent infusions were more centrally targeted within the dorsal hippocampus, we used longer (+ 0.25mm) microinjectors than in Chapter 4. To determine whether an improvement of placement and spread of ODNs was

achieved with the longer microinjectors, two rats were infused with biotinylated antisense *Zif268* ODNs and 90 minutes later the brains were processed for histological visualisation.

The second group of rats (Group 2) received dorsal hippocampal infusions of antisense ODNs targeting *c-Fos* and/or *Zif268*, and was then tested on two spatial memory tasks (Figure 5-1). Firstly, the modified version of the radial arm maze task as described in Chapter 4 (Experiment 1) and secondly an object-in-place task. As shown in Figure 5-2, the rats were infused with antisense ODNs targeting either *Zif268* or *c-Fos* mRNA independently, or with a cocktail combination of the ODNs, before the 3-hour delay with maze rotation variant of the radial arm maze task. The infusions were administered 90 minutes before the sample phase of the task as previous studies have shown that these antisense ODN sequences become behaviourally effective 1-2 hours post-infusion (Hebb & Robertson, 1997; Lee et al., 2004; Malkani et al., 2004; Seoane et al., 2012; Tolliver et al., 2000).

To establish whether any behavioural effects were task-specific, animals were subsequently tested on the object-in-place task after having been infused with a cocktail solution of antisense ODNs targeting both *c-Fos* and *Zif268* transcripts (Figure 5-3). The object-in-place task has been designed to determine whether animals are sensitive to the location of specific objects in a test arena and the task relies on rats' preference for novelty (Dix & Aggleton, 1999). The object-in-place task can be divided into a sample and a test phase. During the sample phase, the animals explore four different objects located at the four corners of the test arena, while in the test phase the same objects are used but two of them swapped positions. Rats preferentially explore the two displaced objects in comparison to the non-displaced objects, and this behaviour has been interpreted as a memory for the original position of all objects in the test arena (Dix & Aggleton, 1999). This preference is spontaneous and does not require previous training (because animals can be directly tested after a few sessions of habituation to the test arena) or reinforcement. These features eliminate the possible confounding effects of over-training or motivation on the animals' performance. A variable time-delay can be interposed between the sample and the test phase of the object-in-place task, and it has been shown that animals still discriminate between the displaced/non-displaced objects after 3 hours (Seoane et al., 2012). In this experiment, the antisense ODNs were infused 90 minutes before the sample phase and the subsequent effect on the test phase was assessed 3 hours later. The object-in-place task is sensitive to both hippocampal (Barker & Warburton,

2011) and retrosplenial cortex lesions (Vann & Aggleton, 2002). In contrast, animals with these same lesions are still able to discriminate between familiar and novel objects (e.g. Barker & Warburton, 2011; Vann & Aggleton, 2002). Thus, the impairment on the object-in-place task is thought to be due to an impoverished representation of the spatial environment or an inability to combine object and place information.

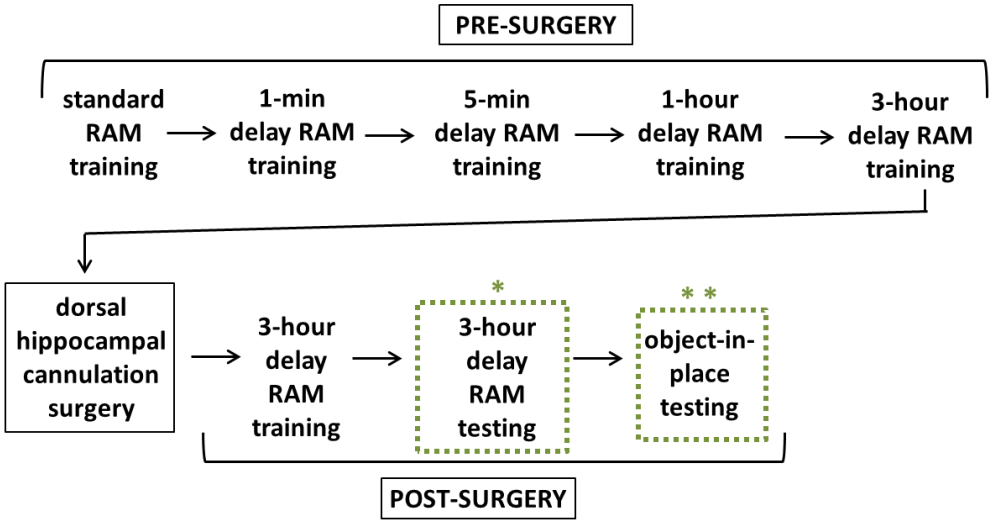

Figure 5-1. Schematic behavioural protocol for Group 2. All the delayed radial arm maze (RAM) tasks involved also a maze rotation between the sample and the test phase of the task. The protocol for the 3-hour delay with maze rotation radial arm maze testing (*) is reported in more details in Figure 5-2. The protocol for the object-in-place testing (**) is reported in more details in Figure 5-3.

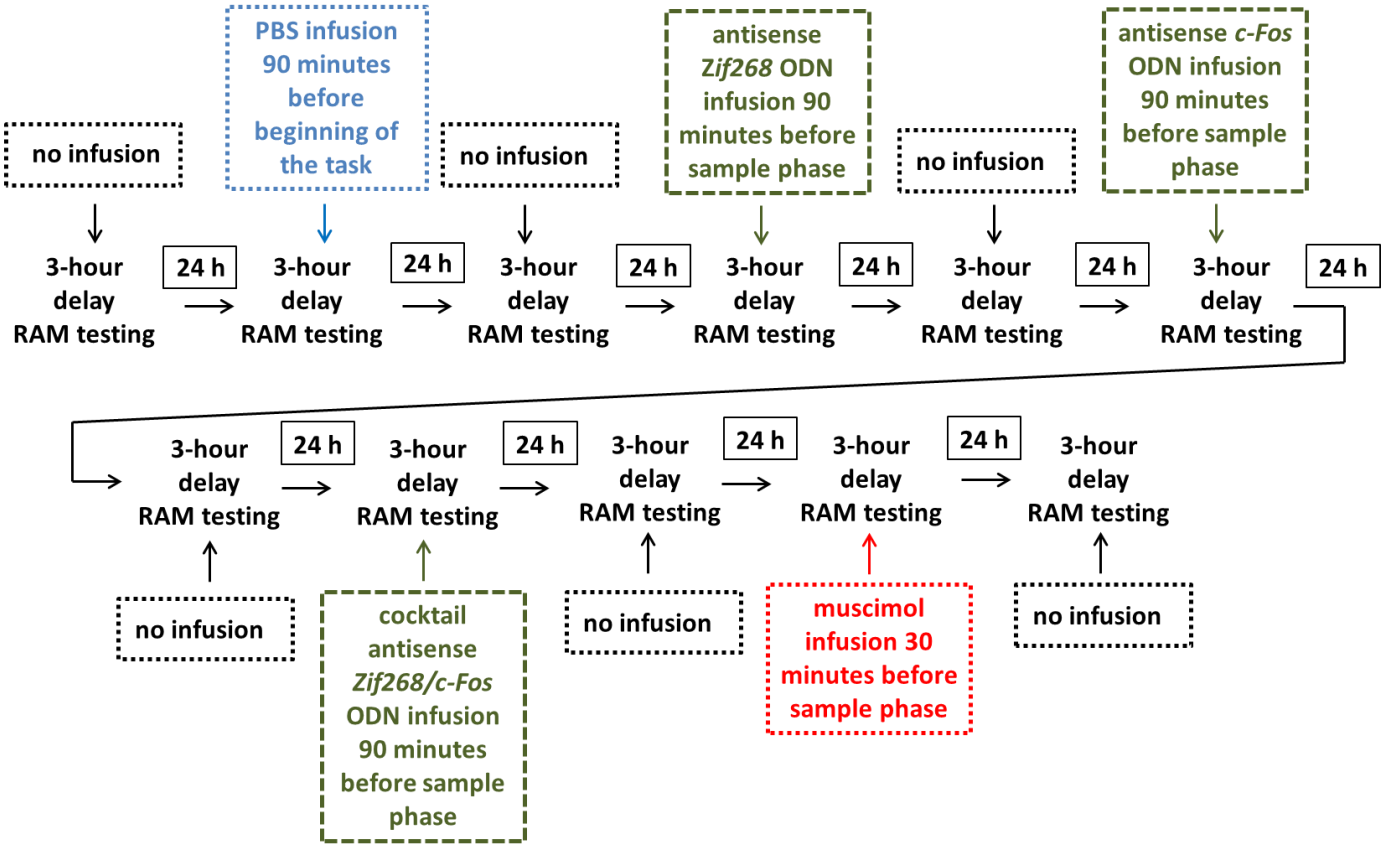

Figure 5-2. Schematic behavioural protocol for radial arm maze (RAM) post-surgery testing for Group 2. A maze rotation was interposed between the sample and the test phase in all sessions. PBS (phosphate buffer saline, i.e. the control infusion solution in this experiment), antisense *Zif268* ODN, antisense *c-Fos* ODN and cocktail antisense *Zif268/c-Fos* ODN infusions were 1.0 µl/infusion site, while muscimol infusions were 0.3 µl/infusion site.

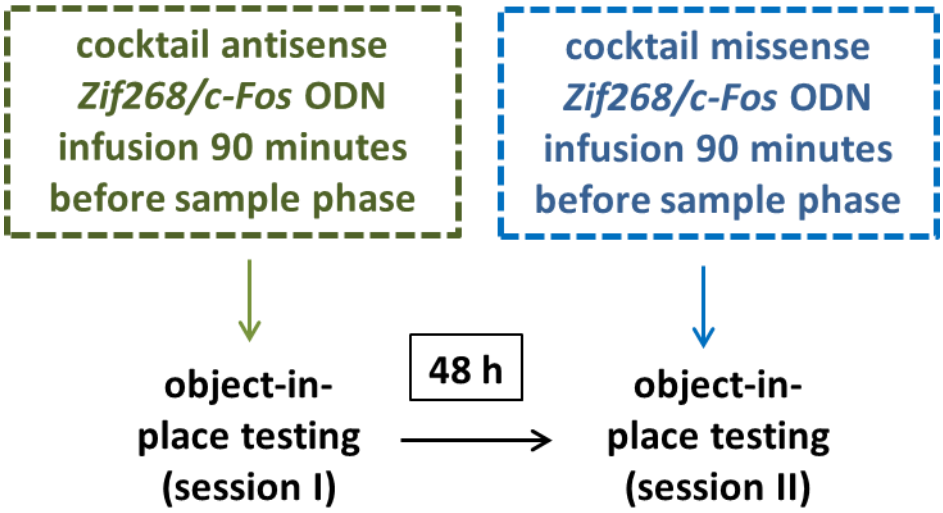

Figure 5-3. Schematic behavioural protocol for object-in-place post-surgery testing for Group 2. Cocktail antisense *Zif268/c-Fos* ODN and cocktail missense *Zif268/c-Fos* ODN infusions were 1 µl/infusion site.

The third group of animals (Group 3) was used to verify the efficacy of antisense ODN infusions in reducing the levels of c-Fos and Zif268 proteins in the dorsal hippocampal tissue in response to activity (Figure 5-4). Ninety minutes after either cocktail antisense or cocktail missense *Zif268/c-Fos* infusions, rats were allowed to freely explore a novel environment (a radial arm maze placed in an unfamiliar room). This behavioural task was chosen because exposure to a novel environment has been associated with an increase of both c-Fos (Hess et al., 1995; Jenkins, Dias, Amin, Brown, et al., 2002; Zhu et al., 1997) and Zif268 (Gheidi et al., 2013; Hall et al., 2000) levels in the dorsal hippocampus. The antisense ODNs infused before the task should block this elicited increase. We chose to infuse a cocktail of both antisense ODNs in order to obtain the maximum amount of information with the smallest number of animals. The animals were perfused 90 minutes after the behavioural task, as this is the time required for Zif268 and c-Fos proteins to be expressed after neuronal stimulation (Bullitt, 1990; Vann, Brown, & Aggleton, 2000; Vann, Brown, Erichsen, et al., 2000a). During this 90-minute delay, the animals were placed in a dark and quiet room to ensure the expression of Zif268 and c-Fos proteins was mainly induced by the neuronal activation following the exploration of the novel environment (Dragunow & Faull, 1989). Afterwards, the animals were euthanised, their brains extracted and the dorsal hippocampi microdissected for protein extraction. An additional four animals were euthanised directly from the home-cage (without undergoing surgery or

behavioural testing), and their dorsal hippocampi removed after brain extraction, in order to have unoperated home-cage control data for comparison. This would enable us to ascertain whether protein levels, following infusion of the antisense or missense ODNs, were raised above baseline levels. Western blot analysis was used to examine Zif268 and c-Fos protein levels. As both proteins (Bullitt, 1990; Curran, Miller, Zokas, & Verma, 1984; Davis et al., 2003; Herrera & Robertson, 1996) act as transcription factors in the nuclei of neurones, we measured their levels in extracts of dorsal hippocampal tissue enriched for nuclear proteins.

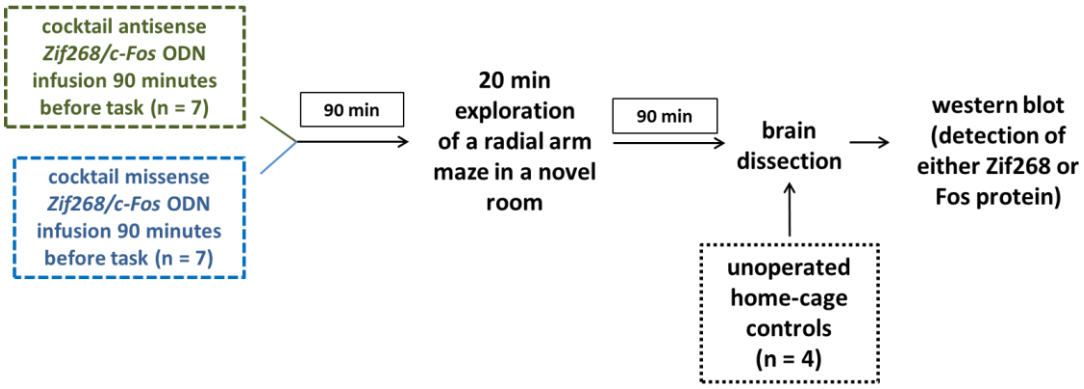

Figure 5-4. Schematic procedure protocol for Group 3. Cocktail antisense *Zif268/c-Fos* ODN and cocktail missense *Zif268/c-Fos* ODN infusions were 1 µl/infusion site. After the infusions, the animals were left 90 minutes in their home-cages in the holding room. After the maze exploration, the animals were left for 90 minutes in a dark and quiet room before euthanasia and brain extraction/dissection. Unoperated home-cage controls, instead, were unoperated naïve animals that were euthanised directly from the home-cage.

5.2 Methods

5.2.1 Subjects

Subjects in Group 1 were two male naïve Lister Hooded rats (Harlan, UK), weighing 302 and 310 g at the time of surgery; these animals were used for visualisation of biotinylated antisense *Zif268* ODNs diffusion into the dorsal hippocampus.

Subjects in Group 2 were six male naïve Lister Hooded rats (Harlan, UK), weighing 287-317 g at the time of surgery; they underwent behavioural procedures before and after cannulation surgery.

Subjects in Group 3 consisted of eighteen male Lister Hooded rats (Harlan, UK); fourteen animals in Group 3 received surgery (weight 278 – 319 g) prior to the behavioural procedure, while the remaining four animals acted as naïve home-cage controls (they did not receive surgery or behavioural testing).

All rats were initially housed in pairs, but animals that underwent surgery were housed individually after the operation, to maintain placement and patency of the implanted cannulae. Water was freely available for the course of the experiment. Rats were kept under diurnal light conditions (14 h light/10 h dark); all behavioural testing was carried out in the light phase. Animals that underwent behavioural testing were food deprived to not below 85 % of their free feeding weight for the duration of the behavioural test. For the remaining animals, food was available *ad libitum* throughout. All animals were thoroughly handled before the study began in order to habituate them to the handling procedure. The experiment was carried out in accordance with UK Animals (Scientific Procedures) Act, 1986 and associated guidelines.

5.2.2 Behavioural procedures

Group 2 – behavioural assessment of antisense ODN infusions into the dorsal hippocampus

5.2.2.1 Radial arm maze task

Apparatus

The apparatus was identical to that described in Chapter 4 (Section 4.2.1.2)

Pre-surgery behavioural procedure

The procedure was identical to that described in Chapter 4 (Section 4.2.1.2).

Post-surgery behavioural procedure

After animals in Group 2 had recovered from surgery, they were re-trained on the 3-hour delay version of the radial arm maze task. Once they reached the criterion level (no more than one error and all arms visited for at least two consecutive sessions), animals underwent infusion test sessions. Before the beginning of the sample phase, animals were infused with either PBS (phosphate buffer saline, used as control infusion solution), antisense *Zif268* ODNs, antisense *c-Fos* ODNs, cocktail antisense *c-Fos/Zif268* ODNs or muscimol (Figure 5-2).

Animals were infused with muscimol in the last test session in order to verify successful hippocampal infusion and cannula patency. Animals underwent infusion test sessions on alternate days; on the days in-between the infusion sessions, rats were tested without any infusions.

5.2.2.2 Object-in-Place task

Apparatus.

Rats in Group 2 were tested in a 'bowtie' maze, which was in the shape of a bowtie with wooden floor and walls. The maze was 120 cm long, with two triangular ends 50 cm wide at their widest point. A corridor, 12 cm wide, joined the apices of these two triangles. The widest end of each triangle had two food wells recessed into the floor, which were covered by the objects being explored. The maze was placed on a table positioned in the centre of a rectangular room.

All the four objects used in each task session were heavy enough that they could not be displaced by the rat, and were tall enough that the animals could not easily jump on top of them. The experiment used two duplicate sets of junk objects (one for each of the two sessions performed in this experiment) that were made of glass, metal, or plastic, e.g. metal cans, plastic containers or glass bottles. The two ends of the maze were slightly different so animals were able to distinguish the location of the objects. At one end of the maze, the food wells were separated from each other by a steel dividing wall 48 cm high, that extended 15 cm from the middle of the back wall of the maze. The dividing wall was removed from the other end of the maze and a sheet of white bench-guard paper was attached to the maze wall. A camera fixed to the ceiling above the maze was used to record onto DVD the animals' object exploration for subsequent analysis.

Post-surgery behavioural procedure

Five days following the completion of radial arm maze task the rats in Group 2 were habituated to the bow-tie maze. Rats were brought to the testing room individually in their home-cages covered with a towel to prevent the animal from seeing outside. Prior to the test day, all animals were given two habituation sessions, during which each rat was placed in the maze for 5 minutes. No objects were present in the maze during habituation.

Behavioural testing involved a sample phase followed by a test phase. During the sample phase, four different objects were placed in the maze. Each rat was placed in the centre of the maze and allowed to explore the objects for 5 minutes. At the end of the sample phase the rat was removed from the testing room and moved back to the holding room. The time delay between the sample and the test phase was 3 hours, during which the maze was wiped down with 20% ethanol to reduce odour cues as far as possible, and the objects were removed and replaced with replicas. Before the test phase, two of the objects, diagonally opposing each other, were swapped ("displaced") so that they were now in different positions in the arena, while the other two objects remained in the same position as in the sample phase (Figure 5-5). Following the 3-hour delay, the rat was returned to the maze for a 3-minute test phase, during which the time spent exploring the displaced and the non-displaced objects was recorded.

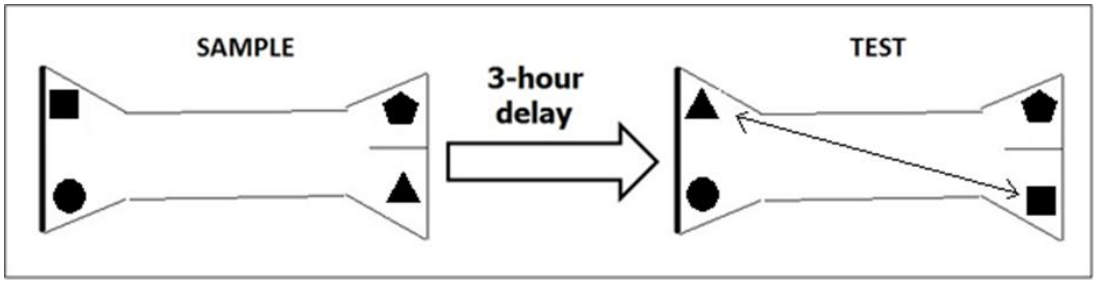

Figure 5-5. The object-in-place task. In the "sample phase" each animal was allowed to explore four different objects in a bow-tie maze for 5 minutes. The rat was then removed from the maze for 3 hours during which the maze was cleaned to remove odour cues. All the objects were substituted with identical replicas and two of the replicas swapped their positions from the sample phase. At the end of the 3 hours the animal was re-introduced in the maze and allowed to explore the objects for 3 minutes ("test phase").

There were two object-in-place task sessions, 48 hours apart, each involving a different set of duplicate objects. Both the object pairs and the positions that were swapped in the test phase were counterbalanced across sessions and animals.

Group 3 – molecular assessment of antisense ODN infusions into the dorsal hippocampus

5.2.2.3 Free exploration of a radial arm maze

Apparatus

The apparatus was identical to that described in Chapter 4 (Section 4.2.1.2)

Post-surgery behavioural procedure

Seven days after surgery, the fourteen cannulated rats in Group 3 were allowed to freely explore a radial maze located in a novel room for 20 minutes. All the guillotine doors that gave access to the maze arms were left open. To encourage the exploration of the maze, sugar pellets (to which rats had been previously habituated in their home-cages; 5TUT/1811251 45 mg, TestDiet, St Louis, Missouri, US) were scattered down the arms and continuously replaced, so that the animals were always motivated to explore. The position and number of arms explored was noted in order to evaluate a possible exploration difference between the two infusion groups. At the end of the exploration, rats remained in a dark and quiet room for 90 minutes before

being euthanised. The four unoperated home-cage control animals remained in their home-cages for the course of the experiment, before being euthanised for brain extraction/dissection. The animals were divided into five sub-groups (Table 5-1) and processed on consecutive days in order to extract the brains at approximately the same time of the day.

DAY 1	DAY 2	DAY 3	DAY 4	DAY 5
antisense (n = 2)	missense (n = 2)	antisense (n = 2)	missense (n = 2)	antisense (n = 1)
missense (n = 1)	antisense (n = 1)	missense (n = 1)	antisense (n = 1)	missense (n = 1)
home-cage control (n = 1)	home-cage control (n = 1)	home-cage control (n = 1)	home-cage control (n = 1)	

Table 5-1. Subdivision of Group 3 animals into five sub-groups that were processed on five consecutive days. "antisense" = group infused with cocktail antisense *Zif268/c-Fos* ODNs (seven animals in total); "missense" = group infused with cocktail missense *Zif268/c-Fos* ODNs (seven animals in total); "control" = unoperated home-cage control group which received no infusion (four animals in total).

5.2.3 Surgical procedure

All animals in Groups 1 and 2 and 14 animals in Group 3 were implanted with bilateral dorsal hippocampal cannulae (the animals in Group 2 underwent surgery once after they had reached criterion on the 3-hour delay with maze rotation variant of the radial arm maze task).

The procedure was identical to that described in Chapter 4 (Section 4.2.1.3).

5.2.4 Infusions

Each rat was gently wrapped in a soft towel whilst awake and the stylets were manually removed before dual microinjectors (28 gauge, 3.8 mm centre-to-centre, 1.5 mm projection beyond the tip of the guide cannulae, so 0.25 mm longer than the ones used in the previous experiments described in Chapter 4; PlasticsOne, Virginia United States) were inserted slowly into the surgically implanted guide cannulae. The microinjectors were connected via polyethylene tubings (PE 0.38x0.355 mm; Scientific Laboratory Supplies, United Kingdom) to two 5 µl syringes (800 Series, Cemented Needle; Hamilton, United States) fixed in a microinjection pump (model 11 plus, dual syringe pump; Harvard Apparatus, United Kingdom). At the end of each infusion, the microinjectors were kept in place inside the brain for further 2 minutes to

allow any solution to diffuse away from the microinjector tip. The injectors were then gently removed and the stylets replaced.

To habituate the rats to the infusion procedure and to test cannula patency, they received an infusion of sterile phosphate buffered saline (PBS, 0.1 M pH 7.4; 1 µl/infusion site at a rate of 0.167 µl/minute) into the dorsal hippocampus at least 3 days before any test session.

PAGE-purified phosphorothioate end-capped 15-mer and 18-mer ODNs (Sigma-Genosys, Sigma-Aldrich, UK) were re-suspended in sterile PBS. Their sequences were designed based on previous studies: antisense *Zif268* ODN, 5'-GGT AGT TGT CCA TGG TGG-3' (concentration 1 nmol/µl) and missense *Zif268* ODN, 5'-GTG TTC GGT AGG GTG TCA-3' (concentration 1 nmol/µl) (Lee et al., 2004); antisense *c-Fos* ODN, 5'-GAA CAT CAT GGT CGT-3' (concentration 2 nmol/µl) and missense *c-Fos* ODN, 5'-GTA CCA ATC GGG ATT-3' (concentration 2 nmol/µl) (Katche et al., 2013). All ODN sequences were subjected to a BLAST search on the National Center for Biotechnology Information BLAST server using the Genbank database. Antisense sequences had positive matches only for their target mRNA sequences, and no other rat or human coding sequences. Control missense sequences did not generate any full matches to identified gene sequences in the database. A cocktail antisense *Zif268/c-Fos* ODN solution was prepared by combining the antisense *Zif268* ODN and the antisense *c-Fos* ODN solutions (or the single missense solutions for the missense cocktail *Zif268/c-Fos* ODN solution). The final concentrations in the cocktail solutions were 1 nmol/µl *Zif268* ODNs and 2 nmol/µl *c-Fos* ODNs.

The two animals in Group 1 were exclusively used for visualising the spread of the infusion of ODNs into the dorsal hippocampus with the longer microinjectors (0.25 mm longer than those employed in the experiments described in Chapter 4). They were infused with 1 µl/infusion site of biotinylated antisense *Zif268* ODNs (1 nmol/µl; Sigma-Genosys, Sigma-Aldrich, UK) at the rate of 0.167 µl/min.

For the animals in Group 2, the infusion details were different for the two behavioural tasks employed. For the 3-hour delay with maze rotation variant of the radial arm maze task, the animals were tested for 11 consecutive days, receiving one infusion before the task on alternate days (Figure 5-2). It was important to insert a reasonable time interval between one ODN infusion and the next, in order to avoid neurotoxicity

effects (like gliosis or morphological rearrangements), as underlined by Chiasson et al. (1994). On the infusion days, rats were infused with different solutions in the following order: PBS (90 minutes before the sample phase), antisense *Zif268* ODNs (90 minutes before the sample phase), antisense *c-Fos* ODNs (90 minutes before the sample phase), cocktail antisense *Zif268/c-Fos* ODNs (90 minutes before the sample phase) and finally muscimol (30 minutes before the sample phase). Muscimol was infused at a volume of 0.3 µl/infusion site and at an infusion rate of 0.3 µl/minute (this volume and infusion rate were shown to be effective in Experiment 3 of Chapter 4). PBS, antisense *Zif268* ODN, antisense *c-Fos* ODNs and cocktail antisense *Zif268/c-Fos* ODNs were infused at a volume of 1 µl/infusion site (Katche et al., 2013; Lee et al., 2004) and at an infusion rate of 0.167 µl/minute. As animals in Group 2 already received a considerable number of infusions (six for each animal), we decided to test them in the object-in-place task only after cocktail antisense (or missense) *Zif268/c-Fos* ODN infusions (the cocktail solution was preferred to the single antisense ODNs in order to maximize the effect of the infusion). The rats were tested on two consecutive sessions of the object-in-place task (Figure 5-3). In the first session (Session I) they were infused with cocktail antisense *Zif268/c-Fos* ODNs (90 minutes before the sample phase), and in the second session (Session II) they were infused with cocktail missense *Zif268/c-Fos* ODNs (90 minutes before the sample phase). In both cases the volume of the infusate was 1 µl/infusion site, infused at an infusion rate of 0.167 µl/minute. Two days were interposed between the first and second object-in-place test session, in order to be sure that the infusate was completely cleared out from the infused area and to minimise any possible memory interference of the first test session on the second test session.

Fourteen rats in Group 3 were infused with either cocktail missense *Zif268/c-Fos* ODNs (seven rats) or cocktail antisense *Zif268/c-Fos* ODNs (seven rats) 90 minutes before behavioural manipulation; in both cases the volume of the infusate was 1 µl/infusion site, infused at an infusion rate of 0.167 µl/minute. During the time interval of 90 minutes before the behavioural task, the animals were returned to their home-cages in the holding room.

5.2.5 SDS-PAGE and Western blotting

Animals in Group 3 were euthanised either 90 minutes after completion of the behavioural task (fourteen infused rats) or straight from the home-cage (four unoperated control rats), by an overdose injection of sodium pentobarbital (60 mg/kg, Euthatal i.p., Rhone Merieux, Harlow, UK). After euthanasia, the rats were decapitated and their brain quickly removed and placed on dry ice. The dorsal hippocampal regions were microdissected and frozen on dry ice prior to storage at –80°C. As the proteins of interest (Zif268 and c-Fos) act as transcription factors in the neuronal nuclei (Bullitt, 1990; Curran et al., 1984; Davis et al., 2003; Herrera & Robertson, 1996), a lysis protocol for nuclear protein fraction extraction was used. TBP (TATA-box Binding Protein, a protein implicated in the initiation of DNA transcription inside the cellular nucleus; e.g. Ahn et al., 2012) was chosen as nuclear fraction loading control protein (previous studies working with nuclear protein fractions extracted from the hippocampus had also used TBP as loading control; e.g. Chen et al. 2011; Jackson, Rani, Kumar, & Foster, 2009). The efficacy of the protocol for both isolation of the nuclear fraction and visualisation of the antibodies of interest (anti-Zif268, anti-c-Fos and anti-TBP) was confirmed in a pilot experiment employing naïve tissue from three naïve Lister hooded rats. Dorsal hippocampal naïve tissue was used for Zif268 optimisation, while prefrontal cortical naïve tissue was employed for c-Fos (as levels of the latter in naïve dorsal hippocampus appear very low; personal observation, data not shown). Tissue (from both the left and the right dorsal hippocampus) was homogenised manually until solid matter traces completely disappeared using a pestle and a glass tissue grinder in a lysis buffer solution (150 mM NaCl, 50 mM Tris at pH 8.0, 1% Triton X-100, 1 mM EDTA, ddH_2O up to 100 ml) to which a cocktail of protease inhibitors was added to avoid protein degradation (one tablet per 10 ml of buffer, Complete Mini EDTA-free tablets; LifeScience, Roche, UK). The ratio tissue : lysis buffer was 1 : 60. Homogenised samples were stored in centrifuge tubes and kept on ice between protocol steps. The samples were centrifuged for 10 minutes at 2000 RCF (relative centrifugal force) at + 4°C, and the supernatant was either discarded or archived for independent control experiments (it constituted the cytosolic fraction). The pellet was washed in lysis buffer, centrifuged again for 10 minutes at 2000 RCF at + 4°C, and the supernatant discarded. The final nuclear pellet was re-suspended in lysis buffer, 5X of the pellet's volume. Protein concentration was quantified using the Bradford assay (Quick Start™ Bradford 1x Dye Reagent, Bio-Rad, UK), comparing sample dilutions to serial dilutions of the protein standard (Quick Start Bovine Serum Albumin Standard Set, Bio-Rad, UK). For gel

electrophoresis, samples were run on two separate gels (two for each protein of interest, Zif268 and c-Fos) processed simultaneously: one containing four antisense, four missense and two unoperated home-cage control samples, and the other containing the remaining three antisense, three missense and two unoperated home-cage control samples.

The protein samples were diluted in lysis buffer in order to reach a concentration of 10 µg/µl, then reduced adding Laemmli buffer (Laemmli Sample Buffer, Bio-Rad, UK; ratio 1 : 1 with the sample) and finally denatured by heating them at 96°C for 5 minutes on a thermoblock. Samples were loaded onto polyacrylamide gel (7.5% Mini-PROTEAN® TGX™ Gel, 15 well, 15 µl; Bio-Rad, UK) and run in a running chamber filled with electrophoresis running buffer (1X Tris/Glycine/SDS, Bio-Rad, UK), connected to a Bio-Rad PowerPac (115 V constant, for about 1 hour and 30 minutes). A protein ladder was also loaded onto each gel in order to be able to estimate the molecular weight of the target proteins (5 µl for each gel; Precision Plus Protein™ Kaleidoscope™ Standards, Bio-Rad, UK). Proteins were then transferred from the gel to a PVDF (polyvinylidene difluoride) membrane (Amersham Hybond, GE Healthcare Life Sciences, UK) in transfer buffer (3.03 g Tris, 14.4 g glycine, 200 ml 100% methanol, ddH_2O up to 1 L) via wet transfer (Bio-Rad; PowerPac setting: 0.1 A constant, 2 hours) performed on ice. After the transfer, the membranes were incubated for 30 minutes in a blocking solution made up of TBST (0.01M Tris-buffered saline solution containing 0.05% Tween 20) with the addition of 5% non-fat dried milk (Amersham ECL Blocking Agent, GE Healthcare, Life Sciences, UK). Membranes were incubated overnight with the primary antibody, either anti-c-Fos (1:1000, rabbit polyclonal antibody, 226 003, Synaptic Systems, Germany) or anti-Zif268 (1:1000, rabbit polyclonal antibody, SC-189, Santa-Cruz Biotechnology, Texas, US) in TBST containing 5% non-fat dried milk. The membranes were subsequently washed 3X 10 minutes in TBST and incubated with the secondary antibody (1:5000, Goat Anti-Rabbit IgG H&L HRP, ab6721, Abcam, UK) in TBST containing 5% non-fat dried milk for 1 hour at room temperature. The blot was washed again 3X 10 minutes in TBST. After incubating the membrane with the chemiluminescent substrate (2 ml/membrane, Luminata Crescendo Western HRP, Merck Millipore, UK) for 5 minutes, the antibody signal was visualized through ChemiDoc MP imaging (Bio-Rad, UK); different exposure times were recorded for each blot, in order to capture the signal in a linear range. The membranes were subsequently stripped to remove the antibody staining before being probed with the with TBP antibody (nuclear fraction loading control). Membranes were washed 3X 10 minutes in TBST, 2X 15 minutes in stripping buffer

(3 g glycine, 0.2 g SDS, 2 ml Tween 20, pH 2.2, ddH_2O up to 200 ml), and finally 2X 10 minutes in TBST. Subsequently, the membranes were processed as above, except the blocking solution was TBST containing 5% BSA (bovine serum albumin, A2153, Sigma-Aldrich, UK), the primary antibody was anti-TBP (1:1000, Anti-TATA binding protein, ab63766, Abcam, UK) in TBST and 5% BSA, and the secondary antibody (1:3000, Goat Anti-Rabbit IgG H&L HRP, ab6721, Abcam, UK) was diluted in TBST and 5% BSA. Throughout the procedure, the membranes were washed and incubated in plastic opaque boxes placed on an orbital shaker at room temperature, except during primary incubation which was performed at 4°C in a cold room.

The effectiveness in isolating the nuclear proteins was confirmed as the TBP band was present only in the nuclear fraction and not in the cytosolic fraction (Figure 5-6).

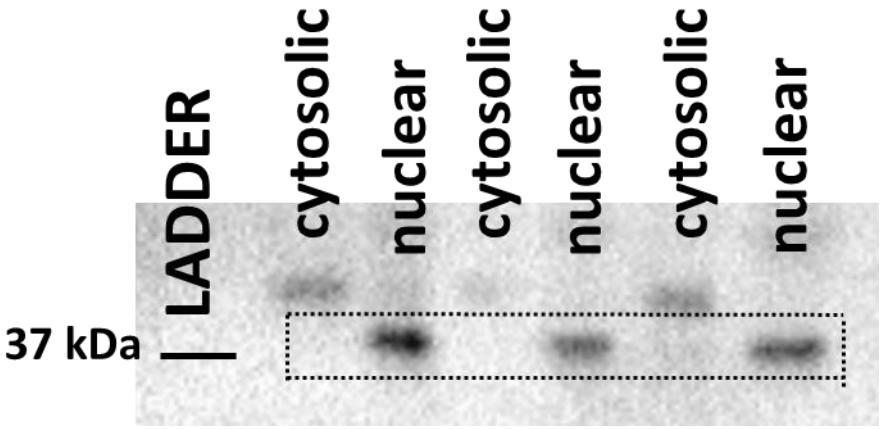

Figure 5-6. Representative blot showing staining for TBP protein during optimisation of the Western blot technique (on samples from additional naïve animals). The first lane on the left was used for running the protein ladder (not visualised in this image and represented by a black horizontal line). Proteins from cytosolic or nuclear fractions of dorsal hippocampi of naïve animals were run in the remaining lanes. The bands representing TBP protein in the nuclear fractions have been enclosed in a dashed rectangle

5.2.6 Histology

5.2.6.1 Infusion of biotinylated antisense *Zif268* ODNs and β-thionin counterstaining to verify infusate diffusion with the longer microinjectors and cannulae placement

This procedure was performed on the two animals in Group 1 in order to verify the spread of the infusate with the longer microinjectors. Ninety minutes after the infusion of the biotinylated antisense *Zif268* ODNs (Section 5.2.4), the animals were irreversibly anaesthetised with sodium pentobarbital (60 mg/kg, Euthatal, Rhone Merieux, Harlow, UK) and perfused transcardially with 0.1 M PBS followed by 4% paraformaldehyde in 0.1 M PBS (PFA). The brains were removed and post-fixed in 4% PFA for 2 hours and then transferred to 20% sucrose (in 0.1M PBS) overnight. Sections were cut at 40 µm on a freezing microtome in the coronal plane, and a one-in-three series of sections was selected and quenched in 50:50 10% methanol (Sigma-Aldrich, UK) and 10% H_2O_2 (Fisher Scientific, US). The sections were rinsed three times in PBS (15 minutes each) and permeabilised in 0.3% Triton overnight. The sections were then incubated in an avidin-biotidin complex (Vectastain Elite ABC kit PK-6100, Vector Laboratories, UK) for 2 hours and again rinsed three times in PBS (15 minutes each). Finally, the sections were exposed to DAB (DAB Peroxidase (HRP) Substrate Kit, 3,3'-diaminobenzidine, Vector Laboratories, UK) until visualisation of biotinylated ODNs was complete (requiring about 1 minute), washed again in cold PBS and left at +4°C overnight. The day after they were mounted onto gelatin-coated slides and air-dried before counterstaining with β-thionin (for histological assessment of cannulae placement). For counterstaining, the sections were immersed in β-thionin (diluted at a concentration of 1% in distilled water; Sigma-Aldrich T7029, UK) for 10 minutes, rinsed in distilled water for 1 minute, then gradually dehydrated in ethanol at increasing concentrations (5 minutes in 70% ethanol, 20 minutes in 90% ethanol and 20 minutes in 100% ethanol), and then immersed in Histoclear (National Diagnostics, UK) for at least 40 minutes. Finally the sections were coverslipped (Gurr DePeX mounting medium, BDH Laboratory Supplies, Poole, UK).

5.2.6.2 Cannulae placement verified through Nissl staining

For the animals in Group 2, cannulae placement was verified through Nissl staining. On completion of the experiment, the animals were irreversibly anaesthetised with sodium pentobarbital (60 mg/kg, Euthatal, Rhone Merieux, Harlow, UK) and perfused transcardially with 0.1 M PBS followed by 10% formol-saline. The brains were removed and post-fixed in 10% formol-saline for 4 hours and then transferred to 25%

sucrose (in 0.1M PBS) overnight. Sections were cut at 40 µm on a freezing microtome in the coronal plane, and a one-in-three series of sections was mounted onto gelatin-coated slides and stained with cresyl violet, a Nissl stain.

5.2.7 Statistical analysis

SPSS software (version 20, IBM Corporation) was used to carry out statistical analyses. The threshold for significance was set at $p < 0.05$ for all statistical tests.

5.2.7.1 Behavioural data

For the 3-hour delay with maze rotation variant of the radial arm maze task (Group 2), the number of correct arm entries in the first eight choices and the total number of errors were recorded for each post-surgery test session. These values were compared across the six test sessions with no infusion and the test session after PBS infusion, using a repeated measures ANOVA. Subsequently, the number of correct arm entries in the first eight choices and the total number of error obtained in the five test sessions after infusion (of either PBS, or antisense *Zif268* ODNs, or antisense *c-Fos* ODNs, or cocktail antisense *Zif268/c-Fos* ODNs, or muscimol) were compared using a repeated measures ANOVA with "Infusion session" as the within-subject factor. Sphericity of data was checked using Mauchly's sphericity test and degree of freedom corrections were applied when necessary. When significant main effects were found, Bonferroni post hoc comparisons were run in order to identify which infusion sessions significantly differed.

For the object-in-place task (Group 2), a preliminary analysis was performed on the total exploration times of the four objects during the "sample" and the "test" phases. The animals were considered to be "exploring" the objects when their nose was less than 1 cm from the object and pointed in that direction. The total exploration times were separately recorded for the "sample" and the "test" phase and compared across cocktail antisense and cocktail missense infusion sessions using paired-samples t-tests. The object exploration times were then further analysed during the 3 minutes of the "test" phase, measuring separately the exploration times for the displaced and the non-displaced object pairs. Successful performance in this task would be reflected by the animals exploring the displaced objects more than the non-displaced objects, due to their relative novelty. A discrimination ratio was calculated from the measures for

the “test” phase of each of the two sessions, using the difference between the time spent exploring the displaced objects minus the time spent exploring the non-displaced objects, divided by the total object exploration time (Dix & Aggleton, 1999). This transformation of the data is able to take into account differences in the individual levels of exploration for each animal. The discrimination ratios were calculated for both the first minute of the “test” phase (which has been shown to be the most sensitive for expression of preference for the displaced objects; e.g. Dix & Aggleton, 1999) and the total 3 minutes of the “test” phase. Paired samples t-test was used to compare performance after the infusion of either cocktail antisense *Zif268/c-Fos* ODN or cocktail missense *Zif268/c-Fos* ODN solution. Each discrimination ratio was also compared against chance level (zero) using one-sample t-test.

For the free exploration of the radial arm maze task (Group 3), the number of arms visited in the 20 minutes was compared between animals infused with either cocktail missense *Zif268/c-Fos* ODNs or cocktail antisense *Zif268/c-Fos* ODNs (the unoperated home-cage controls did not perform the behavioural task) using independent samples t-test.

5.2.7.2 Western blot data

Densitometric analysis was performed using ImageJ (version 1.46r; National Institute of Health, US), using the “Analyze → Gels” tool already installed. The software estimates a “peak profile” from each lane (y-axis) and band (x-axis) of the gel, registering the chemiluminescent signal emitted from the blot as a rising peak emerging from its surface in the third dimension (on the z-axis). The total volume under the three dimensional peak constitutes the “density” of a band. The densitometric data obtained represent arbitrary numbers of optical density (OD). Subtraction of the background noise was performed manually on two-dimensional densitometric lane plots (lane extension on the x-axis and chemiluminescent signal on the y-axis), closing the peaks with a straight line passing through the two points where the peak starts and ends (they were determined arbitrarily for each peak). In order to control for loading variation, the signal for either Zif268 or c-Fos for each sample was standardised by the TBP signal obtained for that specific sample in the same gel. These standardised values were then divided by the average of the TBP-standardised signals for the two control samples present on each gel, obtaining percentages. A one-way ANOVA was used to measure if there was a main effect of the Infusion group between-subject factor (unoperated home-cage control group,

versus cocktail missense *Zif268/c-Fos* ODN infusion group, versus cocktail antisense *Zif268/c-Fos* ODN infusion group) on the protein signal in the blot. When a significant main effect was found, Bonferroni post hoc comparisons were carried out. The Zif268 and c-Fos data were analysed separately.

5.3 Results

5.3.1 Histology

5.3.1.1 Verification of biotinylated antisense ODN *Zif268* diffusion into the dorsal hippocampus with the longer microinjectors (Group 1)

The spread of infusion with the longer microinjectors in animals of Group 1 was optimal, covering the whole extent of the dorsal hippocampus. The infusion did not spread into the ventral hippocampus and there was minimal into the overlying cerebral cortex. In both subjects the cannulae appeared correctly positioned in all the stereotaxical axes (Figure 5-7).

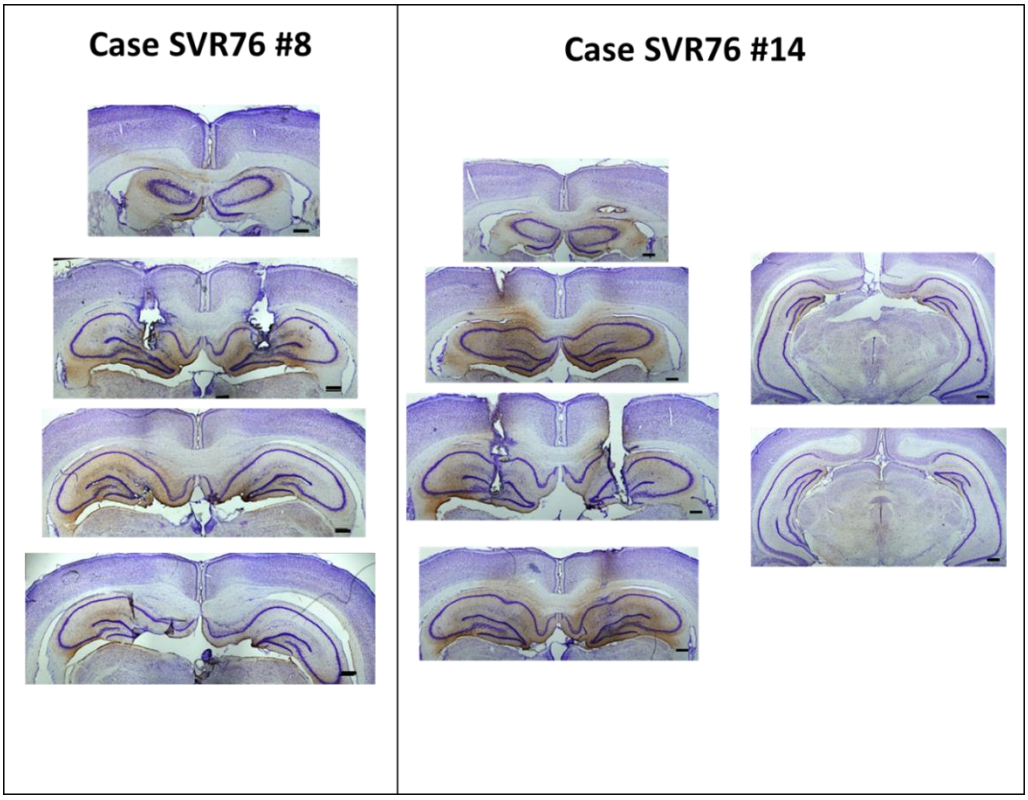

Figure 5-7. Diffusion of biotinylated antisense *Zif268* ODNs infused into the dorsal hippocampus in the two subjects in Group 1. Notice the minimal spread of the infusate in the overlying cortex and in the ventral hippocampus. Scale bar 200 µm.

5.3.1.2 Cannulae placement verified through Nissl staining (Group 2)

In Group 2, the cannulae were correctly placed within the dorsal hippocampus in all three planes (antero-posterior, medio-lateral and dorso-ventral; Figure 5-8 & Figure 5-9).

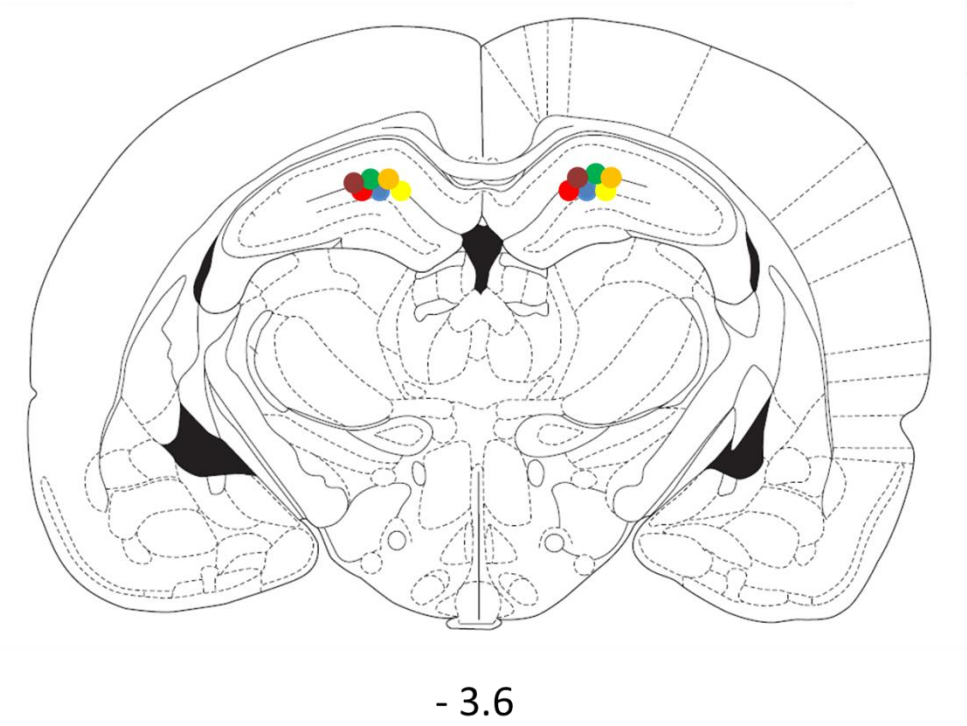

Figure 5-8. Cannulae placement into the dorsal hippocampus (coronal view) in Group 2. Each point represents the position of the tip of the cannula. A different colour has been used to identify cannulae placement for each animal. The distance in mm from bregma is reported. Figure adapted from Paxinos & Watson (1998).

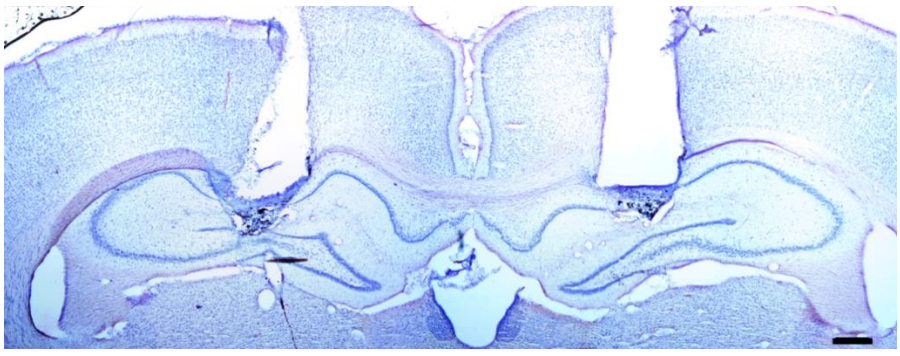

Figure 5-9. Representative coronal section of the dorsal hippocampus showing cannulae placement in one animal in Group 2. Tissue stained with cresyl violet staining. Scale bar 200 µm.

5.3.2 Behaviour (Group 2 and Group 3)

Group 2 – behavioural assessment of the antisense ODN infusions into the dorsal hippocampus

5.3.2.1 Pre-surgery radial arm maze task training

Animals in Group 2 were first trained on the standard working memory version of the radial-arm maze task. Subsequently, delays of increasing length were inserted after the first four arm choices, from 1 minute, to 5 minutes, then to 1 hour and finally to 3 hours. The performances are summarised in Table 5-2. All animals were able to reach the criterion level (i.e. no more than one error and all arms visited for at least two consecutive sessions) in both the standard task and in the variant with maze rotation with each of the delays inserted.

TIME DELAY INSERTED IN THE TASK	Mean NUMBER OF SESSIONS BEFORE REACHING CRITERION ± SEM	Mean NUMBER OF CORRECT ENTRIES (first eight choices) ± SEM	Mean TOTAL NUMBER OF ERRORS ± SEM
NO DELAY (STANDARD RAM task)	9.3 ± 0.7	7.5 ± 0.4	3.5 ± 0.5
1-MINUTE DELAY	5.5 ± 0.8	6.9 ± 0.1	2.6 ± 0.3
5-MINUTE DELAY	4.2 ± 0.8	7.0 ± 0.1	1.6 ± 0.1
1-HOUR DELAY	6.7 ± 0.4	7.3 ± 0.1	1.5 ± 0.3
3-HOUR DELAY	7.1 ± 1.2	7.1 ± 0.2	1.3 ± 0.2

Table 5-2. Summary of performance during pre-surgery behavioural training in the radial arm maze (RAM) task for Group 2.

5.3.2.2 Post-surgery radial arm maze task training/testing

After surgery the rats in Group 2 were re-trained on the 3-hour delay with maze rotation variant of the radial arm maze task until they reached criterion level (at least two consecutive sessions with no more than one error and all arms visited). This took on average 8.0 ± 0.5 (mean ± SEM) sessions. Testing began on the following day (Figure 5-2).

When performance (mean ± SEM) during the six no-infusion test sessions (correct entries: 7.5 ± 0.1, errors: 0.5 ± 0.1) was compared to performance after PBS infusion (correct entries: 7.5 ± 0.2, errors: 0.7 ± 0.3), no significant difference was found ($F < 1$ for comparisons of both correct entries and errors). Thus performance measures after PBS infusion were used as control measurement in the subsequent analyses. Statistical analysis revealed a significant main effect of the Infusion session factor (infusion of either PBS, or antisense *Zif268* ODNs, or antisense *c-Fos* ODNs, or cocktail antisense *Zif268/c-Fos* ODNs, or muscimol) on animals' performances, considering both the number of correct arm entries during first eight choices ($F_{4,20}=11.321$ $p<0.001$) and the total number of errors ($F_{4,20}=40.41$; $p<0.001$). Bonferroni post-hoc comparisons revealed that, for the correct entries in the first eight arm choices (Figure 5-10), performance after muscimol infusion was significantly worse than after antisense *c-Fos* ODN infusion ($p < 0.01$); when considering the number of errors (Figure 5-11), performance after muscimol infusion was significantly impaired compared to infusion of each of the other solutions ($p < 0.01$ in all cases).

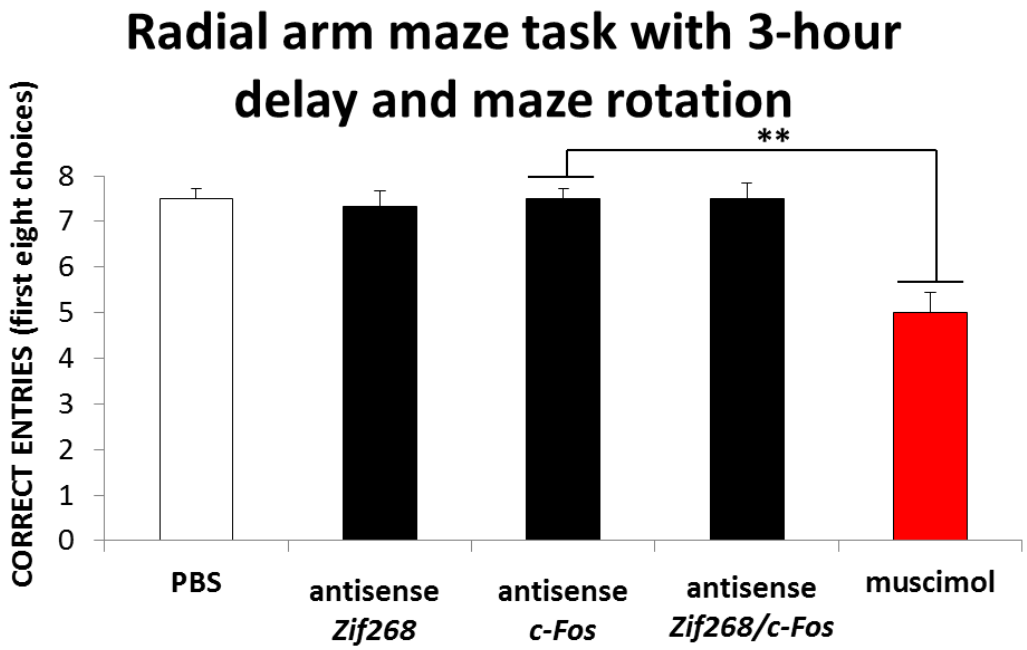

Figure 5-10. Correct entries (mean ± SEM) in the first eight arm choices of the 3-hour delay radial arm maze task with maze rotation for Group 2. Rats received infusions of either PBS, antisense *Zif268* ODNs, antisense *c-Fos* ODNs, cocktail antisense *Zif268/c-Fos* ODNs or muscimol into the dorsal hippocampus before the sample phase. Level of significance: *** $p < 0.01$.

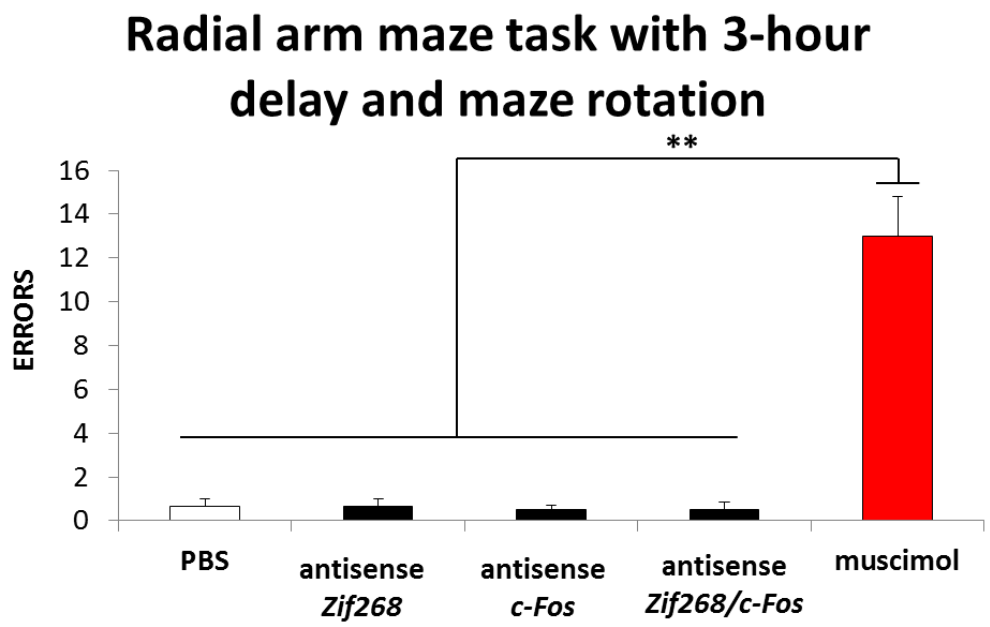

Figure 5-11. Total errors (mean ± SEM) in the 3-hour delay radial arm maze task with maze rotation after dorsal hippocampal cannulation surgery for Group 2. Rats received infusions of either PBS, antisense *Zif268* ODNs, antisense *c-Fos* ODNs, cocktail antisense *Zif268/c-Fos* ODNs or muscimol into the dorsal hippocampus before the sample phase. Level of significance: ** $p < 0.01$.

5.3.2.3 Post-surgery object-in-place task testing

Analysis of the total object exploration times after infusion of either the cocktail antisense *Zif268/c-Fos* ODNs or the cocktail missense ODNs into the dorsal hippocampus of animals in Group 2 did not reveal any significant difference, either in the sample phase (t_5 = -0.2, p = 0.90; Figure 5-12) or in the test phase (t_5 = 0.6, p = 0.57; Figure 5-13).

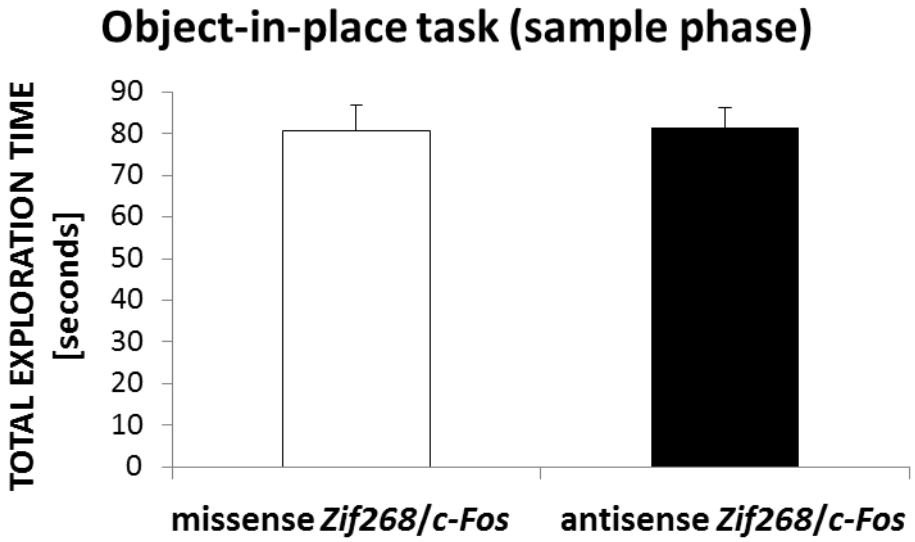

Figure 5-12. Total exploration times (mean ± SEM) in the sample phase of the object-in-place task for Group 2. The animals were infused with either cocktail missense *Zif268/c-Fos* ODNs or cocktail antisense *Zif268/c-Fos* ODNs into the dorsal hippocampus 90 minutes before the sample phase.

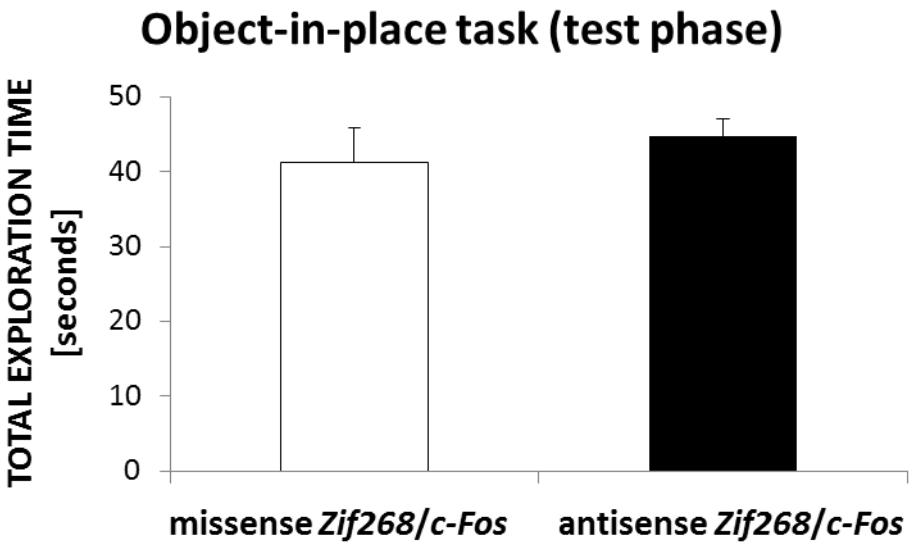

Figure 5-13. Total exploration times (mean ± SEM) in the test phase of the object-in-place task for Group 2. The animals were infused with either cocktail missense *Zif268/c-Fos* ODNs or cocktail antisense *Zif268/c-Fos* ODNs into the dorsal hippocampus 90 minutes before the sample phase. A 3-hour delay was inserted between the sample and the test phase.

To evaluate the ability of the rats in Group 2 to discriminate between the displaced and the non-displaced objects during the test phase, the discrimination ratios for both the first minute and the total 3 minutes of the test phase were compared to zero. The discrimination ratios did not significantly differ from zero following infusions of either the cocktail missense (first minute: $t_5 = 1.0$, $p = 0.35$; total 3 minutes: $t_5 = 0.3$, $p = 0.78$) or the cocktail antisense (first minute: $t_5 = 1.3$, $p = 0.26$; total 3 minutes: $t_5 = 1.1$, $p = 0.31$) *Zif268/c-Fos* ODN solutions. Moreover, the discrimination ratios obtained after the animals were infused with cocktail antisense *Zif268/c-Fos* ODNs were not significantly different from those obtained after the animals were infused with cocktail antisense *Zif268/c-Fos* ODNs (first minute: $t_5 = -0.4$, $p = 0.70$; total 3 minutes: $t_5 = -1.1$, $p = 0.32$; Figure 5-14].

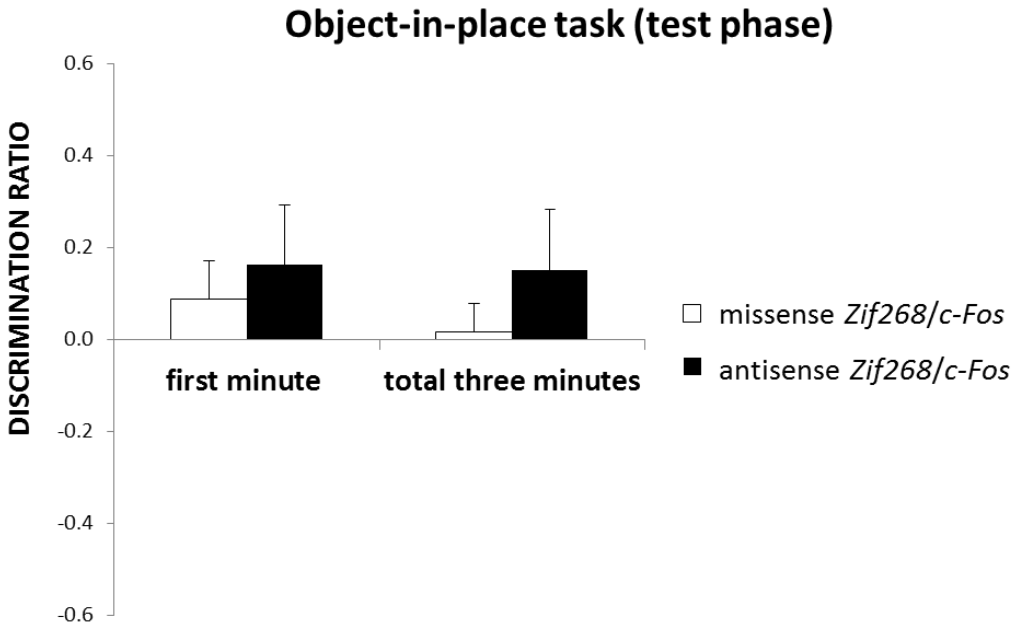

Figure 5-14. Discrimination ratios (mean ± SEM) in the test phase of the object-in-place task for Group 2. The animals were infused with either cocktail missense *Zif268/c-Fos* ODNs or cocktail antisense *Zif268/c-Fos* ODNs into the dorsal hippocampus 90 minutes before the sample phase. A 3-hour delay was inserted between the sample and the test phase.

Group 3 – molecular assessment of antisense ODN infusions into the dorsal hippocampus

5.3.2.4 Post-surgery free exploration of a radial arm maze located in a novel room

No difference was detected in the total number of radial arm maze arms visited following cocktail missense *Zif268/c-Fos* ODNs infusion compared to cocktail antisense *Zif268/c-Fos* ODNs infusion (t_{12} = 1.0, p = 0.33; mean number of arms visited (± SEM): missense 33.1 ± 3.9; antisense 28.0 ± 3.3).

5.3.3 Western blot (Group 3)

5.3.3.1 Identification of bands of interest

Identification of bands of interest for Zif268 and c-Fos on the blots was not obvious as more than one band was stained in each lane of each blot. This result was partially due to the lack of specificity of the antibodies employed, the ability of the antibodies to recognise proteins with similar epitopes to the protein of interest, and/or Zif268 and c-Fos with different post-translational modifications. In order to select the bands to analyse we referred to the estimated molecular weights of the proteins and to the optimisation pilot experiment in which we compared nuclear and cytosolic fraction extracted from hippocampal or prefrontal tissue of naïve animals, focusing the analysis on those protein bands which were present only in the nuclear fraction. The estimated molecular weight of Zif268 is 75 kDa (Lonergan et al., 2010). Figure 5-15 shows the most intense band (band “A”) was found in a region comprising proteins between 50 kDa and 100 kDa. The molecular weight of this band appears to be smaller than 75 kDa, so three other bands (“B”, “C” and “D”) with a higher molecular weight (but not higher than 100 kDa) were also considered. The pilot experiment had previously showed that band “A” was expressed only in the nuclear fraction, while the other three bands were present in both nuclear and cytosolic fractions (Figure 5-16).

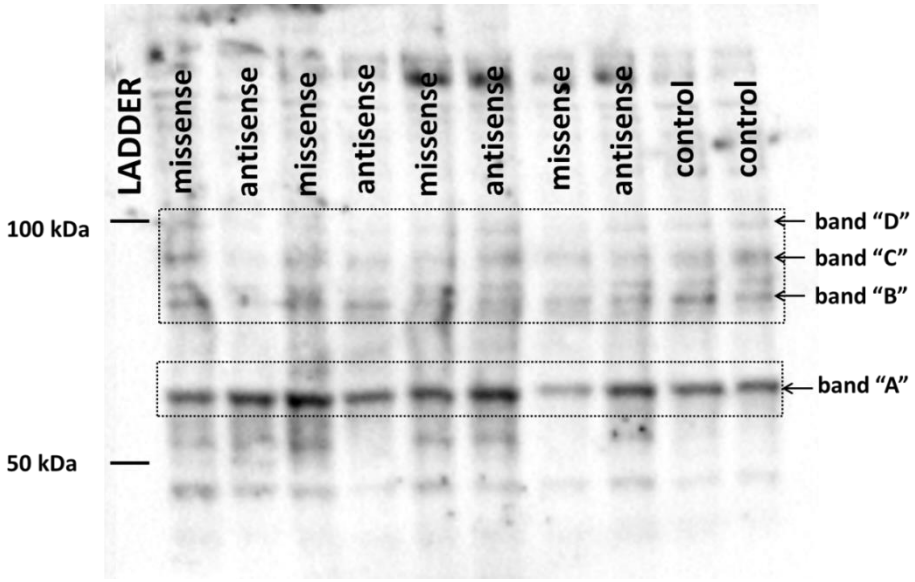

Figure 5-15. Representative blot showing staining for Zif268 protein for Group 3. The first lane on the left was used for running the protein ladder (not visualised in this image and represented by black horizontal lines). Proteins from the nuclear fraction of the dorsal hippocampi of experimental animals were run in the remaining lanes (each lane has been labelled with the name of the respective experimental group: missense = group infused with cocktail missense *Zif268/c-Fos* ODNs 90 minutes before free exploration of a novel environment; antisense = group infused with cocktail antisense *Zif268/c-Fos* ODNs 90 minutes before free exploration of a novel environment; control = unoperated home-cage control group which did not receive any infusion or behavioural training). The four bands of interest have been enclosed in dashed rectangles.

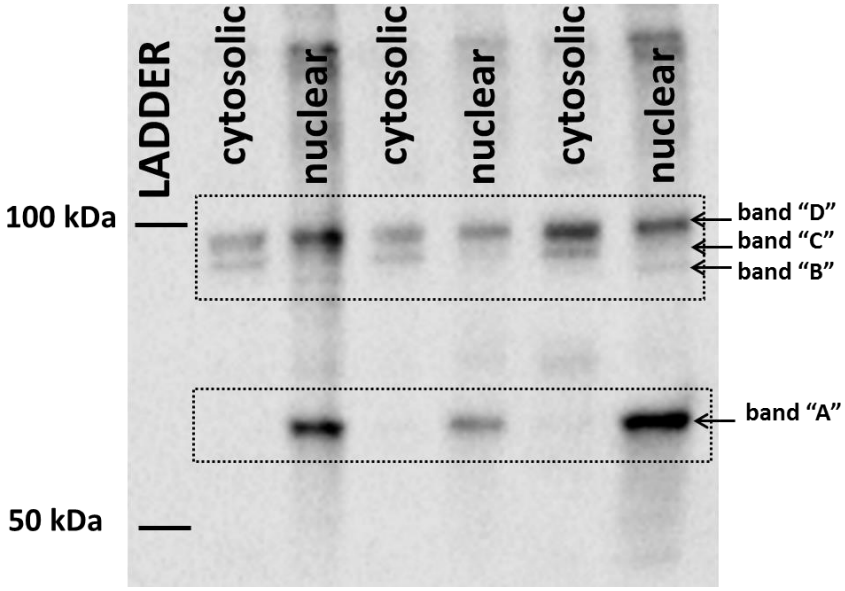

Figure 5-16. Representative blot showing staining for Zif268 protein during the optimisation of the Western blot technique (on samples from additional naïve animals). The first lane on the left was used for running the protein ladder (not visualised in this image and represented by black horizontal lines). Proteins from cytosolic or nuclear fraction of the dorsal hippocampus of naïve animals were run in the remaining lanes. The bands representing the putative Zif268 protein have been enclosed in dashed rectangles.

The estimated molecular weight of c-Fos is 56 kDa (Herrera & Robertson, 1996). As with Zif268, the analysis was performed on four bands whose molecular weight was between 50 and 100 kDa (Figure 5-17). One of these bands (band “A”) has a molecular weight very close to 50 kDa, while all the others (“C”, “D” and “E”) were greater, but appeared not to exceed 75 kDa. All the bands were present in the nuclear but not in the cytosolic fraction in the protocol optimisation (Figure 5-18).

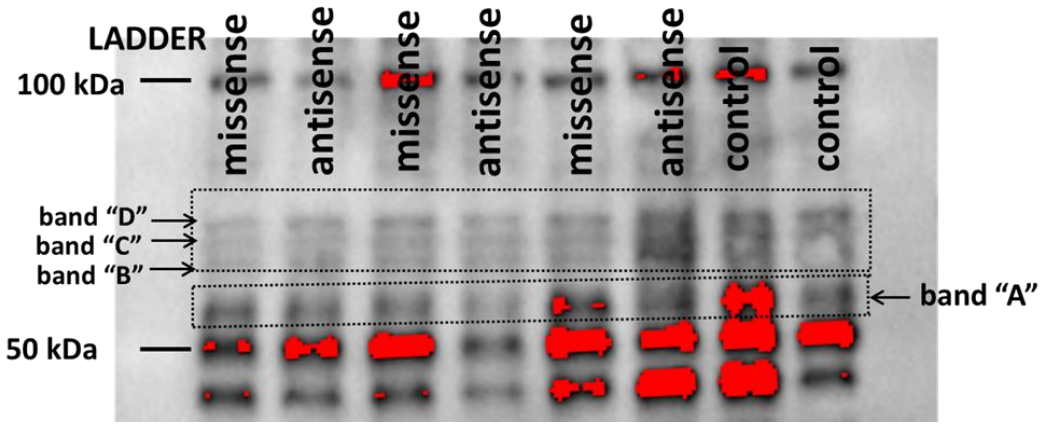

Figure 5-17. Representative blot showing staining for c-Fos protein for Group 3. The first lane on the left was used for running the protein ladder (not visualised in this image and represented by black horizontal lines). Proteins from the nuclear fraction of the dorsal hippocampi of experimental animals were run in the remaining lanes (each lane has been labelled with the name of the respective experimental group: missense = group infused with cocktail missense *Zif268/c-Fos* ODNs 90 minutes before free exploration of a novel environment; antisense = group infused with cocktail antisense *Zif268/c-Fos* ODNs 90 minutes before free exploration of a novel environment; control = unoperated home-cage control group which did not receive any infusion or behavioural training). The four bands of interest have been enclosed in dashed rectangles. Different exposure times have used in order to obtain images with a strong signal for each of the bands and to avoid saturation (which in this specific image was present for band “A”)

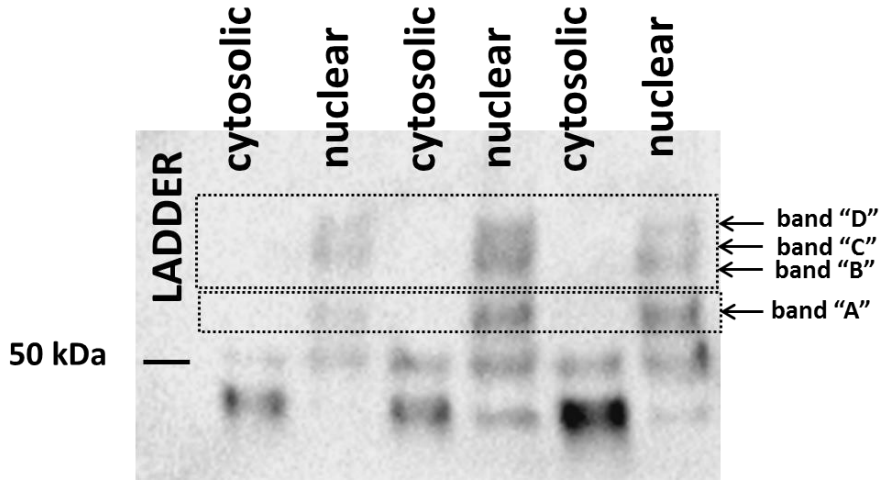

Figure 5-18. Representative blot showing staining for c-Fos protein during the optimisation of the Western blot technique (on samples from additional naïve animals). The first lane on the left was used for running the protein ladder (not visualised in this image and represented by a black horizontal line). Proteins from cytosolic or nuclear fractions of prefrontal cortex of naïve animals were run in the remaining lanes. The bands representing the putative c-Fos protein have been enclosed in dashed rectangles.

TBP has an estimated molecular weight of 38 kDa (as reported in data sheet for anti-TBP antibody ab63766, Abcam, UK) and a band at that level was clearly visible in all blots that were loaded with nuclear fractions (Figure 5-19).

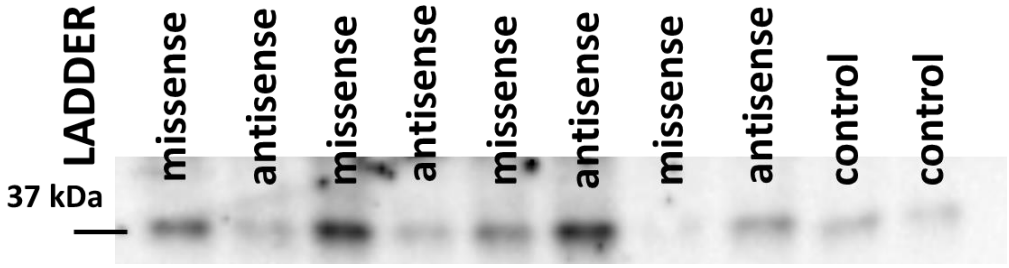

Figure 5-19. Representative blot showing staining for TBP protein (loading control) for Group 3. The first lane on the left was used for running the protein ladder (not visualised in this image and represented by a black horizontal line). Proteins from the nuclear fraction of the dorsal hippocampi of experimental animals were run in the remaining lanes (each lane has been labelled with the name of the respective experimental group: missense = group infused with cocktail missense *Zif268/c-Fos* ODNs 90 minutes before free exploration of a novel environment; antisense = group infused with cocktail antisense *Zif268/c-Fos* ODNs 90 minutes before free exploration of a novel environment; control = unoperated home-cage control group which did not receive any infusion or behavioural training).

5.3.3.2 Zif268 levels in the dorsal hippocampus after free exploration of a radial arm maze

Ninety minutes after the exploration of a novel environment (radial arm maze) there was no significant main effect of “Infusion” on band “A” ($F < 1$; Figure 5-20, left upper panel), the lowest molecular weight band analysed, in the dorsal hippocampal tissue processed with anti-Zif268 antibody. Considering the higher molecular weight bands, there was a non-significant trend in the main effect of “Infusion” ($F_{2,10} = 3.9$, $p = 0.06$) on the band “B” signal, with the antisense-infused rats showing the lowest signal (Figure 5-20, right upper panel). A significant main effect of “Infusion” was seen on band “C” ($F_{2,10} = 4.7$, $p < 0.05$; Figure 5-20, left lower panel) and band “D” ($F_{2,10} = 6.2$, $p < 0.05$; Figure 5-20, right lower panel). Post-hoc analysis revealed that for band “C”, the signal for the antisense-infused group was significantly lower than the missense-infused group ($p < 0.05$), but not the unoperated home-cage control group ($p = 0.08$). In addition, there was a significant decrease in signal in the antisense-infused group compared to both the unoperated home-cage control ($p < 0.05$) and missense-infused ($p < 0.05$) groups in the highest molecular weight band “D”.

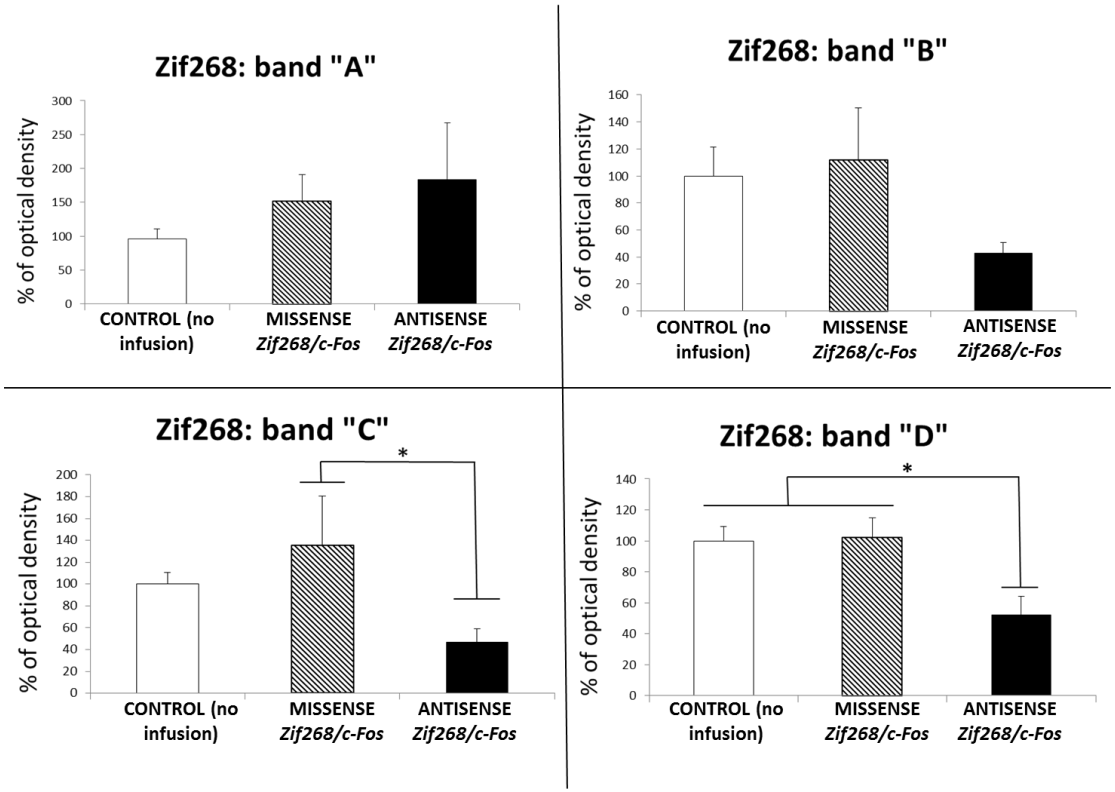

Figure 5-20. Relative signals (mean ± SEM) for band “A” (left upper panel), band “B” (right upper panel), band “C” (left lower panel) and band “D” (right lower panel) in the dorsal hippocampus after exploration of a novel context for Group 3. These bands were obtained after the tissue was processed with Zif268 antibody through Western blot technique. MISSENSE *Zif268/c-Fos* = group infused with cocktail missense *Zif268/c-Fos* ODNs 90 minutes before free exploration of a novel environment; ANTISENSE *Zif268/c-Fos* = group infused with cocktail antisense *Zif268/c-Fos* ODNs 90 minutes before free exploration of a novel environment; CONTROL = unoperated home-cage control group (no infusions or behavioural training). The signal is expressed as a percentage of optical density (OD) and represents the normalised putative Zif268 signal standardised to the OD in the control group (100%). Level of significance: * $p < 0.05$.

5.3.3.3 c-Fos levels in the dorsal hippocampus after free exploration of a radial arm maze

Ninety minutes after exploration of a novel environment (a radial arm maze) there was no significant main effect of “Infusion” on band “A” ($F_{2,15}$ = 1.0, p = 0.38; Figure 5-21, left upper panel), band “B” (F < 1; Figure 5-21, right upper panel), band “C” (F < 1; Figure 5-21, left lower panel) or band “D” (F < 1; Figure 5-21, right lower panel) in the dorsal hippocampal tissue processed with anti-c-Fos antibody.

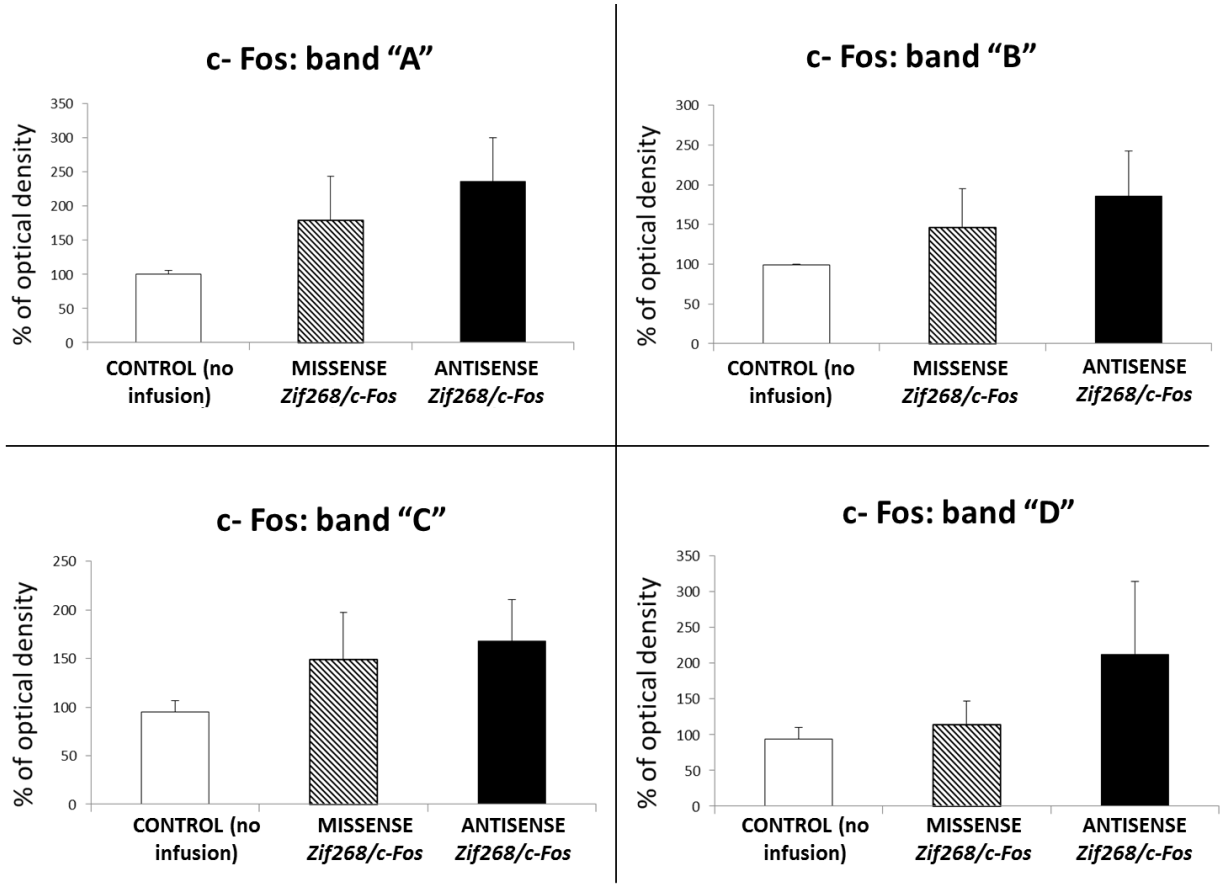

Figure 5-21. Relative signals (mean ± SEM) for band "A" (left upper panel), band "B" (right upper panel), band "C" (left lower panel) and band "D" (right lower panel) in the dorsal hippocampus after exploration of a novel context for Group 3. These bands were obtained after the tissue was processed with c-Fos antibody through Western blot technique. MISSENSE *Zif268/c-Fos* = group infused with cocktail missense *Zif268/c-Fos* ODNs 90 minutes before free exploration of a novel environment; ANTISENSE *Zif268/c-Fos* = group infused with cocktail antisense *Zif268/c-Fos* ODNs 90 minutes before free exploration of a novel environment; CONTROL = unoperated home-cage control group (no infusions or behavioural training). The signal is expressed as a percentage of optical density (OD) and represents the normalised putative c-Fos signal standardised to the OD in the control group (100%).

5.4 Discussion

As the histological analysis showed, the use of longer injectors was effective in increasing the quality for the infusion, as all the biotinylated infusate appeared spread bilaterally within the dorsal hippocampus (Group 1). Injectors of this length were then used for the subsequent two experiments.

In the second experiment (Group 2), the performance in a modified version of the radial arm maze task (with 3-hour delay and maze rotation after the first four arm choices) and in the object-in-place task was not affected by the infusion of antisense ODNs specific for either c-Fos or Zif268 or both molecules into the dorsal hippocampus. These findings are in contrast with the significant impairment observed in the radial arm maze task after infusion of muscimol, in comparison to control solution infusion.

Finally (Group 3), using the Western blot technique, it was possible to verify that the molecular levels of proteins recognised by the anti-c-Fos antibody were not affected by the infusion into the dorsal hippocampus of an antisense ODN cocktail targeting both *c-Fos* and *Zif268* transcripts. Conversely, the signal associated with two protein bands recognised by the anti-Zif268 antibody was decreased after the infusion of the antisense ODN cocktail, in comparison to control levels.

The infusion of antisense ODNs targeting either *c-Fos* or *Zif268* transcripts (individually and combined) was not effective in impairing the performance of the animals on two tasks taxing spatial memory, a modified version of the radial arm maze task (Figure 5-10 and Figure 5-11) and the object-in-place task (Figure 5-14). In contrast, muscimol infusions produced a marked impairment on radial-arm maze performance. The null results following antisense ODN infusions could not be attributed to the misplacement of the cannulae as histological analysis showed them to be well-placed within the dorsal hippocampus. Furthermore, the biotinylated antisense *Zif268* ODN infusion results (Group 1; Figure 5-7) showed that the use of longer infusion microinjectors ensured a complete coverage of the dorsal hippocampi by the infusate. These longer microinjectors were, therefore, used for the infusions of animals in Groups 2 and 3. The contrasting results between antisense ODN infusions and muscimol infusions in the animals in Group 2 would also argue against the null result arising from technical issues relating to surgery or infusion procedures.

The lack of effect of antisense ODN infusions on performance of the modified radial arm maze task are in contrast with the outcome of an earlier study by He et al. (2002).

In that study, infusion of the same sequence antisense *c-Fos* ODNs into the dorsal hippocampus impaired performance on a different version of the radial arm maze task. However, there are differences between the two experiments which may account for the different results. One major difference is the time of infusion of the antisense *c-Fos* ODNs. In the present experiment it was administered 90 minutes before the beginning of the task, while in the He et al. (2002) study it was infused 10-12 hours before the task. In the literature, experiments that have assessed the behavioural effects of antisense *c-Fos* ODN infusion have administered it at two main time points: either 10-12 hours before behavioural testing (Countryman et al., 2005; Hooper et al., 1994; Lamprecht & Dudai, 1996), or about 1-2 hours before testing (Hebb & Robertson, 1997; Seoane et al., 2012; Tolliver et al., 2000). Interestingly, two studies administered the infusion at both time points in order to obtain the maximal impact on the behavioural performance (Grimm et al., 1997; Kemp et al., 2013). The time-window of action of the antisense *c-Fos* ODNs, therefore, appears to be comprised between 1-12 hours post-infusion, and it could be the case that infusing the antisense ODNs at two separate time points could increase the probability of detecting a behavioural effect. To test this, the experiment could be repeated with two infusions, the first 10-12 hours and the second 1-2 hours before the beginning of the task. The efficacy of antisense *Zif268* ODNs in influencing behaviour, instead, has been reported at 90-120 minutes post-infusion (Hebb & Robertson, 1997; Lee et al., 2004; Malkani et al., 2004) which is consistent with the infusion time used in the present experiment.

Another important difference with the experiment run by He et al. (2002) is the version of radial arm maze task employed. They used the reference/working memory version of the radial arm maze task, in which only four arms are constantly baited with the food reward, and the post-infusion test session consisted of 20 consecutive trials of the task, lasting for about 2 hours (while in the experiment presented here one post-infusion session overlapped with one unique trial with a long time delay in the middle). It could be that the higher spatial working memory load caused by the task administered by He et al. (2002) made the animals more sensitive to *c-fos* expression disruption. Furthermore, their study showed that even if the animals infused with the antisense *c-Fos* ODNs made more errors in comparison to the animals infused with a control solution, however, both groups' performance improved over the test session. Thus spatial memory learning was not completely abolished by blocking the expression of *c-fos* in the dorsal hippocampus. It could be that other molecular

mechanisms implicated in spatial memory could overlap those triggered by *c-fos* expression, thus limiting the effects of its loss.

Finally, the modified radial arm maze task employed in the present experiment required a very long training period (about one month), while in the study by He et al. (2002) animals underwent spatial memory testing after the infusion without having any previous training. In the same study they also trained a second group of animals on the reference/working memory variant of the radial arm maze task for five days (five trials/day); immunohistochemical analysis of the rats' brains showed c-Fos protein levels in the dorsal CA3 subfield peaked on the third day of training. The levels on the third day were higher than either the first or the final days of testing. This could indicate that levels of *c-fos* expression are affected by continuous training on the same behavioural task, and after an initial increase while the task is still relatively new for the animal, c-Fos levels gradually decrease when the task becomes familiar. The association between novelty and *c-fos* expression levels increase has been shown in many experiments (Hess et al., 1995; Jenkins, Dias, Amin, Brown, et al., 2002; VanElzakker et al., 2008; Vann, Brown, & Aggleton, 2000; Vann, Brown, Erichsen, et al., 2000a; Wan, Aggleton, & Brown, 1999; Zhu, Brown, McCabe, & Aggleton, 1995; Zhu et al., 1997). Similar issues with over-training could also apply to *zif268* expression. Poirier et al., examined Zif268 levels as animals acquired a reference/working memory task in the radial arm maze and found an effect of training on the protein levels (Poirier, Amin, et al., 2008). The amount of training influenced Zif268 levels in the dorsal dentate gyrus, CA1 and CA3; Zif268 levels in the dentate gyrus correlated with task performance only in animals with a limited amount of training, while for animals that had undergone more training, Zif268 levels in CA1 and CA3 became more relevant in predicting the performance.

To remove the possible confounding effect of over-training on *zif268* and *c-fos* expression from the experiment, the animals in Group 2 were tested on a second behavioural task, the object-in-place task. This task also taxes spatial memory and is dependent on the dorsal hippocampus, but has the benefit of not requiring any training. The overall structure of the protocol used was very similar to that employed for the modified radial arm maze task (since both tasks were divided into a sample phase which required spatial memory consolidation in order to perform in a test phase, and the two phases were separated by a 3-hour delay). No studies so far have investigated the expression of *zif268* and *c-fos* in the bran elicited by this particular behavioural task. However, increased c-*fos* and *zif268* expression in the dentate

gyrus has been reported following similar behavioural tasks that also rely an animals forming associations between objects and locations (Barbosa et al., 2013; Soulé et al., 2008). An object-in-place task with a 3-hour delay interposed between the sample and the test phase has been used in a recent study (Seoane et al., 2012), with the infusion of antisense *c-Fos* ODNs into the perirhinal cortex 1 hour before the sample phase of the task; they showed a significant impairment in performance in the test phase 3 hours later.

In contrast, in the present experiment no difference was found between the discrimination ratios of the animals infused with either the antisense or the missense *Zif268/c-Fos* ODN cocktail. However, at no point the animals were able to successfully discriminate between the displaced and non-displaced objects. The finding that the animals could not discriminate the displaced objects, even after a control infusion (the missense cocktail), makes the null effects more difficult to interpret. One possible explanation for this poor performance is that by the time the animals were tested on the control session of the object-in-place task they had received eight bilateral infusions into the dorsal hippocampus. These infusions may have caused cumulative physical damage to the hippocampal tissue, effectively resulting in a hippocampal "lesion". Chiasson et al. (1994) showed that repeated ODN infusions into the amygdala caused neurotoxicity in the infused area, but increasing the interval between one infusion and the next reduced this effect. Despite an inter-infusion delay of at least 24 hours in this experiment, it is possible that some neurotoxic damage to the dorsal hippocampus occurred and that this time interval was not sufficiently long. Finally, it should be noted that the infusions were not counterbalanced between the two sessions since all animals were infused with cocktail antisense *Zif268/c-Fos* ODN before the first session and with cocktail missense *Zif268/c-Fos* ODN before the second session. This constitutes a further confound in the experiment as it makes difficult to disentangle a possible effect of infusion (cocktail antisense versus cocktail missense) from any impact of the session order on the results.

The Western blot analysis after infusion of the cocktail ODNs (Group 3) showed a significant decrease in Zif268 levels in two of the bands detected by the anti-Zif268 antibody in the novelty-exposed animals infused with the cocktail antisense *Zif268/c-Fos* ODNs compared to animals infused with the cocktail missense *Zif268/c-Fos* ODNs (bands "C" and "D", Figure 5-20). This is consistent with another experiment that showed that the same antisense ODN sequence caused a decrease in the levels

of Zif268 in the hippocampus associated with contextual fear learning (Lee et al., 2004) .

In contrast, no significant differences were found in novelty-induced c-Fos levels in any associated band comparing them after the infusion of the antisense or the missense ODN cocktail (Figure 5-21). These results differ to those from previous studies that detected a decrease in the levels of c-Fos (Hebb & Robertson, 1997; Kemp et al., 2013) using the Western blot technique in animals infused (either in the dorsal hippocampus or in the striatum) with antisense *c-Fos* ODNs in comparison to animals infused with the missense sequence.

One potential issue with the present study was that the antibodies used were not highly specific as multiple bands were detected on the Western blots. It is possible that the antibodies used were able to either pick up other proteins non specifically and/or Zif268 and c-Fos with post-translational modifications. As no band exactly matched with the expected molecular weight of Zif268 and c-Fos, more bands were taken into consideration for the analysis of *zif268* and *c-fos* expression levels. We focused the analysis on those bands whose molecular weight was similar to the expected molecular weight (about 75 kDa for Zif268; Lonergan et al., 2010) and 56 kDa for c-Fos (Herrera & Robertson, 1996)] and which in the optimisation phase (that assured that cytosolic and nuclear protein fractions were separated by the extraction protocol) gave a strong signal in the nuclear protein fraction (Figure 5-16 and Figure 5-18). These bands could represent modified versions of the protein of interest.

Post-translational modifications can increase the molecular weight of the protein of interest by adding functional groups to the aminoacidic side chains or to the N- or C-termini of the protein. For example, both Zif268 and c-Fos can be phosphorylated (Curran et al., 1984; Sambucetti, Schaber, Kramer, Crowl, & Curran, 1986; Veyrac, Besnard, Caboche, Davis, & Laroche, 2014), and Zif268 can also be glycosylated (Veyrac et al., 2014). It is also possible that detecting higher molecular weight bands than expected could be due to the inefficiency of the denaturing protocol in releasing the protein of interest from a protein complex. This could be the case for c-Fos, because when expressed it forms a non-covalent heterodimer with Jun (a 39 kDa nuclear protein), forming the functional AP-1 transcription factor complex which binds to the DNA to regulate the transcription of other genes (Herrera & Robertson, 1996). However, given the individual molecular weights of the two proteins, the AP-1 complex should be around 100 kDa and all the bands analysed for c-Fos were smaller than

this size (Figure 5-17). The proteins of interest could also appear with a smaller molecular weight than expected because they have been subjected to degradation during the extraction process and this could be the case for band “A” detected by the anti-Zif268 antibody (Figure 5-15). It is also well known that the presence of several c-Fos related antigens (FRAs) can give rise to cross-reactions in blots immuno-stained with anti-c-Fos antibodies, as they present epitopes similar to those of c-Fos protein (Herrera & Robertson, 1996). Moreover, their molecular weight is very close to 56 kDa, and their expression can be induced by the same kind of stimuli that trigger c-Fos expression (Sharp, Hisanaga, Sagar, Hicks, & Lowenstein, 1991; Sonnenberg et al., 1989). Thus, it is a possibility that the bands detected on the blot stained with c-Fos antibody did not represent c-Fos protein but these FRAs, and for this reason it was not possible to visualise any change in expression levels because the antisense *c-Fos* ODNs were specifically targeting *c-Fos* transcript sequence.

Significantly lower signals were found in two of the bands recognised by the anti-Zif268 antibody (bands “C” and “D”, Figure 5-20) following infusion of the antisense ODN cocktail compared to the missense ODN cocktail. A previous analysis for the optimisation of the nuclear fraction extraction protocol showed that these bands were present in both the nuclear and the cytosolic fractions extracted from the dorsal hippocampus of naïve animals (Figure 5-16). As Zif268 is a protein which translocates into the nucleus after its translation in the cytoplasm, the bands recognised by the anti-Zif268 antibody could represent proteins other than Zif268. It is unlikely that the nuclear extraction protocol was not optimal because the nuclear protein TBP was higly enriched in the nuclear versus cytosolic fractions (Figure 5-6).

As there was ambiguity regarding the identity of the bands in the present experiment, further investigation would be needed to fully understand the effects of of the antisense ODN infusions at the molecular level. This could involve using different antibodies able to recognise different epitopes on Zif268 and on c-Fos, and/or able to discriminate among the possible different post-translational modification of the proteins.

Another critical point for the Western blot experiment is the lack of a difference in Zif268 and c-Fos levels in the dorsal hippocampus when the levels obtained in the group infused with the missense ODN cocktail were compared to those obtained in the unoperated home-cage control group (Figure 5-20 and Figure 5-21). Higher levels of both proteins were expected in the missense-infused group because the animals

freely explored a novel environment for 20 minutes. This behavioural procedure was chosen as novel environment exploration has been confirmed to increase the levels of both Zif268 (Gheidi et al., 2013; Hall et al., 2000) and c-Fos (Hess et al., 1995; Jenkins, Dias, Amin, Brown, et al., 2002; Zhu et al., 1997) in the dorsal hippocampus. However, it is possible that this task was not sufficiently demanding to allow a significant rise of the expression levels of these two immediate early genes. Consequently, this would also make it harder to detect a difference between the Zif268 and c-Fos protein levels when the animals were infused with the antisense ODNs. Another behavioural task with higher spatial memory demands could be used in future studies in order to produces higher expression levels of Zif268 and c-Fos. For example, consecutive trials of the standard working memory version of the radial arm maze task could be administered over 30 minutes, as in previous studies (Jenkins, Amin, Brown, & Aggleton, 2006; Vann, Brown, Erichsen, & Aggleton, 2000; Vann, Brown, & Aggleton, 2000). It is also important to note that some studies have reported a preferential increase in Zif268 an c-Fos expression levels associated with the exploration of a novel environment in specific subfields of the dorsal hippocampus: CA1 (Hess et al., 1995; VanElzakker et al., 2008) for both Zif268 and c-Fos, and dentate gyrus for Zif268 (Gheidi et al., 2013). Another study (Wan et al., 1999) investigated the expression of c-Fos when animals were presented with novel configurations of visual stimuli compared to familiar configurations and found a different pattern across the three hippocampal subfields: an increase in CA1, no change in CA3 and a decrease in the dentate gyrus. In the experiment reported in this Chapter, nuclear proteins were extracted from the whole dorsal hippocampi. Thus, a consistent increase/decrease in signal of Zif268 and c-Fos levels within a specific subfield could remain undetected because there could be a decrease in the signal-to-noise ratio or it could be obscured by changes in expression in the opposite direction in other subfields. An analysis where the different hippocampal subfields were assessed separately would increase the chance of uncovering any effects.

In conclusion, the experiments presented in this Chapter showed that infusion of antisense ODNs targeting *Zif268* and *c-Fos* transcripts into the dorsal hippocampus did not impair animals' performance on two spatial memory tasks. In contrast, muscimol infusions produced marked impairments on the radial arm maze task, confirming the efficacy of the surgery and of the infusion technique and the sensitivity of the task to hippocampal disruption. The variant of the radial arm maze task we used required a very long behavioural training period which could have affected the levels of the immediate early genes expressed during the task, due to experience-induced

compensatory mechanisms. For this reason, the object-in-place task (which does not require any training) was subsequently employed as an alternative to test animals' spatial memory after infusions of cocktail antisense *Zif268/c-Fos* ODNs. However, the object-in-place task was also insensitive to disruption by intrahippocampal antisense infusion. While these results indicate that there is no causal role for hippocampal Zif268 or c-Fos in spatial learning, we have identified a number of experimental caveats that weaken this interpretation and further experiments would need to be performed to optimise the behavoral and molecular assays. These include:

(i) Determining the optimal time to administer the antisense ODNs by measuring the peak expression of Zif268 and c-Fos in each task.

(ii) Investigating whether the impairment in the object-in-place task after cocktail missense infusions could be related to the toxic effect of repeated ODN infusions into the dorsal hippocampus. If so, it will be necessary to limit the number of total infusions in future experiments. Furthermore, the cocktail ODN missense and antisense infusions were not balanced during the two sessions of the object-in-place task, complicating the interpretation of the results; a balanced experimental design would be more appropriate to be used in any future experiments.

(iii) Determine the specificity of the antibodies to detect the genes of interest using a range of antibodies in Western blotting experiments. This would resolve whether changes in hippocampal Zif268 an c-Fos were associated with the spatial tasks and the efficacy of the ODN sequences to reduce their levels.

Chapter 6 Muscimol and antisense *Zif268* oligodeoxynucleotide infusions into the retrosplenial cortex

6.1 Introduction

The experiments in Chapter 5 showed that the infusion of antisense oligodeoxynucleotides (ODNs) targeting *Zif268* and *c-Fos* transcripts into the dorsal hippocampus of rats did not have any impact on the performance on two spatial memory tasks. While the reasons for this null effect are currently inconclusive, it is possible that blocking the increase of the expression levels of those immediate early genes in the dorsal hippocampus is not detrimental for some spatial memory tasks.

This chapter focuses on another brain area, the retrosplenial cortex, which is anatomically connected to the hippocampus (Wyss & Van Groen, 1992) and also supports spatial memory (Vann et al., 2009). Immediate early gene imaging studies have shown that both *zif268* and *c-fos* are highly expressed in this structure when rats are engaged in spatial memory tasks (He et al., 2002; Pothuizen et al., 2009; Vann, Brown, & Aggleton, 2000). Furthermore, the retrosplenial cortex shows the most dramatic decrease in *zif268* and *c-fos* expression when other structures within the Papez circuit are lesioned; these structures include the anterior thalamic nuclei (Dumont et al., 2012; Jenkins, Dias, Amin, & Aggleton, 2002; Jenkins, Dias, Amin, Brown, et al., 2002; Jenkins et al., 2004; Poirier & Aggleton, 2009; Poirier, Shires, et al., 2008), the mammillothalamic tract (Vann & Albasser, 2009) and the hippocampus (Albasser et al., 2007). This loss of immediate early gene expression has been shown to be persistent over time, with changes found up to 10 months after the lesion (Jenkins et al., 2004). It is possible that these lesion-induced changes to immediate early gene expression disrupt the normal functioning of the retrosplenial cortex and, therefore, contribute to the observed spatial memory deficits that follow lesions of the other structures within the Papez circuit (Aggleton et al., 1996, 1986; Sziklas & Petrides, 2002; Vann & Aggleton, 2003).

We tested this hypothesis by infusing antisense *Zif268* ODNs into the retrosplenial cortex before testing rats on the object-in-place task. The object-in-place task was chosen as it does not require any training (the animals just need to be habituated to

the bow-tie maze), and lesions of the retrosplenial cortex disrupt animals' performance on this task (Vann & Aggleton, 2002). As in Chapter 5, a 3-hour delay was inserted between the sample and test phase of the task to make it suitable for studying the effect on antisense ODN infusions.]

This variant of the object-in-place task was used again in the following experiments, even though it did not give any positive results in the previous Chapter 5. In the experiment with the object-in-place task reported in Chapter 5 it was not possible to conclude if the poor performance of the animals infused with the control solution was due to dorsal hippocampal damage or to some other factors. It does not appear to be the case that the behavioural task was the issue, thus I decided to use it again for the retrosplenial infusion experiments, as it allows the expression of Zif268 protein during the delay between the sample and the test phase, and it does not require a long period of training.

Before testing the effect of antisense *Zif268* ODN infusions, a separate group of animals (Group 1) was tested with muscimol infusions into the retrosplenial cortex. There were a number of reasons for this experiment. It was important to test the efficacy of the surgery, which required two pairs of cannulae implanted into each brain to target both the rostral and the caudal portions of the retrosplenial cortex. Secondly, object-in-place deficits have only ever been reported in chronically lesioned rats (Vann & Aggleton, 2002), so it was necessary to determine whether similar effects were observed when this region was temporarily disrupted. Finally, the previously reported retrosplenial cortex lesion impairments were found with a delay of 15 minutes inserted between the sample and the test phase, so again it was important to be sure the longer delay produced similar results. Rats were infused with either muscimol or a control solution (phosphate buffer saline) and the infusions were counterbalanced across two consecutive object-in-place sessions (Figure 6-1). As in Chapter 5, the infusions were made 30 minutes before the sample phase of the task.

We decided to infuse only the antisense ODNs targeting *Zif268* and not *c-Fos* on the basis of the results obtained in the Western blot experiment carried out in Chapter 5. In that experiment, the infusion of the cocktail antisense *Zif268/c-Fos* ODNs (targeting the transcripts of both immediate early genes) into the dorsal hippocampus was associated with a significant decrease (in comparison to naïve home-cage control levels and to the levels obtained after cocktail missense infusion) only in the signal of two protein bands recognised by the anti-Zif268 antibody. No significant change was observed for the protein bands recognised by the anti-c-Fos antibody. Even if, as

discussed in Chapter 5, those results cannot be considered conclusive, they gave a suggestion that the antisense ODNs might be effective in disrupting *Zif268* but not *c-Fos* translation. For this reason we decided to only infuse the antisense *Zif268* ODNs into the retrosplenial cortex in a second group of animals (Group 2).

The effects of infusing the antisense *Zif268* ODNs into the retrosplenial cortex were also investigated at the molecular level, using an immunohistochemistry protocol for visualising Zif268-positive nuclei in the brain. Following behavioural testing on the object-in-place task, rats in Group 2 were again infused with either antisense or missense *Zif268* ODNs before freely exploring a radial arm maze in a novel room (exploring a novel environment has been shown to increase Zif268 levels in the brain; e.g. Gheidi et al., 2013; Hall et al., 2000). Additional unoperated control rats were also used for the immunohistochemical analysis. One group was processed directly from the home-cage whereas a second group performed the same radial-arm maze task as the cannulated animals. With these additional control groups it was possible not only to make comparisons between the effects of antisense and missense infusion but also to assess whether the infusions/cannulations altered expression levels compared to unoperated animals and whether any levels differed from baseline (Figure 6-2).

Finally, in order to visualise the spread of infusate within the retrosplenial cortex and so help with the interpretation of the behavioural data, two behaviourally naïve rats were infused with biotinylated antisense *Zif268* ODNs 90 minutes before perfusion (Group 3).

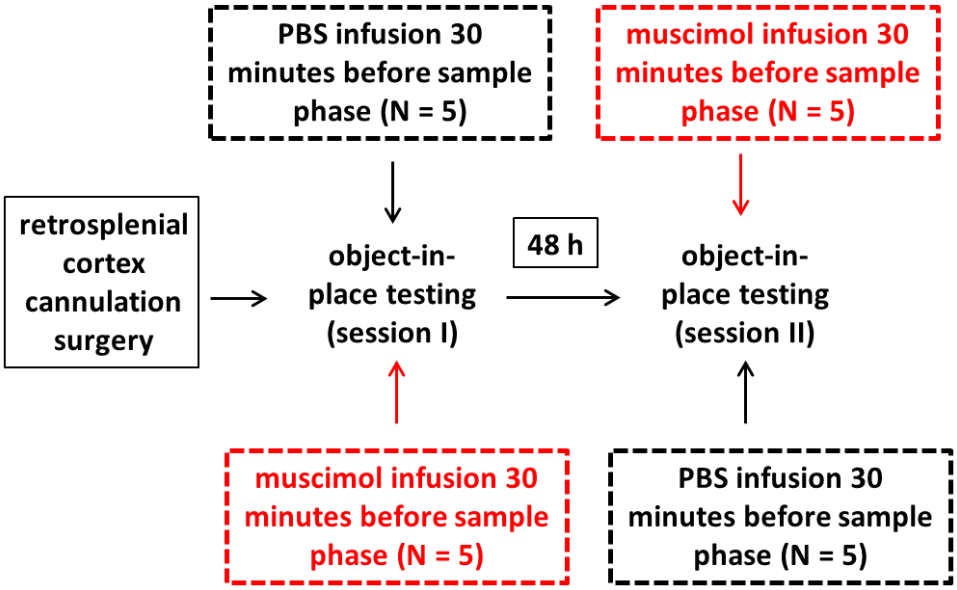

Figure 6-1. Schematic behavioural protocol for Group 1. Half of the animals were infused with PBS in session I and with muscimol in session II; for the other half the infusion order was inverted. In all cases, the volume of the infusate was 0.2 µl/infusion site.

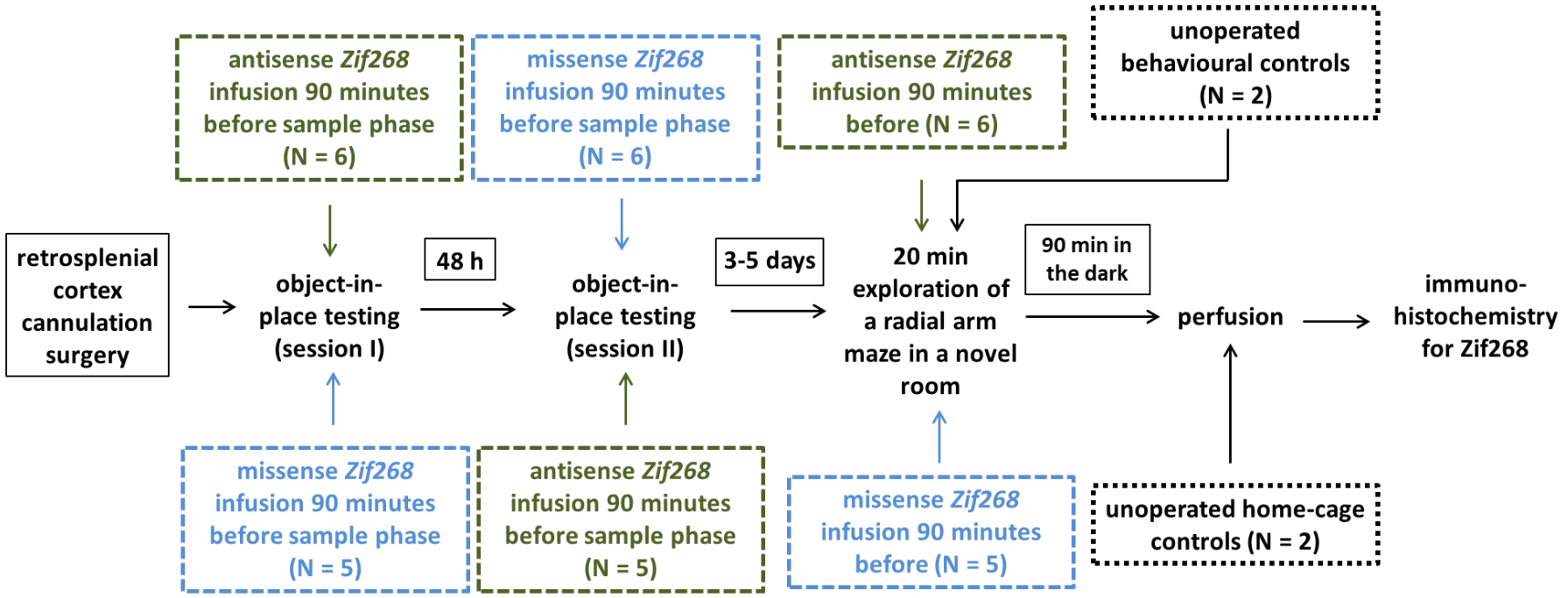

Figure 6-2. Schematic protocol for Group 2. Antisense *Zif268* ODN and missense *Zif268* ODN infusions were 1 µl/infusion site. After all infusions, the cannulated animals were left 90 minutes in their home cages in the holding room. After the free radial arm maze exploration in a novel room (last behavioural procedure), the animals (the unoperated behavioural controls and the animals infused with either missense or antisense *Zif268* ODNs) were left for 90 minutes in a dark and quiet room before perfusion. Unoperated home-cage animals were perfused directly from the home-cage.

6.2 Methods

6.2.1 Subjects

Subjects in Group 1 were 10 male naïve Lister Hooded rats (Charles River, UK), weighing 222–262 g at the time of surgery. These rats were part of a separate behavioural study and after undergoing cannulation surgery the rats were tested on T-maze alternation (Nelson et al., 2015) prior to taking part in the behavioural experiments described below.

Subjects in Group 2 were 15 male naïve Lister Hooded rats (Charles River, UK). Eleven of these rats received surgery (weight 285-311 g) prior to behavioural testing. The remaining four animals in Group 2 acted as unoperated controls for immunohistochemical analysis; two of them were the “unoperated behavioural” controls and they underwent part of the same behavioural procedure as the cannulated animals in the same group (free exploration of a radial arm maze in a novel room); the other two were the “unoperated home-cage” controls and did not undergo either surgery or any behavioural procedure (Figure 6-2).

Subjects in Group 3 were two male naïve Lister Hooded rats (Charles River, UK), weighing 268 and 311 g at the time of surgery; these animals were used for visualisation of biotinylated antisense *Zif268* ODN diffusion into the retrosplenial cortex.

All rats were initially housed in pairs under diurnal light conditions (14 h light/10 h dark). The animals that underwent surgery were housed individually after the operation, due to the implanted cannulae. Water was freely available for the course of the experiment. Animals that underwent behavioural testing were food deprived to not below 85 % of their free feeding weight for the duration of the behavioural test. For the remaining animals, food was available *ad libitum* throughout. All animals were thoroughly handled before the study began in order to habituate them to the handling procedure. All behavioural testing was carried out in the light phase. The experiment was carried out in accordance with UK Animals (Scientific Procedures) Act, 1986 and associated guidelines.

6.2.2 Behavioural procedure

Group 1 and Group 2

6.2.2.1 Object-in-place task

Apparatus

Rats in Group 1 and eleven of the rats in Group 2 were tested in a 'bowtie' maze, which was in the shape of a bowtie with wooden floor and walls. The apparatus was identical to that described in Chapter 5 (Section 5.2.2.2).

Post-surgery behavioural procedure

The post-surgery training procedure was identical to that described in Chapter 5 (Section 5.2.2.2).

Group 2

6.2.2.2 Free exploration of a radial arm maze

Apparatus

The apparatus was identical to that described in Chapter 4 (Section 4.2.1.2)

Post-surgery behavioural procedure

The two unoperated behavioural controls and the eleven cannulated rats in Group 2 were allowed to freely explore a radial ram maze located in a novel room for a 20 minute period. For the cannulated rats, this radial-arm maze session was carried out between 3 and 5 days after the completion of the object-in-place task. Six of the cannulated animals received antisense *Zif268* ODN infusions, while the remaining five received missense *Zif268* ODN infusions before the beginning of the behavioural procedure (Figure 6-2). Animals underwent the behavioural procedure on 1 of 2 days in order to be able to perfuse them at similar times of the day (Table 6-1).

The behavioural procedure was identical to the one described in Chapter 5 (Section 5.2.2.3).

DAY 1	DAY 2
antisense (n = 3)	missense (n = 3)
missense (n = 2)	antisense (n = 3)
unoperated behavioural control (n = 2)	unoperated behavioural control (n = 2)

Table 6-1. The animals in Group 2 which underwent the free exploration of a radial arm maze in a novel room were processed across 2 consecutive days. “antisense” = group infused with the antisense *Zif268* ODNs (six animals in total); “missense” = group infused with the missense *Zif268* ODNs (five animals in total); “unoperated behavioural control” = unoperated control group which underwent the same free exploration of the radial arm maze as the cannulated animals (two animals in total).

6.2.3 Surgical procedure

The surgeries for the experiments reported in this chapter were carried out by Dr A. J. D. Nelson and Dr A. Powell.

All animals in Groups 1 and 3 and 11 animals in Group 2 underwent surgery.

Each animal was deeply anaesthetised with 4% isofluorane (Teva UK Limited) in O_2 in a transparent Plexiglas induction chamber; once anaesthetised, the rat was placed in a stereotaxic frame (David Kopf Instruments, Tujunga, CA) with a specialised mask for continuous anaesthetic flow (1-2 % isofluorane in O_2). The position of the incisor bar of the stereotaxic frame was set at -3.3 mm below the intra-aural line, to maintain the skull flat on the horizontal plane. The incision site was sterilised with surgical scrub (Videne, Ecolab, UK). A midline incision was made on the top of the scalp to expose the dorsal skull. Lidocaine (2% w/v, B. Braun, Germany) was topically applied to the skin to act as a local anaesthetic. Bregma was identified, and antero-posterior coordinates were taken for the implantation of two bilateral guide cannulae (PlasticsOne, Virginia, United States): one targeting the rostral (−2.5 mm posterior to bregma) and the other targeting the caudal (-6.0 mm posterior to bregma) portion of the retrosplenial cortex. The medio-lateral coordinates (±0.7 mm for the anterior cannulae; ±1.0 mm for the posterior cannulae) were taken from the central sinus,

which was revealed by removing a small flap of bone at about −2.5 mm from bregma. The anterior bilateral guide cannulae were 26 gauge, 1.4 mm centre-to-centre, cut to 1.5 mm below the plastic supporting pedestal, while the posterior bilateral guide cannulae were 26 gauge, 2 mm centre-to-centre, cut to 1.7 mm below the plastic support pedestal. Six bone micro screws (Bilaney, United Kingdom) were fitted into six small burr holes in the skull that were made using a handheld drill (Bilaney, United Kingdom), three in each parietal skull plate. The guide cannulae were lowered such that the plastic pedestal rested on the skull surface and was adhered to the skull and to the six bone screws using dental acrylic cement (Kemdent, United Kingdom). Four stainless steel stylets (PlasticsOne, Virginia, United States) were inserted to maintain cannula patency during recovery and prevent infection. To reduce post-operative pain, all animals received a subcutaneous injection of 0.03 ml Metacam (5 mg/ml; Boehringer Ingelheim, Berkshire, UK) before the end of the surgery. On completion of surgery, the skin was loosely sutured around the cannulae and antibiotic powder (Clindamycin Hydrochloride; Pharmacia, Sandwich, United Kingdom) was topically applied on the wound site. Finally, animals received subcutaneous injections of 5 ml glucose saline and were placed in a temperature-controlled recovery box until they awoke from surgery. Rats were allowed to recover for at least 7 days before any further procedures, and during this time their recovery was carefully monitored and their weights checked daily.

6.2.4 Infusions

The infusions for the experiments reported in this chapter were performed by Dr A. J. D. Nelson and Dr A. Powell.

Each rat was gently wrapped in a soft towel whilst awake and the stylets were manually removed before two bilateral microinjectors (33 gauge, either 1.4 mm or 2 mm centre-to-centre, 1.5 mm projection beyond the tip of the guide cannulae; PlasticsOne, Virginia United States) were inserted slowly into the two bilateral guide cannulae surgically implanted into the rostral and caudal portions of the retrosplenial cortex. Each bilateral microinjector was connected via polyethylene tubings (Bilaney, Kent, UK) to two 5 µl Hamilton syringes (Bonaduz, Switzerland) mounted on two infusions pumps (Harvard Apparatus Ltd, Kent, UK), allowing the simultaneous infusion of the rostral and caudal portions of the retrosplenial cortex. At the end of each infusion, the microinjectors were kept in place inside the brain for another minute

to allow any solution to diffuse away from the microinjector tip. The microinjectors were then gently removed and the stylets replaced.

To habituate the rats to the infusion procedure and to test cannula patency, they received an infusion of sterile phosphate buffered saline (PBS, 0.1 M pH 7.4; Group 1: 0.2 µl/infusion site at a rate of 0.2 µl/minute; Groups 2 and 3: 1 µl/infusion site at a rate of 0.167 µl/minute) into both the rostral and the caudal portions of the retrosplenial cortex at least 1 day before any further infusion.

For the first object-in-place testing session (Session I), five of the animals in Group 1 were infused into the retrosplenial cortex with PBS solution and the other five with muscimol solution (diluted in sterile PBS at a concentration of 1 µg/µl; M1523, Sigma-Aldrich, UK). For the second object-in-place testing session (Session II), the infusion groups were swapped, so the animals previously infused with PBS were now infused with muscimol and vice versa (Figure 6-1). In all cases, a volume of 0.2 µl/infusion site of infusate was infused at a rate of 0.2 µl/minute, administered 30 minutes before the sample phase of each object-in-place task session. Two days were interposed between the first and second sessions, to be sure that the infusate was completely cleared from the infused area and to minimise any possible memory interference of the first test session on the second test session.

PAGE-purified phosphorothioate end-capped 18-mer ODNs (Sigma-Genosys, Sigma-Aldrich, UK) were re-suspended in sterile PBS. Their sequences were designed based on previous studies: antisense *Zif268* ODN, 5'-GGT AGT TGT CCA TGG TGG-3' (concentration 1 nmol/µl) and missense *Zif268* ODN, 5'-GTG TTC GGT AGG GTG TCA-3' (concentration 1 nmol/µl) (Lee et al., 2004). Both antisense and missense *Zif268* ODN sequences were subjected to a BLAST search on the National Center for Biotechnology Information BLAST server using the Genbank database. The antisense sequence had positive matches only for its target *Zif268* mRNA sequence, and no other rat or human coding sequences. The control missense sequence did not generate any full matches to identified gene sequences in the database

For the first object-in-place testing session (Session I) of the cannulated animals in Group 2, five rats received missense *Zif268* ODN infusions into the retrosplenial cortex, while the remaining six rats were infused with the antisense *Zif268* ODN solution. For the second object-in-place testing session (Session II) the infusion groups were swapped, so the animals previously infused with missense *Zif268* ODN were now infused with antisense *Zif268* ODN and vice versa. For the free exploration

of the radial arm maze the groups reverted back to receiving the initial infusate (Figure 6-2). In all cases, a volume of 1 µl/infusion site of infusate was infused at a rate of 0.167 µl/minute, administered 90 minutes before each behavioural procedure. As before, at least two days were interposed between one behavioural session and the next, in order to be sure that the infusate was completely cleared out from the infused area and to minimise any possible memory interference of the first test session on the second test session of the object-in-place task.

The two animals in Group 3 were infused with 1 µl/infusion site of biotinylated antisense *Zif268* ODNs (1 nmol/µl; Sigma-Genosys, Sigma-Aldrich, UK) at the rate of 0.167 µl/min, administered 90 minutes before perfusion.

6.2.5 Histology

6.2.5.1 Cannulae placement verified through Nissl staining (Group 1)

For animals in Group 1, cannulae placement was verified through Nissl staining. On completion of the experiment, the animals were irreversibly anaesthetised with sodium pentobarbital (60 mg/kg, Euthatal, Rhone Merieux, Harlow, UK) and perfused transcardially with 0.1 M PBS followed by 10% formol-saline. The brains were removed and post-fixed in 10% formol-saline for 4 hours and then transferred to 25% sucrose (in 0.1M PBS) overnight. Sections were cut at 40 µm on a freezing microtome in the coronal plane, and a one-in-three series of sections was mounted onto gelatin-coated slides and stained with cresyl violet, a Nissl stain before being cover-slipped (DPX, Thermoscientific, UK).

6.2.5.2 Zif268-positive cells immunohistochemistry and Nissl staining for cannulae placement verification (Group 2)

Immunohistochemical analysis was performed for all the animals in Group 2. The rats that underwent the behavioural procedure (the eleven cannulated rats and the two unoperated behavioural controls) were anaesthetised with sodium pentobarbital (60 mg/kg, Euthatal, Rhone Merieux, UK) 90 minutes after the completion of the free exploration of the radial arm maze task; the two unoperated home-cage controls were irreversibly anaesthetised directly from the home-cage. Rats were processed in 2 consecutive days, in order to be able to perfuse them at similar times of the day.

After anaesthesia induction, all animals were transcardially perfused with 0.1 M phosphate buffer saline (PBS) followed by 4% paraformaldehyde in PBS (PFA). The

brains were then extracted and postfixed in 4% PFA for four hours, and then transferred to 25% sucrose in distilled water overnight. On the following day, brains were cut in the coronal plane using a freezing microtome (40 µm slice thickness), and two series (1:3) of sections were collected: one series were collected in PBS for Zif268 staining, the other was mounted directly onto gelatin-coated slides and stained using cresyl violet, a Nissl stain, for verification of the cannulae placement.

For Zif28 staining, sections were processed in five batches, with three subjects per batch. One batch was composed of two antisense-infused cases and one missense-infused case; the remaining four were composed by one missense-infused case, one antisense-infused case and one unoperated control (either behavioural or home-cage) case. The sections were incubated for 10 minutes on a shaker in a solution of 0.3% hydrogen peroxidase (Fisher Scientific, US) in PBST (0.2% Triton in PBS), in order to block endogenous peroxidase activity. Then they were washed four times (10 minutes each) with PBST. Next, sections were incubated with primary anti-Zif268 antibody (Egr-1 (C19): Sc-189; Santa Cruz Biotechnology, Texas, US) diluted 1:3000 in PBST; they were stirred on the shaker in the primary antibody solution for 10 minutes at room temperature and then they were incubated in the same primary antibody solution for 48 hours at +4°C (at the end of the first 24 hours the sections in the primary antibody solution were stirred again for another 10 minutes at room temperature and then returned to the fridge). Sections were then rinsed again four times (10 minutes each) in PBST, and then incubated in biotinylated goat secondary antibody (diluted 1:200 in PBST; Vectastain, Vector Laboratories, Burlingame, USA) and 1.5% normal goat serum, and left on the shaker for 2 hours at room temperature. After this, sections were washed four times (10 minutes each) in PBST and processed with avidin-biotinylated horseradish peroxidase complex in PBST (Vectastain Elite ABC kit PK-6100, Vector Laboratories, UK) for 1 hour at room temperature, again with constant rotation on the shaker. Sections were then rinsed four times (10 minutes each) in PBST, and then washed two times (10 minutes each) in 0.05 M Tris buffer (pH 7.4, prepared diluting Trizma base in distilled water). Finally, sections were incubated with 3.3'-diaminobenzidine (DAB Substrate Kit, Vector Laboratories, UK) until a brown stain was obtained (requiring about one minute); the reaction was stopped in cold PBS. Sections were mounted on gelatin-coated slides, dehydrated through a graded series of alcohols and cover-slipped (DPX mounting medium, Thermoscientific, UK).

6.2.5.3 Infusion of biotinylated antisense *Zif268* ODNs to verify infusate diffusion into the retrosplenial cortex (Group 3)

This procedure was performed only on the two animals in Group 3 that did not undergo any behavioural procedure. Ninety minutes after the infusion of the biotinylated antisense *Zif268* ODNs, the animals were irreversibly anaesthetised with sodium pentobarbital (60 mg⁄kg, Euthatal, Rhone Merieux, Harlow, UK) and perfused transcardially with 0.1M PBS followed by 4% paraformaldehyde in 0.1 M PBS (PFA). The brains were removed and post-fixed in 4% PFA for 2 hours and then transferred to 20% sucrose (in 0.1M PBS) overnight. Sections were cut at 40 µm on a freezing microtome in the coronal plane, and a one-in-three series of sections was selected and quenched in 50:50 10% methanol (Sigma-Aldrich, UK) and 10% H_2O_2 (Fisher Scientific, US). The sections were rinsed three times in PBS (15 minutes each) and permeabilised in 0.3% Triton overnight. The sections were then incubated in an avidin-biotidin complex (Vectastain Elite ABC kit PK-6100, Vector Laboratories, UK) for 2 hours and again rinsed three times in PBS (15 minutes each). Finally, the sections were exposed to DAB (DAB Peroxidase (HRP) Substrate Kit, 3,3'-diaminobenzidine, Vector Laboratories, UK) until visualization of biotinylated ODN was complete (requiring about one minute), washed again in cold PBS and left at +4°C overnight. The day after they were mounted onto gelatin-coated slides and air dried before being cover-slipped (DPX mounting medium, Thermoscientific, UK).

6.2.6 Zif268-*positive cell counts*

Counting procedures were carried out without knowledge of group assignment. Images were viewed on a Leica microscope (5X magnification) and photographed using an Olympus DP70 camera. The program ImageJ (1.46r version, NIH, US) was used to grey-scale the images and to count the number of Zif268-positive neuronal nuclei above threshold (the threshold value was set manually for each picture). Counts were made in a frame area comprising all laminae of the retrosplenial cortex. This counting procedure is not stereological, and so it does not provide a precise account of absolute Zif268-positive cell numbers; however, it provides account of relative numbers, allowing group comparisons. All nuclei above threshold and between 10-100 μm^2 in area size were counted. Zif268-positive cell counts were taken from an average of at least three sections (adjacent to the infusion site and consecutive if possible) per brain, and a mean was calculated for each animal.

The regions of interest were identified in coronal sections, using the nomenclature adopted by Wyss & Van Groen (1992) (Figure 6-3). Counts were made in the three main subregions of the retrosplenial cortex: granular b (Rgb), granular a (Rga), and dysgranular cortex (Rdg), keeping separated the superficial (II and upper III) and deep (lower III to VI) layers (the border between superficial and deep layers is signalled by an abrupt change in cell size and packaging density; e.g. Jenkins et al., 2004; Vann & Albasser, 2009); furthermore, for Rgb and Rdg, counts were taken at both rostral (- 2.56 mm from bregma) and caudal (- 6.04 mm from bregma) levels.

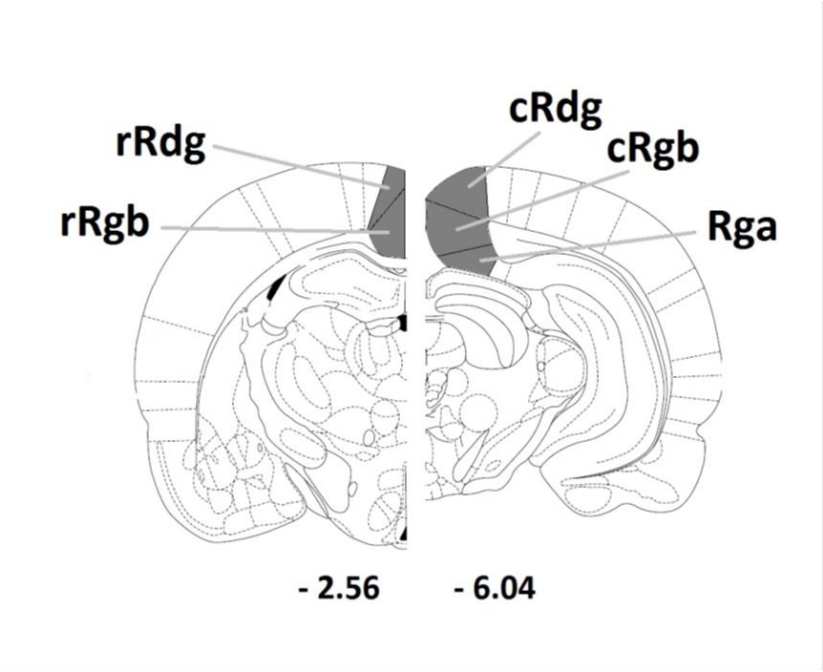

Figure 6-3. Location in coronal schematic sections of the regions of interest where cell counting was performed. Numbers under each section refer to their distance from bregma, referring to the brain atlas Paxinos & Watson, 1998. Pictures were adapted from a digital version of the atlas. cRdg (caudal dysgranular retrosplenial cortex), cRgb (caudal granular b retrosplenial cortex), Rga (granular a retrosplenial cortex), rRdg (rostral dysgranular retrosplenial cortex), rRgb (rostral granular b retrosplenial cortex).

6.2.7 Statistical analysis of behavioural data

SPSS software (version 20, IBM Corporation) was used to carry out all statistical analyses. The threshold for significance was set at $p < 0.05$.

6.2.7.1 Behavioural data

For the object-in-place task (Group 1 and the eleven cannulated animals in Co Group hort 2), a preliminary analysis was performed on the total exploration times of the four objects during the "sample" and the "test" phases. The animals were considered to be "exploring" the objects when their nose was less than 1 cm from the object and pointed in that direction. The total exploration times were separately recorded for the "sample" and the "test" phase and compared across cocktail antisense and cocktail missense infusion sessions using paired-samples t-tests. The object exploration times were then further analysed during the 3 minutes of the "test" phase, measuring separately the exploration times for the displaced and the non-displaced object pairs. Successful performance would be reflected by the animals exploring the displaced objects more than the non-displaced objects, due to their relative novelty. A discrimination ratio was calculated from the measures for the "test" phase of each session, using the difference between the time spent exploring the displaced objects minus the time spent exploring the non-displaced objects, divided by the total object exploration time (Dix & Aggleton, 1999); this transformation of the data is able to take into account differences in the individual levels of exploration for each animal. The discrimination ratios were calculated for both the first minute of each "test" phase [which has been shown to be the most sensitive for expression of preference for the displaced objects (Dix & Aggleton, 1999)] and the total 3 minutes of each "test" phase. Paired samples t-test was used to compare performance after the infusion in each animal of either muscimol or PBS (Group 1), or either antisense *Zif268* ODNs or missense *Zif268* ODNs (Group 2). Each discrimination ratio was also compared against chance level (zero) using one-sample t-test.

For the free exploration of the radial arm maze task (13 animals from Group 2), the number of visited arms was compared across animals infused with either missense *Zif268* ODNs or antisense *Zif268* ODNs or that did not receive any infusions (the unoperated behavioural controls) using one-way ANOVA.

6.2.7.2 Immunohistochemical data

Analyses were carried out on mean raw counts, which were derived by averaging the values obtained for all the sections for each area of interest in each brain. Two different mixed ANOVA designs were performed for analysing the cell counts in the retrosplenial cortex, grouping the subregions on the basis of their rostro-caudal location.

Analysis of the rostral retrosplenial cortex was carried out with “Group” as between-subject factor, with four levels: unoperated home-cage controls (N = 2), unoperated behavioural controls (N = 2), animals infused with missense *Zif268* ODNs before the behavioural procedure (N = 5), animals infused with antisense *Zif268* ODNs before the behavioural procedure (N = 6). “Region” (two levels: rostral Rgb and rostral Rdg) and “Layer” (two levels: superficial and deep) were, instead, the within-subject factors. Similarly, analysis of the caudal retrosplenial cortex was carried out with “Group” as between-subject factor, with four levels: unoperated home-cage controls (N = 2), unoperated behavioural controls (N = 2), animals infused with missense *Zif268* ODNs before the behavioural procedure (N = 5), animals infused with antisense *Zif268* ODNs before the behavioural procedure (N = 6). “Region” (three levels: caudal Rgb, caudal Rdg and Rga) and “Layer” (two levels: superficial and deep) were, instead, the within-subject factors.

When sphericity assumption was violated, Greenhouse-Geisser correction was applied to the degrees of freedom. When significant interactions were found, the simple effects for each brain region were analysed as recommended by Winer (1971) using the pooled error term. The main effects of “Region” and “Layer” were not considered because all regions of interest are different in size, thus the comparison would not be meaningful.

6.3 Results

6.3.1 Histology

6.3.1.1 Cannulae placement verified through Nissl staining (Group 1 and Group 2)

For all animals in Group 1 and Group 2 the two pairs of cannulae were correctly placed within the rostral and caudal portion of the retrosplenial cortex (Figure 6-4 and Figure 6-5).

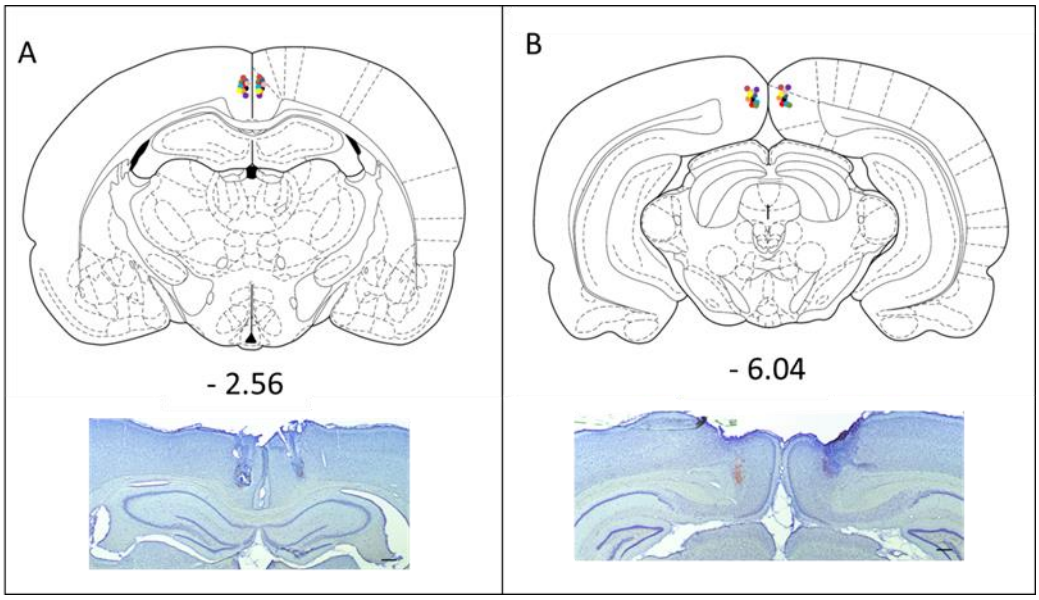

Figure 6-4. Cannulae placement into the retrosplenial cortex in Group 1. Panel A: cannulae placement into the rostral portion of the retrosplenial cortex (upper), and representative coronal section taken at the same antero-posterior level (lower). Panel B: cannulae placement into the caudal portion of the retrosplenial cortex (upper), and representative coronal section taken at the same antero-posterior level (lower). Each point in the diagrams represents the position of the tip of the cannula. A different colour has been used to identify cannulae placement for each animal. The distance in mm from bregma is reported. Figure adapted from Paxinos & Watson (1998). The tissue was stained with cresyl violet staining. Scale bar 100 µm.

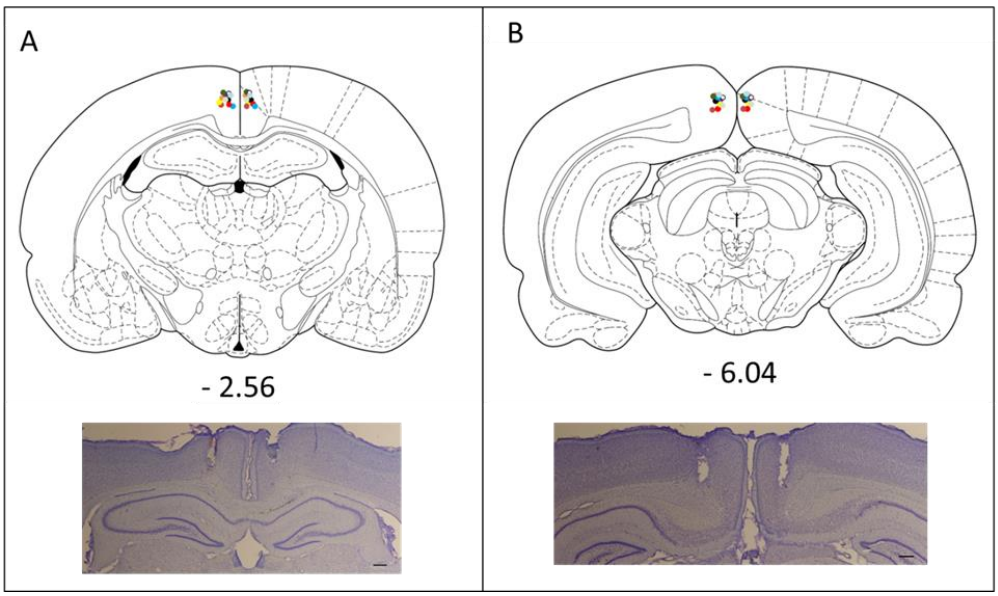

Figure 6-5. Cannulae placement into the retrosplenial cortex in Group 2. Panel A: cannulae placement into the rostral portion of the retrosplenial cortex (upper), and representative coronal section taken at the same antero-posterior level (lower). Panel B: cannulae placement into the caudal portion of the retrosplenial cortex (upper), and representative coronal section taken at the same antero-posterior level (lower). Each point in the diagrams represents the position of the tip of the cannula. A different colour has been used to identify cannulae placement for each animal. The distance in mm from bregma is reported. Figure adapted from Paxinos & Watson (1998). The tissue was stained with cresyl violet staining. Scale bar 100 µm.

6.3.1.2 Verification of biotinylated antisense Zif268 ODNs diffusion into the retrosplenial cortex (Group 3)

For both subjects in Group 3, the spread of the infusate was bilateral and covered all the three subregions (Rga, Rgb and Rdg) in the caudal portion of the retrosplenial cortex. However, in the rostral portion it was optimal in the left hemisphere (covering all retrosplenial subregions) but not in the right hemisphere (only Rgb was covered); this could due to the asymmetric positions of the anterior guide cannulae in both subjects. Furthermore, the anterior guide cannulae in one animal were implanted excessively rostrally, resulting in the spread of the infusate into the anterior cingulate cortex (Figure 6-6, case SVR94#1).

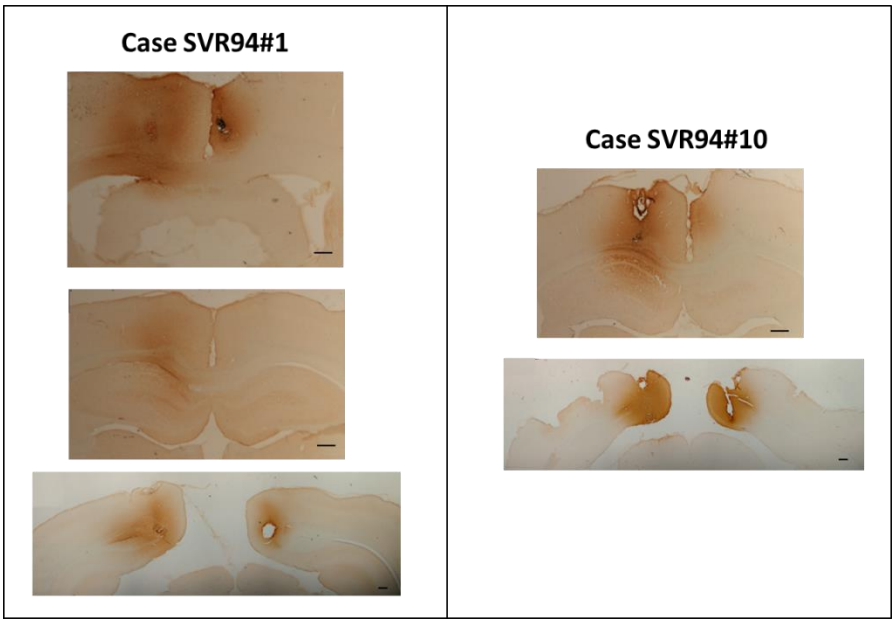

Figure 6-6. Diffusion of biotinylated antisense *Zif268* ODN infused into the retrosplenial cortex in the two subjects in Group 3. Two pairs of cannulae were implanted into the rostral and the caudal portion of the retrosplenial cortex (about – 2.5 mm and – 6.0 mm from bregma, respectively). Scale bar 100 µm.

6.3.2 Behaviour

Group 1 – behavioural assessment of muscimol infusions into the retrosplenial cortex

6.3.2.1 Post-surgery object-in-place testing

There was no difference between the total object exploration times following infusions with either PBS or with muscimol in the sample (t_9 = -0.752, p = 0.471; Figure 6-7) or in the test phase (t_9 = -0.55, p = 0.596; Figure 6-8).

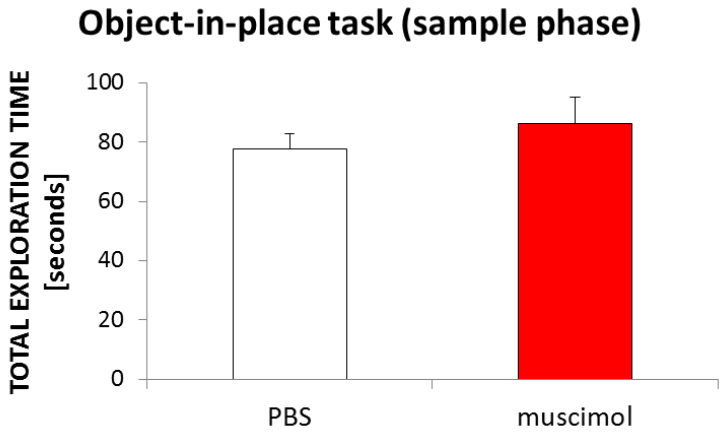

Figure 6-7. Total exploration times (mean ± SEM) in the sample phase of the object-in-place task for Group 1. The animals were infused with either PBS or muscimol into the retrosplenial cortex 30 minutes before the sample phase.

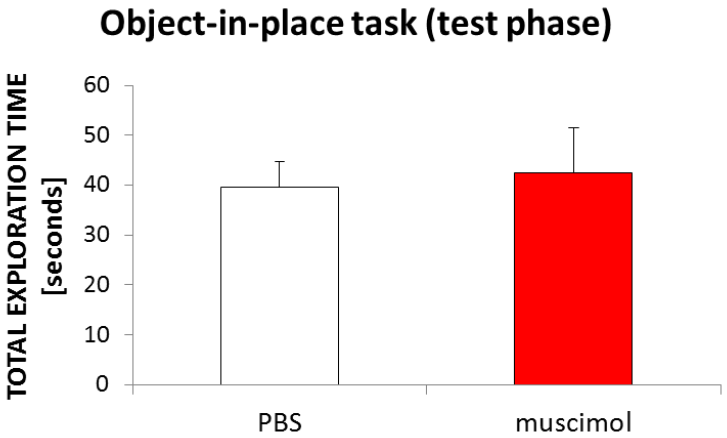

Figure 6-8. Total exploration times (mean ± SEM) in the test phase of the object-in-place task for Group 1. The animals were infused with either PBS or muscimol into the retrosplenial cortex 30 minutes before the sample phase. A 3-hour delay was inserted between the sample and the test phase.

Independent-samples t-tests were used to compare animals' performance (discrimination ratios calculated for either the first minute or the total 3 minutes of the test phase) between Session I and II, after infusion with either PBS or muscimol (Figure 6-9). As no significant difference was detected (first minute PBS: $t_8 = -0.6$, $p = 0.60$; first minute muscimol: $t_8 = -0.2$, $p = 0.82$; total 3 minutes PBS: $t_8 = -0.3$, $p = 0.74$; total 3 minutes muscimol: $t_8 = -0.2$, $p = 0.86$), data from Session I and Session II were combined for subsequent analyses.

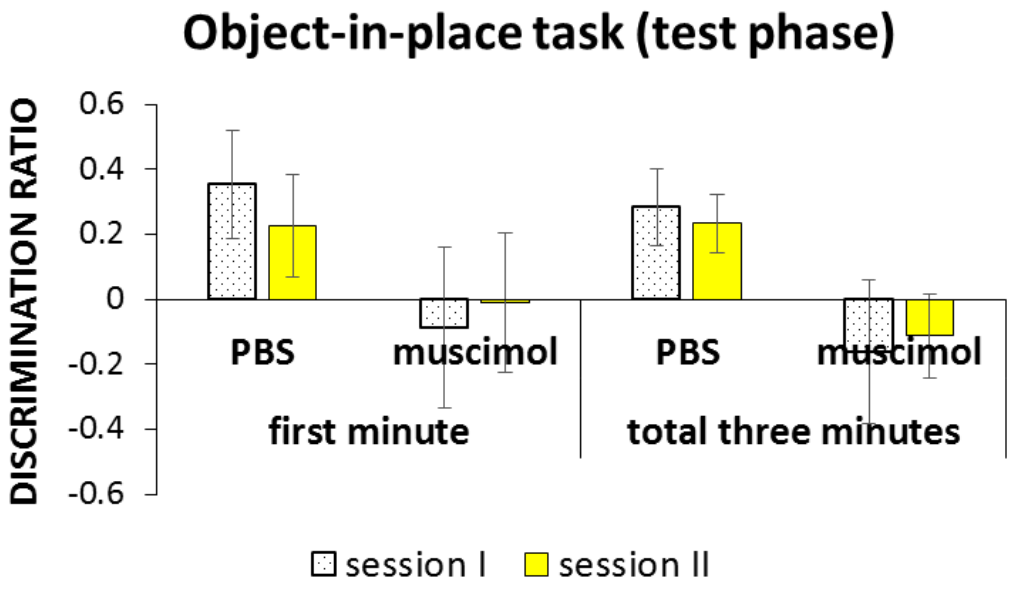

Figure 6-9. Discrimination ratios (mean ± SEM) for the two sessions of the test phase (considering either the first or the total 3 minutes) of the object-in-place memory task for Group 1, after muscimol or PBS infusions 30 minutes before the sample phase. A 3-hour delay was inserted between the sample and the test phase.

To evaluate the ability of the rats in Group 1 to discriminate between the displaced and the non-displaced objects during the test phase, the discrimination ratios for both the first minute and the total 3 minutes of the test phase were compared to zero. The discrimination ratios significantly differed from zero following infusions of PBS for both the first minute (t_9 = 2.6, p <0.01) and the total 3 minutes (t_9 = 3.6, p <0.01) of the test phase; however, after muscimol infusions, this difference was no longer significant, either after the first minute (t_9 = -0.3, p = 0.76) or in the total 3 minutes (t_9 = -1.1, p = 0.29) of the test phase. Furthermore, after muscimol infusions the discrimination ratios were smaller than after PBS infusions. This difference was statistically significant for the total 3 minutes of test phase (t_9 =2.4, p < 0.05), but not for the first minute (t_9 =1.4, p = 0.20) (Figure 6-10).

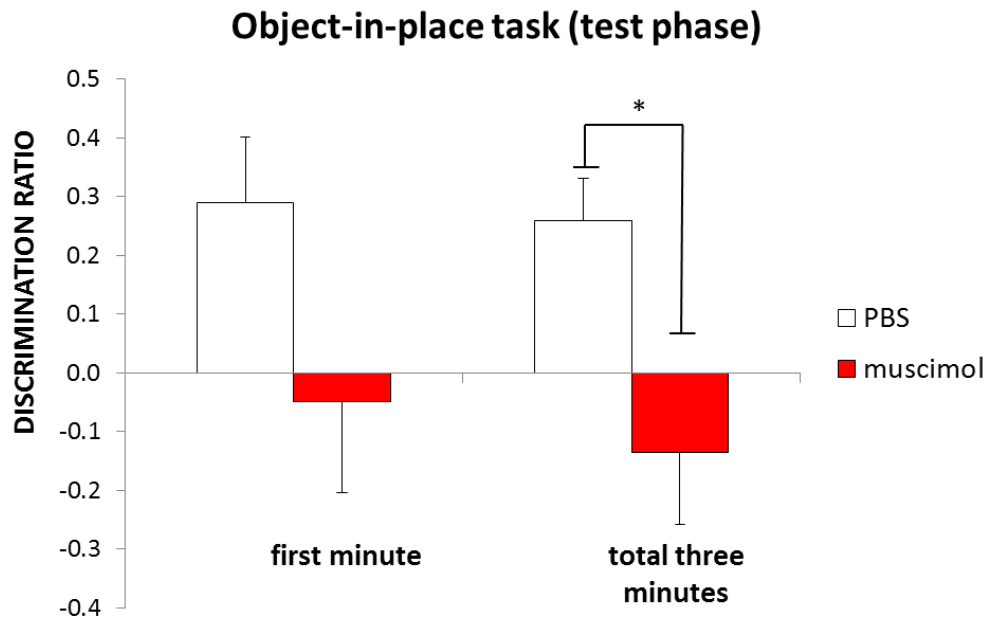

Figure 6-10. Discrimination ratios (mean ± SEM) in the test phase of the object-in-place task for Group 1. The animals were infused with either either PBS or muscimol into the retrosplenial cortex 30 minutes before the sample phase. A 3-hour delay was inserted between the sample and the test phase. Results for both the first minute and the total 3 minutes of test exploration are reported. Level of significance: *p < 0.05.

Group 2 – behavioural assessment of antisense Zif268 ODN infusions into the retrosplenial cortex

6.3.2.2 Post-surgery object-in-place testing

There was no difference between the total object exploration times of rats infused with either missense or antisense *Zif268* ODNs for either the sample (t_{10} = 0.1, p = 0.94; Figure 6-11) or the test phase (t_{10} = 0.5, p = 0.66; Figure 6-12).

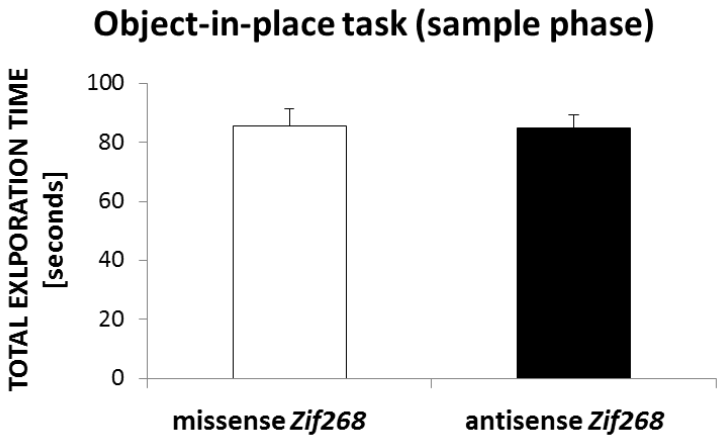

Figure 6-11. Total exploration times (mean ± SEM) in the sample phase of the object-in-place task for Group 2. The animals were infused with either missense or antisense *Zif268* ODNs into the retrosplenial cortex 90 minutes before the sample phase.

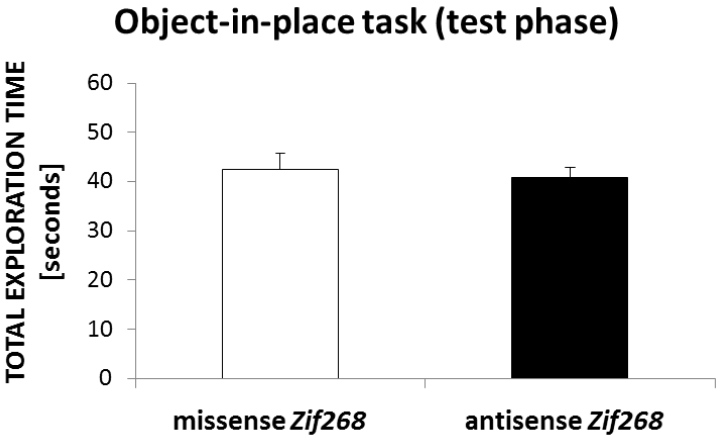

Figure 6-12. Total exploration times (mean ± SEM) in the test phase of the object-in-place task for Group 2. The animals were infused with either missense or antisense *Zif268* ODNs into the retrosplenial cortex 90 minutes before the sample phase. A 3-hour delay was inserted between the sample and the test phase.

Independent-samples t-tests were used to compare animals' performance (discrimination ratios calculated for either the first minute or the total 3 minutes of the test phase) between Session I and II, after infusion with either missense or antisense *Zif268* ODNs (Figure 6-13). As no significant difference was detected (first minute missense *Zif268* ODNs: $t_9 = -0.3$, $p = 0.74$; first minute antisense *Zif268* ODNs: $t_9 = -1.0$, $p = 0.35$; total 3 minutes missense *Zif268* ODNs: $t_9 = 0.0$, $p = 0.97$; total 3 minutes antisense *Zif268* ODNs: $t_9 = -0.3$, $p = 0.78$), data from Session I and Session II were combined for subsequent analyses.

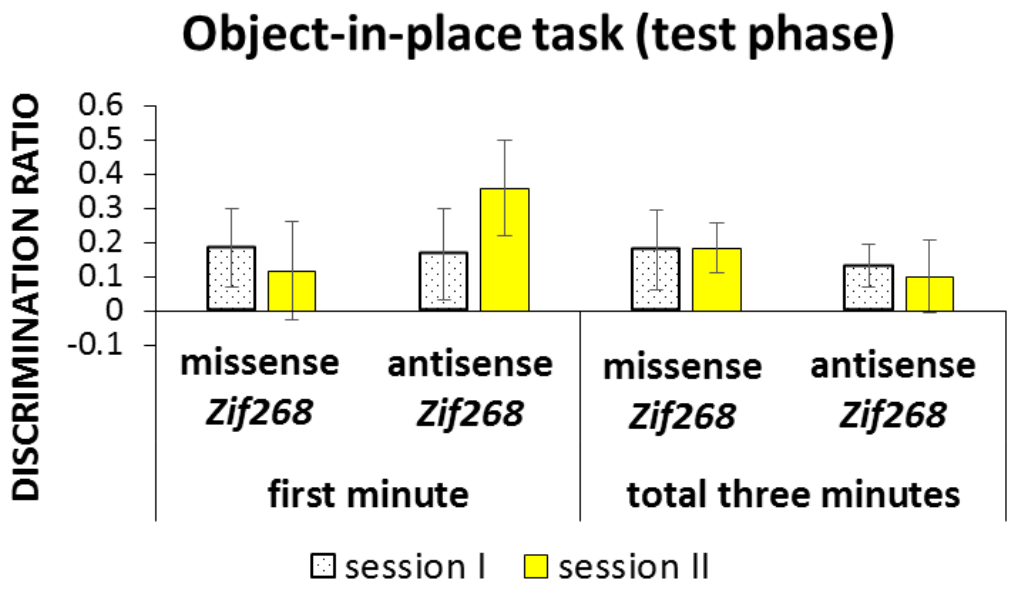

Figure 6-13. Discrimination ratios (mean ± SEM) for the two sessions of the test phase (considering either the first or the total 3 minutes) of the object-in-place memory task for Group 2, after missense or antisense *Zif268* ODN infusions 90 minutes before the sample phase. A 3-hour delay was inserted between the sample and the test phase.

The discrimination ratios after missense and antisense *Zif268* ODN infusions were compared to chance level (zero) in order to verify if the animals were able to discriminate the displaced from the non-displaced objects: in the first minute of the test phase only the discrimination ratios of the animals infused with antisense *Zif268* ODNs were significantly above zero (missense: $t_{10} = 1.6$, $p = 0.13$; antisense: $t_{10} = 2.6$, $p < 0.05$); when considering the total 3 minutes, instead, only the discrimination ratios of the animals infused with the missense solution were significantly above zero (missense: $t_{10} = 2.9$, $p < 0.05$; antisense: $t_{10} = 2.1$, $p = 0.06$). However, there was no significant difference between discrimination ratios following antisense infusion compared to missense infusion (first minute: $t_{10} = -1.0$, $p = 0.36$; total 3 minutes: $t_{10} = 0.8$, $p = 0.44$) (Figure 6-14).

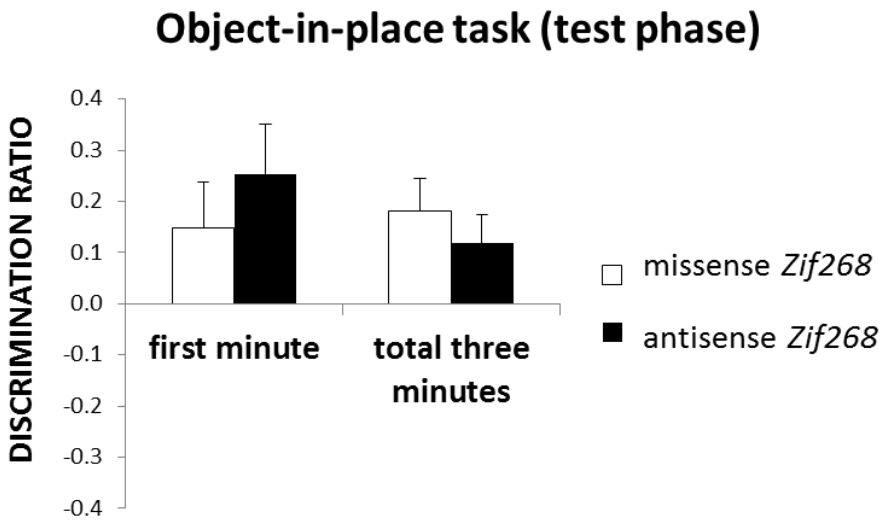

Figure 6-14. Discrimination ratios (mean ± SEM) in the test phase of the object-in-place task for Group 2. The animals were infused with either missense or antisense *Zif268* ODNs into the retrosplenial cortex 90 minutes before the sample phase. A 3-hour delay was inserted between the sample and the test phase.

6.3.2.3 Post-surgery free exploration of a radial arm maze located in a novel room

No difference was detected in the total number of radial arm maze arms visited following either missense *Zif268* ODNs infusion, antisense *Zif268* ODNs infusion or no infusion (unoperated behavioural controls) ($F < 1$; mean number of arms visited ± SEM: missense 29.0 ± 5.2; antisense 31.0 ± 2.9; unoperated behavioural controls: 28.0 ± 3.0).

6.3.3 Counting of Zif268-positive cells

Looking at Zif268 levels in the rostral portion of retrosplenial cortex (comprising rostral Rgb and rostral Rdg; Figure 6-15 and Figure 6-16), statistical analysis revealed a significant main effect of the Group factor ($F_{3,11} = 4.3$, $p < 0.05$). There was also a significant Group x Region interaction ($F_{3,11} = 4.0$, $p < 0.05$). None of the other interactions reached significance (Group x Layer: $F_{3,11} = 2.9$, $p = 0.09$; Group x Region x Layer: $F_{3,11} = 2.0$, $p = 0.17$).

Analysis of simple effects showed that the number of Zif268-positive cells was significantly higher in rostral Rdg in the unoperated behavioural control group in comparison to the missense *Zif268* ODN infused group ($p < 0.05$).

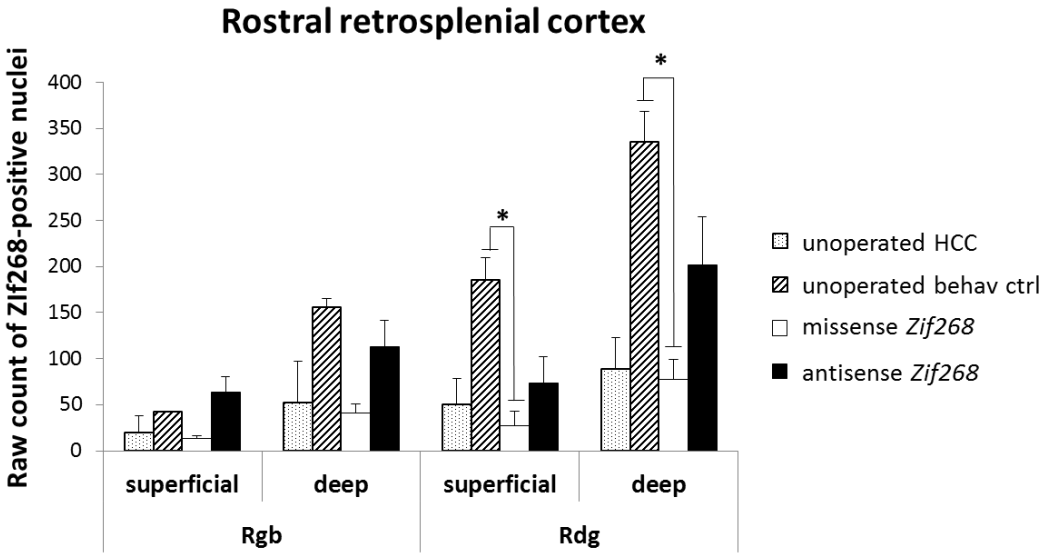

Figure 6-15. Mean raw counts of Zif268-positive nuclei (± SEM) in the rostral portion of the retrosplenial cortex (rostral Rgb and rostral Rdg) in Group 2. HCC = home-cage control group; behav ctrl = behavioural control group. Level of significance: * p<0.05.

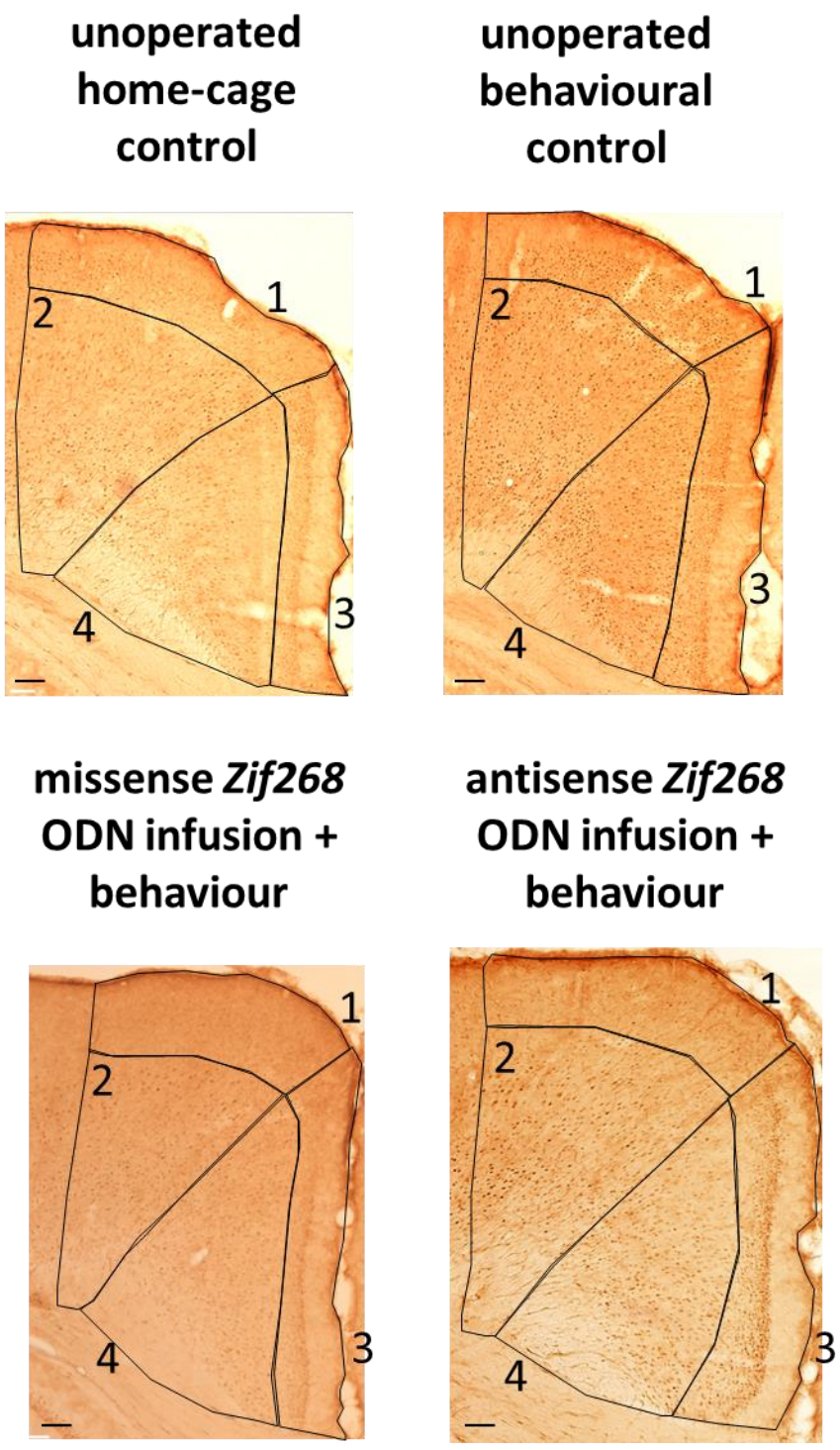

Figure 6-16. Representative coronal sections of the rostral portion of the retrosplenial cortex from the four different groups. The different retrosplenial subregions are indicated by numbers (1: rostral Rdg superficial layer; 2: rostral Rdg deep layer; 3: rostral Rgb superficial layer; 4: rostral Rgb deep layer). Scale bar 100 µm.

For the caudal portion of the retrosplenial cortex (comprising caudal Rgb, caudal Rdg and Rga; Figure 6-17 and Figure 6-18), there was no main effect of the Group factor on Zif268 levels ($F_{3,9}$ = 2.5, p = 0.13). While the interaction Group x Layer was statistically significant ($F_{3,9}$ = 33.9, p < 0.001), none of the simple effects reached significance. None of the other interactions reached significance (Group x Region: F < 1; Group x Region x Layer: $F_{6,18}$ = 1.5, p = 0.23).

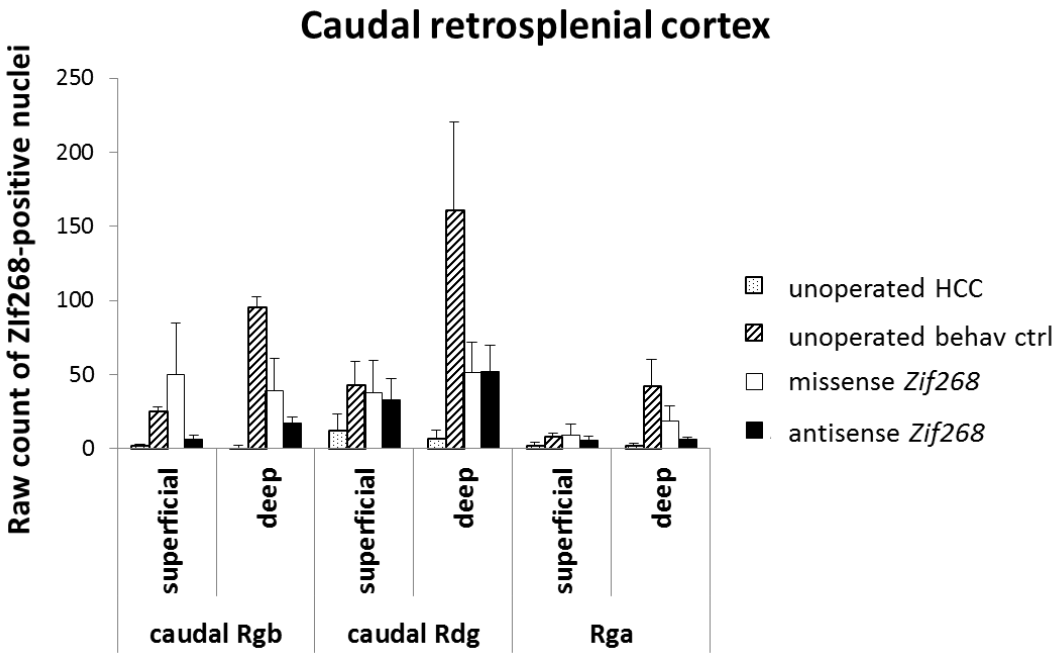

Figure 6-17. Raw counts (mean ± SEM) of Zif268-positive nuclei (± SEM) in caudal portion of the retrosplenial cortex (caudal Rgb, caudal Rdg and Rga, which is present only at caudal level) in Group 2. HCC = home-cage control group; behav ctrl = behavioural control group.

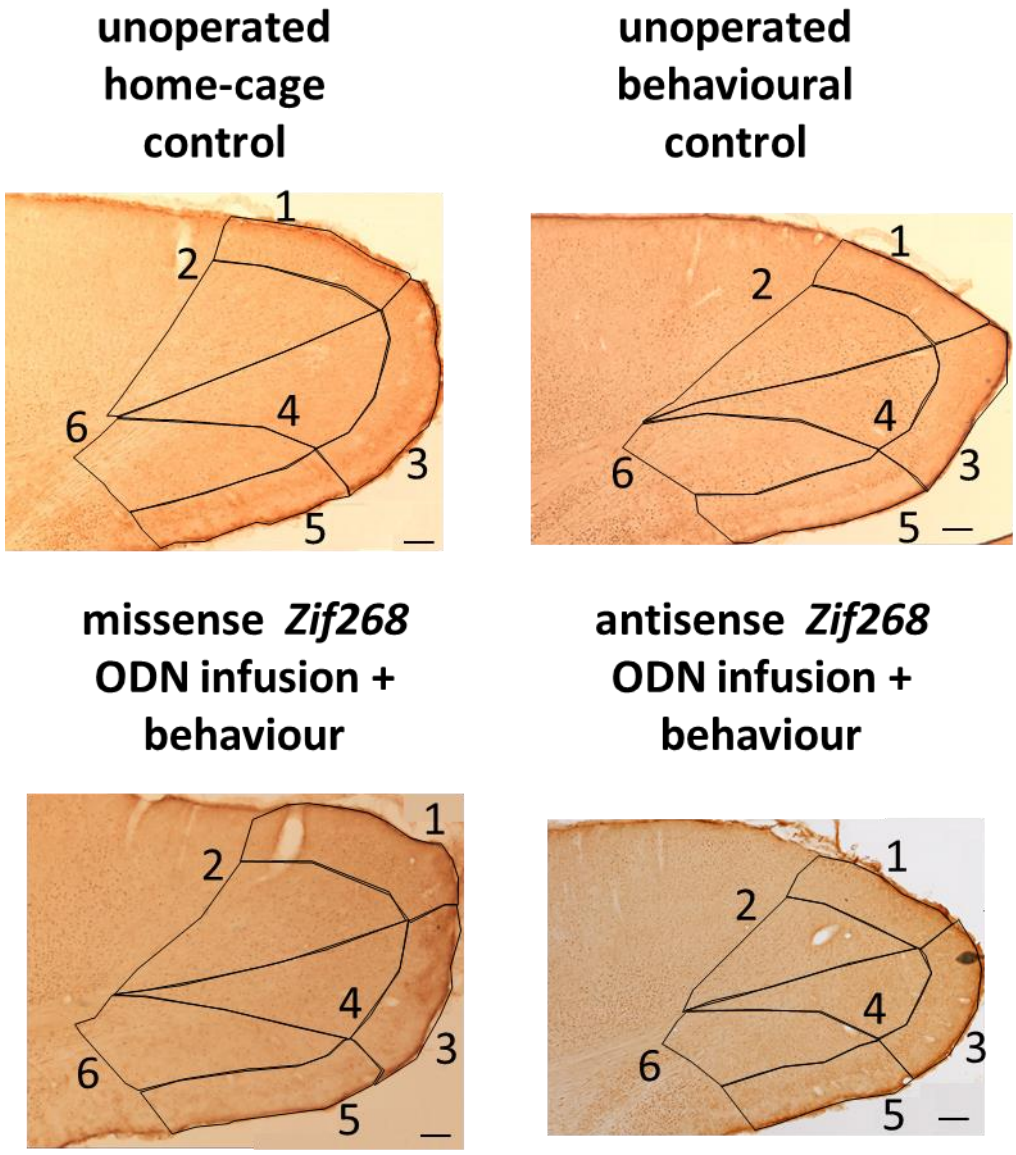

Figure 6-18. Representative coronal sections of the caudal portion of the retrosplenial cortex from the four different groups. The different retrosplenial subregions are indicated by numbers (1: caudal Rdg superficial layer; 2: caudal Rdg deep layer; 3: caudal Rgb superficial layer; 4: caudal Rgb deep layer; 5: Rga superficial layer; 6: Rga deep layer). Scale bar 100 µm.

6.4 Discussion

The retrosplenial cannulation surgery and infusion procedure appeared optimal at the level of the caudal portion of the retrosplenial cortex and slightly asymmetrical and too anterior in the rostral portion of the retrosplenial cortex, as verified through infusion of biotinylated antisense *Zif268* ODNs (Group 3).

The behavioural experiment with muscimol infusion before the test on the object-in-place task (Group 1), revealed an impairment, measured as a shorter time spent exploring the displaced pair of objects than after infusion of a control solution. This result confirmed at the behavioural level the efficacy of the surgical and cannulation procedures.

A third group of animals (Group 2) was infused with the antisense *Zif268* ODN, and tested on the object-in-place task: no impairment was detected in comparison to the same animals performing the same task after a control solution. Finally, the third group of animals was let free to explore a new arm maze apparatus in a new room after being infused with either the antisense *Zif268* ODN or a control solution; then the animals' brains were analysed for Zif268 expression using immunochemistry. No significant difference in Zif268 levels was found between animals infused either with antisense *Zif268* ODN or with the control solution.

This experiment has shown that muscimol infusions into the retrosplenial cortex in Group 1 impaired animals' performance on the object-in-place task in which the sample and the test phase were separated by a delay of 3 hours (Figure 6-10). Not only performance following muscimol infusions was significantly worse than performance following PBS infusion, but performance following muscimol infusion was at chance, i.e., the animals could no longer discriminate between the displaced and non-displaced objects.

A previous lesion study found an impairment after retrosplenial lesions on the same task, but with a 15 minute delay inserted between the sample and the test phase (Vann & Aggleton, 2002). Thus, the present outcome after muscimol infusions extends that result showing that the normal functionality of the retrosplenial cortex is necessary for animals to show a preference for the displaced objects in the object-in-place task, even after a longer delay between sample and test phase. The consistent findings following temporary inactivation with muscimol and chronic neurotoxic lesions would suggest that the lesion effects are not due to longer-term changes such as retrograde degeneration (typically seen in the anterior thalamic nuclei after

retrosplenial cortex lesions). The current muscimol findings on the object-in-place task extend earlier studies that have reported effects on spatial working memory tasks following muscimol or tetracaine retrosplenial infusions (Cooper & Mizumori, 1999, 2001; Nelson et al., 2015).

In contrast, infusions of antisense ODNs targeting *Zif268* transcript in the retrosplenial cortex in Group 2 did not have any consistent effect on the behavioural performance on the object-in-place task with the 3-hour delay (Figure 6-14). Neither of the groups was consistently above chance over the 3 minute test period and there was never a significant difference in performance following infusion of the antisense ODNs compared to missense ODNs.

Visualisation of the spread of biotinylated antisense *Zif268* ODNs into the retrosplenial cortex in Group 3 showed that at the rostral level the infusion was not optimal (Figure 6-6), probably because the guide cannulae were not positioned symmetrically on the two sides of the midline and/or because there was an occlusion in the microinjectors/guide cannulae during the infusion. In some of the subjects in both Groups 1 and 2 the position of the rostral guide cannulae (verified through Nissl stain) was also slightly asymmetric (Figure 6-4 and Figure 6-5). The spread of the infusate was not verified in these animals, and may not have been optimal in the rostral portion of the retrosplenial cortex. However, it has been shown that inactivation of the caudal portion of the retrosplenial cortex (- 6 mm from bregma) via infusions of tetracaine and neurotoxic lesions restricted to the caudal retrosplenial portion are sufficient to impair animals' performance on spatial memory tasks (Cooper, Manka, & Mizumori, 2001; Cooper & Mizumori, 1999; Vann, Wilton, et al., 2003). Furthermore, the results from an immediate early gene imaging experiment (Pothuizen et al., 2009) implicated the posterior portion of the retrosplenial cortex in spatial memory, as levels of Zif268 were significantly increased in caudal Rgb and not in rostral Rgb when animals performed a radial arm maze task. This difference in activation between rostral and caudal portions of the retrosplenial cortex was related to the intrinsic connections within the retrosplenial cortex: rostral retrosplenial cortex projects to the more caudal retrosplenial regions but this projection is not reciprocated (Shibata et al., 2009), resulting in more information being integrated in the caudal retrosplenial subdivision. Taking into account these earlier studies and the observed deficit following muscimol infusions in the present experiment, it seems unlikely that the null results after antisense *Zif268* ODN infusions were due to cannulae misplacement or blocking of the microinjectors/ during the infusion procedure.

A possible explanation for the lack of an effect of antisense *Zif268* ODN infusions into the retrosplenial cortex on the performance on the object-in-place task is that retrosplenial expression levels of this immediate early gene are not relevant for the task. However, a number of studies have reported the increase of Zif268 levels across brain regions when animals are engaged in various spatial memory tasks. Ninety minutes after the completion of a radial arm maze task, levels of the protein Zif268 appeared higher than in controls in the retrosplenial cortex, anteroventral thalamic nucleus, subicular complex, anterior cingulate cortex, entorhinal cortex, postrhinal and perirhinal cortices, primary auditory cortex and amygdala (Jenkins et al., 2006; Pothuizen et al., 2009). Another study found an increase in *Zif268* mRNA levels in the dorsal hippocampus 30 minutes after training in the reference memory version of the water maze task (Guzowski et al., 2001). An experiment using a long-term memory object-place recognition task found an increase of Zif268 levels in the dentate gyrus 60 minutes after the task (Soulé et al., 2008). Transgenic mice overexpressing Zif268 protein in the forebrain (including the hippocampus) have been shown to be better than wild-type controls in a long-term memory version of the object-place recognition task (Penke et al., 2014), while knock-out mice lacking the expression of Zif268 protein were impaired on both the object-place recognition task (Bozon, Davis, & Laroche, 2002) and the reference memory version of the water maze task (Jones et al., 2001).

To date, no study has analysed expression levels of *zif268* in the retrosplenial cortex after the object-in-place task. This information could be useful to evaluate the null results from the current experiment, especially regarding the suitability of using the object-in-place task. However, even if this task was able to increase the expression levels of Zif268 in the retrosplenial cortex, the exact role of this protein would still remain uncertain, i.e. if it is necessary for task performance or if an increase in its levels is just a secondary effect of retrosplenial activation.

The effect of antisense *Zif268* ODN infusions into the retrosplenial cortex was further analysed at the molecular level by immunohistochemically processing the brains with an antibody specific for Zif268 (the same anti-Zif268 antibody used in Chapters 2 and 5). Counts of Zif268-positive nuclei were carried out in all retrosplenial cortex subregions, at both rostral and caudal levels. Animals infused with the missense control solution were expected to have a comparable number of Zif268-positive nuclei with the unoperated behavioural control group, while the counts were expected to be significantly lower in the antisense-infused group and in the unoperated home-cage

control group. However, a significant difference was detected only in rostral Rdg (in both superficial and deep layers), with the unoperated behavioural control group showing a significantly higher number of Zif268-positive nuclei in comparison to the group infused with missense *Zif268* ODNs. One limit of the experimental protocol was that the unoperated behavioural control group was not properly matched to the antisense and missense infusion groups, as these last two groups were tested on the object-in-place task before the free exploration of the radial arm maze, unlike the unoperated behavioural control group. The free exploration of the radial arm maze was the first instance the unoperated behaviour control group experienced another environment outside the home-cage. It could be the case that, even if an increase in Zif268 levels is expected when animals explore a novel environment, in the case of the unoperated behavioural control group, this increase could have been further potentiated by never having been outside their home-cage before. This may make direct comparisons with the antisense and missense-infused groups hard to interpret. The lower counts in the missense group could also imply that the surgery and any infusion are sufficient to disrupt normal immediate early gene expression in the retrosplenial cortex. Additional controls that had undergone surgery but not received any infusions, or having an unoperated behavioural group that was more fully matched to the infusion groups may be one way to clarify this. Furthermore, the quality of Zif268 immunostaining was very poor, giving rise to a very weak signal of the positive nuclei in all groups. For all these reasons the results provided by this last experiment may not be reliable, however, they would suggest there is no clear difference in Zif268 expression following antisense *Zif268* ODN infusions compared to missense *Zif268* ODN infusions.

In conclusion, muscimol infusions into the retrosplenial cortex are able to impair performance of an object-in-lace task with a 3-hour delay between the sample and the test phase. Infusions of antisense *Zif268* ODNs into the retrosplenial cortex did not seem to cause any memory deficit in the same task. However, the efficacy of the antisense *Zif268* ODN solution in significantly decreasing the expression levels of Zif268 in the retrosplenial cortex was not demonstrated, thus limiting any conclusions from the behavioural results.

Chapter 7 General Discussion

Damage to the medial diencephalon has been repeatedly shown to cause episodic memory impairments in humans and spatial memory impairments in rodents. However, it is still not fully understood why this region is important for memory. In addition to the memory impairments observed, medial diencephalic damage has also been associated with distal dysfunction in other structures within the Papez circuit, in particular the retrosplenial cortex and hippocampus. It is possible that these distal effects contribute to, and exacerbate, the memory impairments observed after medial diencephalic damage. The overall aim of this body of work was to investigate the distal changes following medial diencephalic damage and whether these changes can affect spatial memory. Mammillothalamic tract lesions were used as a model of diencephalic amnesia for two reasons: vascular diencephalic amnesia is most consistently associated with damage to this tract; secondly, this tract does not directly innervate the key regions under investigation, i.e. the hippocampus and retrosplenial cortex, so any effects cannot simply be interpreted in terms of deafferentation.

In this body of work, the distal effects of mammillothalamic tract lesions were investigated using immediate early imaging and analysis of dendritic microstructure. Furthermore, I used infusions of antisense oligodeoxynucleotides (ODNs) in selected components of the Papez circuit in order to assess if the loss of the immediate early genes expression was sufficient to disrupt spatial memory processes. An overview of the results obtained in this body of work is given in Table 7-1, Table 7-2, Table 7-3 and Table 7-4.

Previous studies have shown changes in c-Fos expression in the retrosplenial cortex, hippocampus and prelimbic cortex following mammillothalamic tract lesion rats (Vann & Albasser, 2009; Vann, 2013). The aim of Chapter 2 was to expand on these findings and see whether this effect was specific to c-*fos* or could be generalised to another immediate-early gene, *zif268*. The lesioned rats carried out a forced-run version of the radial arm maze task in a novel room; exploring a novel environment has repeatedly been shown to trigger immediate early gene expression in the brain in control animals (Gheidi et al., 2013; Hall et al., 2000; Jenkins, Dias, Amin, Brown, et al., 2002; VanElzakker et al., 2008; Zhu et al., 1997).

Significantly fewer Zif268-positive cells were measured in Rdg and Rgb subregions of the retrosplenial cortex (Table 7-1). This result was similar to that obtained after c-Fos imaging in mammillothalamic tract lesioned-animals (Vann & Albasser, 2009; Vann, 2013), and also overlaps with the loss of Zif268 levels within the retrosplenial cortex after anterior thalamic (Dumont et al., 2012) and hippocampal lesions (Albasser et al., 2007). The functionality of the retrosplenial cortex appears particularly sensitive to the integrity of the Papez circuit, even when the connections with the lesioned structures are indirect, as for the case of the mammillothalamic tract.

None of the other regions measured (dorsal hippocampus, presubiculum, parasubiculum, postsubiculum, and anterior cingulate, prelimbic and infralimbic cortices) showed any significant changes in Zif268 levels, in contrast to the changes detected in c-Fos levels after mammillothalamic tract lesions in some of those regions (a decrease in the dorsal hippocampus, postsubiculum and prelimbic cortex, and an increase in the parasubiculum, see Figure 7-1). This highlights the differences between these two immediate early genes and suggests c-Fos might be a more sensitive marker to detect dysfunction within the system. Other experiments have reported differential expression of c-Fos and Zif268 in the brain after performing tasks that engage different memory processes. For example, one study reported an increase of c-Fos but not Zif268 levels in the perirhinal cortex and the hippocampus of animals tested on the one-trial object recognition task in comparison to controls (Barbosa et al., 2013). Another study investigated immediate early gene expression in animals processing novel temporal configurations of stimuli (Amin, Pearce, Brown, & Aggleton, 2006); c-Fos (but not Zif268) levels were lower in both the dorsal CA1 subfield and retrosplenial cortex, while Zif268 (but not c-Fos) levels were increased in the anteroventral thalamic nuclei, in comparison to control animals processing familiar temporal configurations of stimuli. It is important to underline that even if some immediate early gene imaging studies have used them as generic neuronal-activation markers, c-Fos and Zif268 immediate early genes have different basal levels of expression in different brain regions (Davis et al., 2003; Herrera & Robertson, 1996) and they have been shown to support different forms of synaptic plasticity: c-Fos long term depression induction in the CA1 subfield (Kemp et al., 2013), while Zif268 long term potentiation maintenance in the dentate gyrus (Richardson et al., 1992). Thus their differential expression after medial diencephalic lesion in the other structures within the Papez circuit could be related to their different functionality.

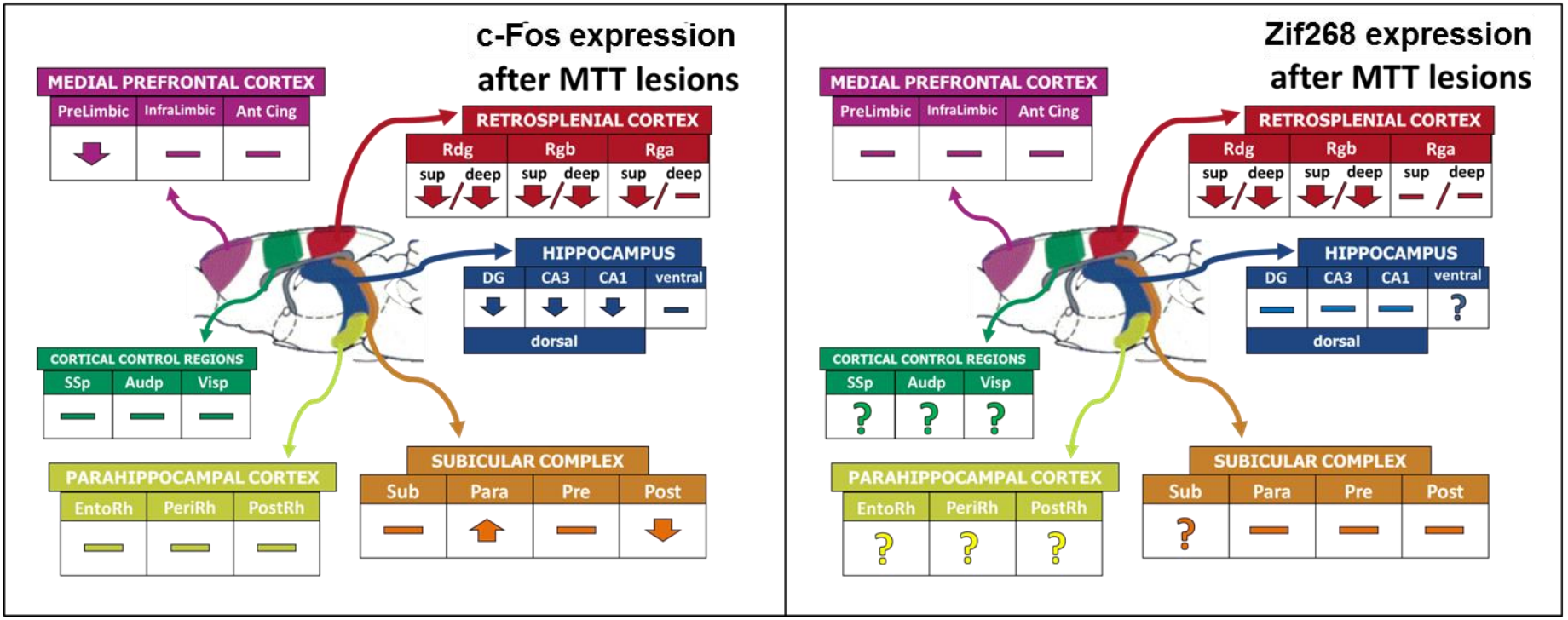

Figure 6-19. Summary of results for c-Fos (Vann & Albasser, 2009; Vann, 2013) and Zif268 (current thesis) expression levels after mammillothalamic tract lesions (MTT lesions) in the Papez circuit and connected structures (figure adapted from Vann & Albasser, 2009). A down arrow indicates a decrease in immediate early gene levels in the mammillothalamic tract-lesioned animals compared to the surgical/behavioural controls, an up arrow indicates an increase, while the horizontal bar indicates no significant change; a question mark indicates that Zif268 levels in that area have not been investigated yet. The areas analysed are: anterior cingulate cortex (Ant Cing), auditory primary cortex (Audp), CA3 (dorsal hippocampus), CA1 (dorsal hippocampus), dentate gyrus (DG, in dorsal hippocampus), entorhinal cortex (EntoRh), infralimbic cortex, parasubiculum (Para), perirhinal cortex (PeriRh), postsubiculum (Post), postrhinal cortex (PostRh), presubiculum (Pre), prelimbic cortex, Rdg, Rga, Rgb, somatosensory primary cortex (SSp), subiculum (Sub), ventral hippocampus (ventral), visual primary cortex (Visp). sup = superficial layers of retrosplenial cortex (II-upper III); deep = deep layers of retrosplenial cortex (lower III-VI).

c-Fos and Zif268 are probably involved in different processes implicated in signalling and plasticity within the Papez circuit, and thus it does not seem unreasonable to suppose that their expression changes in a different way after mammillothalamic tract lesions. A possible further investigation would be analysing the expression levels of other molecular plasticity markers, such as CREB, a constitutive transcription factor upstream of the activation of both c-Fos (e.g. Sheng & Greenberg, 1990) and Zif268 (Davis et al., 2003), or Arc, a transcription factor involved in remodelling of dendrites at active synapses (Shepherd & Bear, 2011). The assessment of different molecules would allow to enable a more complete analysis of the effects of medial diencephalic lesions.

The findings from the mammillothalamic tract lesions were also remarkably similar to those findings from anterior thalamic tract lesions, where hippocampal changes were found using c-Fos but not Zif268 imaging. The similarity between mammillothalamic tract and anterior thalamic tract lesions also suggests that the changes following anterior thalamic tract lesions are mainly driven by the loss of their inputs from the mammillary bodies.

The aim of Chapter 3 was to determine whether the lesion-induced changes in immediate early gene expression reported in Chapter 2 coincided with any microstructural changes in the retrosplenial cortex. An analysis was carried out of the dendritic microstructure of the small pyramidal cells located in the superficial layers of Rgb, which receive most of the medial diencephalic input (Table 7-1). In mammillothalamic tract-lesioned rats, in comparison to control animals, the dendritic arbor complexity, measured through Sholl analysis, appeared slightly lower in the distal part of the apical arbors and in the middle part of the basal arbors. This difference, however, did not reach statistical significance in either case. Analysis of apical dendritic spine density did not reveal any difference when comparing the lesioned and non-lesioned animals. This result differs from the findings of a similar study assessing the effects of anterior thalamic nuclei lesions that detected a decrease in thin spines on the apical arbors of small fusiform pyramids in the superficial layers of Rgb (Harland et al., 2014). This different pattern of findings may reflect the direct deafferentation of the retrosplenial cortex in the case of the anterior thalamic nuclei lesions. Another factor to consider is that the technique used for visualising dendritic spines (the Golgi staining) may not be the most suitable, and subtle changes could be instead detected using a more sensitive technique.

However, given that anterior thalamic and mammillothalamic tract lesions have very similar effects on c-Fos and Zif268 expression in the retrosplenial cortex, but only anterior thalamic lesions appear to affect dendritic spine density, the immediate-early gene changes are clearly not just a reflection of changes at the microstructural level of the cell.

Having found further evidence that medial diencephalic damage, and more specifically mammillothalamic tract lesions, result in distal changes in immediate early gene expression, the remaining experiments were aimed at better understanding these changes. More specifically, the goal was to assess whether disrupting c-Fos and Zif268 expression in the hippocampus and retrosplenial cortex could disrupt spatial memory.

In the first instance, a behavioural task needed to be developed that would be suitable for studying the effects of knocking down c-Fos and Zif248 expression, using antisense ODNs, and also tax the retrosplenial cortex and hippocampus. A variant of the working memory version of the radial arm maze task was used, in which the animals were removed from the maze after making their first four arm choices; the maze was rotated and they were returned to the maze after a given time-delay. Animals were tested with gradually longer time-delays until the animals were able to remember their initial arm choices over a 3-hour delay. The findings from Chapter 2 (Table 7-2) showed that animals were able to successfully learn this task and also that this task was hippocampal dependent, as infusions of muscimol into the dorsal hippocampus, disrupted performance of this task.

Once a suitable task had been developed, the next step was to assess whether knocking down c-Fos and Zif268 expression in the dorsal hippocampus affected performance of this task (Chapter 5; Table 7-3). Surprisingly, animals infused with antisense ODNs performed the task at control levels, while infusions of muscimol in the same animals, markedly disrupted performance of the task. It is possible that the extended training required for the acquisition of the modified radial arm maze task meant that c-Fos and Zif268 expression in the hippocampus no longer contributed to the performance of this task. c-Fos expression is most strongly associated with novelty (see Section 1.4.5.1), and Zif268 expression in the hippocampal subfields varies in association with training levels (Poirier, Amin, et al., 2008). For this reason, the same group of rats was further tested on a spatial memory task that does not require training, the object-in-place task, again with a 3-hour delay between the

sample and the test phase. However, animals were unable to discriminate the displaced objects after infusions of the cocktail antisense *Zif268/c-Fos* ODNs or with cocktail missense (control), i.e. the poor performance of the animals following the control infusion meant it was not possible to assess whether there was an effect of the antisense infusion. By the time animals received these two last infusions they had already been infused eight times, thus it could have been that the dorsal hippocampus was damaged, explaining the poor performance after infusion of the control solution.

A further group of animals received either cocktail antisense *Zif268/c-Fos* ODN or cocktail missense infusions and then freely explored a radial arm maze in a novel room for 20 minutes. Their dorsal hippocampi were dissected and c-Fos and Zif268 protein levels were analysed using the Western blot technique and compared to those of a group of naïve home-cage animals. The analysis revealed a decrease in the levels of some of the proteins detected by the anti-Zif268 antibody in the antisense-infused group; no change was detected by the anti-c-Fos antibody among the groups. The outcome of this last experiment appeared inconclusive mainly because of the lack of specificity of the antibodies used (it was not possible to be certain if the bands detected on the blots were c-Fos or Zif268, one of their post-translational modifications or some other related protein). These antibodies are commonly used in immediate early gene immunohistochemical studies for detecting the expression of specific proteins in the brain. However the result of this experiment suggests that these antibodies are not specific enough to reliably detect just one protein, but they bind to many others, possibly to either the post-translational modifications of the protein of interest or to some related proteins (for example belonging to the same family). This confirms the importance of validating an experimental result using a variety of different techniques.

In Chapter 6 (Table 7-4), the effect of reducing the expression level of Zif268 in the retrosplenial cortex was tested using the object-in-place task. We decided to knock-down only Zif268 and not c-Fos levels because the previous Western blot experiment found a decrease only in protein levels detected by the anti-Zif268 antibody. The retrosplenial cortex is the most sensitive brain area to lesion within the Papez circuit in terms of loss of immediate early gene expression; thus it appears as the main area to be tested if a behavioural dysfunction is associated with that loss. No impairment was detected when animals were infused with the antisense Zif268 ODNs in comparison to missense infusions, and, in both cases, animals were able to perform the task (considering either the first or the total 3 minutes of test). In contrast, infusions

of muscimol into the retrosplenial cortex before the same object-in-place task significantly impaired performance in comparison to control infusions.

Finally, the levels of Zif268 expression in the retrosplenial cortex were analysed using immunohistochemistry in animals infused with either the antisense or missense *Zif268* ODNs and subsequently left free to explore a novel environment; two additional control groups were also used for comparisons (an unoperated group that underwent the same behavioural testing and a naïve home-cage control group). The only significant outcome was an increase in the levels of Zif268 in rostral Rdg in the unoperated behavioural control group in comparison to the missense-infused group. However, there were issues with the quality of the staining, so these findings would need to be replicated.

As a main conclusion, this piece of work adds to the evidence that lesions in the medial diencephalon cause distal effects in the retrosplenial cortex, in terms of a decrease in immediate early gene expression. Specifically, it has been shown that, similarly to c-Fos levels, Zif268 levels also decrease in the retrosplenial cortex after mammillothalamic tract lesions. Lesions in the anterior thalamic nuclei cause the same hypoactivity in the retrosplenial cortex for both immediate early genes and they disrupt the induction of long-term depression in the superficial layers of the granular retrosplenial cortex (Garden et al., 2009). It would be interesting to assess whether this loss of long-term plasticity is present also after mammillothalamic tract lesions. However, in contrast to what was found after anterior thalamic lesions, mammillothalamic tract lesions did not appear able to induce a significant change in the dendritic microstructure of the retrosplenial neurones. This functional pathology at the level of the retrosplenial cortex after mammillothalamic tract lesions, thus, appears "covert", without a structural counterpart.

Regarding the lack of an effect of the antisense ODN infusions in Chapter 5 and 6, the main issue was the difficulty in establishing at the molecular level the efficacy of the infusions as both the Western blot experiment of Chapter 5 and the immunohistochemical experiment of Chapter 6 gave unreliable results. In the case of the Western blot experiment, one additional finding was the non-specificity of the antibodies used to measure c-Fos and Zif268 levels. This is quite relevant when these antibodies are used in immediate early gene experiments to verify the expression of those specific proteins in different areas within the brain. The issue arises once those immediate early genes are not considered just as mere markers of neuronal activity,

but also as proteins with a specific function inside the neurones. For example, those experiments in which c-Fos and Zif268 changes of expression levels detected through immunohistochemical techniques are correlated with memory processes; if the antibodies used do not bind just to the target molecules but also to other related proteins, it is difficult to sustain the significance of those correlations. For those reasons it is important to support the findings of immunohistochemical immediate early gene studies with complementary techniques, able to assess the same phenomenon from a different perspective. For example, using *in situ* hybridization, a technique that uses nucleic acidic probes to recognise specific mRNA strands, thus avoiding the complications related with the use of antibodies. Also the use of specific transgenic and/or knock-out mice could be informative in assessing a putative role of the immediate early genes on spatial memory processes. Different mice lines have been created that would allow further investigation of c-Fos and Zif268 overexpression or lack of expression: e.g. transgenic c-Fos line (Robertson et al, 1995), knock out c-Fos line (Fleischmann et al, 2003), transgenic Zif268 line (Penke et al, 2014), Zif268 knock-out line (Topilko et al, 1997).

From the experiments reported in this thesis, it would appear that the infusion of antisense ODNs in the retrosplenial cortex did not disrupt spatial memory performance on a specific behavioural task. The importance of immediate early gene expression into the retrosplenial cortex has also been investigated in a recent set of experiments that have assessed the effects of environmental enrichment on spatial memory performance of rats with anterior thalamic lesions. After about 1 month of housing in enriched home-cages, these animals partially recovered their ability to perform a reinforced T-maze alternation task and a radial arm maze task sensitive to anterior thalamic and retrosplenial cortical lesions. However, in the same animals, no restoration of c-Fos and Zif268 expression levels was detected in the retrosplenial cortex (Loukavenko, Wolff, Poirier, & Dalrymple-Alford, 2015; Mercer, 2015) suggesting that memory improvements after anterior thalamic lesions do not require an increase of immediate early gene expression in the retrosplenial cortex back to normal levels. From this finding, it could be inferred that reduced c-Fos and Zif268 expression in the retrosplenial cortex does not have any detrimental effect on spatial memory. However, it is also possible that the improvements observed in those enriched animals were mediated by regions other than the retrosplenial cortex and reflected a level of compensation within the system. Furthermore, the observed spatial memory improvements were partial and not consistent across all behavioural tasks: for example, the enriched lesioned animals were as impaired as the non-

enriched lesioned group on a water-maze task (Mercer, 2015). Immediate early gene functionality within the retrosplenial cortex could then be necessary for a complete restoration of spatial memory behaviour.

Thus, there is still no definitive conclusion regarding the functional importance of the reduction in c-Fos and Zif268 expression in the retrosplenial cortex after medial diencephalic lesions. Further investigations are then required. A possible experiment that would be able to investigate the phenomenon with a different approach to the one exposed in this thesis would be lesioning the medial diencephalon (either the anterior thalamic nuclei or the mammillothalamic tract) in one hemisphere and knocking-down c-Fos and Zif268 expression levels in the retrosplenial cortex in the other hemisphere through antisense ODN infusions. In this way, a decrease of immediate early gene expression would be induced bilaterally, but on one side it would be possible to experimentally control the temporal pattern of the decrease, making its relevance for spatial memory processes amenable to be tested.

Finally, another interesting approach would be recording directly electrical activity within the retrosplenial cortex *in vivo* after medial diencephalic lesions. In particular, measuring the activity of those retrosplenial neurones that show a marked decrease in immediate early gene expression levels after lesions of the medial diencephalon; this would determine the extent to which these cells are abnormally functioning and shed light on the origin of the retrosplenial covert pathology.

CHAPTER	EXPERIMENT	OUTCOMES
2	Zif268 imaging in the Papez circuit after MTT lesions.	Levels of Zif268 significantly reduced in the retrosplenial subregions Rgb and Rdg of the MTT-lesioned animals in comparison to controls. No significant change in the other regions examined (dorsal HPC, ParaSub, PreSub, PostSub, IL, PL and ACC).
3 [analysis of dendritic microstructure in Rgb after MTT lesions]	Analysis of complexity of apical and basal dendritic arbors of small pyramidal neurones located in the superficial layers of Rgb.	No significant difference between MTT-lesioned animals and controls.
	Spine density measurement on the apical dendrites of small pyramidal neurones located in the superficial layers of Rgb.	No difference between MTT-lesioned animals and controls, also considering different spine shapes (thin, mushroom, stubby and other).

Table 6-2. Summary of results of the experiments described in Chapters 2 and 3. ACC = anterior cingulate cortex; HPC = hippocampus; IL = infralimbic cortex; MTT = mammillothalamic tract; ParaSub = parasubiculum; PostSub = postsubiculum; PreSub = presubiculum; PL = prelimbic cortex.

CHAPTER	EXPERIMENT	OUTCOMES
4/(exp 1) [3h-RAM pilot]	Piloting of a modified version of the radial arm maze task (3h-RAM).	Animals able to learn the task gradually, inserting increasing time delays in the middle of the task (one minute, five minutes, one hour and three hours).
	Muscimol infusions (0.5 µl/infusion site) into the dorsal HPC 30 min before the beginning of the 3h-RAM.	No impairment after muscimol infusions in comparison to performance with no infusion.
4/(exp 2) [dorsal HPC cannulations and infusions optimisation]	Muscimol infusions into the dorsal HPC 30 min before 1min-RAM (two different muscimol doses), continuous alternation T-maze task and standard T-maze task.	Significant impairment in comparison to performance with no infusion only when animals were tested on the 1min-RAM and infused with the highest dose of muscimol (1 µl/infusion site). No effect in all the other tests (0.5 µl/infusion site).
4/(exp 3) [dorsal HPC cannulations and infusions optimisation]	Muscimol infusions (0.3 µl/infusion site) into the dorsal HPC 30 min before standard T-maze task and 1min-RAM	Significant impairment after muscimol infusions in comparison to performance after PBS infusions in both the standard T-maze task and in the 1min-RAM.

Table 6-3. Summary of results of the experiments described in Chapter 4. 3h-RAM =modified version of the radial arm maze task with a 45 ° maze rotation and a 3-hour time delay inserted after the first four arm choices; 1min-RAM =modified version of the radial arm maze task with a 45 ° maze rotation and a 1-minute time delay inserted after the first four arm choices; HPC = hippocampus; PBS = phosphate-buffered saline.

CHAPTER	EXPERIMENT	OUTCOMES
5/(I) [dorsal HPC infusions of antisense *c-Fos* and *Zif268* ODNs and effect on spatial memory tasks]	Antisense *Zif268* ODNs infusions into the dorsal HPC 90 min before 3h-RAM.	No impairment in comparison to performance after PBS infusions
	Antisense *c-Fos* ODNs infusions into the dorsal HPC 90 min before 3h-RAM.	
	Cocktail antisense *Zif268/c-Fos* ODNs infusions into the dorsal HPC 90 min before 3h-RAM	
	Muscimol infusions (0.3 µl/infusion site) into the dorsal HPC 30 min before 3h-RAM.	Significant impairment in comparison to performance after PBS infusions
	Infusion of either cocktail antisense or missense *Zif268/c-Fos* ODNs into the dorsal HPC 90 min before 3h-object-in-place task.	No impairment in the animals infused with cocktail antisense ODNs in comparison to their performance after cocktail missense ODN infusions. All the animals were not able to discriminate the displaced objects from the non-displaced ones
5/(II) [dorsal HPC infusions of cocktail antisense *Zif268/c-Fos* ODNs and effect on c-Fos and Zif268 protein levels (Western blot)]	Infusion of either cocktail antisense or missense *Zif268* ODNs into the dorsal HPC 90 min before free exploration of a RAM in a novel room (+ unoperated home-cage animals).	Significant decrease in the levels of Zif268 in the group infused with the cocktail antisense in two of the bands detected by the anti-Zif268 antibody. No difference for any of the bands associated with anti-c-Fos antibody.

Table 6-4. Summary of results of the experiments described in Chapter 5. 3h-object-in-place task = object-in-place task with a 3-hour delay inserted between the sample and the test phase; 3h-RAM =modified version of the radial arm maze task with a 45 ° maze rotation and a 3-hour time delay inserted after the first four arm choices; HPC = hippocampus; ODNs = oligodeoxynucleotides; PBS = phosphate-buffered saline.

CHAPTER	EXPERIMENT	OUTCOMES
6/(I)	Infusions of muscimol into the RSC 30 min before 3h-object-in-place task.	Significant impairment after muscimol infusions in comparison to PBS infusions. The animals were able to discriminate between the displaced and non-displaced objects only after PBS infusions.
6/(II) [infusions of antisense or missense *Zif268* ODNs into the RSC and effect on spatial memory and on Zif268 protein levels (immunohistochemistry)]	Infusion of either antisense or missense *Zif268* ODNs into the RSC 90 min before 3h-object-in-place task.	No difference in performance on the objects-in-place task when animals were infused with the antisense *Zif268* ODNs or the missense *Zif268* ODNs. In both cases, animals were able to discriminate displaced and non-displaced objects.
	Infusion of either antisense or missense Zif268 ODNs into the RSC 90 min before free exploration of a RAM in a novel room (+ unoperated home-cage animals + unoperated behavioural control animals).	Levels of Zif268 significantly increased in the rostral Rdg of unoperated behavioural control group in comparison to the missense infused group.

Table 6-5. Summary of results of the experiments described in Chapter 6. 3h-object-in-place task = object-in-place task with a 3-hour delay inserted between the sample and the test phase; ODNs = oligodeoxynucleotides; PBS = phosphate-buffered saline; RAM = radial arm maze; RSC = retrosplenial cortex.

References

Aggleton, J. P. (2008). Understanding anterograde amnesia: disconnections and hidden lesions. *Quarterly Journal of Experimental Psychology*, *61*(10), 1441–1471.

Aggleton, J. P., & Brown, M. W. (1999). Episodic memory, amnesia, and the hippocampal-anterior thalamic axis. *The Behavioral and Brain Sciences*, *22*(3), 425–444; discussion 444–489.

Aggleton, J. P., & Brown, M. W. (2005). Contrasting hippocampal and perirhinal cortex function using immediate early gene imaging. *The Quarterly Journal of Experimental Psychology. B, Comparative and Physiological Psychology*, *58*(3-4), 218–233.

Aggleton, J. P., Hunt, P. R., Nagle, S., & Neave, N. (1996). The effects of selective lesions within the anterior thalamic nuclei on spatial memory in the rat. *Behavioural Brain Research*, *81*, 189–198.

Aggleton, J. P., Hunt, P. R., & Rawlins, J. N. P. (1986). The effects of hippocampal lesions upon spatial and non-spatial tests of working memory. *Behavioural Brain Research*, *19*, 133–146.

Aggleton, J. P., Hunt, P. R., & Shaw, C. (1990). The effects of mammillary body and combined amygdalar-fornix lesions on tests of delayed non-matching-to-sample in the rat. *Behavioural Brain Research*, *40*, 145–157.

Aggleton, J. P., Keith, A. B., & Sahgal, A. (1991). Both fornix and anterior thalamic, but not mammillary, lesions disrupt delayed non-matching-to-position memory in rats. *Behavioural Brain Research*, *44*(2), 151–161.

Aggleton, J. P., McMackin, D., Carpenter, K., Hornak, J., Kapur, N., Halpin, S., … Gaffan, D. (2000). Differential cognitive effects of colloid cysts in the third ventricle that spare or compromise the fornix. *Brain : A Journal of Neurology*, *123*, 800–815.

Aggleton, J. P., Neave, N., Nagle, S., & Hunt, P. R. (1995). A comparison of the effects of anterior thalamic , mamillary body and fornix lesions on reinforced spatial alternation. *Behavioural Brain Research*, *68*, 91–101.

Aggleton, J. P., Neave, N., Nagle, S., & Sahgal, A. (1995). A Comparison of the Effects of Medial Prefrontal , Cingulate Cortex , and Cingulum Bundle Lesions on Tests of Spatial Memory : Evidence of a Double Dissociation between Frontal and Cingulum Bundle Contributions. *The Journal of Neuroscience*, *15*, 7270–7281.

Aggleton, J. P., & Nelson, A. D. (2014). Why do lesions in the rodent anterior thalamic nuclei cause such severe spatial deficits? *Neuroscience & Biobehavioral Reviews*, *54*, 131–144.

Aggleton, J. P., O'Mara, S. M., Vann, S. D., Wright, N. F., Tsanov, M., & Erichsen, J. T. (2010). Hippocampal-anterior thalamic pathways for memory: Uncovering a network of direct and indirect actions. *European Journal of Neuroscience*, *31*(12), 2292–2307.

Aggleton, J. P., Poirier, G. L., Aggleton, H. S., Vann, S. D., & Pearce, J. M. (2009). Lesions of the fornix and anterior thalamic nuclei dissociate different aspects of hippocampal-dependent spatial learning: implications for the neural basis of scene learning. *Behavioral Neuroscience*, *123*(3), 504–519.

Aggleton, J. P., & Saunders, R. C. (1997). The relationships between temporal lobe and diencephalic structures implicated in anterograde amnesia. *Memory*, *5*, 49–71.

Ahn, S., Huang, C.-L., Ozkumur, E., Zhang, X., Chinnala, J., Yalcin, A., … Irani, R. J. (2012). TATA binding proteins can recognize nontraditional DNA sequences. *Biophysical Journal*, *103*(7), 1510–1517.

Albasser, M. M., Poirier, G. L., Warburton, E. C., & Aggleton, J. P. (2007). Hippocampal lesions halve immediate-early gene protein counts in retrosplenial cortex: distal dysfunctions in a spatial memory system. *The European Journal of Neuroscience*, *26*(5), 1254–1266.

Alberini, C. M. (2009). Transcription factors in long-term memory and synaptic plasticity. *Physiological Reviews*, *89*(1), 121–145.

Albo, Z., Di Prisco, G. V, & Vertes, R. P. (2003). Anterior thalamic unit discharge profiles and coherence with hippocampal theta rhythm. *Thalamus and Related Systems*, *2*(2), 133–144.

Allen, G. V, & Hopkins, D. A. (1988). Mamillary body in the rat: a cytoarchitectonic, Golgi, and ultrastructural study. *The Journal of Comparative Neurology*, *275*(1), 39–64.

Allen, G. V, & Hopkins, D. A. (1989). Mamillary body in the rat: topography and synaptology of projections from the subicular complex, prefrontal cortex, and midbrain tegmentum. *The Journal of Comparative Neurology*, *286*(3), 311–336.

Allen, G. V, & Hopkins, D. A. (1990). Topography and Synaptology of Mammillary Body projections to the Mesencephalon and Pons in the Rat. *The Journal of Comparative Neurology*, *301*, 214–231.

Amaral, D. G. (1993). Emerging principles of intrinsic hippocampal organisation. *Current Opinion in Neurobiology*, *3*, 225–229.

Amin, E., Pearce, J. M., Brown, M. W., & Aggleton, J. P. (2006). Novel temporal configurations of stimuli produce discrete changes in immediate-early gene expression in the rat hippocampus. *The European Journal of Neuroscience*, *24*(9), 2611–2621.

Amin, E., Wright, N., Poirier, G. L., Thomas, K. L., Erichsen, J. T., & Aggleton, J. P. (2010). Selective lamina dysregulation in granular retrosplenial cortex (area 29) after anterior thalamic lesions: an in situ hybridization and trans-neuronal tracing study in rats. *Neuroscience*, *169*(3), 1255–1267.

Arikan, R., Blake, N. M. J., Erinjeri, J. P., Woolsey, T. A., Giraud, L., & Highstein, S. M. (2002). A method to measure the effecti v e spread of focally injected muscimol into the central ner v ous system with electrophysiology and light microscopy. *Journal of Neuroscience Methods*, *118*, 51–57.

Babb, S. J., & Crystal, J. D. (2005). Discrimination of what, when, and where: Implications for episodic-like memory in rats. *Learning and Motivation*, *36*, 177–189.

Baird, A. J., Futter, J. E., Muir, J. L., & Aggleton, J. P. (2004). On the transience of egocentric working memory: evidence from testing the contribution of limbic brain regions. *Behavioral Neuroscience*, *118*(4), 785–97.

Bannerman, D. M., Yee, B. K., Good, G. A., Heupel, M. J., Iversen, S. D., & Rawlins, J. N. P. (1999). Double dissociation of function within the hippocampus: A comparison of dorsal, ventral, and complete hippocampal cytotoxic lesions. *Behavioral Neuroscience*, *113*(6), 1170–1188. doi:10.1037/0735-7044.113.6.1170

Barbizet, J., & Jardine, D. K. (1971). *Human memory and its pathology*. W.H.Freeman.

Barbosa, F. F., Santos, J. R., Meurer, Y. S. R., Macêdo, P. T., Ferreira, L. M. S., Pontes, I. M. O., … Silva, R. H. (2013). Differential Cortical c-Fos and Zif-268 Expression after Object and Spatial Memory Processing in a Standard or Episodic-Like Object Recognition Task. *Frontiers in Behavioral Neuroscience*, *7*(August), 1–12.

Barker, G. R. I., & Warburton, E. C. (2011). When is the hippocampus involved in recognition memory? *The Journal of Neuroscience*, *31*(29), 10721–10731.

Bassant, M. H., & Poindessous-Jazat, F. (2001). Ventral tegmental nucleus of Gudden: A pontine hippocampal theta generator? *Hippocampus*, *11*(6), 809–813.

Bassett, J. P., Tullman, M. L., & Taube, J. S. (2007). Lesions of the tegmentomammillary circuit in the head direction system disrupt the head direction signal in the anterior thalamus. *The Journal of Neuroscience*, *27*(28), 7564–7577.

Becker, J. T., Walker, J. A., & Olton, D. S. (1980). Neuroanatomical bases of spatial memory. *Brain Research*, *200*, 307–320.

Beracochea, D. J., & Jaffard, R. (1990). Effects of Ibotenic Lesions of Mammillary Bodies on Spontaneous and Rewarded Spatial Alternation in Mice. *Journal of Cognitive Neuroscience*, *2*(2), 133–140.

Beracochea, D. J., & Jaffard, R. (1987). Impairment of spontaneous alternation behavior in sequential test procedures following mammillary body lesions in mice: evidence for time-dependent interference-related memory deficits. *Behavioral Neuroscience*, *101*(2), 187–197.

Beracochea, R., Micheau, J., & Jaffard, D. J. (1995). Alteration of cortical and hippocampal cholinergic activities following lesion of the mammillary bodies in mice. *Brain Research*, *670*, 53–58.

Blackstad, T. W. (1956). Commissural connections of the hippocampal region in the rat, with special reference to their mode of termination. *The Journal of Comparative Neurology*, *105*, 417–537.

Blair, H. T., Cho, J., & Sharp, P. E. (1998). Role of the lateral mammillary nucleus in the rat head direction circuit: A combined single unit recording and lesion study. *Neuron*, *21*(6), 1387–1397.

Bonham, M. A., Brown, S., Boyd, A. L., Brown, P. H., Bruckenstein, D. A., Hanvey, J. C., … Bisi, J. E. (1995). An assessment of the antisense properties of RNase H-competent and steric-blocking oligomers. *Nucleic Acids Research*, *23*(7), 1197–1203.

Borst, J. G., Leung, L. W., & MacFabe, D. F. (1987). Electrical activity of the cingulate cortex. II. Cholinergic modulation. *Brain Research*, *407*(1), 81–93.

Bourne, & Harris. (2007). Do thin spines learn to be mushroom spines that remember? *Current Opinion in Neurobiology*, *17*(3), 381–6.

Bozon, B., Davis, S., & Laroche, S. (2002). Regulated transcription of the immediate-early gene Zif268: mechanisms and gene dosage-dependent function in synaptic plasticity and memory formation. *Hippocampus*, *12*(5), 570–577.

Bozon, B., Kelly, A., Josselyn, S. A., Silva, A. J., Davis, S., & Laroche, S. (2003). MAPK, CREB and zif268 are all required for the consolidation of recognition memory. *Philosophical Transactions of the Royal Society of London. Series B, Biological Sciences*, *358*(1432), 805–814.

Bulley, S. J., Drew, J. G., & Morton, A. J. (2012). Direct Visualisation of Abnormal Dendritic Spine Morphology in the Hippocampus of the R6/2 Transgenic Mouse Model of Huntington's Disease. *Journal of Huntington's Disease*, *1*, 267–273.

Bullitt, E. (1990). Expression of C-fos-Like Protein as a Marker for Neuronal Activity Following Noxious Stimulation in the Rat. *The Journal of Comparative Neurology*, *296*, 517–530.

Burgess, N., & O'Keefe, J. (2011). Models of place and grid cell firing and theta rhythmicity. *Current Opinion in Neurobiology*, *21*(5), 734–744.

Bussey, T. J., Duck, J., Muir, J. L., & Aggleton, J. P. (2000). Distinct patterns of behavioural impairments resulting from fornix transection or neurotoxic lesions of the perirhinal and postrhinal cortices in the rat. *Behavioural Brain Research*, *111*(1-2), 187–202.

Byatt, G., & Dalrymple-Alford, J. C. (1996). Both anteromedial and anteroventral thalamic lesions impair radial-maze learning in rats. *Behavioral Neuroscience*, *110*(6), 1335–1348.

Camacho-Abrego, I., Tellez-Merlo, G., Melo, A. I., Rodríguez-Moreno, A., Garcés, L., De La Cruz, F., … Flores, G. (2014). Rearrangement of the dendritic morphology of the neurons from prefrontal cortex and hippocampus after subthalamic lesion in Sprague-Dawley rats. *Synapse*, *68*(3), 114–26.

Carlesimo, G. A., Lombardi, M. G., & Caltagirone, C. (2011). Vascular thalamic amnesia: A reappraisal. *Neuropsychologia*, *49*(5), 777–789.

Carlesimo, G. A., Serra, L., Fadda, L., Cherubini, A., Bozzali, M., & Caltagirone, C. (2007). Bilateral damage to the mammillo-thalamic tract impairs recollection but not familiarity in the recognition process: a single case investigation. *Neuropsychologia*, *45*(11), 2467–2479.

Cassel, J. C., Cassel, S., Galani, R., Kelche, C., Will, B., & Jarrard, L. (1998). Fimbria-fornix vs selective hippocampal lesions in rats: effects on locomotor activity and spatial learning and memory. *Neurobiology of Learning and Memory*, *69*, 22–45.

Célérier, A., Ognard, R., Decorte, L., & Beracochea, D. (2000). Deficits of spatial and non-spatial memory and of auditory fear conditioning following anterior thalamic lesions in mice: Comparison with chronic alcohol consumption. *European Journal of Neuroscience*, *12*(7), 2575–2584.

Chan, J. H. P., Lim, S., & Wong, W. S. F. (2006). Antisense oligonucleotides: from design to therapeutic application. *Clinical and Experimental Pharmacology and Physiology*, *33*(February), 533–540.

Chaudhuri, A. (1997). Neural activity mapping with inducible trancription factors. *NeuroReport*, *8*(13).

Chen, J., Pan, H., Lipsky, R. H., Pérez-Gómez, A., Cabrera-Garcia, D., Fernández-Sánchez, M. T., … Marini, A. M. (2011). Cellular and molecular responses of cultured neurons to stressful stimuli. *Dose-Response*, *9*(3), 416–433.

Chen, L. L., Green, E. J., Barnes, C. A., & McNaughton, B. L. (1994). Head-direction cells in the rat posterior cortex - I . anatomical distribution and behavioral modulation. *Experimental Brain Research*, *101*, 8–23.

Chiasson, B. J., Armstrong, J. N., Hooper, M. L., Murphy, P. R., & Robertson, H. A. (1994). The application of antisense oligonucleotide technology to the brain: Some pitfalls. *Cellular and Molecular Neurobiology*, *14*(5), 507–521.

Child, N. D., & Benarroch, E. E. (2013). Functional organization and clinical implications. *Neurology*, *81*(21), 1869–1876.

Chudasama, Y., Doobay, V. M., & Liu, Y. (2012). Hippocampal-Prefrontal Cortical Circuit Mediates Inhibitory Response Control in the Rat. *Journal of Neuroscience*, *32*(32), 10915–10924.

Cimadevilla, J. M., Miranda, R., López, L., & Arias, J. L. (2005). Partial unilateral inactivation of the dorsal hippocampus impairs spatial memory in the MWM. *Cognitive Brain Research*, *25*(3), 741–746.

Cirelli, C., Pompeiano, M., & Tononi, G. (1995). In vivo antisense approaches to the role of immediate early gene expression in the brain. *Regulatory Peptides*, *59*(2), 151–162.

Clark, B. J., Rice, J. P., Akers, K. G., Candelaria-Cook, F. T., Taube, J. S., & Hamilton, D. A. (2013). Lesions of the dorsal tegmental nuclei disrupt control of navigation by distal landmarks in cued, directional, and place variants of the Morris water task. *Behavioral Neuroscience*, *127*(4), 566–81.

Clarke, S., Assal, G., Bogousslavsky, J., Regli, F., Townsend, D. W., Leenders, K. L., & Blecic, S. (1994). Pure amnesia after unilateral left polar thalamic infarct: topographic and sequential neuropsychological and metabolic (PET) correlations. *Journal of Neurology, Neurosurgery, and Psychiatry*, *57*, 27–34.

Clayton, D. F. (2000). The genomic action potential. *Neurobiology of Learning and Memory*, *74*(3), 185–216.

Clayton, N. S., Griffiths, D. P., Emery, N. J., & Dickinson, a. (2001). Elements of episodic-like memory in animals. *Philosophical Transactions of the Royal Society of London. Series B, Biological Sciences*, *356*(1413), 1483–1491.

Clayton, N. S., Salwiczek, L. H., & Dickinson, A. (2007). Episodic memory. *Current Biology*, *17*(6), 189–191.

Colchester, A., Kingsley, D., Lasserson, D., Kendall, B., Bello, F., Rush, C., … Kopelman, M. D. (2001). Structural MRI volumetric analysis in patients with organic amnesia, 1: methods and comparative finidings across diagnostic groups. *Journal of Neurology, Neurosurgery, and Psychiatry*, *71*(1), 13–33.

Comeau, W. L., McDonald, R. J., & Kolb, B. E. (2010). Learning-induced alterations in prefrontal cortical dendritic morphology. *Behavioural Brain Research*, *214*, 91–101.

Conde', F., Audinat, E., Maire-Lepoivre, E., & Crepel, F. (1990). Afferent Connections of the Medial Frontal Cortex of the Rat . A Study Using Retrograde Transport of Fluorescent Dyes . I . Thalamic Afferents. *Brain Research Bulletin*, *24*, 341–354.

Cooper, B. G., Manka, T. F., & Mizumori, S. J. (2001). Finding your way in the dark: The retrosplenial cortex contributes to spatial memory and navigation without visual cues. *Behavioral Neuroscience*, *115*(5), 1012–1028.

Cooper, B. G., & Mizumori, S. J. Y. (1999). Retrosplenial cortex inactivation selectively impairs navigation in darkness. *Learning and Memory*, *10*(3), 625–630.

Cooper, B. G., & Mizumori, S. J. Y. (2001). Temporary Inactivation of the Retrosplenial Cortex Causes a Transient Reorganization of Spatial Coding in the Hippocampus. *The Journal of Neuroscience*, *21*(11), 3986–4001.

Corcoran, K., Desmond, T., Frey, K., & Maren, S. (2005). Hippocampal inactivation disrupts the acquisition and contextual encoding of fear extinction. *The Journal of Neuroscience*, *25*(39), 8978–2987.

Corcoran, K., & Maren, S. (2001). Hippocampal Inactivation Disrupts Contextual Retrieval of Fear Memory after Extinction. *The Jounal of Neuroscience*, *21*(5), 1720–1726.

Countryman, R. A., Kaban, N. L., & Colombo, P. J. (2005). Hippocampal c-fos is necessary for long-term memory of a socially transmitted food preference. *Neurobiology of Learning and Memory*, *84*(3), 175–183.

Cruce, J. A. F. (1975). An autoradiographic study of the projections of the mammillothalamic tract in the rat. *Brain Research*, *85*, 211–219.

Cruce, J. A. F. (1977). An autoradiographic study of the descending connections of the mammillary nuclei of the rat. *The Journal of Comparative Neurology*, *176*(4), 631–644.

Curran, T., Miller, A. D., Zokas, L., & Verma, I. M. (1984). Viral and Cellular fos Proteins : A Comparative Analysis. *Cell*, *36*(February), 259–268.

Czerniawski, J., Yoon, T., & Otto, T. (2009). Dissociating space and trace in dorsal and ventral hippocampus. *Hippocampus*, *19*(1), 20–32.

D'Esposito, M., Verfaellie, M., Alexander, M. P., & Katz, D. I. (1995). Amnesia following traumatic bilateral fornix transection. *Neurology*, *45*(8), 1546–1550.

Davila, M. D., Shear, P. K., Lane, B., Sullivan, E. V, & Pfefferbaum, A. (1994). Mammillary body and cerebellar shrinkage in chronic alcoholics: An MRI and neuropsychological study. *Neuropsychology*, *8*(9), 433–444.

Davis, S., Bozon, B., & Laroche, S. (2003). How necessary is the activation of the immediate early gene zif268 in synaptic plasticity and learning? *Behavioural Brain Research*, *142*(1-2), 17–30.

Delay, J., & Brion, S. (1969). *Le Syndrome de Korsakoff*. Masson.

Dere, E., Huston, J. P., & De Souza Silva, M. A. (2005). Episodic-like memory in mice: Simultaneous assessment of object, place and temporal order memory. *Brain Research Protocols*, *16*(1-3), 10–19.

Dhanrajan, T. M., Lynch, M. A., Kelly, A., Popov, V. I., Rusakov, D. A., & Stewart, M. G. (2004). Expression of long-term potentiation in aged rats involves perforated synapses but dendritic spine branching results from high-frequency stimulation alone. *Hippocampus*, *14*(2), 255–264. doi:10.1002/hipo.10172

Dias, N., & Stein, C. A. (2002). Antisense Oligonucleotides : Basic Concepts and Mechanisms Minireview Antisense Oligonucleotides : Basic Concepts and Mechanisms. *Molecular Cancer Therapeutics*, *1*, 347–355.

Dillingham, C. M., Erichsen, J. T., O'Mara, S. M., Aggleton, J. P., & Vann, S. D. (2015). Fornical and nonfornical projections from the rat hippocampal formation to the anterior thalamic nuclei. *Hippocampus*, *16*, 1–16.

Dillingham, C. M., Holmes, J. D., Wright, N. F., Erichsen, J. T., Aggleton, J. P., & Vann, S. D. (2015). Calcium-binding protein immunoreactivity in Gudden's tegmental nuclei and the hippocampal formation: differential co-localization in neurons projecting to the mammillary bodies. *Frontiers in Neuroanatomy*, *9*(August), 1–15.

Dix, S. L., & Aggleton, J. P. (1999). Extending the spontaneous preference test of recognition: evidence of object-location and object-context recognition. *Behavioural Brain Research*, *99*(2), 191–200.

Dixon, G., Garrick, T., Whiteman, I., Sarris, M., Sithamparanathan, S., & Harper, C. G. (2004). Characterization of gabaergic neurons within the human medial mamillary nucleus. *Neuroscience*, *127*(2), 365–372. doi:10.1016/j.neuroscience.2004.05.009

Douglas, R. J. (1966). Cues for spontaneous alternation. *Journal of Comparative and Physiological Psychology*, *62*(2), 171–183.

Dragunow, M., Abraham, W. C., Goulding, M., Mason, S. E., Robertson, H. A., & Faull, R. L. M. (1989). Long-term potentiation and the induction of c-fos mRNA and proteins in the dentate gyrus of unanesthetized rats. *Neuroscience Letters*, *101*, 274–280.

Dragunow, M., & Faull, R. (1989). The use of c-fos as a metabolic marker in neuronal pathway tracing. *Journal of Neuroscience Methods*, *29*, 261–265.

Dudchenko, P. A. (2001). How do animals actually solve the T maze? *Behavioral Neuroscience*, *115*(4), 850–860.

Dudchenko, P. A., & Davidson, M. (2002). Rats use a sense of direction to alternate on T-mazes located in adjacent rooms. *Animal Cognition*, *5*, 115–118.

Dudchenko, P. A., Wood, E. R., & Eichenbaum, H. (2000). Neurotoxic Hippocampal Lesions Have No Effect on Odor Span and Little Effect on Odor Recognition Memory But Produce Significant Impairments on Spatial Span , Recognition , and Alternation. *The Journal of Neuroscience*, *20*(8), 2964–2977.

Dumitriu, D., Rodriguez, A., & Morrison, J. H. (2013). High throughput, detailed, cell-specific neuroanatomy of dendritic spines using microinjections and confocal microscopy. *Nature Protocols*, *6*(9), 1391–1411.

Dumont, J. R., Amin, E., Poirier, G. L., Albasser, M. M., & Aggleton, J. P. (2012). Anterior thalamic nuclei lesions in rats disrupt markers of neural plasticity in distal limbic brain regions. *Neuroscience*, *224*, 81–101.

Dupire, A., Kant, P., Mons, N., Marchand, A. R., Coutureau, E., Dalrymple-Alford, J., & Wolff, M. (2013). A role for anterior thalamic nuclei in affective cognition: interaction with environmental conditions. *Hippocampus*, *23*(5), 392–404.

Dusoir, H., Kapur, N., Byrnes, D. P., McKinstry, S., & Hoare, R. D. (1990). The role of diencephalic pathology in human memory disorder. Evidence from a penetrating paranasal brain injury. *Brain*, *113*, 1695–1706.

Dwyer, J. a, Ingram, M. L., Snow, A. C., Thorpe, C. M., Martin, G. M., & Skinner, D. M. (2013). The Effects of Bilateral Lesions to the Dorsal Tegmental Nucleus on Spatial Learning in Rats. *Behavioral Neuroscience*, *127*(6), 867–877.

Edeline, J.-M., Hars, B., Hennevin, E., & Cotillon, N. (2002). Muscimol diffusion after intracerebral microinjections: a reevaluation based on electrophysiological and autoradiographic quantifications. *Neurobiology of Learning and Memory*, *78*(1), 100–124.

Engelhordt, E., & Da Mota Gomes, M. (2013). Shock, diaschisis and von Monakow. *Arquivos de Neuro-Psiquiatria*, *71*(7), 487–489.

Fadda, F., Cocco, S., & Stancampiano, R. (2000). Hippocampal acetylcholine release correlates with spatial learning performance in freely moving rats. *NeuroReport*, *11*(10), 2265–2269.

Fazio, F., Perani, D., Gilardi, M. C., Colombo, F., Cappa, S. F., Vallar, G., … Lenzi, G. L. (1992). Metabolic Impairment in Human Amnesia : A PET Study of Memory Networks. *Journal of Cerebral Blood Flow and Metabolism*, *12*, 353–358.

Feeney, D. M., & Baron, J.-C. (1986). Diaschisis. *Stroke*, *17*(5), 817–830.

Fenton, A. A., & Bures, J. (1993). Place navigation in rats with unilateral tetrodotoxin inactivation of the dorsal hippocampus: Place but not procedural learning can be lateralized to one hippocampus. *Behavioural Neuroscience*, *107*(4), 552–564.

Fiala, J. C., Feinberg, M., Popov, V., & Harris, K. M. (1998). Synaptogenesis Via Dendritic Filopodia in Developing Hippocampal Area CA1. *The Journal of Neuroscience*, *18*(21), 8900–8911.

Field, T. D., Rosenstock, J., King, E. C., & Greene, E. (1978). Behavioral role of the mammillary efferent system. *Brain Research Bulletin*, *3*(5), 451–456.

Finger, S., Koehler, P. J., & Jagella, C. (2014). The Monakow Concept of Diaschisis. *History of Neurology*, *61*, 283–288.

Flavell, S. W., & Greenberg, M. E. (2008). Signaling mechanisms linking neuronal activity to gene expression and plasticity of the nervous system. *Annual Review of Neuroscience*, *31*, 563–590.

Fleischmann, A., Hvalby, O., Jensen, V., Strekalova, T., Zacher, C., Layer, L. E., Kvello, A., Reschke, M., Spanagel, R., Sprengel, R., Wagner, E. F., & Grass, P. (2003). Impaired long-term memoryand N2RA-type NMDA receptor-dependent synaptic plasticity in mice lacking c-Fos in the CNS. *The Journal of Neuroscience*, *23*(27), 9116–9122.

Foster, B. L., Kaveh, A., Dastjerdi, M., Miller, K. J., & Parvizi, J. (2013). Human retrosplenial cortex displays transient theta phase locking with medial temporal cortex prior to activation during autobiographical memory retrieval. *The Journal of Neuroscience*, *33*(25), 10439–10446.

Freed, D. M., Corkin, S., & Cohen, N. J. (1987). Forgetting in H.M.: a second look. *Neuropsychologia*, *25*(3), 461–471.

French, P. J., O'Connor, V., Jones, M. W., Davis, S., Errington, M. L., Voss, K., … Bliss, T. V. (2001). Subfield-specific immediate early gene expression associated with hippocampal long-term potentiation in vivo. *The European Journal of Neuroscience*, *13*(5), 968–976.

Fritts, M. E., Asbury, E. T., Horton, J. E., & Isaac, W. L. (1998). Medial prefrontal lesion deficits involving or sparing the prelimbic area in the rat. *Physiology & Behavior*, *64*(3), 373–380.

Futter, J. E., & Aggleton, J. P. (2006). How rats perform spatial working memory tasks: limitations in the use of egocentric and idiothetic working memory. *Quarterly Journal of Experimental Psychology*, *59*(1), 77–99.

Gabriel, M., Lambert, R. W., Foster, K., Orona, E., Sparenborg, S., & Maiorca, R. R. (1983). Anterior Thalamic Lesions and Neuronal Activity in the Cingulate and Retrosplenial Cortices During Discriminative Avoidance Behavior in Rabbits. *Behavioural Neuroscience*, *97*(5), 675–696.

Gaffan, D., & Gaffan, E. A. (1991). Amnesia in man following transection of the fornix. A review. *Brain*, *114*, 2611–2618.

Gaffan, E. A., Gaffan, D., & Hodges, J. R. (1991). Amnesia following damage to the left fornix and to other sites. A comparative study. *Brain*, *114*, 1297–1313.

Galani, R., Lehmann, O., Bolmont, T., Aloy, E., Bertrand, F., Lazarus, C., … Cassel, J.-C. (2002). Selective immunolesions of CH4 cholinergic neurons do not disrupt spatial memory in rats. *Physiology & Behavior*, *76*(1), 75–90.

Gan, W.-B., Grutzendler, J., Wong, W. T., Wong, R. O. L., & Lichtman, J. W. (2000). Multicolor " DiOlistic " Labeling Lipophilic Dye Combinations. *Neurotechnique*, *27*, 219–225.

Garcia-Bengochea, F., & Friedman, W. A. (1987). Persistent memory loss following section of the anterior fornix in humans. A historical review. *Surgical Neurology*, *27*(4), 361–364.

Garden, D. L. F., Massey, P. V, Caruana, D. A., Johnson, B., Warburton, E. C., Aggleton, J. P., & Bashir, Z. I. (2009). Anterior thalamic lesions stop synaptic plasticity in retrosplenial cortex slices: expanding the pathology of diencephalic amnesia. *Brain*, *132*(Pt 7), 1847–1857.

Gass, P., Herdegen, T., Bravo, R., & Kiessling, M. (1992). Induction of immediate early gene encoded proteins in the rat hippocampus after bicucculine-induced seizures: differential expression of Krox-24, Fos and Jun proteins. *Neuroscience*, *48*(2), 315–324.

Gheidi, A., Azzopardi, E., Adams, A. A., & Marrone, D. F. (2013). Experience-dependent persistent expression of zif268 during rest is preserved in the aged dentate gyrus. *BMC Neuroscience*, *14*(1), 100.

Ginty, D. D. (1997). Calcium regulation of gene expression: Isn't that spatial? *Neuron*, *18*(2), 183–186.

Goh, J. J., & Manahan-Vaughan, D. (2013). Spatial object recognition enables endogenous LTD that curtails LTP in the mouse hippocampus. *Cerebral Cortex*, *23*(5), 1118–1125.

Golgi, C. (1873). Sulla sostanza grigia del cervello. *Gazz. Med. Ital. Lombardia*, *6*, 244–246.

Gonzalo-Ruiz, A., Alonso, A., Sanz, J. M., & Llinas, R. R. (1992). Afferent projections to the mammillary complex of the rat, with special reference to those from surrounding hypothalamic regions. *Journal of Comparative Neurology*, *321*(2), 277–299.

Gonzalo-Ruiz, A., Morte, L., & Sanz, J. M. (1998). Glutamate/aspartate and leu-enkephalin immunoreactivity in mammillothalamic projection neurons of the rat. *Brain Research Bulletin*, *47*(6), 565–574.

Gonzalo-Ruiz, A., Romero, J. C., Sanz, J. M., & Morte, L. (1999). Localization of amino acids, neuropeptides and cholinergic neurotransmitter markers in identified projections from the mesencephalic tegmentum to the mammillary nuclei of the rat. *Journal of Chemical Neuroanatomy*, *16*(2), 117–133.

Good, M., & Honey, R. C. (1997). Dissociable effects of selective lesions to hippocampal subsystems on exploratory behavior, contextual learning, and spatial learning. *Behavioral Neuroscience*, *111*(3), 487–493.

Gottlieb, D. I., & Cowan, W. M. (1973). Autoradiographic Studies of the Commissural and Ipsilateral Association Connections of the Hippocampus and Dentate Gyrus of the Rat. *The Journal of Comparative Neurology*, *149*(4), 393–422.

Graff-Radford, N. R., Tranel, D., Van Hoesen, G. W., & Brandt, J. P. (1990). Diencephalic amnesia. *Brain*, *113*, 1–25.

Greene, E., & Naranjo, J. N. (1986). Thalamic role in spatial memory. *Behavioural Brain Research*, *19*(2), 123–131.

Grimm, R., Schicknick, H., Riede, I., Gundelfinger, E. D., Herdegen, T., Zuschratter, W., & Tischmeyer, W. (1997). Suppression of c-fos induction in rat brain impairs retention of a brightness discrimination reaction. *Learning & Memory*, *3*(5), 402–413.

Gurdjian, E. S. (1927). The diencephalon of the albino rat. *Journal of Comparative Neurology*, *43*(1), 1–114.

Guzowski, J. F. (2002). Insights into immediate-early gene function in hippocampal memory consolidation using antisense oligonucleotide and fluorescent imaging approaches. *Hippocampus*, *12*(1), 86–104. doi:10.1002/hipo.10010

Guzowski, J. F., Setlow, B., Wagner, E. K., & McGaugh, J. L. (2001). Experience-dependent gene expression in the rat hippocampus after spatial learning: a comparison of the immediate-early genes Arc, c-fos, and zif268. *The Journal of Neuroscience : The Official Journal of the Society for Neuroscience*, *21*(14), 5089–5098.

Hall, J., Thomas, K. L., & Everitt, B. J. (2000). Rapid and selective induction of BDNF expression in the hippocampus during contextual learning. *Nature Neuroscience*, *3*(6), 533–535.

Hallock, H., Arreola, A., Shaw, C., & Griffin, A. (2013). Dissociable roles of the dorsal striatum and dorsal hippocampus in conditional discrimination and spatial alternation T-maze tasks. *Neurobiology of Learning and Memory*, *100*, 108–116.

Harding, A., Halliday, G., Caine, D., & Kril, J. (2000). Degeneration of anterior thalamic nuclei differentiates alcoholics with amnesia. *Brain*, *123*, 141–154.

Harker, K. T., & Whishaw, I. Q. (2002). Impaired Spatial Performance in Rats with Retrosplenial Lesions : Importance of the Spatial Problem and the Rat Strain in Identifying Lesion Effects in a Swimming Pool. *The Journal of Neuroscience*, *22*(3), 1155–1164.

Harland, B. (2013). Recovery of function after lesions of the anterior thalamic nuclei: CA1 neuromorphology. *Ph.D. Thesis*, *Univerisity of Canterbury (New Zealand)*.

Harland, B. C., Collings, D. A., McNaughton, N., Abraham, W. C., & Dalrymple-Alford, J. C. (2014). Anterior thalamic lesions reduce spine density in both hippocampal CA1 and retrosplenial cortex, but enrichment rescues CA1 spines only. *Hippocampus*, *24*(10), 1232–47.

Harper, D. N., McLean, A. P., & Dalrymple-Alford, J. C. (1994). Forgetting in rats following medial septum or mammillary body damage. *Behavioral Neuroscience*, *108*(4), 691–702.

Harris, K. M., & Stevens, J. K. (1989). Dendritic Spines of CA1 Pyramidal Cells in the Rat Hippocampus : Serial Electron Microscopy with Reference to Their Biophysical Characteristics. *The Journal of Neuroscience*, *9*(8), 2982–2997.

Hayakawa, T., & Zyo, K. (1989). Retrograde double-labeling study of the mammillothalamic and the mammillotegmental projections in the rat. *The Journal of Comparative Neurology*, *284*(1), 1–11.

He, J., Yamada, K., & Nabeshima, T. (2002). A Role of Fos Expression in the CA3 Region of the Hippocampus in Spatial Memory Formation in Rats. *Neuropsychopharmachology*, *26*(2), 260–268.

Hebb, M. O., & Robertson, H. A. (1997). Coordinate suppression of striatal ngfi-a and c-fos produces locomotor asymmetry and up-regulation of IEGs in the globus pallidus. *Molecular Brain Research*, *48*(1), 97–106.

Heck, N., Betuing, S., Vanhoutte, P., & Caboche, J. (2012). A deconvolution method to improve automated 3D-analysis of dendritic spines: application to a mouse model of Huntington's disease. *Brain Structure & Function*, *217*, 421–34.

Henry, J., Petrides, M., St-Laurent, M., & Sziklas, V. (2004). Spatial conditional associative learning: effects of thalamo-hippocampal disconnection in rats. *Neuroreport*, *15*(15), 2427–2431.

Herdegen, T., & Leah, J. D. (1998). Inducible and constitutive transcription factors in the mammalian nervous system: control of gene expression by Jun, Fos and Krox, and CREB/ATF proteins. *Brain Research Reviews*, *28*(3), 370–490.

Hering, & Sheng. (2001). Dendritic spines: structure, dynamics and regulation. *Nature Reviews. Neuroscience*, *2*(December), 880–888.

Herrera, D. G., & Robertson, H. A. (1996). Activation of c-fos in the brain. *Progress in Neurobiology*, *50*, 83–107.

Hess, U. S., Lynch, G., & Gall, C. M. (1995). Regional Patterns of c-fos mRNA Expression in Rat Hippocampus Following Exploration of a Novel Environment versus Performance of a Well-Learned Discrimination. *The Journal of Neuroscience*, *15*(December), 7796–7809.

Hildebrandt, H., Müller, S., Bussmann-Mork, B., Goebel, S., & Eilers, N. (2001). Are Some Memory Deficits Unique to Lesions of the Mammillary Bodies? *Journal of Clinical and Experimental Neuropsychology*, *23*(4), 490–501.

Hodges, J. R., & Carpenter, K. (1991). Anterograde amnesia with fornix damage following removal of IIIrd ventricle colloid cyst. *Journal of Neurology, Neurosurgery, and Psychiatry*, *54*(7), 633–638.

Holahan, M. R. (2005). Complementary roles for the amygdala and hippocampus during different phases of appetitive information processing. *Neurobiology of Learning and Memory*, *84*(2), 124–131.

Holscher, C. (1999). Stress impairs performance in spatial water maze learning task. *Behavioural Brain Research*, *100*, 225-235.

Holt, W., & Maren, S. (1999). Muscimol Inactivation of the Dorsal Hippocampus Impairs Contextual Retrieval of Fear Memory. *The Journal of Neuroscience*, *19*(20), 124–131.

Honda, Y., & Ishizuka, N. (2004). Organization of Connectivity of the Rat Presubiculum: I. Efferent Projections to the Medial Entorhinal Cortex. *Journal of Comparative Neurology*, *473*(4), 463–484.

Honda, Y., Umitsu, Y., & Ishizuka, N. (2008). Organization of Connectivity of the Rat Presubiculum: II. Associational and Commissural Connections. *The Journal of Comparative Neurology*, *506*, 640–658.

Hooper, M. L., Chiasson, B. J., & Robertson, H. A. (1994). Infusion into the brain of an antisense oligonucleotide to the immediate-early gene c-fos suppresses production of Fos and produces a behavioral effect. *Neuroscience*, *63*(4), 917–924.

Hunkin, N. M., & Parkin, A. J. (1993). Recency judgements in Wernicke-Korsakoff and post-encephalitic amnesia: influences of proactive interference and retention interval. *Cortex*, *29*(3), 485–499.

Hunt, P. R., & Aggleton, J. P. (1998). An examination of the spatial working memory deficit following neurotoxic medial dorsal thalamic lesions in rats. *Behavioural Brain Research*, *97*(1-2), 129–141.

Hunt, S. P., Pini, A., & Evan, G. (1987). Induction of c-fos-like protein in spinal cord neurons following sensory stimulation. *Letters to Nature*, *328*, 632–63.

Huppert, F. A., & Piercy, M. (1979). Normal and abnormal forgetting in organic amnesia: effect of locus of lesion. *Cortex*, *15*(3), 385–390.

Insausti, R., Annese, J., Amaral, D. G., & Squire, L. R. (2013). Human amnesia and the medial temporal lobe illuminated by neuropsychological and neurohistological findings for patient E.P. *Proceedings of the National Academy of Sciences of the United States of America*, *110*(21), E1953–E1962.

Iordanova, M. D., Good, M. A., & Honey, R. C. (2008). Configural learning without reinforcement: integrated memories for correlates of what, where, and when. *Quarterly Journal of Experimental Psychology*, *61*(12), 1785–1792.

Ishizuka, N., Weber, J., & Amaral, D. G. (1990). Organization of intrahippocampal projections originating from CA3 pyramidal cells in the rat. *The Journal of Comparative Neurology*, *295*(4), 580–623.

Jackson, J., Goutagny, R., & Williams, S. (2011). Fast and slow gamma rhythms are intrinsically and independently generated in the subiculum. *The Journal of Neuroscience*, *31*(34), 12104–12117.

Jackson, T. C., Rani, a, Kumar, a, & Foster, T. C. (2009). Regional hippocampal differences in AKT survival signaling across the lifespan: implications for CA1 vulnerability with aging. *Cell Death and Differentiation*, *16*(3), 439–48.

Jay, T., Glowinski, J., & Thierry, A.-M. (1989). Selectivity of the hippocampal projection to the prelimbic area of the prefrontal cortex in the rat. *Brain Research*, *505*, 337–340.

Jay, T., & Witter, M. P. (1991). Distribution of hippocampal CA1 and subicular efferents in the prefrontal cortex of the rat studied by means of anterograde transport of Phaseolus vulgaris-leucoagglutinin. *Journal of Comparative Neurology*, *313*(4), 574–586.

Jeffery, K. J., Abraham, W. C., Dragunow, M., & Mason, S. E. (1990). Induction of Fos-like immunoreactivity and the maintenance of long-term potentiation in the dentate gyrus of unanesthetized rats. *Brain Research. Molecular Brain Research*, *8*(4), 267–274.

Jenkins, T. A., Amin, E., Brown, M. W., & Aggleton, J. P. (2006). Changes in immediate early gene expression in the rat brain after unilateral lesions of the hippocampus. *Neuroscience*, *137*(3), 747–759.

Jenkins, T. A., Dias, R., Amin, E., & Aggleton, J. P. (2002). Changes in Fos expression in the rat brain after unilateral lesions of the anterior thalamic nuclei. *European Journal of Neuroscience*, *16*(8), 1425–1432.

Jenkins, T. A., Dias, R., Amin, E., Brown, M. W., & Aggleton, J. P. (2002). Fos imaging reveals that lesions of the anterior thalamic nuclei produce widespread limbic hypoactivity in rats. *The Journal of Neuroscience*, *22*(12), 5230–5238.

Jenkins, T. A., Vann, S. D., Amin, E., & Aggleton, J. P. (2004). Anterior thalamic lesions stop immediate early gene activation in selective laminae of the retrosplenial cortex : evidence of covert pathology in rats ? *European Journal of Neuroscience*, *19*(April), 3291–3304.

Ji, Y., Gong, Y., Gan, W., Beach, T., Holtzman, D. M., & Wisniewski, T. (2003). Apolipoprotein E isoform-specific regulation of dendritic spine morphology in apolipoprotein E transgenic mice and Alzheimer's disease patients. *Neuroscience*, *122*, 305–315.

Johnston, G. A. R. (2014). Muscimol as an ionotropic GABA receptor agonist. *Neurochemical Research*, *39*(10), 1942–7.

Jones, E. G., Manger, P. R., & Woods, T. M. (1997). Maintenance of a somatotopic cortical map in the face of diminishing thalamocortical inputs. *Proceedings of the National Academy of Sciences of the United States of America*, *94*(20), 11003–11007.

Jones, M. W., Errington, M. L., French, P. J., Fine, A., Bliss, T. V. P., Garel, S., … Davis, S. (2001). A requirement for the immediate early gene Zif268 in the expression of late LTP and long-term memories. *Nature Neuroscience*, *4*(3), 289–296.

Jorgensen, M. B., Deckert, J., Wright, D. C., & Gehlert, D. R. (1989). Delayed c-fos proto-oncogene expression in the rat hippocampus induced by transient global cerebral ischemia : an in situ hybridization study. *Brain Research*, *484*, 393–398.

Jung, M. W., Wiener, S. I., & McNaughton, B. L. (1994). Comparison of spatial firing characteristics of units in dorsal and ventral hippocampus of the rat. *The Journal of Neuroscience*, *14*(12), 7347–7356.

Kalisman, N., Silberberg, G., & Markram, H. (2003). Deriving physical connectivity from neuronal morphology. *Biological Cybernetics*, *88*(3), 210–218.

Katche, C., Bekinschtein, P., Slipczuk, L., Goldin, A., Izquierdo, I. A., Cammarota, M., & Medina, J. H. (2010). Delayed wave of c-Fos expression in the dorsal hippocampus involved specifically in persistence of long-term memory storage. *Proceedings of the National Academy of Sciences of the United States of America*, *107*(1), 349–354.

Katche, C., Dorman, G., Gonzalez, C., Kramar, C. P., Slipczuk, L., Rossato, J. I., … Medina, J. H. (2013). On the role of retrosplenial cortex in long-lasting memory storage. *Hippocampus*, *23*(4), 295–302.

Kemp, A., & Manahan-Vaughan, D. (2004). Hippocampal long-term depression and long-term potentiation encode different aspects of novelty acquisition. *Proceedings of the National Academy of Sciences of the United States of America*, *101*(21), 8192–8197.

Kemp, A., Tischmeyer, W., & Manahan-Vaughan, D. (2013). Learning-facilitated long-term depression requires activation of the immediate early gene, c-fos, and is transcription dependent. *Behavioural Brain Research*, *254*, 83–91.

Kim, J., & Lee, I. (2011). Hippocampus is necessary for spatial discrimination using distal cue-configuration. *Hippocampus*, *21*(6), 609–621.

Kirk, I. J., & Mackay, J. C. (2003). The role of theta-range oscillations in synchronising and integrating activity in distributed mnemonic networks. *Cortex*, *39*(4-5), 993–1008.

Kiyama, H., Shiosaka, S., Sakamoto, N., Michel, J. P., Pearson, J., & Tohyama, M. (1986). A neurotensin-immunoreactive pathway from the subiculum to the mammillary body in the rat. *Brain Research*, *375*(2), 357–359.

Kocsis, B., Di Prisco, G. V, & Vertes, R. P. (2001). Theta synchronization in the limbic system: The role of Gudden's tegmental nuclei. *European Journal of Neuroscience*, *13*(2), 381–388.

Kocsis, B., & Vertes, R. P. (1994). Characterization of neurons of the supramammillary nucleus and mammillary body that discharge rhythmically with the hippocampal theta rhythm in the rat. *The Journal of Neuroscience*, *14*(11), 7040–7052.

Kolb, B., Cioe, J., & Comeau, W. (2008). Contrasting effects of motor and visual spatial learning tasks on dendritic arborization and spine density in rats. *Neurobiology of Learning and Memory*, *90*, 295–300.

Kopelman, M. D. (1991). Frontal dysfunction and memory deficits in the alcoholic Korsakoff syndrome and Alzheimer-type dementia. *Brain*, *114*, 117–137.

Kopelman, M. D. (2002). Disorders of memory. *Brain*, *125*, 2152–2190.

Kopelman, M. D. (2015). What does a comparison of the alcoholic Korsakoff syndrome and thalamic infarction tell us about thalamic amnesia? *Neuroscience & Biobehavioral Reviews*, *54*, 46–56.

Kopelman, M. D., Stanhope, N., & Kingsley, D. (1997). Temporal and spatial context memory in patients with focal frontal, temporal lobe, and diencephalic lesions. *Neuropsychologia*, *35*(12), 1533–1545.

Koyama, Y. (2013). The unending fascination with the Golgi method. *OA Anatomy*, *1*(3), 1–8.

Krebs-Kraft, D. L., & Parent, M. B. (2009). Hippocampal infusions of glucose reverse memory deficits produced by co-infusions of a GABA receptor agonist. *Neurobiology of Learning and Memory*, *89*(2), 142–152.

Krieckhaus, E. E., & Randall, D. (1967). Lesions of the mammillothalamic tract in rat produce no decrements in recent memory. *Journal of Neurology*, (1964), 369–378.

Krieg, W. J. S. (1932). The hypothalamus of the albino rat. *The Journal of Comparative Neurology*, *55*(1), 19–89.

Lamprecht, R., & Dudai, Y. (1996). Transient expression of c-Fos in rat amygdala during training is required for encoding conditioned taste aversion memory. *Learning & Memory*, *3*(1), 31–41.

Lecosnier, S., Cordier, C., Simon, P., François, J.-C., & Saison-Behmoaras, T. E. (2011). A steric blocker of translation elongation inhibits IGF-1R expression and cell transformation. *The FASEB Journal : Official Publication of the Federation of American Societies for Experimental Biology*, *25*(7), 2201–2210.

Lee, I., & Kesner, R. P. (2003). Time-Dependent Relationship between the Dorsal Hippocampus and the Prefrontal Cortex in Spatial Memory. *The Journal of Neuroscience*, *23*(4), 1517–1523.

Lee, J. L. C., Everitt, B. J., & Thomas, K. L. (2004). Independent cellular processes for hippocampal memory consolidation and reconsolidation. *Science*, *304*(5672), 839–843.

Leonetti, J. P., Mechti, N., Degols, G., Gagnor, C., & Lebleu, B. (1991). Intracellular distribution of microinjected antisense oligonucleotides. *Proceedings of the National Academy of Sciences of the United States of America*, *88*(7), 2702–2706.

Levine, N. D., Rademacher, D. J., Collier, T. J., O'Malley, J. A., Kells, A. P., Sebastian, S. S., … Steece-Collier, K. (2013). Advances in thin tissue Golgi-Cox impregnation: fast, reliable methods for multi-assay analyses in rodent and non-human primate brain. *Journal of Neuroscience Methods*, *213*(2), 214–227.

Li, H., Matsumoto, K., & Watanabe, H. (1999). Different effects of unilateral and bilateral hippocampal lesions in rats on the performance of radial maze and odor-paired associate tasks. *Brain Research Bulletin*, *48*(1), 113–119.

Little, A. G., Kocha, K. M., Lougheed, S. C., & Moyes, C. D. (2010). Evolution of the nuclear-encoded cytochrome oxidase subunits in vertebrates. *Physiological Genomics*, *42*(1), 76–84.

Lo, D. C., McAllister, A. K., & Katz, C. L. (1994). Neuronal Transfection in Brain Slices Using Particle-Mediated Gene Transfer. *Neurotechnique*, *13*, 1263–1268.

Loke, S. L., Stein, C. A., Zhang, X. H., Mori, K., Nakanishi, M., Subasinghe, C., … Neckers, L. M. (1989). Characterization of oligonucleotide transport into living cells. *Proceedings of the National Academy of Sciences of the United States of America*, *86*(10), 3474–3478.

Lonergan, M. E., Gafford, G. M., Jarome, T. J., & Helmstetter, F. J. (2010). Time-dependent expression of Arc and zif268 after acquisition of fear conditioning. *Neural Plasticity*, *2010*, 139891.

Longair, M. H., Baker, D. A., & Armstrong, J. D. (2011). Simple Neurite Tracer: open source software for reconstruction, visualization and analysis of neuronal processes. *Bioinformatics (Oxford, England)*, *27*(17), 2453–2454.

Loukavenko, E. A., Wolff, M., Poirier, G. L., & Dalrymple-Alford, J. C. (2015). Impaired spatial working memory after anterior thalamic lesions: recovery with cerebrolysin and enrichment. *Brain Structure and Function*.

Lukoyanov, N. V, Lukoyanova, E. A., Andrade, J. P., & Paula-Barbosa, M. M. (2005). Impaired water maze navigation of Wistar rats with retrosplenial cortex lesions: effect of nonspatial pretraining. *Behavioural Brain Research*, *158*(1), 175–82.

Mair, W. G., Warrington, E. K., & Weiskrantz, L. (1979). Memory disorder in Korsakoff's psychosis: a neuropathological and neuropsychological investigation of two cases. *Brain*, *102*(4), 749–783.

Malkani, S., Wallace, K. J., Donley, M. P., & Rosen, J. B. (2004). Infused Into the Amygdala Disrupts Fear Conditioning. *Learning & Memory*, *1*, 617–624.

Markowska, A. L., Olton, D. S., Murray, E. A., & Gaffan, D. (1989). A comparative analysis of the role of fornix and cingulate cortex in memory: rats. *Experimental Brain Research*, *74*, 187–201.

Marmolejo, Paez, Levitt, & Jones. (2012). Early postnatal lesion of the medial dorsal nucleus leads to loss of dendrites and spines in adult prefrontal cortex. *Developmental Neuroscience*, *34*(6), 463–76.

Marquis, Goulet, & Dore'. (2008). Neonatal ventral hippocampus lesions disrupt extra-dimensional shift and alter dendritic spine density in the medial prefrontal cortex of juvenile rats. *Neurobiology of Learning and Memory*, *90*(2), 339–46.

Martin, J. H. (1991). Autoradiographic estimation of the extent of reversible inactivation produced by microinjection of lidocaine and muscimol in the rat ctivi : *Neuroscience Letters*, *127*, 160–164.

Martin, S. J., Grimwood, P. D., & Morris, R. G. M. (2000). Synaptic plasticity and memory: An Evaluation of the Hypothesis. *Annual Review of Neuroscience*, (23), 649–711. doi:10.1146/annurev.neuro.23.1.649

Matus-Amat, P., Higgins, E. A., Barrientos, R. M., & Rudy, J. W. (2004). The role of the dorsal hippocampus in the acquisition and retrieval of context memory representations. *The Journal of Neuroscience*, *24*(10), 2431–2439.

Mayes, A. R., Meudell, P. R., Mann, D., & Pickering, A. (1988). Location of lesions in Korsakoff's syndrome: neuropsychological and neuropathological data on two patients. *Cortex*, *24*(3), 367–388.

McHugh, S. B., Niewoehner, B., Rawlins, J. N. P., & Bannerman, D. M. (2008). Dorsal hippocampal N-methyl-D-aspartate receptors underlie spatial working memory performance during non-matching to place testing on the T-maze. *Behavioural Brain Research*, *186*(1), 41–47. doi:10.1016/j.bbr.2007.07.021

McKee, R. D., & Squire, L. R. (1992). Equivalent forgetting rates in long-term memory for diencephalic and medial temporal lobe amnesia. *The Journal of Neuroscience*, *12*(10), 3765–3772.

Mechta-Grigoriou, F., Gerald, D., & Yaniv, M. (2001). The mammalian Jun proteins: redundancy and specificity. *Oncogene*, *20*(19), 2378–2389.

Meibach, R. C., & Siegel, A. (1977). Thalamic projections of the hippocampal formation: evidence for an alternative pathway involving the internal capsule. *Brain Research*, *134*, 1–12.

Mendez, M., Arias, N., Uceda, S., & Arias, J. L. (2015). c-Fos expression correlates with performance on novel object and novel place recognition tests. *Brain Research Bulletin*, *117*, 16–23.

Mendez-Lopez, M., Arias, J. L., Bontempi, B., & Wolff, M. (2013). Reduced cytochrome oxidase activity in the retrosplenial cortex after lesions to the anterior thalamic nuclei. *Behavioural Brain Research*, *250*, 264–73.

Menzel, C. R. (1999). Unprompted recall and reporting of hidden objects by a chimpanzee (Pan troglodytes) after extended delays. *Journal of Comparative Psychology*, *113*(4), 426–434.

Mercer, S. A. (2015). *Enrichment Facilitates Recovery of Spatial Memory but not Retrosplenial Immediate Early Gene Hypoactivation after Anterior Thalamic Lesions*. PhD Thesis. University of canterbury (New Zealand).

Milosević, N. T., & Ristanović, D. (2007). The Sholl analysis of neuronal cell images: Semi-log or log-log method? *Journal of Theoretical Biology*, *245*(1), 130–140.

Minoshima, S., Giordani, B., Berent, S., Frey, K. A., Foster, N. L., & Kuhl, D. E. (1997). Metabolic reduction in the posterior cingulate cortex in very early Alzheimer's disease. *Annals of Neurology*, *42*(1), 85–94.

Mitchell, A., & Dalrymple-Alford, J. (2006). Lateral and anterior thalamic lesions impair independent memory systems. *Learning & Memory*, *13*, 388–396.

Mitchell, S. J., & Ranck, J. B. (1980). Generation of theta rhythm in medial entorhinal cortex of freely moving rats. *Brain Research*, *189*, 49–66.

Morel, A., Magnin, M., & Jeanmonod, D. (1997). Multiarchitectonic and stereotactic atlas of the human thalamus. *The Journal of Comparative Neurology*, *387*(4), 588–630.

Mori, E., Yamadori, A., & Mitani, Y. (1986). Left thalamic infarction and disturbance of verbal memory: a clinicoanatomical study with a new method of computed tomographic stereotaxic lesion localization. *Annals of Neurology*, *20*(6), 671–676.

Morris, R. G., Garrud, P., Rawlins, J. N., & O'Keefe, J. (1982). Place navigation impaired in rats with hippocampal lesions. *Nature*.

Moser, M. B., & Moser, E. I. (1998). Distributed Encoding and Retrieval of Spatial Memory in the Hippocampus. *The Journal of Neuroscience*, *18*(18), 7535–7542.

Naggara, O., Varlet, P., Page, P., Oppenheim, C., & Meder, J. F. (2005). Suprasellar paraganglioma: A case report and review of the literature. *Neuroradiology*, *47*(10), 753–757.

Nasrallah, F. A., Pagès, G., Kuchel, P. W., Golay, X., & Chuang, K.-H. (2013). Imaging brain deoxyglucose uptake and metabolism by glucoCEST MRI. *Journal of Cerebral Blood Flow and Metabolism*, *33*(8), 1270–1278.

Neave, Lloyd, Sahgal, & Aggleton. (1994). Lack of effect of lesions in the anterior cingulate cortex and retrosplenial cortex on certain tests of spatial memory in the rat. *Behavioural Brain Research*, *65*, 89–101.

Neave, N., Nagle, S., & Aggleton, J. P. (1997). Evidence for the Involvement of the Mammillarv Bodies and Cingulum Bundle in Allocentric Spatial Processing by Rats. *European Journal of Neuroscience*, *9*, 941–955.

Neave, N., Nagle, S., Sahgal, A., & Aggleton, J. P. (1996). The effects of discrete cingulum bundle lesions in the rat on the acquisition and performance of two tests of spatial working memory. *Behavioural Brain Research*, *80*(1-2), 75–85.

Nelson, A. J. D., Powell, A. L., Holmes, J. D., Vann, S. D., & Aggleton, J. P. (2015). What does spatial alternation tell us about retrosplenial cortex function? *Frontiers in Behavioral Neuroscience*, *9*(May), 1–15.

Nelson, A. J. D., & Vann, S. D. (2014). Mammilliothalamic Tract Lesions Disrupt Tests of Visuo-Spatial Memory. *Behavioural Neuroscience*, *128*(4), 494–503.

Nestor, P. J., Fryer, T. D., Smielewski, P., & Hodges, J. R. (2003). Limbic hypometabolism in Alzheimer's disease and mild cognitive impairment. *Annals of Neurology*, *54*(0364-5134), 343–351.

Newman, L. A., & McGaughy, J. (2011). Attentional effects of lesions to the anterior cingulate cortex: How prior reinforcement influences distractibility. *Behavioral Neuroscience*, *125*(3), 360–371.

O'Keefe, J. (1976). Place units in the hippocampus of the freely moving rat. *Experimental Neurology*, *51*(1), 78–109.

Ogawa, S., Brown, H. E., Okano, H. J., & Pfaff, D. W. (1995). Cellular uptake of intracerebrally administered oligodeoxynucleotides in mouse brain. *Regulatory Peptides*, *59*(2), 143–149.

Olton, D. S., & Samuelson, R. J. (1976). Animal Behavior Processes Remembrance of Places Passed : Spatial Memory in Rats. *Journal of Experimental Psychology*, *2*(2), 97–116.

Paller, K. A. (1997). Consolidating dispersed neocortical memories: the missing link in amnesia. *Memory*, *5*(1-2), 73–88.

Paller, K. A., Acharya, A., Richardson, B. C., Plaisant, O., Shimamura, A. P., Reed, B. R., & Jagust, W. J. (1997). Functional Neuroimaging of Cortical Dysfunction in Alcoholic Korsakoff's Syndrome. *Journal of Cognitive Neuroscience*, *9*(2), 277–293.

Pantano, P., Baron, J. C., Samson, Y., Bousser, M. G., Derousene, C., & Comar, D. (1986). Crossed cerebellar diaschisis: further studies. *Brain*, *109*, 677–694.

Papez, J. W. (1937). A proposed mechanism of emotion. *Archives of Neurology & Psychiatry*, *38*(4), 725–743.

Parkin, a J., Leng, N. R., & Hunkin, N. M. (1990). Differential sensitivity to context in diencephalic and temporal lobe amnesia. *Cortex*, *26*(3), 373–380.

Parkin, A. J. (1984). Amnesic syndrome: a lesion-specific disorder? *Cortex*, *20*(4), 479–508.

Paxinos, G., & Watson, C. (1998). The Rat Brain in stereotaxic coordinates. *Academic Press*, *4th Ed.*

Penke, Z., Morice, E., Veyrac, A., Gros, A., Chagneau, C., LeBlanc, P., … Laroche, S. (2014). Zif268/Egr1 gain of function facilitates hippocampal synaptic plasticity and long-term spatial recognition memory. *Philosophical Transactions of the Royal Society of London. Series B, Biological Sciences*, *369*(1633), 1–9. doi:10.1098/rstb.2013.0159

Pitkänen, A., Pikkarainen, M., Nurminen, N., & Ylinen, A. (2006). Reciprocal Connections between the Amygdala and the Hippocampal Formation, Perirhinal Cortex, and Postrhinal Cortex in Rat: A Review. *Annals of the New York Academy of Sciences*, *911*(1), 369–391.

Poirier, G. L., & Aggleton, J. P. (2009). Post-surgical interval and lesion location within the limbic thalamus determine extent of retrosplenial cortex immediate-early gene hypoactivity. *Neuroscience*, *160*(2), 452–469.

Poirier, G. L., Amin, E., & Aggleton, J. P. (2008). Qualitatively different hippocampal subfield engagement emerges with mastery of a spatial memory task by rats. *The Journal of Neuroscience*, *28*(5), 1034–1045.

Poirier, G. L., Shires, K. L., Sugden, D., Amin, E., Thomas, K. L., & Carter, J. P. (2008). Anterior thalamic lesions produce chronic and profuse transcriptional de-regulation in retrosplenial cortex: A model of retrosplenial hypoactivity and covert pathology. *Thalamus & Related Systems*, *4*(1), 59–77.

Poletti, C. E., & Creswell, G. (1977). Fornix system efferent projections in the squirrel monkey: an experimental degeneration study. *The Journal of Comparative Neurology*, *175*(1), 101–128.

Poreh, A., Winocur, G., Moscovitch, M., Backon, M., Goshen, E., Ram, Z., & Feldman, Z. (2006). Anterograde and retrograde amnesia in a person with bilateral fornix lesions following removal of a colloid cyst. *Neuropsychologia*, *44*(12), 2241–2248.

Pothuizen, Davies, Albasser, Aggleton, & Vann. (2009). Granular and dysgranular retrosplenial cortices provide qualitatively different contributions to spatial working memory: evidence from immediate-early gene imaging in rats. *The European Journal of Neuroscience*, *30*(5), 877–88.

Pothuizen, H. H. J., Aggleton, J. P., & Vann, S. D. (2008). Do rats with retrosplenial cortex lesions lack direction? *The European Journal of Neuroscience*, *28*(12), 2486–2498.

Pothuizen, H. H. J., Davies, M., Aggleton, J. P., & Vann, S. D. (2010). Effects of selective granular retrosplenial cortex lesions on spatial working memory in rats. *Behavioural Brain Research*, *208*(2), 566–75.

Potvin, O., Allen, K., Thibaudeau, G., Doré, F. Y., & Goulet, S. (2006). Performance on spatial working memory tasks after dorsal or ventral hippocampal lesions and adjacent damage to the subiculum. *Behavioral Neuroscience*, *120*(2), 413–422.

Racine, R. J., & Kimble, D. P. (1965). Hippocampal lesions and delayed alternation in the rat. *Psychonomic Science*, *3*, 285–286.

Ransone, L. J., Visvader, J., Sassone-Corsi, P., & Verma, I. M. (1989). Fos-Jun interaction: mutational analysis of the leucine zipper domain of both proteins. *Genes & Development*, *3*(6), 770–781.

Redburn, J. L., & Leah, J. D. (1997). Accelerated breakdown and enhanced expression of c-Fos in the rat brain after noxious stimulation. *Neuroscience Letters*, *237*(2-3), 97–100.

Reed, L. J., Lasserson, D., Marsden, P., Stanhope, N., Stevens, T., Bello, F., … Kopelman, M. D. (2003). FDG-PET findings in the Wernicke-Korsakoff syndrome. *Cortex*, *39*, 1027–1045.

Reed, L. J., Marsden, P., Lasserson, D., Sheldon, N., Lewis, P., Stanhope, N., … Kopelman, M. D. (1999). FDG-PET analysis and findings in amnesia resulting from hypoxia. *Memory*, *7*(5-6), 599–612.

Richardson, C. L., Tate, W. P., Mason, S. E., Lawlor, P. A., Dragunow, M., & Abraham, W. C. (1992). Correlation between the induction of an immmediate early gene, zif268, and long-term potentiation in the dentate gyrus. *Brain Research*, *580*, 147–154.

Richter-Levin, G., Thomas, K. L., Hunt, S. P., & Bliss, T. V. P. (1998). Dissociation between genes activated in long-term potentiation and in spatial learning in the rat. *Neuroscience Letters*, *251*(1), 41–44.

Roberts, W. A. (2002). Are animals stuck in time? *Psychological Bulletin*, *128*(3), 473–489.

Robertson, L.M., Kerppola, T. K., Vendrell, M., Luk, D., Smeyne, J. R., Bocchiaro, C., Morgan, J. I., & Curran, T. (1995). Regulation of c-fos expression in transgenic mice requires mutliple interdependent transcription control elements *Neuron*, *128*(3), 473–489.

Rogers, J. L., Hunsaker, M. R., & Kesner, R. P. (2006). Effects of ventral and dorsal CA1 subregional lesions on trace fear conditioning. *Neurobiology of Learning and Memory*, *14*, 241–252.

Roland, J., & Savage, L. (2007). Blunted hippocampal, but not striatal, acetylcholine efflux parallels learning impairment in diencephalic-lesioned rats. *Neurobiology of Learning and Memory*, *87*(1), 123–132.

Rose, J. E., & Woolsey, C. N. (1948). Structure and relations of limbic cortex and anterior thalamic nuclei in rabbit and cat. *The Journal of Comparative Neurology*, *89*(3), 279–347.

Rosenstock, J., Field, T. D., & Greene, E. (1977). The role of mammillary bodies in spatial memory. *Experimental Neurology*, *55*(2), 340–352.

Sagar, S. M., Sharp, F. R., & Curran, T. (1988). Expression of c-fos protein in brain: metabolic mapping at the cellular level. *Science*, *240*(4857), 1328–1331.

Saito, S., Okada, A., Ouwa, T., Kato, A., Akagi, M., & Kmei, C. (2010). Interaction between Hippocampal g -Aminobutyric Acid A and N -Methyl- D - aspartate Receptors in the Retention of Spatial Working Memory in Rats. *Biological and Pharmaceutical Bulletin*, *33*(March), 439–443.

Sakata, J. T., Crews, D., & Gonzalez-Lima, F. (2005). Behavioral correlates of differences in neural metabolic capacity. *Brain Research. Brain Research Reviews*, *48*(1), 1–15.

Sambucetti, L. C., Schaber, M., Kramer, R., Crowl, R., & Curran, C. (1986). The fos gene product undergoes extensive post-translational modification in eukaryotic but not in prokaryotic cells. *Gene*, *43*, 69–77.

Sang, Y., & Lee, I. (2011). Disconnection of the hippocampal-perirhinal circuits severely disrupts object-place paired associative memory. *The Journal of Neuroscience*, *30*(29), 9850–9858.

Santín, L. J., Rubio, S., Begega, A., & Arias, J. L. (1999). Effects of mammillary body lesions on spatial reference and working memory tasks. *Behavioural Brain Research*, *102*, 137–150.

Sassone-Corsi, P., Sisson, J. C., & Verma, I. M. (1988). Transcriptional autoregulation of the proto-oncogene fos. *Nature*, *334*, 314–334.

Sato, K., Morimoto, K., Suemaru, S., Sato, T., & Yamada, N. (2000). Increased synapsin I immunoreactivity during long-term potentiation in rat hippocampus. *Brain Research*, *872*(1-2), 219–222.

Saunders, C. R., & Aggleton, J. P. (2007). Origin and topography of fibers contributing to the fornix in the macaque monkey. *Hippocampus*, *17*, 396–411.

Savage, L. M., Chang, Q., & Gold, P. E. (2003). Diencephalic damage decreases hippocampal acetylcholine release during spontaneous alternation testing. *Learning & Memory*, *10*(4), 242–6.

Savage, L. M., Hall, J. M., & Vetreno, R. P. (2011). Anterior thalamic lesions alter both hippocampal-dependent behavior and hippocampal acetylcholine release in the rat. *Learning & Memory*, *18*(12), 751–758.

Schindelin, J., Arganda-Carreras, I., Frise, E., Kaynig, V., Longair, M., Pietzsch, T., … Cardona, A. (2012). Fiji - an Open Source platform for biological image analysis. *Nature Methods*, *9*, 676–682.

Schmahmann, J. D. (2003). Vascular syndromes of the thalamus. *Stroke*, *34*(9), 2264–2278.

Scoville, W. B., & Milner, B. (1957). Loss of recent memory after bilateral hippocampal lesions. *The Journal of Neuropsychiatry and Clinical Neurosciences*, *20*(11), 11–21.

Seki, M., & Zyo, K. (1984). Anterior thalamic afferents from the mamillary body and the limbic cortex in the rat. *The Journal of Comparative Neurology*, *229*(2), 242–256.

Seoane, A., Tinsley, C. J., & Brown, M. W. (2012). Interfering with Fos expression in rat perirhinal cortex impairs recognition memory. *Hippocampus*, *22*(11), 2101–2113.

Serrano-Pozo, A., Frosch, M. P., Masliah, E., & Hyman, B. T. (2011). Neuropathological Alterations in Alzheimer Disease pic hallmarks. *Cold Spring Harbor Perspective in Medicine*, *1*, 1–23.

Shankaranarayana, R. B. S., Govindaiah, Laxmi, T. R., Meti, B. L., & Raju, T. R. (2001). Subicular lesions cause dendritic atrophy in CA1 and CA3 pyramidal neurons of the RAT hippocampus. *Neuroscience*, *102*(2), 319–327.

Shankaranarayana, R. B. S., & Raju, T. R. (2004). The Golgi Techniques for Staining Neurons. In T. R. Raju, B. M. Kutty, T. N. Sathyaprabha, & R. B. S. Shankaranarayana (Eds.), *Brain and Behavior* (pp. 108– 111). NIMH and Neuro Sciences.

Sharp, F. R., Hisanaga, K., Sagar, M., Hicks, K., & Lowenstein, D. (1991). c-fos mRNA, Fos, and Fos-related antigen induction by hypertonic saline and stress. *The Journal of Neuroscience*, *7*(August), 2321–2331.

Sharp, P. E., & Koester, K. (2008). Lesions of the mammillary body region severely disrupt the cortical head direction, but not place cell signal. *Hippocampus*, *18*(8), 766–784.

Sharp, P. E., Tinkelman, A., & Cho, J. (2001). Angular velocity and head direction signal recorded from the dorsal tegmental nucleus of Gudden in the rat. *Behavioral Neuroscience*, *115*(3), 571–588.

Shaw, C., & Aggleton, J. P. (1993). The effects of fornix and medial prefrontal lesions on delayed non-matching-to-sample by rats. *Behavioral Brain Research*, *54*, 91–102.

Sheedy, D., Lara, A., Garrick, T., & Harper, C. (1999). Size of mammillary bodies in health and disease: useful measurements in neuroradiological diagnosis of Wernicke's encephalopathy. *Alcoholism, Clinical and Experimental Research*, *23*(10), 1624–1628.

Sheng, M., & Greenberg, M. E. (1990). The regulation and function of c-fos and other immediate early genes in the nervous system. *Neuron*, *4*(4), 477–485.

Shepherd, J. D., & Bear, M. F. (2011). New views of Arc, a master regulator of synaptic plasticity. *Nature Neuroscience*, *14*(3), 279–284.

Shibata, H. (1992). Topographic organization of subcortical projections to the anterior thalamic nuclei in the rat. *The Journal of Comparative Neurology*, *323*(1), 117–127.

Shibata, H. (1993a). Direct Projections From the Anterior Thalamic Nuclei to the Retrohippocampal Region in the Rat. *The Journal of Comparative Neurology*, *337*, 431–445.

Shibata, H. (1993b). Efferent projections from the anterior thalamic nuclei to the cingulate cortex in the rat. *The Journal of Comparative Neurology*, *330*(4), 533–542.

Shibata, H., Honda, Y., Sasaki, H., & Naito, J. (2009). Organization of intrinsic connections of the retrosplenial cortex in the rat, *84*, 280–292.

Shibata, H., & Kato, A. (1993). Topographic relationship between anteromedial thalamic nucleus neurons and their cortical terminal fields in the rat. *Neuroscience Research*, *17*(1), 63–69.

Shibata, H., Kondo, S., & Naito, J. (2004). Organization of retrosplenial cortical projections to the anterior cingulate, motor, and prefrontal cortices in the rat. *Neuroscience Research*, *49*(1), 1–11.

Shibata, H., & Naito, J. (2005). Organization of anterior cingulate and frontal cortical projections to the anterior and laterodorsal thalamic nuclei in the rat. *Brain Research*, *1059*(1), 93–103.

Sholl, D. A. (1953). Dendritic organization of the neurons of the visual and motor cortices of the cat. *Journal of Anatomy*, *87*(4), 387–406.

Sjöström, P. J., Rancz, E. A., Roth, A., & Häusser, M. (2008). Dendritic excitability and synaptic plasticity. *Physiological Reviews*, *88*(2), 769–840.

Smith, D. L., Pozueta, J., Gong, B., Arancio, O., & Shelanski, M. (2009). Reversal of long-term dendritic spine alterations in Alzheimer disease models. *Proceedings of the National Academy of Sciences of the United States of America*, *106*(39), 16877–82.

Sommer, W., Cui, X., Erdmann, B., Wiklund, L., Bricca, G., Heilig, M., & Fuxe, K. (1998). The spread and uptake pattern of intracerebrally administered oligonucleotides in nerve and glial cell populations of the rat brain. *Antisense & Nucleic Acid Drug Development*, *8*(2), 75–85.

Sonnenberg, J. L., Mitchelmore, C., Macgregor-Leon, P. F., Hempstead, J., Morgan, J. I., & Curran, T. (1989). Glutamate receptor agonists increase the expression of Fos, Fra, and AP-1 DNA binding activity in the mammalian brain. *Journal of Neuroscience Research*, *24*(1), 72–80.

Soulé, J., Penke, Z., Kanhema, T., Alme, M. N., Laroche, S., & Bramham, C. R. (2008). Object-place recognition learning triggers rapid induction of plasticity-related immediate early genes and synaptic proteins in the rat dentate gyrus. *Neural Plasticity*, *2008*, 1–12.

Squire, L. R. (1981). Two forms of human amnesia: an analysis of forgetting. *The Journal of Neuroscience*, *1*(6), 635–640.

Sripanidkulchai, & Wyss. (1986). Thalamic projections to retrosplenial cortex in the rat. *The Journal of Comparative Neurology*, *254*(2), 143–165.

Staffend, N. A., & Meisel, R. L. (2011). DiOlistic labeling in fixed brain slices: phenotype, morphoogy and dendritic spines. *Current Protocols in Neuroscience*, *Chapter2* (Unit 2.13), 1–23.

Storm-Mathisen, J., & Woxen Opsahl, M. (1978). Asparate and/or glutamate may be transmitters in hippocampal efferents to septum and hypothalamus. *Neuroscience Letters*, *9*, 65–70.

Suddendorf, T., & Busby, J. (2003). Mental time travel in animals? *Trends in Cognitive Sciences*, *7*(9), 391–396.

Sugar, Witter, Strien, V., & Cappaert. (2011). The retrosplenial cortex: intrinsic connectivity and connections with the (para)hippocampal region in the rat. An interactive connectome. *Frontiers in Neuroinformatics*, *5*(July), 1–13.

Sutherland, R. J., & Hoesing, J. M. (1993). Posterior cingulate cortex and spatial memory: a microlimnology analysis. In A. B. Vogt & M. Gabriel (Eds.), *Neurobiology of cingulate cortex and limbic thalamus: a comprehensive handbook* (p. 1993). Birkhauser.

Swanson, L. W., & Cowan, W. M. (1975). Hippocampo-Hypothalamic Connections : Origin in Subicular Cortex , Not Ammon's Horn. *Science*, (July), 303–304.

Swanson, L. W., & Cowan, W. M. (1979). The connections of the septal region in the rat. *The Journal of Comparative Neurology*, *186*(4), 621–655.

Swanson, L. W., Kohler, C., & Bjorklund, A. (1987). The limbic region. I: The septohippocampal system. In A. Bjorklund, T. Hokfelt, & L. W. Swanson (Eds.), *Handbook of chemical neuroanatomy, Vol.5: Integrated systems of the CNS part 1* (pp. 125–277). Elsevier.

Sziklas, V., & Petrides, M. (1998). Memory and the region of the mammillary bodies. *Progress in Neurobiology*, *54*(1), 55–70.

Sziklas, V., & Petrides, M. (1999). The effects of lesions to the anterior thalamic nuclei on object – place associations in rats. *Neuroscience*, *11*(May 1998), 559–566.

Sziklas, V., & Petrides, M. (2000). Selectivity of the spatial learning deficit after lesions of the mammillary region in rats. *Hippocampus*, *10*(3), 325–328.

Sziklas, V., & Petrides, M. (2002). Effects of lesions to the hippocampus or the fornix on allocentric conditional associative learning in rats. *Hippocampus*, *12*(4), 543–550.

Sziklas, V., Petrides, M., & Leri, F. (1996). The effects of lesions to the mamillary region and the hippocampus on conditional associative learning by rats. *European Journal of Neuroscience*, *8*(June 1995), 106–115.

Takeuchi, Y., Allen, G. V, & Hopkins, D. A. (1985). Transnuclear transport and axon collateral projections of the mamillary nuclei in the rat. *Brain Research Bulletin*, *14*(5), 453–468.

Tako, A. N., Beracochea, D., & Jaffard, R. (1988). Accelerated rate of forgetting for spatial information following mammillary bodies lesion in mice : a retrieval deficit alleviated by a context change occuring on the retention test. *Psychobiology*, *16*(1), 45–53.

Tanaka, D. J. (1976). Thalamic Projections of the Dorsomedial Prefrontal Cortex in the Rhesus Monkey (Macaca Mulatta). *Brain Research*, *110*, 21–38.

Tashiro, & Yuste. (2003). Structure and molecular organization of dendritic spines. *Histology and Histopathology*, *18*, 617–634.

Taube, J. S. (1995). Head direction cells recorded in the anterior thalamic nuclei of freely moving rats. *The Journal of Neuroscience*, *15*(1), 70–86.

Taube, J. S., Muller, R. U., & Ranck, J. B. (1990). Head-direction cells recorded from the postsubiculum in freely moving rats. II. Effects of environmental manipulations. *The Journal of Neuroscience*, *10*(2), 436–447.

Thiel, G., Schoch, S., & Petersohn, D. (1994). Regulation of Synapsin I Gene Expression by the Zinc Finger Transcription Factor zif268/egr-1. *Biochemistry*, (21), 15294–15301.

Thomas, G. J., & Gash, D. M. (1985). Mammillothalamic tracts and representational memory. *Behavioral Neuroscience*, *99*(4), 621–630. Retrieved from

Tischmeyer, W., & Grimm, R. (1999). Activation of immediate early genes and memory formation. *Cellular and Molecular Life Sciences : CMLS*, *55*(4), 564–74.

Tolliver, B. K., Sganga, M. W., & Sharp, F. R. (2000). Suppression of c-fos induction in the nucleus accumbens prevents acquisition but not expression of morphine-conditioned place preference. *European Journal of Neuroscience*, *12*(9), 3399–3406.

Tønnesen, J., Katona, G., Rózsa, B., & Nägerl, U. V. (2014). Spine neck plasticity regulates compartmentalization of synapses. *Nature Neuroscience*, *17*(5), 678–85.

Topilko, P., Schneider-Maunoury, S., Levi, G., Trembleau, A., Gourdji, D., Driancourt, M. A., Rao, C. V., & Charnay, P. (1997). Multiple pituitary and ovarian defects in Krox-24 (NGFI-A, Egr-1) – targeted mice. *Molecular Endocrinology*, *108*, 678–85.

Torres-García, M. E., Solis, O., Patricio, A., Rodríguez-Moreno, A., Camacho-Abrego, I., Limón, I. D., & Flores, G. (2012). Dendritic morphology changes in neurons from the prefrontal cortex, hippocampus and nucleus accumbens in rats after lesion of the thalamic reticular nucleus. *Neuroscience*, *223*, 429–38.

Trivedi, M. A., & Coover, G. D. (2004). Lesions of the ventral hippocampus , but not the dorsal hippocampus , impair conditioned fear expression and inhibitory avoidance on the elevated T-maze. *Neurobiology of Learning and Memory*, *81*, 172–184.

Tronel, S., Fabre, A., Charrier, V., Oliet, S. H. R., Gage, F. H., & Abrous, D. N. (2010). Spatial learning sculpts the dendritic arbor of adult-born hippocampal neurons. *Proceedings of the National Academy of Sciences of the United States of America*, *107*(17), 7963–8.

Tsivilis, D., Vann, S. D., Denby, C., Roberts, N., Mayes, A. R., Montaldi, D., & Aggleton, J. P. (2008). A disproportionate role for the fornix and mammillary bodies in recall versus recognition memory. *Nature Neuroscience*, *11*(7), 834–842.

Tulving, E. (2002). Episodic Memory: From Mind to Brain. *Annual Review of Psychology*, *53*(1), 1–25.

Vaerman, J. L., Moureau, P., Deldime, F., Lewalle, P., Lammineur, C., Morschhauser, F., & Martiat, P. (1997). Antisense oligodeoxyribonucleotides suppress hematologic cell growth through stepwise release of deoxyribonucleotides. *Blood*, *90*(1), 331–339.

Valenstein, E., Bowers, D., Verfaellie, M., Heilman, K. M., Day, A., & Watson, R. T. (1987). Retrosplenial amnesia. *Brain*, *110*, 1631–1646.

Van der Werf, Y. D., Witter, M. P., Uylings, H. B. M., & Jolles, J. (2000). Neuropsychology of infarctions in the thalamus: a review. *Neuropsychologia*, *38*(5), 613–627.

Van Groen, T., Kadish, I., & Wyss, J. M. (1999). Efferent connections of the anteromedial nucleus of the thalamus of the rat. *Brain Research Reviews*, *30*(1), 1–26.

Van Groen, T., Kadish, I., & Wyss, J. M. (2002). The role of the laterodorsal nucleus of the thalamus in spatial learning and memory in the rat. *Behavioural Brain Research*, *136*(2), 329–337.

Van Groen, T., Kadish, I., & Wyss, J. M. (2004). Retrosplenial cortex lesions of area Rgb (but not of area Rga) impair spatial learning and memory in the rat. *Behavioural Brain Research*, *154*(2), 483–491.

Van Groen, T., & Wyss, J. M. (1990a). Connections of the retrosplenial granular a cortex in the rat. *The Journal of Comparative Neurology*, *300*(4), 593–606.

Van Groen, T., & Wyss, J. M. (1990b). The connections of presubiculum and parasubiculum in the rat. *Brain Research*, *518*(1-2), 227–243.

Van Groen, T., & Wyss, J. M. (1990c). The postsubicular cortex in the rat: characterization of the fourth region of the subicular cortex and its connections. *Brain Research*, *529*(1-2), 165–177.

Van Groen, T., & Wyss, J. M. (2003). Connections of the retrosplenial granular b cortex in the rat. *The Journal of Comparative Neurology*, *463*(3), 249–263.

Van Groen, T. V, & Wyss, J. M. (1992). Connections of the retrosplenial dysgranular cortex in the rat. *The Journal of Comparative Neurology*, *315*(2), 200–216.

Van Groen, T. V, & Wyss, J. M. (1995). Projections From the Anterodorsal and Anteroventral Nucleus of the Thalamus to the Limbic Cortex in the Rat. *The Journal of Comparative Neurology*, *358*, 584–604.

VanElzakker, M., Fevurly, R. D., Breindel, T., & Spencer, R. L. (2008). Environmental novelty is associated with a selective increase in Fos expression in the output elements of the hippocampal formation and the perirhinal cortex. *Learning & Memory*, *15*(12), 899–908.

Vanhoutte, P., Barnier, J. V, Guibert, B., Pagès, C., Besson, M. J., Hipskind, R. a, & Caboche, J. (1999). Glutamate induces phosphorylation of Elk-1 and CREB, along with c-fos activation, via an extracellular signal-regulated kinase-dependent pathway in brain slices. *Molecular and Cellular Biology*, *19*(1), 136–146.

Vann, S. D. (2005). Transient spatial deficit associated with bilateral lesions of the lateral mammillary nuclei. *The European Journal of Neuroscience*, *21*(3), 820–824.

Vann, S. D. (2009). Guddens ventral tegmental nucleus is vital for memory: Re-evaluating diencephalic inputs for amnesia. *Brain*, *132*(9), 2372–2384.

Vann, S. D. (2010). Re-evaluating the role of the mammillary bodies in memory. *Neuropsychologia*, *48*(8), 2316–2327.

Vann, S. D. (2011). A role for the head-direction system in geometric learning. *Behavioural Brain Research*, *224*(1), 201–206.

Vann, S. D. (2013). Dismantling the Papez circuit for memory in rats. *eLife*, *2*, e00736.

Vann, S. D., & Aggleton, J. P. (2002). Extensive cytotoxic lesions of the rat retrosplenial cortex revel consistent deficits on tasks that tax allocentric spatial memory. *Behavioral Neuroscience*, *116*(1), 85–94.

Vann, S. D., & Aggleton, J. P. (2003). Evidence of a spatial encoding deficit in rats with lesions of the mammillary bodies or mammillothalamic tract. *The Journal of Neuroscience : The Official Journal of the Society for Neuroscience*, *23*(8), 3506–3514.

Vann, S. D., & Aggleton, J. P. (2004a). Testing the importance of the retrosplenial guidance system: effects of different sized retrosplenial cortex lesions on heading direction and spatial working memory. *Behavioural Brain Research*, *155*, 97–108.

Vann, S. D., & Aggleton, J. P. (2004b). The mammillary bodies: two memory systems in one? *Nature Reviews. Neuroscience*, *5*(1), 35–44.

Vann, S. D., & Aggleton, J. P. (2005). Selective dysgranular retrosplenial cortex lesions in rats disrupt allocentric performance of the radial-arm maze task. *Behavioral Neuroscience*, *119*(6), 1682–1686.

Vann, S. D., Aggleton, J. P., & Maguire, E. A. (2009). What does the retrosplenial cortex do? *Nature Reviews. Neuroscience*, *10*(11), 792–802.

Vann, S. D., & Albasser, M. M. (2009). Hippocampal, retrosplenial, and prefrontal hypoactivity in a model of diencephalic amnesia: Evidence towards an interdependent subcortical-cortical memory network. *Hippocampus*, *19*(11), 1090–1102.

Vann, S. D., Brown, M. W., & Aggleton, J. P. (2000). Fos expression in the rostral thalamic nuclei and associated cortical regions in response to different spatial memory tests. *Neuroscience*, *101*(4), 983–991.

Vann, S. D., Brown, M. W., Erichsen, J. T., & Aggleton, J. P. (2000a). Fos imaging reveals differential patterns of hippocampal and parahippocampal subfield activation in rats in response to different spatial memory tests. *The Journal of Neuroscience : The Official Journal of the Society for Neuroscience*, *20*(7), 2711–2718.

Vann, S. D., Brown, M. W., Erichsen, J. T., & Aggleton, J. P. (2000b). Using fos imaging in the rat to reveal the anatomical extent of the disruptive effects of fornix lesions. *The Journal of Neuroscience : The Official Journal of the Society for Neuroscience*, *20*(21), 8144–8152.

Vann, S. D., Denby, C., Love, S., Montaldi, D., Renowden, S., & Coakham, H. B. (2008). Memory loss resulting from fornix and septal damage: impaired supra-span recall but preserved recognition over a 24-hour delay. *Neuropsychology*, *22*(5), 658–668.

Vann, S. D., Erichsen, J. T., O'Mara, S. M., & Aggleton, J. P. (2011). Selective disconnection of the hippocampal formation projections to the mammillary bodies produces only mild deficits on spatial memory tasks: implications for fornix function. *Hippocampus*, *21*, 945–57.

Vann, S. D., Honey, R. C., & Aggleton, J. P. (2003). Lesions of the mammillothalamic tract impair the acquisition of spatial but not nonspatial contextual conditional discriminations. *European Journal of Neuroscience*, *18*(8), 2413–2416.

Vann, S. D., & Nelson, A. J. D. (2015). The mammillary bodies and memory : more than a hippocampal relay. *Progress in Brain Reserach*, *219*, 163–185.

Vann, S. D., Wilton, L. A. K., Muir, J. L., & Aggleton, J. P. (2003). Testing the importance of the caudal retrosplenial cortex for spatial memory in rats. *Behavioural Brain Research*, *140*, 107–118.

Vertes, R. P. (2004). Differential Projections of the Infralimbic and Prelimbic Cortex in the Rat. *Synapse*, *51*(1), 32–58.

Vertes, R. P. (2005). Hippocampal theta rhythm: A tag for short-term memory. *Hippocampus*, *15*(7), 923–935.

Veyrac, A., Besnard, A., Caboche, J., Davis, S., & Laroche, S. (2014). The transcription factor Zif268/Egr1, brain plasticity, and memory. *Progress in Molecular Biology and Translational Science*, *122*, 89–129.

Victor, M., Adams, R. D., & Collins, G. (1989). *The Wernicke-Korsakoff syndrome and realted neurological disorders due to alcoholism and malnutrition (Contemporary neurology)*. F. A. Davis Company.

Victor, M., & Yakovlev, P. I. (1955). S.S. Korsakoff's psychic disorder in conjunction with peripheral neuritis; a translation of Korsakoff's original article with comments on the author and his contribution to clinical medicine. *Neurology*, *5*(6), 394–406.

Villain, N., Desgranges, B., Viader, F., de la Sayette, V., Mézenge, F., Landeau, B., … Chételat, G. (2008). Relationships between hippocampal atrophy, white matter disruption, and gray matter hypometabolism in Alzheimer's disease. *The Journal of Neuroscience*, *28*(24), 6174–6181.

Vogt, B. A., Vogt, L., & Farber, N. B. (2004). Cingulate Cortex and Disease Models. In *The Rat Nervous System, Third Edition* (pp. 705–727).

Vogt, & Peters. (1981). Form and distribution of neurons in rat cingulate cortex: areas 32, 24, and 29. *The Journal of Comparative Neurology*, *195*(4), 603–25.

Von Cramon, D. Y., Hebel, N., & Schuri, U. (1985). A contribution to the anatomical basis of thalamic amnesia. *Brain*, *108*, 993–1008.

Wan, H., Aggleton, J. P., & Brown, M. W. (1999). Different contributions of the hippocampus and perirhinal cortex to recognition memory. *The Journal of Neuroscience*, *19*(3), 1142–1148.

Warburton, E. C., & Aggleton, J. P. (1999). Differential deficits in the Morris water maze following cytotoxic lesions of the anterior thalamus and fornix transection. *Behavioural Brain Research*, *98*(1), 27–38.

Warburton, E. C., Aggleton, J. P., & Muir, J. L. (1998). Comparing the effects of selective cingulate cortex lesions and cingulum bundle lesions on water maze performance by rats. *European Journal of Neuroscience*, *10*, 622–634.

Warburton, E. C., Baird, A. L., & Aggleton, J. P. (1997). Assessing the magnitude of the allocentric spatial deficit associated with complete loss of the anterior thalamic nuclei in rats. *Behavioural Brain Research*, *87*(2), 223–232.

Warburton, E. C., Baird, A. L., Morgan, A., Muir, J. L., & Aggleton, J. P. (2000). Disconnecting hippocampal projections to the anterior thalamus produces deficits on tests of spatial memory in rats. *European Journal of Neuroscience*, *12*(5), 1714–1726.

Warburton, E. C., Baird, A., Morgan, A., Muir, J. L., & Aggleton, J. P. (2001). The Conjoint Importance of the Hippocampus and Anterior Thalamic Nuclei for Allocentric Spatial Learning : Evidence from a Disconnection Study in the Rat. *The Jounal of Neuroscience*, *21*(18), 7323–7330.

Warrington, E. K., & Weiskrantz, L. (1982). Amnesia: A disconnection syndrome? *Neuropsychologia*, *20*(3), 233–248.

Whishaw, I. Q., Maaswinkel, H., Gonzalez, C. L. R., & Kolb, B. (2001). Deficits in allothetic and idiothetic spatial behavior in rats with posterior cingulate cortex lesions. *Behavioural Brain Research*, *118*(1), 67–76. doi:10.1016/S0166-4328(00)00312-0

Wickstrom, E. (1986). Oligodeoxynucleotide stability in subcellular extracts and culture media. *Journal of Biochemical and Biophysical Methods*, *13*(2), 97–102.

Williams, P. A., Thirgood, R. A., Oliphant, H., Frizzati, A., Littlewood, E., Votruba, M., … Morgan, J. E. (2013). Retinal ganglion cell dendritic degeneration in a mouse model of Alzheimer's disease. *Neurobiology of Aging*, *34*(7), 1799–1806.

Winer, B. J. (1971). *Statistical Principles in Experimental Design*. McGraw-Hill.

Winocur, G. (1982). Radial-arm maze behavior by rats with dorsal hippocampal lesions: Effects of cuing. *Journal of Comparative and Physiological Psychology*, *96*(2), 155–169.

Winocur, G., Oxbury, S., Roberts, R., Agnetti, V., & Davis, C. (1984). Amnesia in a patient with bilateral lesions to the thalamus. *Neuropsychologia*, *22*(2), 123–143.

Winter, S. S., Wagner, S. J., McMillin, J. L., & Wallace, D. G. (2011). Mammillothalamic tract lesions disrupt dead reckoning in the rat. *The European Journal of Neuroscience*, *33*(2), 371–381.

Wisden, W., Errington, M. L., Williams, S., Dunnett, S. B., Waters, C., Hitchcock, D., … Hunt, S. P. (1990). Differential Expression of Immediate Early Genes neurons in the Hippocampus and Spinal Cord. *Neuron*, *4*, 603–614.

Witte, O. W. (1998). lesion-induced plasticity as a potential mechanism for recovery and rehabilitative training. *Current Opinion in Neurobiology*, *11*(6), 655–662.

Woolf, N. (1991). Cholinergic systems in mammalian brain and spinal cord. *Progress in Neurobiology*, *37*(6), 475–524.

Woolsey, R. M., & Nelson, J. S. (1975). Asymptomatic destruction of the fornix in man. *Archives of Neurology*, *32*, 566–568.

Wright, N. F., Erichsen, J. T., Vann, S. D., O'Mara, S. M., & Aggleton, J. P. (2010). Parallel but separate inputs from limbic cortices to the mammillary bodies and anterior thalamic nuclei in the rat. *The Journal of Comparative Neurology*, *518*(12), 2334–54.

Wright, N. F., Vann, S. D., Erichsen, J. T., O'Mara, S. M., & Aggleton, J. P. (2013). Segregation of parallel inputs to the anteromedial and anteroventral thalamic nuclei of the rat. *Journal of Comparative Neurology*, *521*(13), 2966–2986.

Wu, C.-C., Reilly, J. F., Young, W. G., Morrison, J. H., & Bloom, F. E. (2004). High-throughput morphometric analysis of individual neurons. *Cerebral Cortex*, *14*, 543–554. doi:10.1093/cercor/bhh016

Wu, H., Lima, W. F., Zhang, H., Fan, A., Sun, H., & Crooke, S. T. (2004). Determination of the Role of the Human RNase H1 in the Pharmacology of DNA-like Antisense Drugs. *Journal of Biological Chemistry*, *279*(17), 17181–17189. doi:10.1074/jbc.M311683200

Wyss, Groen, V., & Sripanidkulchai. (1990). Dendritic bundling in layer I of granular retrosplenial cortex: intracellular labeling and selectivity of innervation. *The Journal of Comparative Neurology*, *295*(1), 33–42.

Wyss, J. M., Swanson, L. W., & Cowan, W. M. (1979). A study of subcortical afferents to the hippocampal formation in the rat. *Neuroscience*, *4*, 463–476.

Wyss, J. M., & Van Groen, T. (1992). Connections Between the Retrosplenial Cortex and the Hippocampal Formation in the Rat : A Review. *Hippocampus*, *2*(1), 1–12.

Yamauchi, H., Fukuyama, H., Nagahama, Y., Nishizawa, S., & Konishi, J. (1999). Uncoupling of oxygen and glucose metabolism in persistent crossed cerebellar diaschisis. *Stroke; a Journal of Cerebral Circulation*, *30*(7), 1424–1428.

Yee, F., Ericson, H., Reis, D. J., & Wahlestedt, C. (1994). Cellular uptake of intracerebroventricularly administered biotin- or digoxigenin-labeled antisense oligodeoxynucleotides in the rat. *Cellular and Molecular Neurobiology*, *14*(5), 475–486.

Yoneoka, Y., Takeda, N., Inoue, A., Ibuchi, Y., Kumagai, T., Sugai, T., … Ueda, K. (2004). Case Report Acute Korsakoff Syndrome Following Mammillothalamic Tract Infarction. *AJNR. American Journal of Neuroradiology*, (July), 964–968.

Yoon, T., Okada, J., Jung, M. W., & Kim, J. J. (2008). Prefrontal cortex and hippocampus subserve different components of working memory in rats. *Learning & Memory*, 97–105.

Yoshihara, T., & Ichitani, Y. (2004). Hippocampal N-methyl-D-aspartate receptor-mediated encoding and retrieval processes in spatial working memory: delay-interposed radial maze performance in rats. *Neuroscience*, *129*(1), 1–10.

Zangenehpour, S., & Chaudhuri, A. (2002). Differential induction and decay curves of c - fos and zif 268 revealed through dual activity maps. *Molecular Brain Research*, *109*, 221–225.

Zhu, X. O., Brown, M. W., McCabe, B. J., & Aggleton, J. P. (1995). Effects of the novelty or familiarity of visual stimuli on the expression of the IEG c-fos in rat brain. *Neuroscience*, *69*(3), 821–829.

Zhu, X. O., McCabe, B. J., Aggleton, J. P., & Brown, M. W. (1997). Differential activation of the rat hippocampus and perirhinal cortex by novel visual stimuli and a novel environment. *Neuroscience Letters*, *229*(2), 141–143.